



Final Report

Arcadian Renewable Energy System

DSE Group 23

Page intentionally left blank

Final Report

Arcadian Renewable Energy System

by

DSE Group 23

Tutor: Dr.-Ing. R. Schmehl

Coaches: Prof. Dr. D. A. von Terzi
Dr. B. V. S. Jyoti
C. Belo Gomes Brito, MSc.

Students:	F. Corte Vargas	4674529
	M. Géczi	4650379
	S. Heidweiller	4476468
	M. Kempers	4542509
	B. J. Klootwijk	4551516
	F. van Marion	4664965
	D. Mordasov	4658760
	L. H. Orouumova	4681797
	E. N. Terwindt	4543548
	D. Witte	4670302

Delft University of Technology
Faculty of Aerospace Engineering

July 21, 2020



Acknowledgements

"When something is important enough, you do it even if the odds are not in your favor."

Elon Musk

First and foremost, we would like to express our sincere gratitude towards our tutor and coaches: Roland Schmehl, Dominic von Terzi, Botchu Jyoti and Camila Brito. Their guidance and involvement in every step of the design synthesis exercise have allowed us to accomplish this final report.

We would also like to show our great appreciation to the OSSC, the organising committee, who has faced an enormous challenge to facilitate this year's DSE during the COVID-19 pandemic. Their outstanding organisational efforts have definitely contributed to the achievement of this project.

We are also very grateful for the assistance given by the teaching assistants. With their experience, they have provided us with valuable advice on project management and systems engineering.

We would also like to extend our gratitude to all the experts who were keen to offer their expertise whenever we needed advice on technical matters outside of our own field of competence.

Last but not least, our thanks go to our animal companions, who have provided emotional support and helped us recover our energy at the end of the strenuous working days. Thank you to our dogs Vajtík, Jax and Sushi, our cats Zsizsi and Gatto, and our fish Elvis, Paris and Touchy.

Contents

Executive Overview	v
1 Introduction	1
2 Market Analysis	2
2.1 Key Partners	2
2.2 Market	2
2.3 Business Model and SWOT	4
2.4 Financials	5
2.5 Future of the system.	6
3 Sustainability Approach	7
3.1 Environmental Sustainability	7
3.2 Social Responsibility	7
3.3 Financial Sustainability	8
4 Technical Risk Management	9
5 Project Objectives and Requirements	11
5.1 Project Objectives	11
5.2 Requirements	11
6 Functional Analysis	14
7 System Architecture and Interfaces	18
7.1 Diagram of the System Architecture	18
7.2 Summary of the Subsystem Design	19
8 Operations and Logistics	21
8.1 Mission Configuration and Site Characteristics	21
8.2 Launching Procedures	23
8.3 Payload Integration	24
8.4 Landing and Set-Up	25
8.5 System Operations	26
9 System Performance Analysis	31
9.1 Model Description	31
9.2 Model Inputs and Task Execution.	34
9.3 Results and System Sensitivity Analysis	36
9.4 Verification and Validation.	41
9.5 Conclusion and Recommendations.	42
10 Power Management and Distribution System Design	43
10.1 Requirements	43
10.2 Trade-off Summary	43
10.3 System Architecture and Interfaces	43
10.4 Subsystem Sizing	44
10.5 Cost Breakdown	47
10.6 Subsystem Design Results	47
10.7 Risk Assessment	48
10.8 Sustainability and Retirement.	49
10.9 Requirement Compliance and Sensitivity Analysis	49
10.10 Recommendations	50
11 Primary Energy System Design	52
11.1 Requirements	52
11.2 Trade-off Summary	52
11.3 Wind Resource	52
11.4 System Architecture and Interfaces	54
11.5 AWE System Model	55
11.6 AWE System Sizing	60
11.7 Material and Structural Characteristics	65

11.8 Cost Breakdown	66
11.9 Model Verification and Validation	68
11.10 Risk Assessment	70
11.11 Sustainability and Retirement	73
11.12 Requirements Compliance and Sensitivity Analysis	73
11.13 Recommendations	75
12 Secondary Energy System Design	76
12.1 Requirements	76
12.2 Trade-off Summary	76
12.3 Solar Resource	76
12.4 Optimising Secondary Energy System for Mars	77
12.5 Subsystem Sizing	79
12.6 System Architecture and Interfaces	80
12.7 Cost Breakdown	80
12.8 Risk Assessment	81
12.9 Sustainability and Retirement	83
12.10 Requirement Compliance and Sensitivity	84
12.11 Recommendations	84
13 Storage System Design	85
13.1 Requirements	85
13.2 Trade-off Summary	85
13.3 System Architecture and Interfaces	85
13.4 CAES Design Approach and Sizing	86
13.5 Battery Design Approach and Sizing	92
13.6 Subsystem Design Results	94
13.7 Cost Breakdown	95
13.8 Risk Assessment	95
13.9 Sustainability and Retirement	97
13.10 Requirement Compliance and Sensitivity Analysis	97
13.11 Recommendations	98
14 Data and Communication Handling	100
15 Reliability, Availability, Maintainability and Safety	101
15.1 Reliability and Availability	101
15.2 Maintainability	102
15.3 Safety	103
16 Budget Analysis and Resource Allocation	105
16.1 Budget Analysis	105
16.2 Resource Allocation	105
17 LCA of the Primary Energy System	108
17.1 Goal and Scope	108
17.2 Inventory Analysis and Impact Assessment	108
17.3 Interpretation & Next Steps	109
18 System Verification and Validation	111
18.1 Model Verification and Validation	111
18.2 Product Verification and Validation	112
18.3 System Verification and Validation	113
19 Production Plan	114
19.1 Production Strategy	114
19.2 Manufacturing and Assembling Plan	115
20 Compliance Matrix	117
21 Next Steps	121
21.1 Project Gantt Chart	121
21.2 Design and Logic Diagram	121
21.3 Cost Breakdown Structure	123
22 Conclusions and Recommendations	126
Bibliography	129

Executive Overview

The Challenge

The human eye has turned itself back to the sky with the commercialisation of the space industry, and a new goal has been set. Setting foot on the Red Planet is the next stage of the human exploration of the universe. The travel to Mars is very lengthy and costly, nonetheless the planet still shows great potential for sustaining human life. To make this a possibility, there is a need for locally sourced energy. The presence of (re-)usable resources on Mars could pave the way to further expand the exploration to an interplanetary scale, and successfully maintain a human presence outside the Earth's atmosphere. The availability of energy will be a key indicator for the success of the human race in the colonisation of Mars.

The Solution

To answer this call for the need to generate locally sourced energy, the design of a renewable energy system was started by a team of students and staff from the faculty of Aerospace Engineering at Delft University of Technology: The Arcadian Renewable Energy System (ARES). The energy system will power the construction and operations of a Mars habitat, to support the livability of humans. The system will use complementary renewable energy sources integrated into a microgrid, to sustainably harvest energy from local Martian environment and resources. To ensure the design will be able to fulfil its purpose, a mission need statement and a project objective statement are generated:

Mission Need Statement: To provide renewable energy supply of 10 kW to a Mars habitat.

Project Objective Statement: Design a renewable energy supply system, primarily focusing on wind energy, which provides 10kW to a Mars habitat, by 10 students in 10 weeks.

This Design synthesis exercise (DSE) will last a total of 10 weeks, beginning on the 20th of April, ending on the 2nd of July, with a poster session and symposium. The DSE is in collaboration with the Architectural faculty, where a separate team of students is working on a rhizomatic Mars habitat project as part of an ESA competition, which has an ESA-ESTEC feasibility study proposal incorporated. Due to the multi-disciplinary nature of this project, it is important that the DSE team produces a complete and verified design as the outcome.

The Design

The design the DSE has come up with consists of two energy production systems, namely the primary and secondary energy system providing wind and solar energy, respectively. In addition the system also consists of a power management and energy storage system. Figure 1 shows how the systems relate to each other and work together.

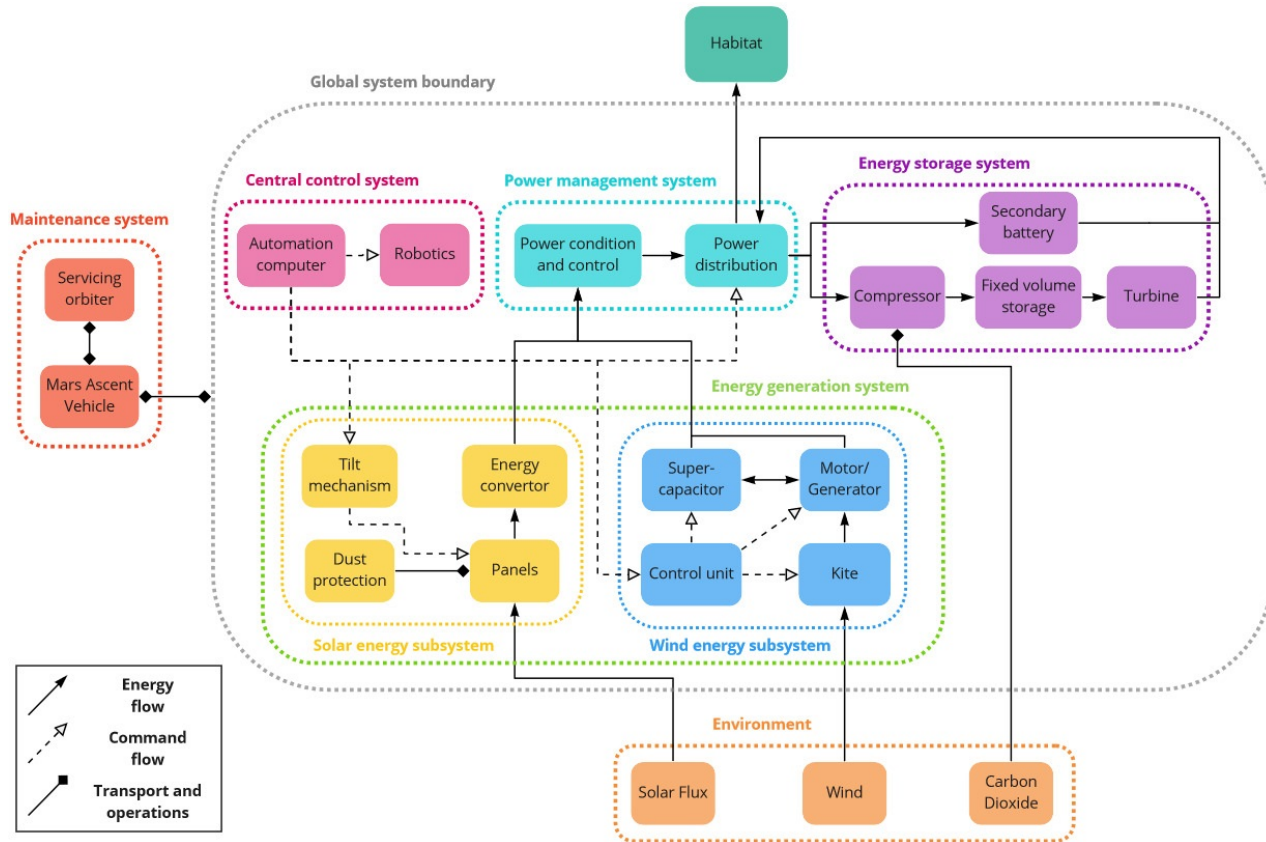


Figure 1: Architecture and Interfacing of the entire renewable energy system

The primary energy system has been chosen to be airborne, and more specifically a kite. It also comes with a ground station in which the mechanical energy produced by the pulling kite tether is transformed into electrical energy. The secondary energy system consists of solar panels which ensure energy is produced from the solar irradiance that reaches the Martian surface. The energy storage systems are seasonal and day-to-day. The former has been designed to be a compressed air storage system (CAES) where energy can be stored for a longer period of time. The day-to-day storage is meant to supply energy during the night when the energy production units are not in use. These are designed as secondary lithium-sulphur batteries. Finally the power management distribution system brings the power efficiently to where it needs to go by means of a DC microgrid with underground cables. The systems will be described more in detail in the following sections.

Market Analysis

Performing a market analysis is critical to determine the financial sustainability and profitability of the energy system. Capital and proper market segmentation is the key driver to ensure the longevity and overall success of the project. Key partners are also important and the team considers the EU administration (ESA), launch site operators, and the subsystem manufacturers to be critical. Requirements are also formed based on cost functions and various demands driven by competitors for other Martian-based energy system designs.

There is a huge potential for Mars colonisation due to public perception growth, technological funding and interest as an aspiring and space-bearing race. Over the next couple of decades, Mars in particular will experience an exponential growth of interest in colonisation missions. Thus, the need for an energy system would naturally follow suit.

The main competition that this DSE team considers in the market study includes:

- **NASA:** Task order NAS3-2S808, "Mars Power System Definition Study" researches various energy technologies specifically for Mars.
- **Shackleton Energy Corporation:** Space energy technologies, power transmission, life support systems and autonomous robots.
- **Kilopower:** Conceptual long-duration and affordable fission nuclear energy systems on planetary surfaces demonstration.

From the SWOT analysis, the key strength of the design is the use of renewable energy and zero use of

nuclear energy. The biggest threats to the project include the launcher not being available currently, launcher program change or cancellations, a delay in the Mars habitat project, and lack of project funding.

For the initial Rhizome project, the system's hardware cost, defined at the point of turnover to the mission operators, is €50 million. It is also a pre-requisite of the project that contractual funding (€500 million) from space administration and national-level is incorporated, as well as subsidies and grants (€150 million) aimed at different subsystem research groups from the company.

Each subsystem has their own intrinsic scientific and economic value. A good framework for this project is to segment the opportunities of each subsystem, in various applications and for monetisation of intellectual property assets that arise from the research. Thus, to position ARES for the future market is to delineate the value opportunity of each subsystem, as a single cost price in competition comparison cannot properly highlight the complete value and assets of the energy system, the research that goes behind it and the production company as a whole.

Risk and Sustainability Approaches

Risk is involved in any project, if one also includes technicalities and high costs, the former only increases. Therefore, a Martian missions that has never been done before brings extreme uncertainties.

Firstly, the risks associated with the project itself are evaluated. The top-level risks include, but are not limited to:

- Project being discontinued/delayed or the top requirements changed substantially.
- Risks associated with launching the payload also including dependence on third-party launcher company.
- Landing module failures.
- Materials and/or water ice is not as abundant as expected or cannot be collected.

Even though these risks generally are outside the control of the DSE group, recommendations are made. The team suggests to send a rover mission to the final habitat location to map the surface in detail for geological composition and subsurface ice content.

On the other hand, failure modes of all subsystems are analysed. The airborne wind energy system technological readiness is low. When the transition to Martian conditions is also taken into account, it is clear that this subsystem brings high risks. A solar subsystem on the other hand does not pose any risks beyond acceptable level, as this is space-proven and has been used in most Martian missions. Lithium-sulphur battery, the short-term storage solution, is a novel technology with promising results in specific power. Due to the low maturity of the concept, this also poses moderate to high risks, but if compared to other lithium-based batteries, like lithium-ion, it is likely to be reliable in due time. Compressed air energy storage, the seasonal storage, despite being used in only four projects on Earth is proven to be reliable. Thus, if the group's recommendations on mapping the site location is satisfied, this aspect of the project only poses moderate risks. Finally, the risks of power management are considered: underground transmission lines greatly reduce the likelihood of an outage during the windy seasons. Also, due to the high readiness level on Earth, the risk associated with this system is expected to stay in the acceptable range.

Sustainable engineering is achieved if the project complies to all three components of sustainability: environmental sustainability, social responsibility and financial sustainability. Environmental sustainability is achieved by the minimisation of waste and use of non-renewable resources. For this, several requirements of the system have been set up: no nuclear energy shall be used and the impact on Mars and Earth shall be minimised. Also, for every subsystem a way to retire the system, preferably on Mars, is being thought of, as this will reduce the impact after life. To get an overview of the impact during production on Earth, a Life Cycle Assessment (LCA) is performed for the primary energy system.

Regarding social responsibility within the mission, the seven key principles are: accountability, transparency, ethical behaviour, respect for stakeholder interests, respect for the rule of law, respect for international norms of behaviour, and respect for human rights.

For financial sustainability, an analysis of the market potential is performed. Additionally, the costs have been estimated so these can be elaborated upon in further design stages.

Operations and Logistics

The complete and adequate specification of a space mission's operations and logistics is critical for its credibility and feasibility. After several rounds of iteration and active collaboration with all involved stakeholders, a first-order concept covering several elements within the mission's design is finalised. To illustrate this concept, a schematic diagram of the mission was developed to provide visual insight into the chronological and logical order of the different stages of the mission as can be seen in figure 2:

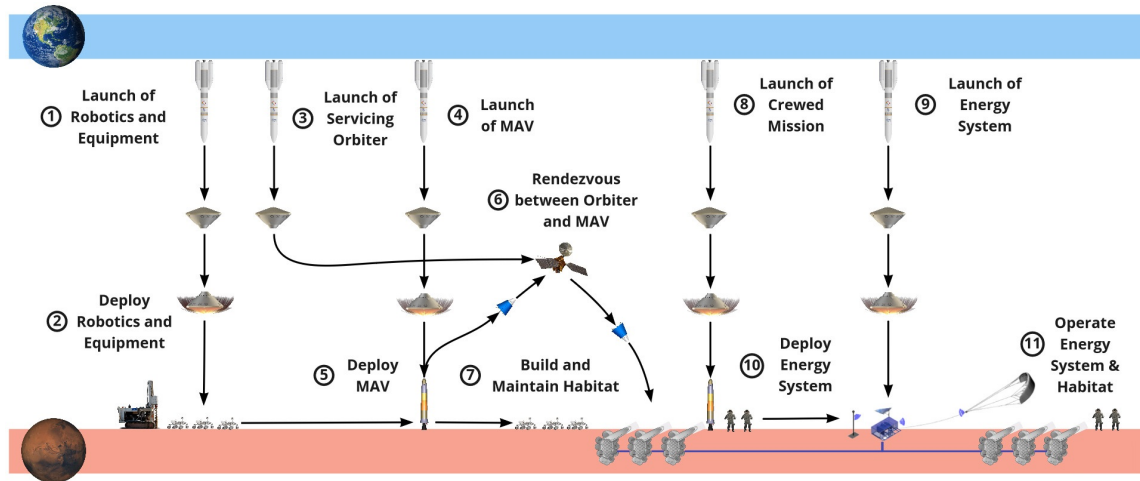


Figure 2: Schematic of the mission configuration

From this figure several important points must be noted; firstly, the order of appearance of all different launches, whether they relate to cargo or to a crewed mission, follows a very particular logic and cannot be interchanged straightforwardly. As it can be expected from the development of a space mission, the complexity of all its constituents can result in an unrealistic gap between theory and practice. For this very reason, special attention must be paid to the user requirements, the sustainability approach of the design, as well as the overall safety and integrity of both machinery and human resources.

Having said this, the site selection and subsequent mission configuration up until this stage resulted in a need for several launches, each with the purpose of fulfilling an independent role towards the completion of a successful colonisation of the Red Planet. More specifically, the mission starts by launching all the necessary equipment and cargo needed to ensure a continuous and fully automated construction of an underground rhizomatic habitat on the Martian surface. Once the entry, descent, and landing procedures of these flights are completed, and once there is a sufficiently complete life-support infrastructure to support human life, the crewed mission along with ARES can make its way to Mars.

Upon successful arrival, the deployment and installation of the system happens in three phases, with slight variations between the subsystems. The first is that astronauts and rovers work in tandem to lay the foundation for the energy system. This means digging trenches for the underground cables, preparing the ground to bury the primary energy system's ground station, drilling the solar panel structure into the ground, excavating the underground storage cavern for the CAES system, and an underground pod for the secondary batteries. The second phase is the transport of these subsystems and components to the desired location (this is done mainly by the rovers) with the direction of the local crew. The last phase is the integration of the subsystems with the power management and this should be completed by a trained astronaut.

Once the power system is producing sufficient energy to sustain the life support functionalities of the habitat, a gateway to a larger colony is opened in preparation for a sustained human presence on the Martian surface. To ensure that all systems are adequately deployed and operated, a specification of the top-level concept for the automation of the primary energy system is presented. Besides this, some important considerations pertaining to the safety and integrity of all astronauts are introduced, as well as their effect on the specification of the system's overall performance.

System Performance

In order to evaluate the complementary interaction between the wind, energy and storage and microgrid sub-systems, a Python model with six code block units was developed. It is paramount to understand that the performance analysis involves multiple iterations between the actual design specification of five sub-systems and the expected performance levels to meet the total demand. For example, the microgrid efficiencies depend on the nominal power inputted in the grid, while the total energy and power generation depend on the microgrid efficiencies. The separate code block units and their description is as follows:

- **Unit 1: Define daily operational conditions** - In this unit the nominal power for work (10 kW) and rest (5 kW) are evaluated for the whole year along with starting times of work (9 o'clock) and rest (23 o'clock) operations. Additionally, the sunrise and sunset times throughout the year are computed because they are relevant for calculating the generation periods of the two sub-systems.
- **Unit 2: Calculate direct supply conditions** - In the second unit, it is evaluated what portion of the total

demand per sol (Martian solar day) can be directly delivered from the wind and solar sub-systems to the habitat. The remaining fraction should be supplied through the storage solutions. As this value depends on the harvesting periods of the respective sub-system, those are evaluated as following. Solar energy is always harvested from sunrise until sunset, while wind energy is harvested from one hour before sunrise until one hour after sunset for spring, summer and autumn. During winter wind energy is harvested from two hours before sunrise until two hours after sunset.

- **Unit 3: Evaluate resource conditions** - This unit of code computes the normalised wind and solar energy available which are also referred to as the resource conditions. The wind conditions are obtained through dividing the annual production of the kite by the required energy supply per sol; resulting in a fraction, where 1 corresponds to a state at which the wind energy could fully meet the daily demand. Similarly, the solar condition is evaluated through normalising the solar irradiance by setting up a maximum solar condition of 0.35 corresponding to the maximum irradiance.
- **Unit 4: Evaluate wind/solar/battery/CAES performance** - This unit is programmed into a Python function which utilises definitions such as dominant and auxiliary condition. Based on the values of the operational and resource conditions, the direct supply, the through-battery supply for wind and solar and the supply through-CAES for each sol are evaluated. Moreover, the excess energy is stored in the CAES facility without considering the efficiencies. An array that represents the net CAES charge through the year is computed through evaluating the absolute charge and discharge energy values.
- **Unit 5: Evaluate power generation for seasonal storage** - Once the daily supply has been evaluated, it must be confirmed that the CAES facility has been provided enough energy to meet the required supply. This is done through transforming the above mentioned data array containing the net CAES charge: the inputted charge is multiplied by the microgrid path and the compression efficiencies. While, the outputted charge is divided by the microgrid path, storage and expansion efficiencies. The inspection if the CAES has been charged sufficiently is performed manually through visual examination.
- **Unit 6: Evaluate power mix values, total energy and nominal powers** - Next, the power mix values can be evaluated in order to examine if the wind energy system meets more than 50% of the total yearly supply. This is done through summing the total wind and solar energy for direct and through battery supply and dividing them by the total supply per sol (190 kWh); the values are as presented in table 1. Following, the energy generation for daily demand is calculated by dividing the direct supply by the direct path efficiencies and the through battery supply by the battery round-trip and microgrid path efficiencies. Hence, the total wind and solar energy generation for the whole year are evaluated through summing the energy to meet the daily and seasonal demand. Moreover, the nominal power production is computed through dividing the total energy generation by the harvesting duration of each sub-systems. Thus, the area of the solar array is calculated through evaluating whether it is sufficient to generate the required nominal power. Moreover, the expected energy generation by the wind system is compared to the actual energy output of the kite.

Table 1: Power mix values for direct and through storage supply on the left and power mix values for sol and seasonal supply on the right

Direct wind	Direct solar	Through battery	Through CAES	Through wind	Through solar	Through CAES
64%	2%	29%	5%	85%	10%	5%

The model computations and results are plotted for clarity, while the final sizes of the sub-systems are as following. The required battery capacity is 116 kWh with 5% contingency as evaluated from the biggest value of the through-battery supply array for a Martian year. The required supply through the CAES is equal to 6.5 MWh for the summer season with a contingency of 10%, as this is the most input sensitive sub-system. Moreover, the solar array must have an area of 70 m² with 5% contingency. The microgrid should be able to facilitate a power input of 26kW with a contingency of 5%. For the model to converge, the kite must be sized and its dimensions are discussed in later sections.

Moreover, to examine the sensitivity of the system design to the power requirements, the model is recomputed for nominal working power required of 7.5 kW and nominal power for rest equal to 5 kW. It is important to note that the energy production of the kite is approximately 80% of the original requirement while the maximum solar condition is still considered to be 35% of what needs to be currently produced. Hence, the new required size for the solar array is equal to 55 m², for the battery it is 93.5 kWh of storage capacity, while the nominal power which should be handled by the grid lowers to approximately 21 kW. Lastly, it is evaluated that the required supply through the CAES facility changes only to 6.25 MWh from 6.55 MWh. This is due to the fact that the CAES meets mainly the supply for the remaining periods where the nominal power required

stays the same as in the original design (5 kW).

Hereafter, the verification and validation procedures are presented for the separate units of code and for the complete model. For the verification Unit 4, verification tests are included in the function which terminated the model computation if for a single sol multiple loops are entered, or if the total evaluated supply through the function is different than the total required demand (190 kW). As for the system verification of the model, to examine if the model computes the correct supply values, the calculations are also performed by hand. To validate the model, the actual sub-system sizes and efficiencies must be known and the actual operations software of the central power control unit must be finalised.

Lastly, it is discussed that the model has an adequate level of precision for the current design stage where the main focus is the evaluation of the performance of different system configuration and performing iterations. Nevertheless, due to the fact that model is not programmed to compute the performance of any kind of system but rather the system at hand, there are modelling errors that could be observed. Therefore, for the future design and the evaluation of the system performance analysis, the model should be tailored for the design at hand.

Power Management and Distribution System

The power management and distribution system ensures the reliable delivery of electrical power to the habitat. After thorough evaluation of a number of configurations, it is concluded that a DC microgrid with underground cabling is most feasible for our project. By setting the grid voltage to 400 V and designing for a nominal power of 26 kW the grid components could be sized. Several power electronic converters are required for an adequate distribution of power, as well as carefully engineered power cables. This resulted in a total mass of 191.2 kg, a volume of 0.235 m³ and an approximate cost of €69,800. An important result of the power management and distribution design are the electrical path efficiencies, which dictate the power losses from the supply side to the demand side. The highest path efficiency is 89.0% while the lowest is 73.2%. The DC microgrid architecture is schematically visualised in figure 3:

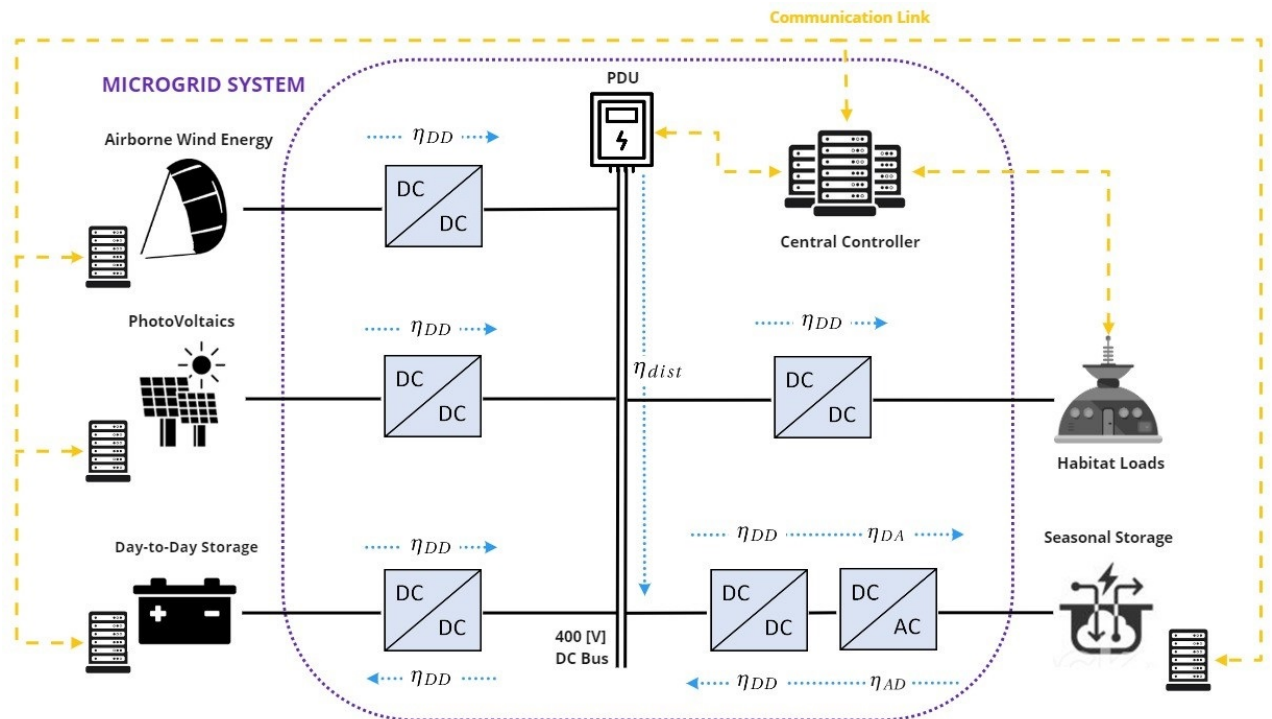


Figure 3: Schematics of the microgrid system architecture

Primary Energy System

Following multiple trade-offs, a pumping kite power system is chosen as the final concept for the primary energy system. After a system architecture is defined and the available wind resource is determined, a software model of the system's performance is generated. The model provided the foundation for the analysis of the power generation throughout the year; the design values were iterated until the system fulfilled its system performance requirements, at the lowest weight possible. This resulted in a primary energy system of a total mass of 288.1 kg, volume of 0.669 m³ and an approximate cost of €68,350. The system configuration consists

of a Tensairity kite of 50 m², a tether rated for a nominal tension of 7.5 kN and a generator rated at a nominal power of 80 kW. The model is considered to be successfully verified, the process of which gave rise to a few possible areas of improvement to the sizing method in the future. Future considerations on how to decrease the system mass are given, along with suggestions on increasing the reliability of the analysis.

Secondary Energy System

After an analysis of the solar resource availability and the light spectrum at the surface of Mars, it is determined that a GaInP/GaAs/Ge triple junction cell technology would be most suitable for the environment. To ensure high performance, the subcells should be current matched, and the panels refrigerated to avoid heat losses. From here the panels could be sized based on the performance analysis of the whole system, leading to a total array area of 70 m². With the required array size known, a mass, volume and cost estimation of the system could be made, including the axis system. From the panel density provided by the chosen manufacturer, Spectrolab, the mass and volume are estimated to be 123.2 kg and 0.63 m³ respectively. Based on the price per cell of €242 for the panels provided by Spectrolab, the total panel price is determined to be €6.78 million.

For the dual axis-system a commercial azimuth tracking axis-system is used as reference. Based on the area, the mass and volume are approximated to be 665 kg and 0.20 m³ respectively when correcting the mass for assuming an aluminium structure. The cost could be estimated to be €7,680.

Storage System

The energy storage system is split into two distinct systems, one for seasonal storage and one for day-to-day energy storage.

The seasonal storage system is selected to be a Martian-adapted CAES system, which consists of a compression segment, storage segment and expansion segment. The former includes the motor and compressor. Its total weight estimation is 500 kg with an efficiency of 76.3% and is required to be supplied with 17.2 kW. The storage segment consists of a plug at the ground surface and the storage cavern, with a volume of 107, 500 m³, holding a pressure of 105.175 Pa with an efficiency of 90%. The main resource for compressed air is CO₂. The final segment expansion which consists of the turbine and generator and is required to output of 18.1 kW. And its total weight is 900 kg with an efficiency of 65%. Overall, the efficiency of the CAES system is 44.6% and is required to store 13.1 MWh of exergy in any given Martian year.

The day-to-day storage system has been designed to be secondary batteries. More specifically they are lithium-sulphur batteries, and as such can be recharged every day. Their working principle is that they are fully charged during the day and depleted during the night to keep the habitat running and safe for the astronauts. The mass of the batteries ends up at 120.4 kg and a volume of 103.3 L. The cost of the batteries is estimated to be around €6.450.

Data and Communication Handling

The data and command flows are established, where the central computer commands the energy and communication systems based on inputs from the astronauts, the habitat and the environmental resources. Furthermore, a watchdog timer is used to protect the system in case of computer failures. Taking the Mars Perseverance rover as reference, it is decided to use a radiation-hardened central processor with PowerPC 750 Architecture and a BAE RAD 750.

Reliability, Availability, Maintainability and Safety

The reliability and availability of the different subsystems are directly related to the technological readiness levels and the reliability of the wind and solar resource availability. Similarly to Earth, renewable energy can be unreliable, but on Mars, the lack of detailed knowledge on the atmosphere adds an additional layer of uncertainty. If only the technical aspect is considered, the following can be said: little information is available on the reliability of airborne wind energy systems, thus this is recommended to be researched later. Meanwhile solar panel reliability on Earth exceeds 99.95%, and has also proven itself during numerous space and Mars missions. Moreover, compressed air storage can be considered reliable if requirements can be met that are dependent on the surface features. Although, lithium-sulphur batteries have little information on its actual performance, based on a conventional lithium-ion battery one can expect that the life cycle can reach or exceed 1200 cycles. Power management&transmission is a complex but developed system on Earth with only local effects in case of an outage. If mitigation measures can be applied on Mars to keep outages local, the reliability is high.

In addition, scheduled hardware and software maintenance are determined for all subsystems in order to reduce the likelihood of failures. These are either automated or require crew operation.

Lastly, safety has to be an integral part of any Mars mission. All stages have been considered: from system production to integration and operation on Mars. The guidelines of the American Institute of Aeronautics and Astronautics are considered and others are suggested as well.

LCA of the Primary Energy System

To get an overview of the impact of the primary energy system during production on Earth, a Life Cycle Assessment (LCA) with a cradle-to-gate approach is performed. The goal of the LCA is to identify the biggest impact areas to be able to reduce those in further design stages. From the LCA analysis performed on the kite energy system, it is concluded that the largest impact reduction could be gained in the acquisition and manufacturing of the materials used for the ground station, as many specialised materials are used for the sub-components.

System Verification and Validation

In order to check whether the design meets all its requirements and fulfils its intended purpose, it is crucial to carefully plan and execute verification and validation procedures on different levels. For the final design stage, computational models are developed to perform a detailed design of the kite power system, and to do a thorough analysis of the renewable energy system's performance. These are verified to some extent, but to ensure the correctness of the models, it is recommended to perform further validation. Next to software V&V, different methods are planned to verify whether or not the final product meets its requirements. Lastly, system-wide verification and validation checks must be carried out. For example, it is suggested to model and simulate the renewable energy system in Simulink. Also, the critical assumption on the available wind resources is addressed in the last section of V&V.

Production Plan

Throughout the production of the energy system, the lean manufacturing methodology must be applied. The approach aims to minimise waste in terms of material, energy, time and human resource, whilst striving to maximise the efficiency, productivity and quality of the process. For the system development team, reduction of waste production in processing, waiting, inventory, and transportation are relevant. The other ways to produce waste (defects, overproduction, motion, non-utilised talent) are considered out of the scope of the project, since the system will not be produced in bulk and manufacturing processes most likely are executed by third party contractors. In this stage of the design, a preliminary production plan is executed. In order to ensure a complete application of the lean manufacturing aspects, in further design stages a more detailed production plan must be created, including a planning for the time management.

Compliance Matrix

In the end, most of the requirements that have been set for the mission are complied with. Unfortunately, there is a small set of requirements that have not been fulfilled yet, which can be seen in table 2. In future design iterations, further investigation will be done in order to get a design that meets these requirements. Different materials will be considered and cooperation with the Mars habitat team will increase.

Table 2: Requirements that are not complied with

Requirement ID	Description
Energy Requirements	
REM-NRG-07	The location of the habitat and its energy system shall be jointly decided by the external Mars habitat project team and the DSE team.
Primary Energy System Requirements	
REM-Sys-N02-01	The primary energy system shall have a maximum mass of 200kg.
REM-Sys-N02-07	The tether shall have a bending fatigue SLL longer than the mission duration.
Secondary Energy System Requirements	
REM-Sys-N12-02	The secondary energy system shall have a maximum mass of 550 kg.
Energy Storage System Requirements	

Continued on next page

Table 2: Continued from previous page

Requirement ID	Description
REM-Sys-N05-04	The components of the total energy storage shall have a maximum mass of 1500 kg.
Launch and Deployment Requirements	
REM-LD-01	The maximum volume for transportation shall be 3 m ³ .
REM-LD-02	The maximum payload shall be 800 kg per flight.

Next Steps

The DSE period of the project has nearly come to an end, however this does not mean that the project needs to be finished. There are still steps and prospects beyond what has been put together during these 10 weeks. More specifically, the model of the design needs to be refined, followed by building a prototype for testing. Finally, a flight model should be built and tested to ensure a correct operation on Mars. The timeline of this mission is stretched over a period of 10 years; of course, the preliminary planning is still very prone to change. Alongside of these design phases, there are also still a multitude of topics that require a considerable amount of research. These include the development of the lithium-sulphur batteries, the wind and solar resources on Mars, and the development of the seasonal storage solution. Finally, the total cost of the mission has been estimated to be at around €1.15 billion.

Recommendations

After designing the renewable energy system, there are still recommendations for the future progression of the project. These are as follows for all the subsystems:

For the system performance analysis, it is considered that it would be for the best if a separate model is developed which is specific to the the design system at hand and the energy resources. Furthermore, this model should include an operational function which is mathematically identical to the software of the power management control unit.

For power management, including a PDU and a central controller in the design, as well as optimising algorithms for power flow is recommended. The latter should increase the efficiency of the DC microgrid, as well as the control. Furthermore, cable protection and grounding need to be investigated for the system. Finally, more should be learned about the power converters for Mars applications.

For the primary energy system, the casing of the KCU needs to be radiation proof and batteries will be needed to power the control unit. These would need to recharge while the kite is on the ground. Kite position tracking is also an important consideration to keep in mind, and is briefly elaborated upon in this report. Furthermore, the system mass needs to be reduced which could be improved by investigating the use of more lightweight materials. Finally, for the optimisation of the system's annual energy production, the cut-in wind speed could be further investigated.

For the secondary energy system, a cooling system as well as a position simulation of the sun path need to be developed. The former is useful for the less dense atmosphere, and the latter should be developed specific to the habitat location. Moreover, the axis-system could be made more lightweight.

Finally, the energy storage system has some ideas for future development. For the CAES, more investigation should be done for the caverns and rock formations in the Martian ground, as the CAES system relies on the their structural properties. Other compressed air storage technologies, such as lightweight tanks should also be investigated as they could be constructed by additive manufacturing on Mars.

For the batteries, thermal insulation and protection from cosmic radiation needs to be researched further and included in the detailed design. Modularity and the general properties of the batteries should also be further developed.

Introduction

In the past century, the human race made advances in technology like one could never dream of. One of the most notable accomplishments was that a man set his foot down on the Moon. Since then, human exploration has stayed within low Earth orbit with the ISS, and the general public lost most interest in the space industry. However, as technology progresses even further, it has come to a point where everyone can contribute. With privately owned businesses in the mix and the new element of commercial competitiveness, the engineering is pushed even further. The plans are to go further than the Moon this time. And not just to visit, but to stay.

To make this a possibility, there are some hurdles left to be overcome. With Mars as the next destination, the prospective living environment is very harsh to humans. A habitat must be developed that is suitable to sustain human life in the Martian conditions. Furthermore, resources must be mined and collected, as water on Mars is not readily available. For all of this, a very important factor is the availability of energy, as without energy there is no life possible there.

The aim of this project is to develop such an energy system to help sustain human life on Mars. This will be done through utilising renewable energy resources, to power the construction and operation of a Rhizomatic Mars habitat. This habitat is developed by an external team of Architecture students as a part of an ESA-ESTEC feasibility study proposal. The objective of this report is to finalise the preliminary design for the wind energy system, as well as further complete the design of the supporting grid and check the total viability of the design, henceforth called the Alien Renewable Energy System (ARES).

To complete this, the report is structured as follows. In chapter 2 a market analysis for the system is performed, followed by the sustainability approach that will be used during the system development as described in chapter 3. Next, it is ensured by means of risk management in chapter 4, that the system is safe to operate. From here, the project objective, requirements and the functional analysis are re-assessed in chapters 5 and 6 respectively. Then, the system architecture, interfaces and their operations and logistics are evaluated in chapter 7 and in chapter 8. Following a careful performance analysis in chapter 9, the separate parts of the systems are sized. Power management can be found in chapter 10, primary energy system sizing can be found in chapter 11, secondary energy system in chapter 12 and energy storage in chapter 13. From here on, the data and communication of the complete system is elaborated upon in chapter 14, followed by the RAMS analysis in chapter 15. Then, chapter 16 contains a budget update and restates the resource allocation, succeeded by the life-cycle assessment of the primary energy system is performed in chapter 17. In chapter 18 the system is verified and validated and in chapter 19 a production plan is developed. To ensure that all the requirements are properly considered throughout the design, chapter 20 contains requirement compliance matrices. Finally, the next steps are discussed in chapter 21, followed by a conclusion to the report in chapter 22.

Market Analysis

For the longevity and overall success of the project, it is critical to be informed about the market milieu and identify the potential sectors that can utilise the technology and its lateral teachings. The market is also a key driver of the functional requirements, which is detailed in section 2.2.3. To provide (financial) sustainability to the project, it is key to identify key partners and resources that can provide support at different stages, even after the project's end-of-life timeline.

Thus, market opportunities, which provides a general framework for market outlook and growth with regards to the energy technology and the value of the Mars mission itself, is critical to ensure longevity and (economic) success of the project. The consequence of the market analysis is to better inform the project team, in how the technology and mission contributes to overall scientific progress and its practical utility in space exploration endeavours. It also informs the project design team to consider new requirements based on cost functions and other demands by the competitive market.

This chapter first introduces the key partners of this project to ensure basic accessibility to the market in section 2.1. Secondly, the target market and opportunities are according highlighted in subsections 2.2.1 and 2.2.2, respectively. Next, a competition analysis is carried out to ensure the maintained competence of unique selling point of the project's outcome in section 2.2.3. Lastly, a SWOT analysis table is presented, highlighting external and internal strengths and weaknesses for the project in section 2.3.

2.1. Key Partners

Key partners are important to ensure market viability and continued competitiveness in the market. These parties are often economic, technical and political gates (or barriers) from market entry to end-of-life continuity of the project. It takes into account adaptation of legislation, manufacturing facilities and technological innovations from the short to long term.

- **EU administration:** From 2015 to 2020, the EU invested over 12 billion euros in space activities, consolidating world-class space projects like Galileo and Copernicus¹. The organisation is the biggest institutional customer for launch services and initiator for space exploration missions in Europe. In this way, it is a key partner to ensure project funding and long-term support.
- **Launch Operation and Site:** Launch operations are essential for the successful initial phase of the mission: sending the designed energy technology to Mars. Thus, many factors come into play including technical compatibility and operational awareness.
- **Energy System Producers:** Since the energy systems chosen (wind, solar, storage and miscellaneous hardware components) for this mission are not built from scratch, but are merely designed, reconfigured and adapted for Martian applications, the power units have to be purchased directly from an external party. This plays a large role in the budgeting and costs of the project.
- **Manufacturing facilities:** It is also important to ensure efficient and regulated workstations in the production process. Currently, the energy system is designed for a one-time use for a one-time mission. Following the success of the mission, it is useful to perform an investigation of available mass-production manufacturing facilities and equipment for the continued developments of an extra-terrestrial energy system.
- **Legislators:** Political support and public perception of the mission is essential. In cases of non-compliance, the entire system would fail to reach its requirements if rules prevent different stages from carrying out. Hence legislative rules can decide the fate of the project's overall success.

2.2. Market

In this section, the target market and market opportunities of the DSE project's outcomes will be analysed.

¹https://www.eib.org/attachments/thematic/future_of_european_space_sector_en.pdf [Cited 30 April 2020]

2.2.1. Target Market

The market for this project is targeted at the space sector, in particular space exploration and colonisation. In recent years, Mars colonisation has received widespread public and private interest, and developments in this direction, whether habitation, materials or energy, are making fast strides. Hence, it is key to keep pace with the critical developments to ensure the project's technical design is still relevant for future projects. The market for the outcomes of this project are directly linked to the habitation study from a separate team of architects and engineers working for ESA-ESTEC [33]. In this way, there is only one target market and the project team is developing the energy system for this particular 'customer'.

However, the outcomes of the project need not just be utilised for a one-off mission, but can be applied to future efforts, which opens the market and economic sustainability of the research and technology. Because one of the main requirements for this project includes the use of renewable energy, the technologies identified will undergo a technology transfer process. This means new intrinsic changes in optimisation and adaptation of the energy technology (to different atmospheric conditions etc.) will instigate new uses and utility of the technology. This is a continual market-capturing process. Hence it is not just the hardware design that is brought into the market, but the novel understandings and technical know-how that can be introduced to future developments. The qualitative and quantitative aspects of this understanding can be applied to new project innovations and can spin-out new products to be introduced to the space-energy market. This sustains the long term market share of the DSE project's outcomes.

2.2.2. Market Growth and Opportunities

On Earth, energy is the biggest industry, valued at over 7.7 trillion euros² with a compounded annual growth rate of 4.1 % in 2018. While for space-derived energy opportunities, as defined by the white-paper released by the EU³, energy technologies are still in its infant emerging state. Thus, for missions similar to this, the next decade will see a rise in application of Earth-based energy sources, such as solar, wind, or nuclear. Naturally, there will be new emerging energy technologies that are designed specifically for these efforts. Hence, it is important to keep pace with the innovations and technical breakthroughs that risk longevity of this design project.

Furthermore, the space industry itself is growing⁴. Currently, the global space industry generates a revenue of 320 billion euros, and is expected to rise to 1 trillion euros as reported by the firm Morgan Stanley⁵. This takes into account terrestrial utilisation of space technologies such as navigation and earth observation systems, but also novel endeavours such as space mining and energy harvesting. This project falls under the latter. Thus, a role is played by the technical developments of this project, supported by the growing space colonisation industry.

Currently, the atmospheric composition of Mars is roughly 95 % carbon dioxide. According to a study by McKinsey⁶, there is a huge potential for Mars colonisation due to efforts done by NASA, in conjunction with MIT, where experiments are carried out to compress the Martian atmosphere and feed it to an electrolysis system, which converts carbon dioxide to unadulterated oxygen. Although these tests are done in labs on a small-scale basis, research and developments similar to this will incite a larger wave of keen parties willing to participate in Martian colonisation efforts. This means that Mars specifically, the closest planet to Earth, will experience an exponential interest in colonisation missions as more humans are able to breathe in the air and form some sort of livelihood aboard Mars. Thus, the growth for the energy demand of Martian systems would naturally follow suit.

2.2.3. Competition

Competition in the 'race to space' colonisation is evident from the fact that governments, space organisations and startups alike are developing solutions for energy production in space. This means that their financial competitive capabilities are diverse. Competition incurs risk in the longevity of the project's outcomes, thus it is key to identify the unique selling points of the competition in order to formulate some for this project, this maintains competitive advantage. The following section summarises the main competition from 3 groups that have projects within this field and can be potential sources of competition.

- **NASA⁷:** NASA has multiple sub-departments that deal with developing a wide range of space colonization technologies. Under NASA's Lewis Research Center in Ohio, a task order NAS3-2S808, entitled

²<https://www.weforum.org/agenda/2017/11/industries-will-make-money-in-space/> [Cited 30 April 2020]

³https://www.eib.org/attachments/thematic/future_of_european_space_sector_en.pdf [Cited 30 April 2020]

⁴<https://spacenews.com/investors-cautiously-optimistic-about-continued-space-industry-growth/> [Cited 30 April 2020]

⁵<https://knowledge.wharton.upenn.edu/article/commercial-space-economy/> [Cited 30 April 2020]

⁶<https://www.mckinsey.com/industries/aerospace-and-defense/our-insights/perspectives-on-the-future-of-space-exploration> [Cited 30 April 2020]

⁷<https://ntrs.nasa.gov/archive/nasa/casi.ntrs.nasa.gov/19950015535.pdf> [Cited 30 April 2020]

"Mars Power System Definition Study" researches various energy technologies specifically for Mars; including solar panels, battery characteristics and nuclear and thermionic reactor power systems.

- **Shackleton Energy Corporation⁸**: Shackleton was founded in 2007 in Texas and are primarily engaged in developing equipment for Moon mining. However, they are also engaged heavily in space energy technologies, such as power transmission, life support systems and autonomous robots.
- **Kilopower⁹** : Kilopower is a spin-off project from NASA and is a near-term conceptual and technological effort to introduce long-duration and affordable fission nuclear energy systems on planetary surfaces. Currently, the Kilopower team is designing mission concepts and risk mitigation strategies to prepare for a future flight demonstration.

As can be inspected, these design and engineering groups are also at the conceptual stage or have just begun preliminary design. It is thus reasonable to believe that this project will produce an outcome that will address certain problems that the other groups might not consider, especially taking into account sustainable design and use of renewable sources of energy.

Implications of Market on Design Requirements

Taking into account stakeholders, the market and the competition, several desired operational functions and design requirements are created and consolidated in table 2.1 below (see the extensive requirements list in section 5.2).

Table 2.1: Requirements Generated from Market Analysis

ID	Description	Justification
REM-Sys-N02-01	Maximum mass 200kg	Mass should be below 3rd party launch-requirements
REM-Sys-N02-07	Lifespan > Operations	Lifespan should be competitive for investment confidence
REM-Sys-N12-02	Maximum mass 550 kg	Same reason as REM-Sys-N02-01
REM-Sys-N12-03	Maximum Volume 1 m ³	Same reason as REM-Sys-N02-01, but for volume budgets
REM-Sys-N05-04	Maximum mass 1500 kg	Same reason as REM-Sys-N02-01
REM-Sys-N05-05	In-situ storage resource > 70%	The complete storage solution should compete with pure battery producers
REM-COST-01	Primary System 0.5 M€	The main product should be affordable for future reproducibility
REM-COST-02	Mission Cost 1150 M€	This price is incurred by customer, should be within market range
REM-Sys-C02-03	Maxmimum Cost 10 M€	Solar array design/technology should be price competitive
REM-Sys-C02-04	Maxmimum Cost 0.7 M€	Power management system should be price competitive

Other general considerations from market and stakeholder needs:

- In the site selection for the energy system, done in subsection 8.1.1, a consideration in relation to the Rhizome Habitat team (as a key stakeholder for initial design) was to place the coupled infrastructures within 10 km to a *theoretical* source of water. This is to ensure nominal accessibility to this important in-situ resource for survival.
- The current Martian energy generation solutions in the market (aboard Rovers) are individual (nuclear-powered) sources. Hence, the general philosophy of this DSE, which is also a top level requirement, is to utilize complementary sources of renewable energy. Here, wind energy, solar energy, compressed air energy storage and battery technology has been integrated in a system.

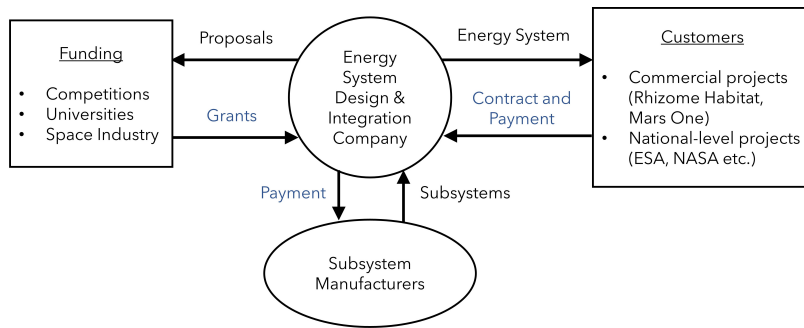
2.3. Business Model and SWOT

The business model for the energy system is relatively straightforward. The team is a long-term dedicated project group designing the integrated system, with manufactured subsystem manufacturers as key partners, and the first customer being ESA, alongside and is dependent on the concept of the Rhizome habitat team. However, there are other market opportunities to apply the Mars renewable energy system.

Mars City Designs, a platform and community connecting industry, university and thought leaders working towards space exploration and colonisation on Mars, was contacted and the DSE project was described. Because the continuous power supply of 10kW is indifferent to its destination, this led to the notion that there are potential collaborators, beside the Rhizome habitat application, that exists, and the business model represents this too (figure 2.1 below). The SWOT Analysis of the design and its market is consolidated in table 2.2.

⁸<http://www.shackletonenergy.com/technology#power-transmission> [Cited 30 April 2020]

⁹<https://www.nasa.gov/directorates/spacetech/kilopower> [Cited 30 April 2020]

**Figure 2.1: Business Model**

	Helpful	Harmful
Internal	<ul style="list-style-type: none"> - Renewable energy ONLY - No nuclear energy - No site selection for geothermal - Opportunities for technological growth and novelty of idea - Home office - Instant messaging - Intensive 10-week preliminary, trade-off and performance design process 	<ul style="list-style-type: none"> - Very novel design and approach - Insufficient task overview - Insufficient background references to Martian environmental resource understanding - No physical testing facilities available - Low face-to-face communication during COVID-19 outbreak - Team development and building is more difficult
External	<ul style="list-style-type: none"> - Very limited competition (novel approach) - Already have a first 'customer' (Rhizome, ESA) - Close collaboration with Rhizome Habitat team - Affiliated with Aerospace eng. and Architecture faculties at TU Delft - Network of research and industry experts - Use of prefabricated and 'off-the-shelf' components for certain subsystems 	<ul style="list-style-type: none"> - Strong reliance on external parties - Launcher program unavailable - Requires strong governmental and public support - Shortage of contractual funds from government and administration due to allocation of resources of COVID-19 outbreak - Capital intensive project - Changes in top level requirements

Figure 2.2: SWOT analysis

2.4. Financials

The energy system should be sold as a complete unit with training to the astronauts. Other costs, including launch, site set-up and habitation initiation, astronaut salary and mission operations of the energy system while on Mars is to be covered by 3rd party space operators, i.e. the customers of the system. Although these details work in tandem with the design of the energy system, as reflected by the requirements generated from market analysis (table 2.1).

Table 2.2 consolidates the costs incurred by the energy system company through the initial 10 year period of research, design and production. The maintenance costs is estimated to be 10% of the value identified in the cost breakdown structure, formed by the cost requirements in table 2.1. This is because, with the facility, only maintenance issues are accounted for, up to the point of the turnkey project to handover the system to the customer once aboard the launcher. The overhead costs are estimated to be 10 % during design and production phase. It is also a pre-requisite of the project that contractual funding from space administration and national-level is be incorporated, including subsidies and grants aimed at different subsystem research groups with the company.

In the event of the continuation of the project and repeat of production, it is estimated that the production and testing costs will decrease by 40 %. This is due to the fact that the deep research and adaptation of simulations and hardware to Martian conditions have been performed and can be validated after the first energy system unit production and operation, leading to a more efficient design update and construction. The specific technology and manufacturing infrastructure is also already set in place. With the same selling price of €50 million, the additional profits would be higher than the initial customer for the Rhizome project. However, it still reflects the value of a 10 year research timeline prior to the actual mission. This is consolidated in table 2.3 below.

Item	M€
Subsystem Hardware Costs	- 35
Production Costs	- 287.5
Labour cost	- 31.5
Testing Costs	- 234.6
Maintenance Costs	- 23.5
Overhead Costs	- 61.2
Subsidies and Grants	+ 150
Contract	+ 500
System Revenue	+ 50
Profit	26.7

Table 2.2: Financials for Rhizome Project

Item	Value [M€]
Subsystem Hardware Costs	- 35
Production Costs	- 172.5
Labour cost	- 30
Testing Costs	- 140.8
Maintenance Costs	- 20
Overhead Costs	- 40
Subsidies and Grants	+ 80
Contract	+ 350
System Revenue	+ 50
Profit	41.7

Table 2.3: Financials for future development

2.5. Future of the system

Besides the 10 kW of power supplied by the designed system for this DSE, the planned energy of a Martian habitat can include many other needs, such as energy peaks, modular charging of rovers and even thermal energy for water filtration and space agriculture. Hence, this is also taken into account for the market analysis in order to have a better estimation of future Martian applications. Figure 2.3 shows what a theoretical Martian Habitat requires and the percentage that the ARES energy system can supply.

There are two key considerations here that allow our system to achieve market competitiveness and future scalability for envisioned Martian energy demand. The first is that assumption that 10 kW can be 'plugged' into future loads that are deemed critical for life support and other operations on Mars. The second is that the components can be adapted to optimize for electrical or heat energy production based on Martian needs. According to *The Journal of the British Interplanetary Society*, each resident (astronaut) on Mars requires anywhere between 1-100 kW capacity each¹⁰ and for a complete Mars settlement a 10 MW supply system is more realistic. For the purpose of this analysis, we estimate an already sizeable settlement with habitat and all life support supports that taps on 10% of the 10 MW supply.

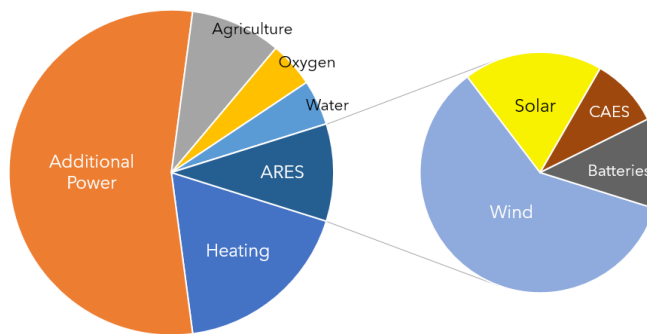


Figure 2.3: Energy demand of a future Mars settlement

As can be seen, additional power for a full Martian settlement requires much more power than can be adapted from the current ARES design. This can come in the form of external sources, namely nuclear energy or geothermal. From this, we can also define a key competitive advantage of our system. Other demands, such as heating and agriculture can use waste heat streams from the CAES system, which is not doable with nuclear sources, such as the ongoing NASA projects and Kilopower mentioned as competition.

The system encompasses a consortium of renewable energy sources that can also exist independently to be integrated with other modular components, such as a nuclear energy source aboard a Mars rover¹¹. Thus, each subsystem possesses their own scientific and economic worth. For instance, the design for the compressed air energy storage system maybe utilised with another Habitat design, without the wind or solar energy sources, but to a geothermal site. Thus, a good recommendation in future market analysis of this project is to delineate the opportunities of each subsystem, as a single value cannot clearly characterise the value and assets of the energy system and its company as a whole.

¹⁰<https://www.forbes.com/sites/brucedorminey/2016/09/30/why-geothermal-energy-will-be-key-to-mars-colonization/#4ca7d6824b25>
[Cited 30 June 2020]

¹¹<https://mars.nasa.gov/mars2020/spacecraft/rover/electrical-power/> [Cited 15 June 2020]

3

Sustainability Approach

With the aim of the mission to provide *renewable* energy to a Mars habitat, the importance of a sustainable design for this project is already highlighted. Nonetheless, sustainable engineering goes beyond generating sustainable energy. Following the ISO 82 Guidelines, sustainability consist of three components: environmental sustainability, social responsibility and economical sustainability¹. If the design complies to these principles, it can be classified as a sustainable design.

For this stage of the design, the focus lays at the environmental sustainability of the system, on which is elaborated in section 3.1. The social responsibility and financial sustainability of the project are discussed in section 3.2 and 3.3 respectively.

3.1. Environmental Sustainability

Environmental sustainability is sustainability in the way that the word is most commonly used in everyday language. It includes the minimisation, and preferably elimination, of waste creation and use of non-renewable resources. For this, the products life time is normally split up in three stages: production, operation and end-of-life. Through all these three stages, minimisation of waste and use of non-renewable resources should be watched.

At the start of the project, several requirements, found in chapter 5, are set up by the stakeholders and the team to ensure the environmental sustainability of the design. First of all, no nuclear energy should be used, as the waste of the process is extremely harmful to the environment and to dispose it in a responsible manner requires a lot of effort, let alone on a planet untrodden. Furthermore, the impact of the design on the Mars during installation and operation as well as on Earth during production should be minimised. This is among others done by researching the possibility to make use of as many as possible resources on Mars. Also, the possibility to retire the (sub)system in a sustainable manner is considered. From a sustainable perspective, a products life cycle would ideally be converted from a linear life cycle to circular one, by revitalising the product after-life into a new phase. Lastly, during the design phase, the minimisation of the amount of launches needed for the system to arrive on Mars is kept in mind, as this leaves a big impact on the Earth as well as Mars environment.

During the first steps of the design phase, all of these requirements are taken into account by the development of the concepts, which again are tested on their sustainability aspect in the subsequent trade-offs. More can be read about this in the Midterm Report [24].

In this report, for all the subsystems, a closer look is taken at their specific sustainability aspects and bottlenecks, which are included in their respective chapters. Furthermore, thought has been put into the retirement of each subsystems: whether it would be able to be recycled or reused on Mars, or should be recycled, reused or disposed on Earth. This is also found in the respective chapters of the subsystems. For the primary energy system, a concise Life Cycle Assessment (LCA) is executed. The LCA makes use of a cradle-to-gate approach and consists of all resources needed to produce the wind energy system on Earth. The LCA can be found in chapter 17. Finally, to make sure the production of the system will also be set in motion in a way that is as sustainable and efficient as possible, the first thoughts have been put in a plan for lean production. This can be found in chapter 19.

3.2. Social Responsibility

Social responsibility is build on the following seven key principles: accountability, transparency, ethical behaviour, respect for stakeholder interests, respect for the rule of law, respect for international norms of behaviour and respect for human rights². As these affects the continuation of the project, all these aspects of social responsibility are ensured during the project. Also, the public perspectives on creating a habitat on Mars can be within controversial margins, hence it is key to ensure public opinion of the team and purpose, to remain on good terms, especially when the project is funded by governmental bodies and commercial financiers.

¹https://iso26000.info/wp-content/uploads/2016/04/ISO_Guide_82_2014E_new_format.pdf

²<https://asq.org/quality-resources/iso-26000>

3.3. Financial Sustainability

A financial sustainability plan describes financial goals, strategies and actionable steps to mitigate financial risks on the short and long term. In this stage of the project, the first steps to get a better view on the projects finances are taken. A market analysis is performed, as can be read in the previous chapter, researching the market potential of the project. Furthermore, for every subsystem a cost estimation is done based on previous projects or literature, which can be found in their belonging chapters. During further design phases, these should be frequently analysed and adjusted in order to make sure the project will continue to be financially healthy.

Technical Risk Management

Risk is defined as the "*probability of an undesired outcome*" and risk management is "*the set of techniques for controlling the uncertainty in a project*". [76] Risks are inherent to any innovative development project that does not follow the me-too philosophy. Judging by the nature of the project, high risks are expected from the first stage. These involve risks related to the project, which are discussed in this chapter and failure mode analysis (FMA) for each subsystem discussed in the respective chapter.

The risk management method is a six-step approach as introduced by Nolberto [79]:

1. *Identification of threats/failure modes*: at this point only the threats/failure modes, but not the risks.
2. *Evaluate threats/failure modes*: in order to assess the risk, the likelihood and impact of each individual threat/failure mode has to be determined. The score definition can be seen in table 4.1. Once, these two parameters are known the risk is given by $\text{Risk} = \text{Likelihood} \cdot \text{Impact}$. The severity of a risk is divided into four categories: low, moderate, high and extreme (table 4.2).
3. *Generate risk matrix* with the identified threats/failure modes and the risk associated with each.
4. *Establish mitigation measures* and guidelines to deal with the risks.
5. *Reevaluate likelihood and impact* of each risk and assess how the severity changed.
6. *Generate risk matrix* after mitigation with the revised likelihood and impact scores.

Table 4.1: Score definition of likelihood and impact

Score	Likelihood	Impact
1	Rare	Negligible
2	Unlikely	Minor
3	Possible	Moderate
4	Likely	Significant
5	Certain	Severe

Table 4.2: Severity of risks

Risk score	Severity
1-3	Low
4-6	Moderate
8-12	High
15-25	Extreme

The top-level threats to the project are detailed in table 4.3. First of all, the project is subjected to numerous external parties, such as the Rhizome habitat project or the project may be discontinued if renewable energy is not deemed suitable for Mars mission by these parties. These threats have a tremendous impact, but the risk associated with it has to be accepted as this cannot be influenced.

The launcher which would transport the energy system to Mars also poses certain threats. This is beyond the scope of the project and is outsourced to a launcher company as usual in aerospace industry. Thus, *LA-1 - LA-3* are outside the reach of this group. On the other hand, *LA-4* and *LA-5* can be mitigation by reducing their likelihood by thorough research. The same applies for the transportation threat: these are the responsibility of the launcher company. The risks related to ISRU can be avoided by thorough research and missions to explore the landing site.

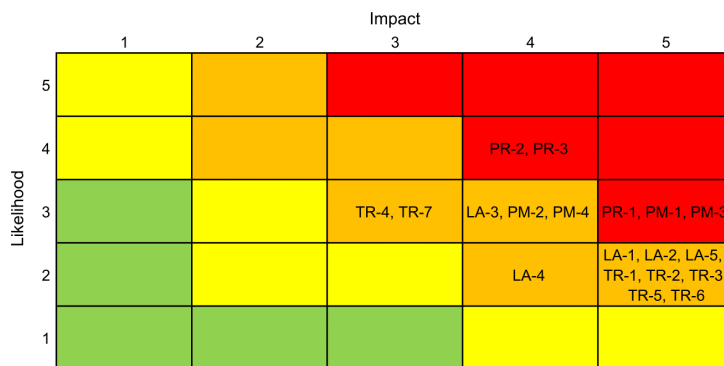
Table 4.3: Top-level risk assessment

ID	Risk description	Likelihood	Impact
PR-1	Project is discontinued	3	5
PR-2	Top requirement(s) change substantially	4	4
PR-3	Project delayed	4	4
LA-1	Launcher fails due to a technical failure	2	5
LA-2	Launcher program cancelled	2	5
LA-3	Launcher program postponed	3	4
LA-4	Unit cannot be integrated in launcher prior to launch	2	4
LA-5	Unit does not survive launch loads	2	5

Continued on next page

Table 4.3: Continued from previous page

ID	Risk description	Likelihood	Impact
TR-1	Launcher cannot reach orbit around Earth	2	5
TR-2	Launcher cannot escape orbit around Earth	2	5
TR-3	S/C cannot enter Martian orbit	2	5
TR-4	Landing module cannot locate landing site	3	3
TR-5	Landing module disintegrates during descent	2	5
TR-6	Landing module crashes upon landing	2	5
TR-7	Landing module performs a hard landing	3	3
PM-1	Materials cannot be collected on Mars	3	5
PM-2	Materials are not as abundant as expected	3	4
PM-3	Water ice cannot be sourced on Mars	3	5
PM-4	Water ice are not as abundant as expected	3	4

**Figure 4.1: Risk matrix of top-level risks before mitigation**

The revised likelihood and impact scores can be seen in table 4.4. Asterisk (*) after the ID means that the score did not change for that risk as it cannot be mitigated due to the reasons mentioned before. The severity risks that are under the control of this group are reduced to moderate after mitigation and the mitigation measures are:

- **LA-4:** Several dress rehearsal shall be held during the design phase and close contact to be maintained with the launcher company.
- **LA-5:** Vibrational analysis and testing shall be conducted during the design phase to validate the structural integrity of the energy system during transportation.
- **PM-1/2/3/4:** The group suggests to send an orbiter and a rover to the landing location to determine the exact geological composition and the water ice content of the ground.

The risk matrix can be seen in figure 4.1. As one can observe, all of the are either extreme or high. This is expected as at this stage of the project, the uncertainties are high and the impact of any of these are extreme. Thus, mitigation is needed for the risks that can be mitigated.

Table 4.4: Revised likelihood&impact scores of the project after mitigation

ID	Likelihood	Impact	ID	Likelihood	Impact
PR-1*	3	5	TR-3*	2	5
PR-2*	4	4	TR-4*	3	3
PR-3*	4	4	TR-5*	2	5
LA-1*	2	5	TR-6*	2	5
LA-2*	2	5	TR-7*	3	3
LA-3*	3	4	PM-1	1	5
LA-4	1	4	PM-2	1	4
LA-5	1	5	PM-3	1	5
TR-1*	2	5	PM-4	1	4
TR-2*	2	5			

5

Project Objectives and Requirements

5.1. Project Objectives

The DSE team 23 is tasked with designing a renewable energy system for a Mars habitat. This system was supposed to provide a continuous renewable energy supply of 10 kW to a Mars habitat. This mission is supposed to last 5 martian years and needs to power the construction of the habitat as well as the astronauts living in the habitat once it is built. The Mission Need Statement and Project Objective Statement for this are found below.

Mission Need Statement: To provide a continuous renewable energy supply of 10 kW to a Mars habitat.

Project Objective Statement: Design a renewable energy supply system, primarily focusing on wind energy, which provides 10 kW to a Mars habitat, by 10 students in 10 weeks.

5.2. Requirements

This section details all the requirements for the design of the system. Many higher level and stakeholder requirements originate from the market analysis of the system while others are derived from those. Sustainability also plays a large role in requirements and design decisions. The full list of requirements is present in table 5.1.

Most of these requirements have already been presented in the baseline report [25], however some changes and additions have been made since then. There are a few requirements that have a strike through, meaning they have either been removed or replaced by a new requirement.

Starting with requirement REM-NRG-01, it has been removed and replaced by REM-NRG-12 and REM-NRG-13. This change was negotiated with the stakeholders as it improved the odds of being able to reasonably produce the amount of energy renewably. At night time it is considered that the astronauts would need less power as they would be resting rather than working on experiments or completing other daily tasks. This will be detailed further in the mission operations chapter 8 as well as the chapter on systems performance, chapter 9.

Furthermore, requirement REM-Sys-N02-10 is removed and replaced by REM-Sys-N02-12 and REM-Sys-N02-13 as these two speeds are different and needed their own requirements.

Finally, requirements REM-Sys-N05-01, REM-Sys-N06-02, REM-Sys-N06-03 and REM-Sys-N06-04 have been removed as they are not directly relevant to the project in its current state.

Any left over TBD's belong mostly to requirements that are not directly relevant to the design as of yet and would need further research to come up with. They would thus be filled in later along in the project if it were to be continued.

Table 5.1: Requirements List

Requirement ID	Description
Energy Requirements	
REM-NRG-01	Energy system shall provide a continuous power output of 10 kW.
REM-NRG-12	The energy system shall provide a continuous power output of 10kW for 14 martian hours per sol.
REM-NRG-13	The energy system shall provide a continuous power output of 5kW for 10 martian hours per sol.
REM-NRG-02	The primary energy system shall be based on wind energy.
REM-NRG-03	The primary energy system shall provide more than 50% of the power output of the entire energy system.
REM-NRG-04	The energy system shall be designed for a lifetime of 5 Martian years.

Continued on next page

Table 5.1: Continued from previous page

Requirement ID	Description
REM-NRG-05	The power management system shall have an energy storage system.
REM-NRG-06	The power management system shall have a power distribution system.
REM-NRG-07	The location of the habitat and its energy system shall be jointly decided by the external Mars habitat project team and the DSE team.
REM-NRG-08	The system shall withstand an impact of [TBD] N m ⁻¹ by flying particles during dust storms.
REM-NRG-09	The system shall withstand wind speeds up to 30 m s ⁻¹ for 4 Martian months.
Primary Energy System Requirements	
REM-Sys-N02-01	The primary energy system shall have a maximum mass of 200kg.
REM-Sys-N02-02	The primary energy system shall have a cut-in wind speed of 7 m s ⁻¹ .
REM-Sys-N02-03	The primary energy system shall have a cut-out wind speed of 35 m s ⁻¹ .
REM-Sys-N02-04	The wind-energy system shall have a nominal operational wind speed of [TBD] m/s.
REM-Sys-N02-05	The tether shall withstand a tether force of up to 11250 N.
REM-Sys-N02-06	The tether shall have a creep SSL longer than the mission duration.
REM-Sys-N02-07	The tether shall have a bending fatigue SLL longer than the mission duration.
REM-Sys-N02-08	The ground station total mechanical-to-electric power efficiency at nominal wind velocity shall be above 90 %.
REM-Sys-N02-09	The ground station generator shall be rated at 80 kW.
REM-Sys-N02-10	The ground station motor shall support a reel-out and reel-in speed of [TBD] m/s.
REM-Sys-N02-12	The ground station motor shall support a reel-out speed of 8 m/s.
REM-Sys-N02-13	The ground station motor shall support a reel-in speed of 25 m/s.
REM-Sys-N02-11	The ground station shall be able to power the motor with 18.5 kW.
Secondary Energy System Requirements	
REM-Sys-N12-02	The secondary energy system shall have a maximum mass of 550 kg.
REM-Sys-N12-03	The secondary energy system shall have a maximum volume of 1 m ³
REM-Sys-N12-04	The secondary energy system shall provide less than 50% of the total power.
REM-Sys-N12-05	The secondary energy system shall have a life-time of more than 5 Martian years.
REM-Sys-N12-06	The dust removal percentage shall be more than 90%
REM-Sys-N12-07	The axis-system shall maintain an accumulative sun tracking error of less than 1% per sol
Energy Storage System Requirements	
REM-Sys-N05-01	The energy storage system shall have an energy capacity able to sustain solely life support functions for [TBD] time.
REM-Sys-N05-02	The seasonal energy storage system shall have an energy capacity of 13.1 MWh.
REM-Sys-N05-03	The combined energy storage system shall have a rated power of 10 kW.
REM-Sys-N05-04	The components of the total energy storage shall have a maximum mass of 1500 kg.
REM-Sys-N05-05	The energy storage subsystem should make use of ISRU storage options by at least 70%.
REM-Sys-N05-06	The seasonal storage system shall have a compression efficiency of at least 70%.
REM-Sys-N05-07	The seasonal storage system shall have a storage efficiency of at least 96%.
REM-Sys-N05-08	The seasonal storage system shall have an expansion efficiency of at least 60%.
REM-Sys-N05-09	The day-to-day energy storage system shall have an energy capacity of at least 117 kWh.
Power Management System Requirements	
REM-Sys-N06-01	The power distribution system shall be able to support a peak power input of 26 kW.
REM-Sys-N06-02	Cable losses between primary energy unit and the combined unit path shall be less than [TBD] %.
REM-Sys-N06-03	Cable losses between secondary energy unit and the combined unit path shall be less than [TBD] %.

Continued on next page

Table 5.1: Continued from previous page

Requirement ID	Description
REM-Sys-N06-04	Cable losses between combined unit and the habitat path shall be less than [TBD] %.
REM-Sys-N06-05	The power distribution system shall have a maximum mass of 400 kg.
REM-Sys-N06-06	The overall efficiency of the power management and distribution system shall be at least 85%.
Mars Environmental Requirements	
REM-MENV-01	No nuclear energy shall be used.
REM-MENV-02	The impact on Mars' environment shall be minimal at end of life.
REM-Sys-M02-01	At least [TBD]% of the material for this system shall be sourced from Mars.
REM-Sys-M02-02	At least [TBD]% of the system materials shall be reused or recycled at end-of-life.
Earth Environmental Requirements	
REM-EENV-01	The impact on Earth's environment shall be minimal.
REM-Sys-E01-01	The generated manufacturing and production waste shall not exceed [TBD] M€.
Launch and Deployment Requirements	
REM-LD-01	The maximum volume for transportation shall be 3 m ³ .
REM-LD-02	The maximum payload shall be 800 kg per flight.
REM-LD-03	The number of flights shall not exceed [TBD] for the system to be deployed and fully operational.
REM-LD-04	The deployment time on Mars shall not exceed [TBD].
Cost Requirements	
REM-COST-01	The cost shall be a maximum of €500 000 for the primary energy unit (excluding costs not directly related to the production of the unit).
REM-COST-02	The mission cost shall not exceed 1150 M€.
REM-Sys-C02-01	Cost per launch and deployment shall be less than [TBD] M€.
REM-Sys-C02-02	Cost per primary energy source shall be less than 0.5 M€.
REM-Sys-C02-03	Cost per secondary energy source shall be less than 10 M€.
REM-Sys-C02-04	Cost of power management system shall be less than 0.7 M€.
Legal Requirements	
REM-LEG-01	The project shall adhere to the legal guidelines established by the resolution 2222 (XXI) of the United Nations General Assembly on space operations.
REM-LEG-02	The mission shall not interfere or preclude the planning or operation of other missions on Mars.
REM-LEG-03	The project shall adhere to the legal guidelines working paper A/AC.105/C.2/L.315 of the United Nations General Assembly on space resource activities.
Integration and Safety Requirements	
REM-IAS-01	Astronauts shall be equipped with all necessary safety gear as established by the American Institute of Aeronautics and Astronautics.
REM-IAS-02	The system's parts and components should be fully replaceable/repairable on site with the existing materials and/or equipment.
REM-IAS-03	The number of maintenance flights shall not exceed [TBD] for the duration of the mission.
REM-Sys-I01-01	The astronauts shall not be exposed to more than 1 Sv of radiation for the duration of the mission.

6

Functional Analysis

In this chapter the reiterated functional flow diagram (FFD) and functional breakdown structure (FBS) can be found. The initial FFD and FBS are developed for the Baseline Report [25]. The FBS can be found in figure 6, where the functions of the system have been broken down into their sub-level components. In figure 6 the FBS can be found, where the aforementioned functions are displayed by their relation, to illustrate the flow of how the system operates.

The FBS has seven top-level functions which are broken up into sub-level functions. These seven functions are:

1. Manufacture payload
2. Transport payload
3. Perform basic energy system integration on Mars
4. Manufacture on-site structures
5. Perform complete system integration on Mars
6. Operate energy systems
7. Perform communication

Each of these functions describes a phase of the development and execution of the system. The sub-level function break these down into separate tasks to show more detail. Note that the functions in the FBS are not per definition in chronological order. The FBS only serves to show the separate tasks which need to be completed. The chronological order follows from the FFD. In the FFD the communication is also captured. This is usually not the case, as the FFD does not depict information flows between systems and software for example. In this case it is added as this type of information flow is important to the functioning of the system and should be accounted for. The moments of communication are part of function 7 and are depicted in the FFD by means of reference points A and B.

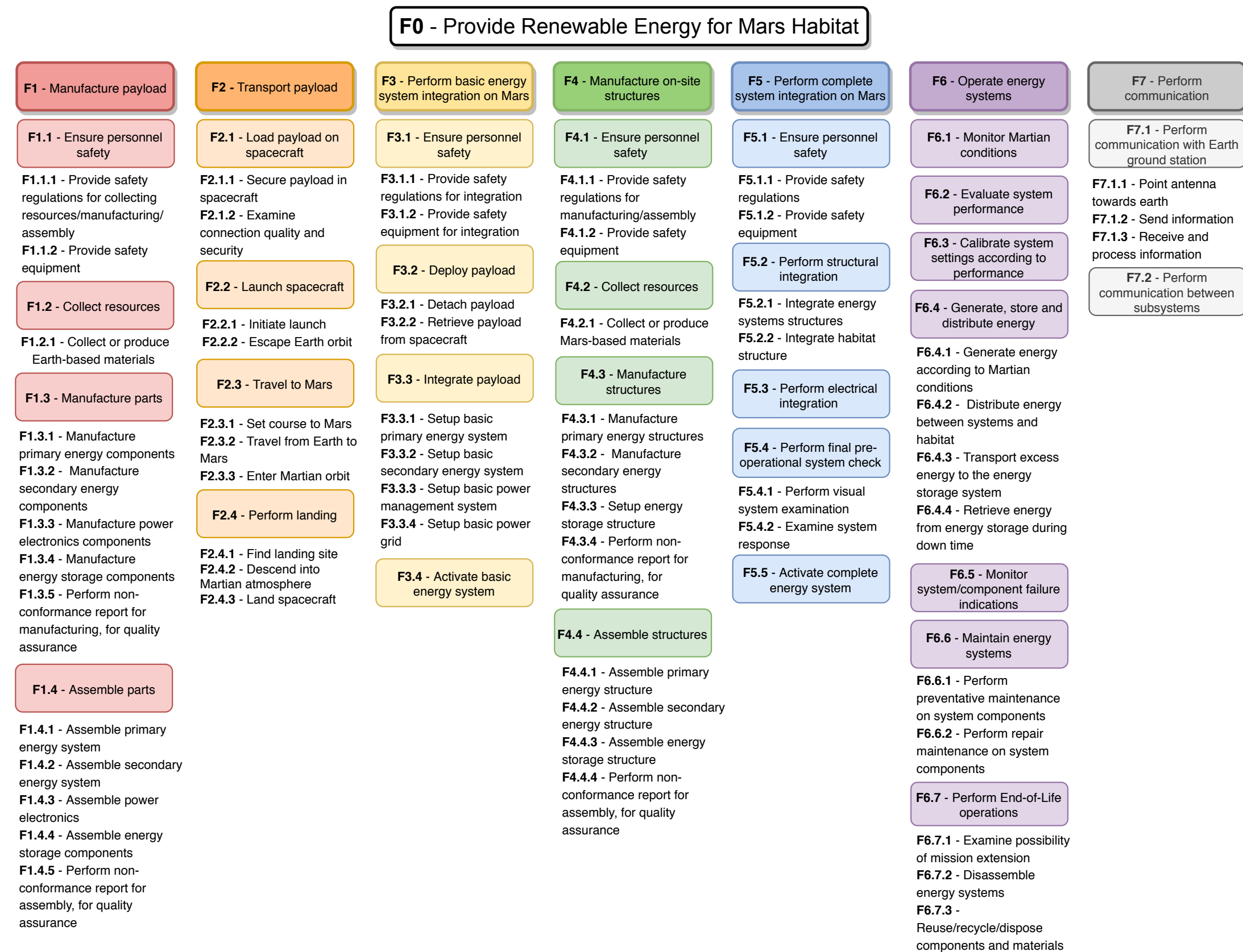


Figure 6.1: Functional Breakdown Structure

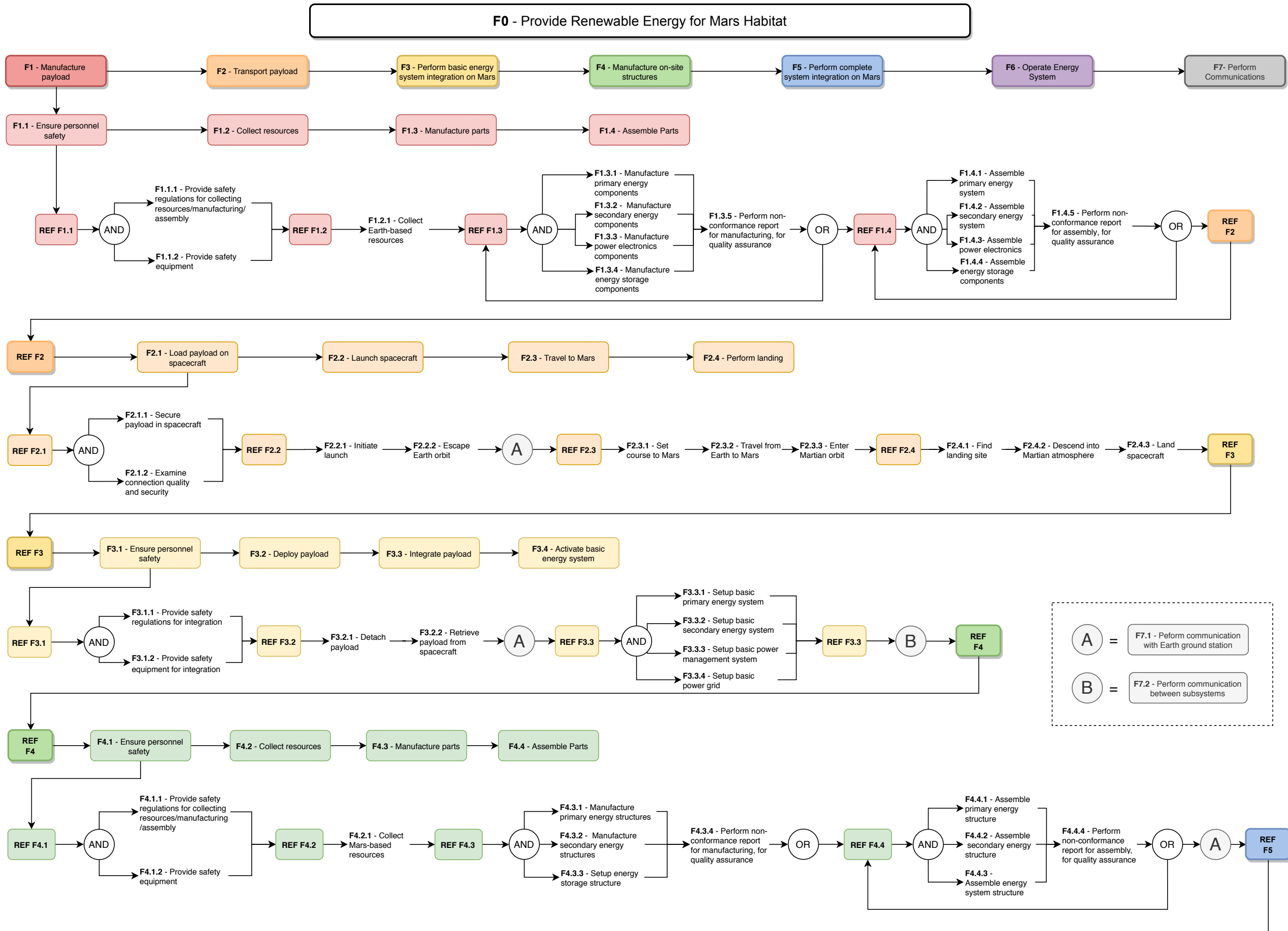
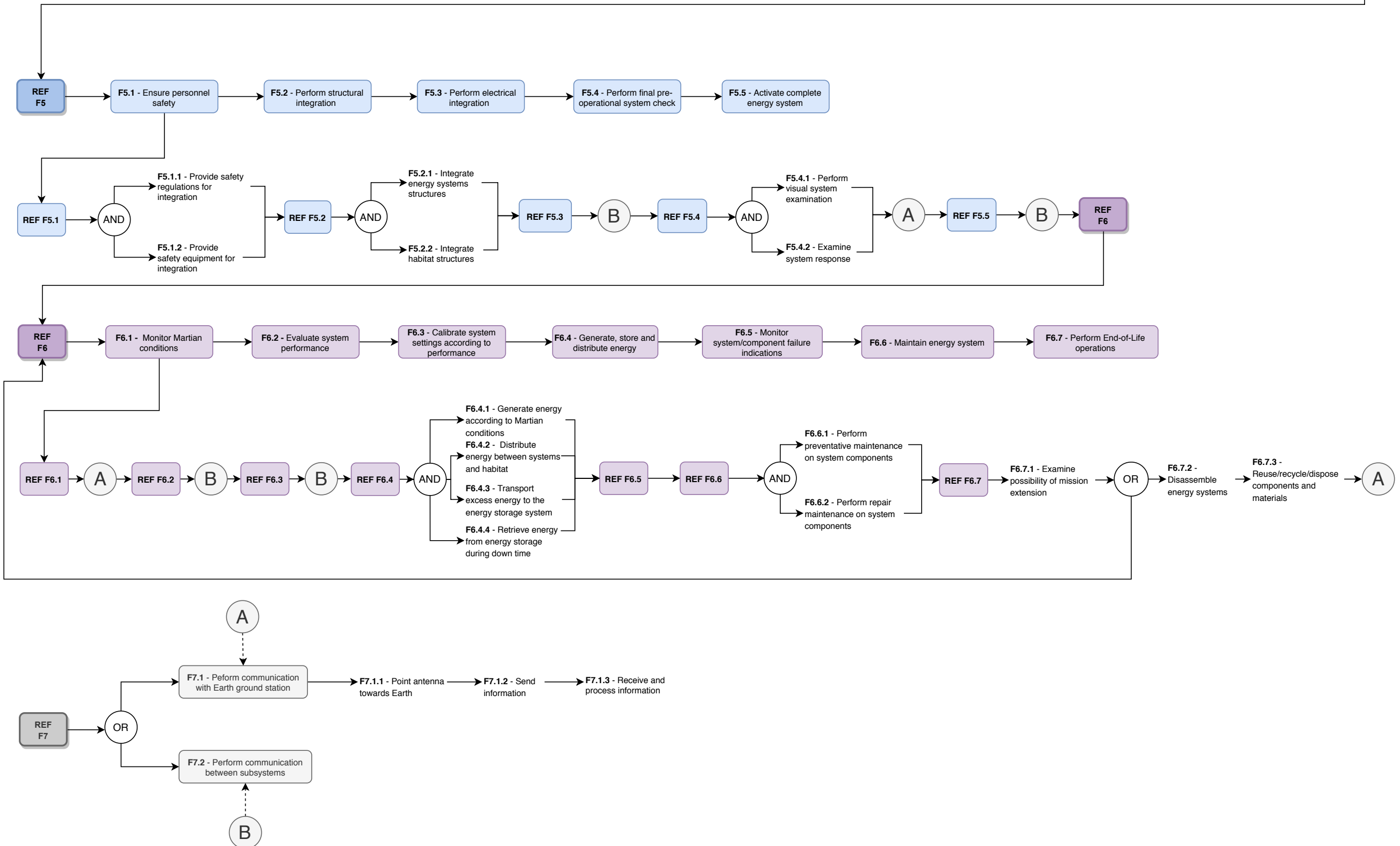


Figure 6.2: Functional Flow Diagram



System Architecture and Interfaces

Before diving deep into the details of every subsystem, an overview of the global system and its interactions will be given. This chapter can always be used to look back on if the system starts to get complex. The first section will focus on the diagram of the entire system and explain an overview of its workings. In the following section a summary table will be presented showing all of the design parameters of the system.

7.1. Diagram of the System Architecture

Figure 7.1 shows the connections and interfaces of all the subsystems as well as with the external factors of the environment, habitat and maintenance system. As can be seen in the figure, there are 5 main systems in the renewable energy system design. These are: the power management system, energy storage system, central control system, solar energy subsystem and the wind energy subsystem. The legend indicates whether the arrows show an energy flow, a command flow or transport and operations actions.

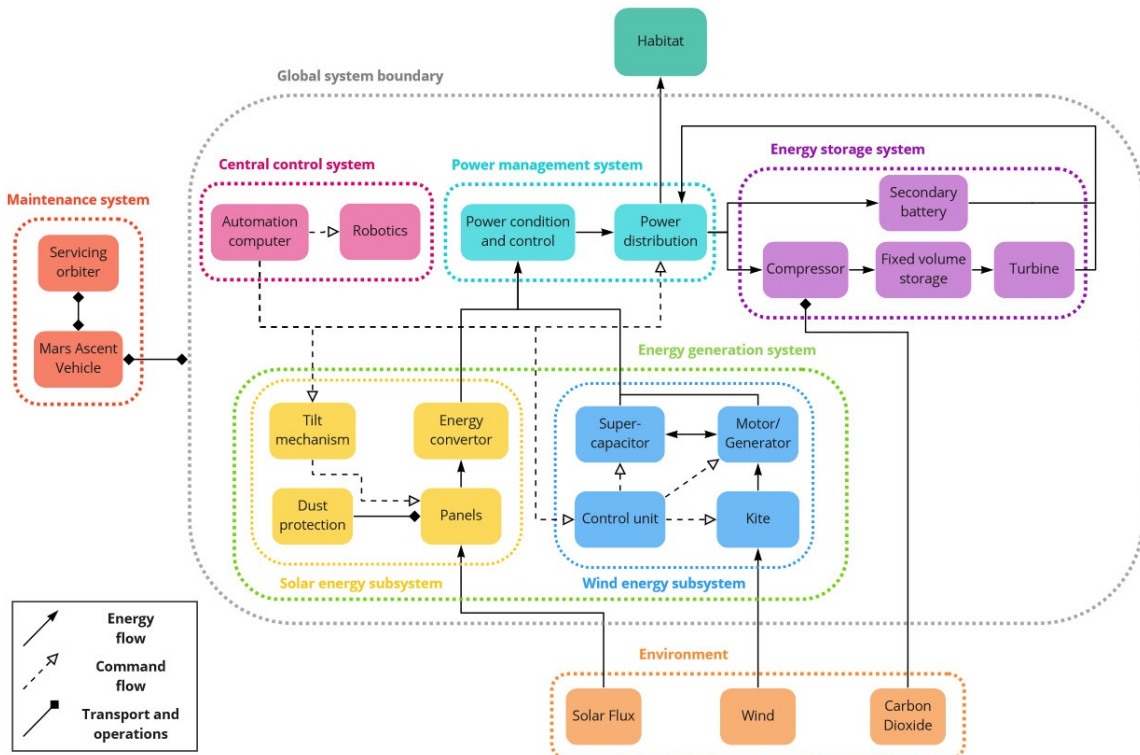


Figure 7.1: Architecture and Interfacing of the entire renewable energy system

Firstly the environment of Mars influences the system and is needed for energy production. Solar flux is used directly by the solar panels to flow through an energy converter which brings the power into the power management system. In addition, the solar energy subsystem also has dust protection and a tilting mechanism used to tilt the panels accordingly to ensure the best incidence angle by the sun rays. The wind's energy is harvested by the airborne wind energy system where a kite is used. The energy then passes through the ground station and into the power distribution unit. In addition, this subsystem also has its own control unit and a super-capacitor.

Since the harvested energy also needs to be transported to the correct locations and stored, power management and storage systems are included in the design. The power management system is central to the flow of energy between energy generators, energy storage units and the habitat, as it ensures efficient flow between each unit. The energy storage system consists of two storage units. One is the day-to-day storage

which acts as a power provider during the night. It will be in the form of secondary batteries, more specifically lithium-sulphur batteries, as will be elaborated upon in chapter 13. The other system is the seasonal storage in the form of compressed air energy storage. It thus includes a compressor and turbine for the carbon dioxide stored in an underground cavity.

For communication flow, the central control system is important. Here communication to other systems originates and commands are given such that the global system functions properly.

Lastly, the maintenance system acts on the global system in order to keep everything maintained and to avoid any tragic failures of the system.

7.2. Summary of the Subsystem Design

This section will provide another overview of the renewable energy system, but this time in the shape of a table and including the main parameters of each system. Table 7.1 shows a global overview of the important factors for each subsystem and as well as some general properties.

Table 7.1: Summary of Design Specifications per Sub-System

Complete System		Total mass system: 2812.4 kg Total volume system: 7.9 m ³ Total cost system: €9 million
Primary Energy System	General Properties	Total mass: 288.1 kg Total volume: 0.669 m ³ Total cost: €68350 Power output: 25 kW
Kite	Wing	Mass: 5.4 kg Volume: 0.006 m ³ Area: 50 m ² Material: Dyneema and Dacron
	Kite Control Unit	Mass: 5.0 kg Volume: 0.025 m ³
	Bridle System	Mass: 2.0 kg Volume: 0.003 m ³
	Pump	Mass: 0.3 kg Volume: 0.001 m ³
Tether		Mass: 12.7 kg Volume: 0.013 m ³ Diameter: 0.0065 m Material: Dyneema DM20 XBO
Ground station	Generator/Motor	Mass: 152.6 kg Volume: 0.119 m ³
	Drum	Mass: 48.3 kg Volume: 0.349 m ³
	Brakes	Mass: 3.0 kg Volume: 0.005 m ³
	Converters	Mass: 24.3 kg Volume: 0.018 m ³
	Spindle	Mass: 25.2 kg Volume: 0.120 m ³
	Super capacitor	Mass: 9.3 kg Volume: 0.010 m ³
Secondary Energy System	General Properties	Total mass: 788 kg Total volume: 0.83 m ³ Total cost: €6 800 000 Power output: 5 kW
PV Panel	GalnP/GaAs/Ge XTE-LILT cells	Mass: 123.2 kg Volume: 0.63 m ³ Area: 70 m ²
Axis system	Azimuth tracking	Mass: 665.1 kg Volume: 0.2 m ³

Continued on the next page

Table 7.1: Continued from previous page

Energy Storage	General Properties	Total mass: 1520 kg Total volume: 6.3 m ³ Total cost: €2 006 500 Total Capacity: 14.12 MWh
CAES	Compressor	Mass: 400 kg Gas: CO ₂ Pressure ratio: 13.5
	Turbine	Mass: 660 kg Pressure ratio: 5.7
	Generator	Mass: 240 kg
	Motor	Mass: 100 kg
	Plug	
	Cavern lining	
Secondary Battery Storage	Lithium-Sulphur battery	Mass: 120.4 kg Volume: 0.1 m ³
		Capacity: 117 kWh
Power Management	General Properties	Total mass: 191 kg Total volume: 0.24 m ³ Total cost: €69800
Cables		Mass: 116.4 kg Volume: 0.10 m ³
	Converters	Mass: 74.8 kg Volume: 0.13 m ³
DC Bus		Voltage: 400 V

Operations and Logistics

This chapter delves into the numerous elements that constitute the mission's operations and logistics. Section 8.1 provides an overview of the main constituent elements for the mission concept, as well as other important considerations pertaining the characteristics of the selected site on Mars. Following this, section 8.2 delves into some of the top-level considerations that need to be considered in the determination of the launching procedures for the ARES mission. Likewise, sections 8.3 and 8.4 list the most important considerations that have shaped the ARES mission design in terms of payload integration, landing, and payload installation on Mars. Finally, section 8.5 will delve into some of the main developments in terms of the system's operations: the concept for maintenance and retirement of the mission has been finalised; a preliminary control architecture for the automated control of the primary energy system is briefly elaborated upon, and an explanation pertaining to the relation between astronaut scheduling and the performance requirements of the system as a whole is presented.

8.1. Mission Configuration and Site Characteristics

Figure 8.1 illustrates an iteration of the first-order concept for the mission configuration that was produced for the midterm report [24]. Moreover, as it was mentioned already in the midterm, the assertion that the following mission configuration is subject to modifications based on future reiterations still applies.

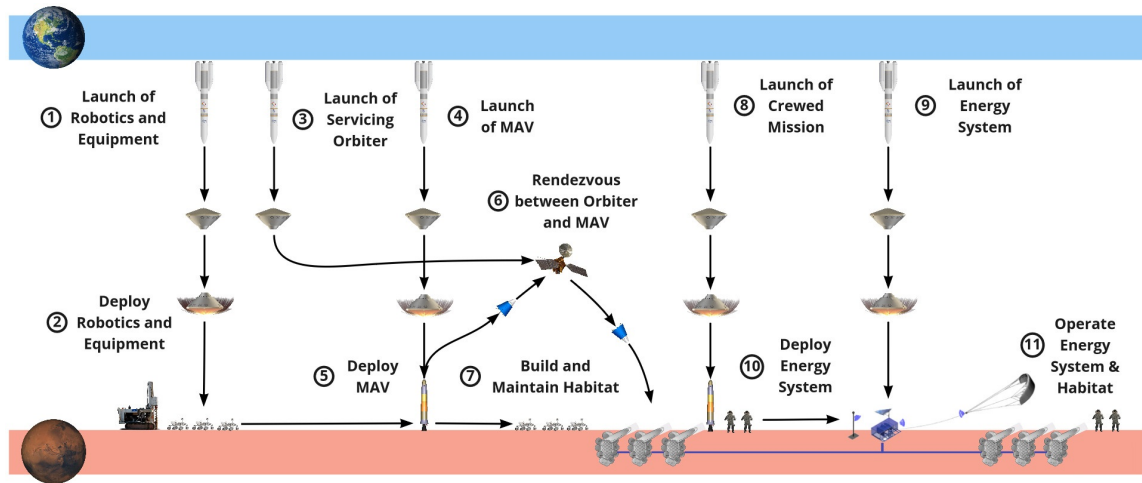


Figure 8.1: Reiteration of the schematic of the mission configuration

From this figure, several important points from the previous mission configuration are still valid, and are summarised hereafter: the mission is designed such that a landing site is ready-for-crew and an operational habitat ready for occupancy prior to any human travel in order to guarantee the mission. This is a key enabling factor that must be fulfilled in order to ensure a sustained human presence on Mars. This ensures that nobody is put into unnecessary danger in trying to install and operate an on-surface station without a proper life support infrastructure; additionally, it improves safety, affordability, and minimises operational risks, as explained by Moses and Bushnell [78]. It was furthermore discussed that tele-operation add a superfluous layer of complexity, due to the 20 minute communication delay between Earth and Mars [78]. For this reason, there is an undeniable need for a high level of automation and Earth-independence to be adapted within the architecture of the mission and its commissioning [75]; at least until the first crewed mission can arrive to the Martian surface.

Following these considerations, the mission will still start by sending the necessary equipment to build the habitat to Mars. A major point of discussion in the development of this mission pertained to the assumption on whether said equipment required the 10 kW continuous power output to be provided by ARES. The biggest challenge is that the current state-of-the-art technology would not provide a sufficient degree of reliability

to not only operate, but also to deploy and maintain a system of such complexity without human input. A paradoxical roadblock thus appeared: a crewed mission would rely on the equipment being able to construct a ready-for-occupancy habitat, while said equipment would require a power system that could only be set in place by humans. For this reason, it was assumed that the equipment would be able to fulfil its function with an independent power system. As soon as said independent power system is producing sufficient energy to power the construction equipment, the habitat can start to be built.

Next, the servicing orbiter and Mars Ascent Vehicle will be sent to the Martian Surface. The details and motivation for the selection of this concept for maintenance is further explored in subsection 8.5.1. Once the habitat and life support infrastructure has been constructed, the first crewed mission will be able to land on the Martian surface. With this, the renewable energy system (ARES) will be ready to launch, and will have to possibly be launched simultaneously with the crewed mission. The main reason for this is that since humans are required for the installation and operation of the system, the two launches will have to occur in parallel.

After both the crew and the ARES cargo have landed, the crew vehicle will have to provide life support to the astronauts while the energy system is installed and initiated. As soon as ARES is producing sufficient energy to power the habitat and the life support, the habitat can be occupied, and the colonisation on Mars will officially be a reality.

8.1.1. Site Characteristics

The following section will discuss some important considerations for the specification of the rest of the mission logistics. Deuteronilus Mensae (39.11°N , 23.199°E) was selected to be the landing site after a thorough trade-off [24]. The location is excellent in all aspects that makes the mission successful: the area provides rich scientific objectives, contains samples from all three major geological eras, abundant stores of water ice, offers great opportunities for In-Situ Resource Utilisation (ISRU) and Civil Engineering¹. The location of the site can be seen in figure 8.2.

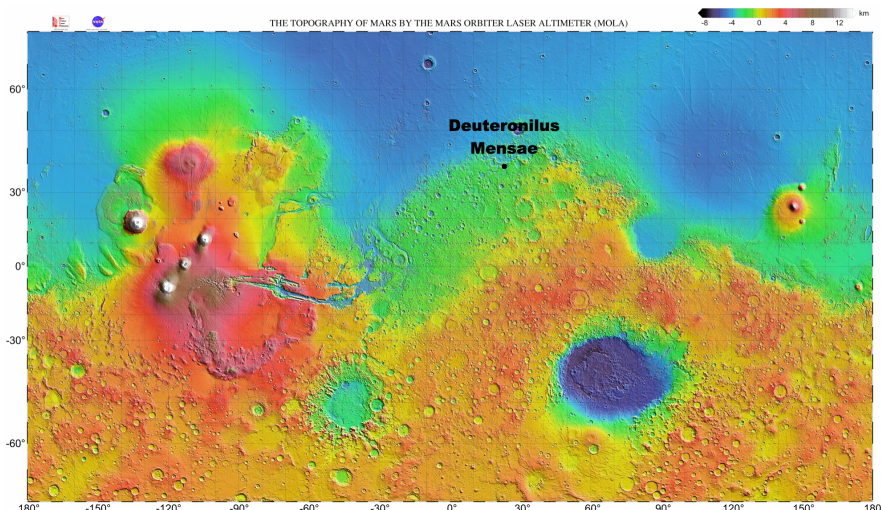


Figure 8.2: Location of Deuteronilus Mensae on the MOLA map²

The presence of water ice at the location has long been suspected due to the lobate debris aprons (LDA) nearby. These surface features are 100s of m thick masses ranging 10s of km. As concluded by Squyres [92] amongst many others, LDAs contain water ice. Later, SHARAD, a subsurface radar sounder, onboard MRO showed that high-grade, high concentration of continuous water ice located in 10-15 m from the surface [82]. This can not only be utilised as a resource for the habitat, but also has scientific implication: LDAs and lineated valley fill are suspected to be the remnants of cold-based glaciers, which were covered by debris and could not sublime [52].

Moreover, there are six regions of interest (ROI) for scientific research at Deuteronilus Mensae, which can be seen in figure 8.3. As one can observe majority of the area at an altitude of -4 km or below, which is advantageous for entry, descent & landing (EDL). The landing site is located at the white star in figure 8.3 and 8.4 as also suggested by the NASA site selection workshop¹.

The regions of interest are³:

¹<https://www.hou.usra.edu/meetings/explorationzone2015/pdf/1033.pdf> [Cited 9 June 2020]

²[https://commons.wikimedia.org/wiki/File:Mars_topography_\(MOLA_dataset\)_HiRes.jpg](https://commons.wikimedia.org/wiki/File:Mars_topography_(MOLA_dataset)_HiRes.jpg) [Cited 9 May 2020]

³https://www.nasa.gov/sites/default/files/atoms/files/exploration_zones_briefing_naochis_terra_deuteronilus_mensae_and_phlegra_dorsa_tagged.pdf [Cited 10 June 2020]

- *ROI 1*: characterised by the uplifting of a Noachian-aged crater central peak exposing deeper crustal material; latitude-dependent mantle (LDM) deposits that expose climate record and potentially water resource
- *ROI 2*: base of LDA with water ice history record; rock material which include Noachian and Hesperian samples
- *ROI 3*: 10s of m thick LDM containing Amazonian climate record and nearly pure ice; cliff face from Noachian-Hesperian volcanic for stratigraphic investigation
- *ROI 4*: distinctive LDA glacial ice record; peak ring of Noachian-aged crater and Noachian-Hesperian volcanics
- *ROI 5*: peak ring of Noachian-aged crater and Noachian-Hesperian volcanics; LDA ice lobe on both sides
- *ROI 6*: LDA ice and climate history; possibly location of ancient lavas; Noachian, Hesperian and Amazonian samples and processes

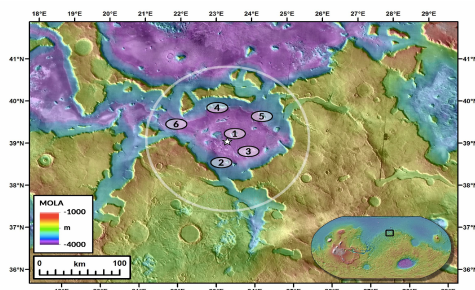


Figure 8.3: Regions of interest in Deuteronilus Mensae region¹



Figure 8.4: Geological map of Deuteronilus Mensae⁴

The circled area in figure 8.4 is approximately 100 by 60 nm and has three main surface features: HNPs (blue) and NPlsu (red), Ada (beige). Majority of the region is covered by smooth plains material (HNPs) from Early Hesperian to Late Noachian. These are relatively featureless lands with some scattered clusters of small circular or irregular knobs. The size and the lack of surface obstacle are in favour of landing and makes traversing easy. Sparsely, there are also upper smooth plateau materials (NPlsu) from Middle Noachian or older. These are portions of continuous cratered highlands modified by impact cratering and minor fluvial activity. This implies that these regions are hard to approach and traverse, thus not making it suitable for the habitat nor the energy generation units. LDAs located on the skirt of the region are made up of debris apron material from Middle to Early Amazonian. This is the region where the previously described ice is located as the remnant of glaciers⁴.

Two elements are indispensable for life: water and energy. As detailed earlier, water ice is abundant at Deuteronilus Mensae. This supports human life and may contain evidence of life on Mars, thus the scientific significance of the site cannot be neglected. The energy aspect is going to be elaborated on in sections 11.3 and 12.3. Furthermore, the site satisfies EDL requirements being located at an elevation of -4 km⁵ and the geological features allow for ISRU and Civil Engineering opportunities.

8.2. Launching Procedures

The definition of the launching procedures for a Mars mission follow straightforwardly from the basic requirement that transfer energy should be minimised as much as possible. This is implicitly specified by user requirement **REM-LD-03**:

Table 8.1: Requirements on launching procedures

Requirement ID	Description
REM-LD-03	The number of flights shall not exceed [TBD] for the system to be deployed and fully operational.
REM-Sys-C02-01	Cost per launch and deployment shall be less than [TBD] M€.

⁴<https://astropedia.astrogeology.usgs.gov/download/Mars/Geology/year-2000/Mars-Geologic-Map-of-MTM-35337-40337-and-45337-Quadrangles-Deuteronilus-Mensae-Region.pdf> [Cited 10 June 2020]

⁵https://marsnext.jpl.nasa.gov/workshops/2014_05/05_LSW1_EDL_Eng_Constraints_v6.pdf [Cited 10 June 2020]

The number of launches directly depends on the available launcher performance in terms of mass and volume that can be transported to Mars, as well as the REM-Sys-C02-01). To maximise the chances of meeting these requirements, special attention must be paid in defining an optimal transportation strategy to ensure that the transfer energy is minimised. The theoretical optimum occurs when departure from Earth and arrival at Mars occur in conjunction. For this, a Hohmann transfer is used, which is based on a departure from Earth and arrival to Mars when both planets are on opposite sides of the sun.

In addition to this, the optimal launch dates for minimum departure energy must be clearly defined, which occur every synodic period. According to Burke et al. [18], the synodic period is the time required for any phase angle to repeat, which for Mars with respect to the Earth is 779.935 Earth days (approximately 2.14 years).

With these two major considerations taken into account, the next step is to select the launch vehicle that is best suited for the ARES system. Since the context and concept for this mission are quite novel, it is nor possible nor logical to make a fixed selection on the launch vehicle. This is mainly due to the fact that the development of launch vehicles for Mars missions is a current trend within the industry; for this reason, the most reasonable strategy for this is to rely on assumptions on the launch vehicle capabilities, based on the design goals of the main launch vehicle manufacturers. As an example, SpaceX's Starship is aiming towards enabling launches of up to 100 mT to the Martian surface [32]; this not only would enormously alleviate the mass constraints currently imposed on the ARES payload, but it could possibly increase the affordability of the concept tremendously.

8.3. Payload Integration

Payload integration in the launching vehicle is one of the most driving factors to fill the gap between conceptual and actual design. User requirements REM-LD-01 and REM-LD-02 set important constraints to the payload integration of the ARES system:

Table 8.2: Requirements on payload integration

Requirement ID	Description
REM-LD-01	The maximum volume for transportation shall be 3 m ³ .
REM-LD-02	The maximum payload shall be 800 kg per flight.

The sensitivity analysis and compliance matrix found in chapter 20 address these requirements on a more detailed extent. At this stage of the design, however, it is not straightforward to increase the amount of detail in the specification of the payload integration within the launching vehicle. One of the main reasons for this is that since the launching vehicle is not a fixed choice, the payload integration cannot be fully specified.

It is possible, however, to provide some context into the considerations that must be taken into account to ensure an adequate payload integration within the launching vehicle. For the sake of clarity and brevity, only a set of requirements that follow from manufacturers of launching vehicles will be included [31], to serve as a starting point for the next steps of the design, during which the payload integration should be looked at in more detail:

Table 8.3: Payload integration requirements as specified by the Falcon 9/Heavy User Manual [31]

Customer Deliverables	Description
Payload safety data	Provides detailed payload information to support SpaceX generation of range safety submittals, requirements tailoring and launch operations planning. Includes hazard analyses and reports, vehicle break-up models and detailed design/test information
Finite-element and CAD models	Used in coupled loads analyses and compatibility assessments. Specific format and other requirements are supplied during the mission integration process
Environment analysis inputs	Payload inputs for SpaceX environment analyses. Includes payload thermal model and others, as required
Environmental test statement and data	Defines the payload provider's approach to qualification and acceptance testing, including general test philosophy, testing to be performed, objectives, test configuration, methods and schedule. Actual test procedures are not required. Specific qualification and acceptance test data may be required prior to launch to demonstrate compatibility with the SpaceX launch service

8.4. Landing and Set-Up

To guarantee a successful landing, the mission has to address many challenges; these include a very short time window in which all entry, descent, and landing (EDL) procedures must be performed, extremely limited communication capacity due to the delays, as well as very limited aerodynamic braking capabilities due to the low air density of the Martian atmosphere. Besides this, surface hazards such as large boulders, craters, and even dust storms can potentially jeopardise the integrity of the system.

For a mission such as ARES, in which a manned lander will be sent to the Martian surface, special attention must be paid to ensure the safety and integrity of both crew and cargo. In order to be able to land large masses, several parameters must be taken into consideration in the future development of the EDL strategy of the ARES mission, such as the diameter of the aeroshell, parachute and ballistic coefficient [14].

Just as for the launching vehicles, many manufacturers are currently exploring new possibilities to ensure that landing a mission like ARES on Mars will not only be possible, but also affordable, reliable, and safe. According to Biswal and Annavarapu [14], for a successful soft-landing with the readily available technology, the following requirements must be fulfilled:

- Masses should lie between 0.6 to 0.9 ton.
- Ballistic coefficient should be $<35 \text{ kg m}^{-2}$.
- The diameter of aeroshell should be $<4.6 \text{ m}$ (70°spherical cone aeroshell).
- The parachute diameter should be limited to $< 30 \text{ m}$ with Mach 2.7 disk-gap band parachute.
- Need to use supersonic retro propulsion systems.
- Need to enter the lander from orbit.

As to be expected, these constraints will most likely become less demanding as the technological developments ensue. For this very reason, defining very strict requirements on EDL procedures for the ARES mission does not result logical or necessary.

8.4.1. Deployment and Installation

Table 8.4: Requirements on deployment and installation

Requirement ID	Description
REM-LD-04	The deployment time on Mars shall not exceed [TBD].

Because some of the components of the energy system are manufactured by third parties and partners or purchased off-the-shelf, there are certain considerations that have to be implemented when adapting the system for Martian utility. This section describes how the components integrate as a system to maintain reliable functionality on Mars, the strategies can be divided into each subsystem detailing the main Martian adaptation and methodologies to verify these are detailed below. The deployment time requirement, REM-LD-04, is left undetermined as it is highly dependent on the further research within each subsystem and especially pertaining to site selection and characteristics.

Primary Energy System

Before the system can begin to open its kite and start to function, which is performed manually by the astronauts, the ground needs to be prepared by the rovers. The energy system is then transported by rovers and buried in the ground. This is a key consideration for maintaining the system in place during dust storms. The kite deployment is done by the astronauts and as well as the integration of power cables with the power management system.

Secondary Energy System

The first step would be to deploy the structures for the panels, which are embedded in the ground by drilling. This is done in part by the astronauts, who position the drilling machinery at the considered site, or could possibly be part of a specific rover's functions. Then, the astronauts would have to manually place the solar panels on these structures by screwing. Welding is a more permanent option but needs to be investigated further as temperatures on Mars might not be conducive to this process. Lastly, the astronauts attach the power interface and integrate the grid cables.

A last note is that the solar radiance model considers full sunlight coverage during day, apart from dust storm, which means shadows from interfering elements such as the habitat or the kit and might affect predictions. Thus, the distance between subsystems should have a minimal limit to ensure design compliance and continuous.

Compressed Air Energy Storage System

Before deployment, it is assumed that further investigation is already performed to validate our understanding of the structure and rigidity of the Martian rock mass formation to estimate the maximum volume and pressures (and thus maximum energy stored) that the underground cavern can support. The time frame for this research is approximately 2 years. This is also described in further recommendations in section 13.11.

Parallel to this, as the Rhizome Habitat team progresses in research to gather more information about the type of rock, including the bulk modulus, material density and thermal conductivity, in determining whether the 3D printed in-situ regolith resource can be used as a structurally sound, air-tight inner storage wall filling. If the design is proven feasible, the storage cavern would have to first be prepared by the Habitat team, including additional excavation and structural construction for the cavern walls and plug at the ground surface.

The compressor, turbine and generator systems will be integrated at a later stage by the rovers in conjunction with the astronauts, who work in tandem. The deployment of the CAES system requires multiple detailed steps, as it encompasses the bulk of Martian construction, thermodynamic calibration of components and power management integration of the energy system as a whole. These steps have been greatly condensed in this report, but further extensive deployment procedures will be defined which stems from future studies described above.

Battery System

Because Martian temperatures variate significantly throughout the day, as well as at different seasons, the secondary battery system is to be placed underground. This means that an underground compartment space needs to be dug by rovers, also see figure 13.1. The cable integration is done manually by the astronauts.

Power Management

The cables should be insulated from radiation and significant temperature variance, this led to a design consideration where cables should be placed underground. Firstly, specific rovers are utilised and trenches of approximately 0.75 m wide, stretched between the subsystems, should be dug in accordance to the distances and configuration set in chapter 10. Then, the cables are laid parallel to the trenches and inserted into ground once the layout is set. Finally, the rovers should cover the top with the accumulated dug-out rock mass material, and lightly compressed to avoid wind erosion and unwanted cable exposure. The converters of the system follows a similar procedure, in which the rovers have to account for a increase in trench width at specific points in the grid. The computer interface of the power management system is integrated into the habitat to allow astronaut accessibility and controllability.

8.5. System Operations

As it was mentioned in the midterm report, the system operations must be designed such that there is a guaranteed energy supply even during the most undesired of conditions [24]. Chapter 9 delves into the details of how the system operation is defined in terms of its performance, and analyses the ulterior requirements that will drive the design of the energy generation systems. Additional to this, a plan to ensure that the system can be maintained and decommissioned is set in place:

8.5.1. Plan for Maintenance and Retirement

The Martian environment is known for being very hostile, which poses a potentially major threat to the integrity of the mission. In order to ensure that the system will be able to comply with the life-span requirement of five Martian years (i.e. 9.41 years on Earth), a well-defined maintenance approach must be defined.

For this, two concepts were adapted from other mission architectures to make sure that the associated requirements on maintenance listed on table 8.5. Firstly, a servicing orbiter needs to be present in which in-orbit servicing, assembly, and manufacturing (OSAM) processes can be adapted to this mission to manufacture, assemble, and perform maintenance on larger than payload structures [83]. This not only increases the system's overall redundancy by introducing the possibility of making components on demand, but it also offers a good opportunity for the decommissioning of parts and components that cannot be disposed or re-utilised in the Habitat. This is possible because this concept is adapted from a Mars sample return mission, which also considers the inclusion of a similar orbiter to serve as a gateway between the Martian surface and planet Earth, thus increasing the system's overall reliability. Moreover, it alleviates the constraints imposed on the manufacturing equipment that is needed for the mission (e.g. ability to withstand launch and EDL loads, resistance to radiation and corrosion, low required power, etc.). Additional to this, the inclusion of the necessary on-surface equipment and infrastructure for manufacturing and servicing with local resources is already taken care of by the habitat construction mission, as designed by Bier et al. [13].

Sending a manned mission to Mars sets an implicit need for a space vehicle that is able to not only get

to Mars, but also to safely return back to Earth. One of the most actively explored concepts within the realm of Mars exploration missions is the Mars ascent vehicle (MAV). Fundamentally, the MAV is a space vehicle concept that is able to repeatedly ascend from or descend to the Martian surface from orbit [23, 86, 104]. This concept is currently being explored in conjunction with the Mars transfer vehicle (MTV) which essentially enables the possibility to transfer to or from the Martian Low Orbit (MLO) from or towards Earth. In this way, the MAV plays a major role as the connecting link to make the purpose of the servicing orbiter more evident. By combining the two concepts together, the possibility to have a fully operational on-demand maintenance and decommissioning infrastructure becomes a more feasible concept, thereby increasing the array of options to ensure an adequate sustainability approach in the design of the ARES mission. Following this rationale, the necessity for requirement REM-IAS-03 becomes irrelevant, considering that this requirement was formulated with the assumption that the maintenance flights would require cargo vehicles with the necessary parts and spares to be sent directly from Earth.

Table 8.5: Requirements on maintenance

Requirement ID	Description
REM-IAS-02	The system's parts and components should be fully replaceable/repairable on site with the existing materials and/or equipment.
REM-IAS-03	The number of maintenance flights shall not exceed [TBD] for the duration of the mission.

Table 8.6: Requirements on mission's EOL

Requirement ID	Description
REM-MENV-02	The impact on Mars' environment shall be minimal at end of life.
REM-Sys-M02-02	At least [TBD]% of the system materials shall be reused or recycled at end-of-life.

8.5.2. Automated Operation of the Primary Energy System

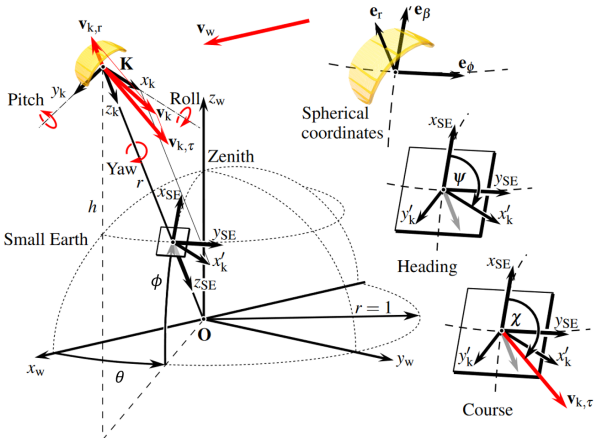


Figure 8.5: Reference frame of AWE system

In order to achieve some degree of automated operation for the primary energy system, a preliminary control architecture must be defined. This not only provides insight on how the kite moves in the air, but also on what the role is of each of the different elements of the control system.

For this, the reference frames that are used in the definition of the control structure are presented in figure 8.5. From this picture, a few important parameters can be distinguished: first, the origin **O** is located at the attachment point to the ground station; next, a spherical frame, denoted Small Earth, is defined by the elevation and azimuth angles (ϕ and θ respectively) at unit radius. On the plane tangent to the Small Earth frame, the local frame x_{SE}, y_{SE}, z_{SE} is defined as the North, East, Down (NED) frame. In this frame, the heading and course angles (ψ and χ respectively) are defined.

Assuming a fully tensioned tether with no sag, the pitch and roll of the kite are kinematically coupled to the angular velocity of the kite, defined by $\omega = v_{k,r}/r$. The tangential velocity of the kite is in turn described by the course angle χ , and its rate of change (yaw rate, denoted by $\dot{\chi}$) which are controlled by the actuation system of the kite. Figure 8.6 illustrates the control architecture of the automated kite control unit (KCU), which was adapted from a concept developed by Fechner and Schmehl [44].

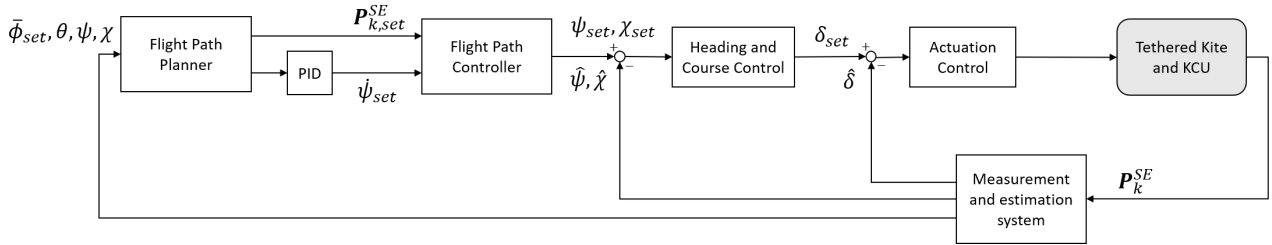


Figure 8.6: Control feedback structure for the automated control of the AWE system

As it can be observed, the kite steering mechanism is controlled by a flight path planner (FPP), which takes a set value for the average elevation angle, as well as the measured azimuth, heading, and course angle. From this the FPP determines whether the kite is flying towards a so-called attraction point (i.e. it sets the coordinates of the attraction point $P_{k,SE}$), or whether it should make a turn of a specified radius (i.e. it sets a specified value for the turn rate of the kite $\dot{\psi}_{set}$). Besides this, the FPP also takes into account the input of an optimiser that maximises the power while meeting basic safety guidelines, as well as a supervisory control system that enables the system to react to a changing wind field. For the sake of simplicity, the complete internal control architecture of the FPP is not shown in figure 8.6 and is instead illustrated as a single block.

Based on this, the flight path control (FPC) sets a course and a heading, which is then processed into the heading and course control, which in turn control the steering actuators of the KCU. A simple feedback loop structure is shown to denote that the measurement and estimation system of the KCU works in conjunction with the FPC to ensure that the kite is adequately controlled [43]. An advantage of using this control architecture is that it offers great controllability, without compromising agility and reeling efficiency. Moreover, the assumption of roll and pitch control being kinematically coupled to the kite course is not always true, but it can be dealt with by adding a secondary micro-winches for pitch control. This will ensure that a proper kite depowering can occur, thereby reducing the energy losses generated during the recovery phase of the power generation cycle.

8.5.3. Astronaut Schedule and Power Consumption

As for the purposes of this mission, renewable energy sources will be utilised to provide energy for the human habitat, it is paramount to examine the power demand behaviour of such an installation and how the supply could accommodate it. Moreover, it is of key importance to understand that for such energy systems is not only the supply that has to be reevaluated, but the demand must also alter based on energy resource availability. It was established that the previous power requirement to provide 10kW of continuous power is not representative of the demand of a Martian habitat. This is concluded through the examination of daily energy consumption patterns for residential and administrative buildings [49, 59] and it is evident that there is a severe power demand drop over night time. It is speculated that a similar behaviour would be encountered during the habitat operations. However, to gain insight in astronaut power demand and reevaluate the power demand, first their behaviour must be examined and the mission aspects affecting it must be discussed.

First, as space exploration becomes part of human life, it becomes more evident how much mankind is dependent on the conditions observed on the blue planet. Especially, due to the fact that the human body has a natural internal circadian clock of 24 hours which is in sync with the rotation of the Earth. Hence, once a person leaves the surface of the Earth, their circadian clock does not have a calibration reference and sleep regimes become hard to follow. Furthermore, irregular sleeping times lead to fatigue and under-performing bodily functions which are serious concern for the astronauts' health⁶ [60]. Hence, the aspects that influence a person's sleep is a research area of interest for multiple astronaut involved organisation where thorough investigations have been made on the sleeping environment, schedules, food regimes, etc⁷ [19], [11].

Nevertheless, so far the human race has not lived on a different planet than Earth so the implementations of the discrepancies between the 24 hour circadian clock of an Earth born human and the 24.6 hour duration of a Martian sol are not definitely identified. However, it is speculated by scientist that it could have disastrous consequences for a human based mission if it is not seriously considered and the consequences mitigated⁸. A simplified explanation for the experience of 24.6 hour days is comparing it to the feeling of being under a constant jet lag. Therefore, in order to address the concerns about the astronauts' well being, for the purposes of the project at hand, a set yearly time schedule is proposed for the astronaut operations. This is not only beneficial from human point of view but also, a set behavioural patterns result in set daily power demand distribution which is predictable and easy to meet.

⁶<https://www.cqu.edu.au/research/research-excellence/impact/case-studies/astronaut-fatigue-on-nasas-radar>

⁷<https://spaceflight.nasa.gov/history/shuttle-mir/science/hls/neuro/sc-hls-sleep.htm>

⁸https://www.huffpost.com/entry/mars-colonizers-sleep_n_56a7ad18e4b0172c65944022

However, before the schedule is created it is important to decide what time keeping model will be implemented on the surface of the red planet as the conventional 24 hour Earth clock would result inaccurate as sols are 24 hours and 37 minutes long. Hence, to accommodate the astronaut experience and to ease time keeping on Mars for people and electronics, a sol of 24 equally lasting hours is considered. Furthermore, every hour consist of 60 equally lasting minutes and each minute is also composed of 60 seconds. Hence the time difference between Martian sols and Earth days is accounted in the second definition where a second on Mars is approximately 1.0275 times longer than a second on Earth⁹. It is paramount to note that this would result in a difference between a kWh of energy on Earth and on Mars. For the purposes of this mission, the energy produced would be considered only for Martian hours.

In order, to create the schedule as presented below in figure 8.7, data from experiments in the Hawaii Space Exploration Analog and Simulation (HI-SEAS) are examined and interpreted [12, 37, 38]. The purpose of that investigation was to evaluate approximately the start and end point of the increase in power demand and the difference in power consumption during the day. However, from the HI-SEAS data it is quickly noticed that the astronaut power demand is not driven by the day and night times but it is rather differentiated in work and rest periods. The work period is characterised by high power demand of 10kW as a result of scientific and domestic activities such as research, lab time, cooking, clothes washing/drying, etc. as on top off the base loads and activities for the habitat. While the rest period is characterised by lowered power consumption as accounting for the base habitat activities such as the use of personal laptops, lighting, bathroom, etc. and the base loads of the life-sustaining systems.

Hence, from the power measurements in the HI-SEAS facility [37, 38] it becomes evident that first increase in power consumption happens between 9 and 10 o'clock in the morning. Therefore, 9 o'clock Martian Local Mean Time (LMT) is considered to be the start of work time and the point from which 10kW must be supplied. Additionally, it is noticed that approximately at 22 to 23 o'clock the power demand of the habitat significantly decreases. Therefore, 23 o'clock LMT is considered the start of rest time. Hence there is a total of 14 work Martian hours and 10 rest ones. Additionally, the power demand for work is equal to 10kW while the one for rest is equal to 5kW. Even though, in the reference data examined, it could be observed that the power demand drops to zero during rest time, it is reasoned that the HI-SEAS facility does not have a heavy duty heating, pressurising or oxygen-production systems; hence, it is not fully representative to the Mars mission at hand. Therefore, it is concluded that 5kW should be a good first approximation of the rest-time demand and the requirements **REM-NRG-12** and **REM-NRG-13** are formulated accordingly.

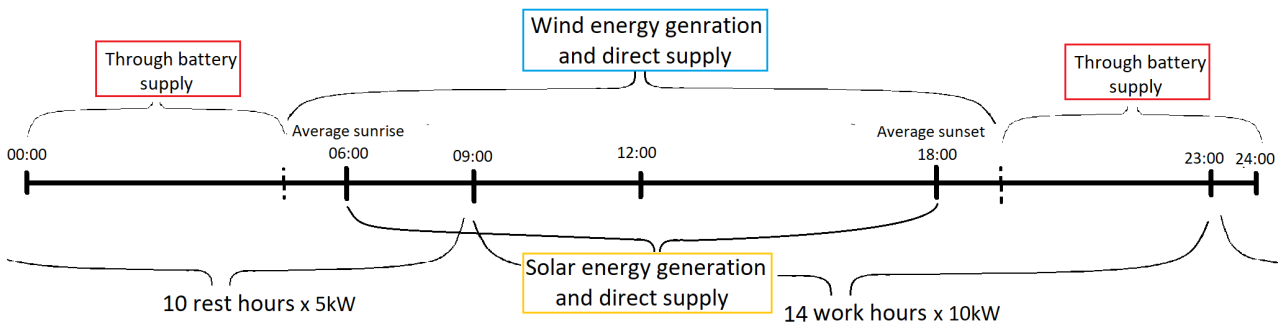


Figure 8.7: Yearly operational schedule for astronauts as visualised for a solar equinox and the respective nominal power demand of the habitat.

Lastly, it is important to note that the demand is ruled by the work and rest schedule and demand of the astronauts while the energy generation and direct supply is driven by the generation periods of the solar array and airborne kite system as seen in figure 8.7 above. For the solar system, the generation period is from sunrise to sunset while the generation period of the kite system is with an offset from those times as there is a strong diurnal characteristics of Martian winds as later explained in section 11.3. Moreover, during the rest of the sol, the demand needs to be met by the secondary battery.

8.5.4. Astronaut Safety and Integrity

Lastly, a few preliminary requirements on astronaut safety are specified in the requirements list:

⁹url

Table 8.7: Requirements on astronaut safety and integrity

Requirement ID	Description
REM-IAS-01	Astronauts shall be equipped with all necessary safety gear as established by the American Institute of Aeronautics and Astronautics.
REM-Sys-I01-01	The astronauts shall not be exposed to more than 1 Sv of radiation for the duration of the mission.

The details on how these requirements will be complied strongly relies on the astronaut scheduling explained in subsection 8.5.3, as well as the adequate selection of the space suits and equipment. The details of this are deemed to be out of the scope of this report, but are an important consideration for the future development of the mission.

System Performance Analysis

The performance analysis regarding the renewable hybrid energy system discusses the power supply and generation required to meet the demand of the habitat. The purpose for this analysis is to evaluate the compatibility of the energy generation subsystems (wind and solar) with the energy storage subsystems (battery and CAES) and the energy distribution subsystem (microgrid). Additionally, as the analysis is dependent on the performance characteristics and efficiencies of all the subsystems and also the other way around, it is paramount to understand that this is an iterative process. Hence, the outputs of the model are inputs for the system sizing as described in the following chapters, while the outputs of the system sizing are inputs to the performance model.

Hence, to clarify the system compatibility and performance analysis in the following chapter, in sections 9.1 and 9.2 the model description will be presented along with a discussion regarding the parameters and inputs used. Following are the results and its sensitivity analysis, presented in section 9.3, while the fidelity of the model is examined in the section 9.4. Lastly, the conclusion and recommendations for the system performance analysis are discussed in section 9.5.

9.1. Model Description

In order to evaluate the yearly performance of all the wind, solar, battery and CAES subsystems, a code model has been developed where the following computations are performed. The whole model is split in six units which are described in the following section.

Units 1 and 3: The first and third units are presented in a code block diagram (figure 9.1). The first unit is computing the yearly operational conditions where the work/rest times and power demands are as explained in figure 8.7. The third step involves quantifying the wind and solar resource available in terms of energy demand. This is done so as to have a quantified relationship of the energy production in different seasons for a given kite or solar array. The computation process is as explained in the section below. Nevertheless, the wind conditions depend on the output of Unit 2, namely, the direct energy supply fraction as described below.

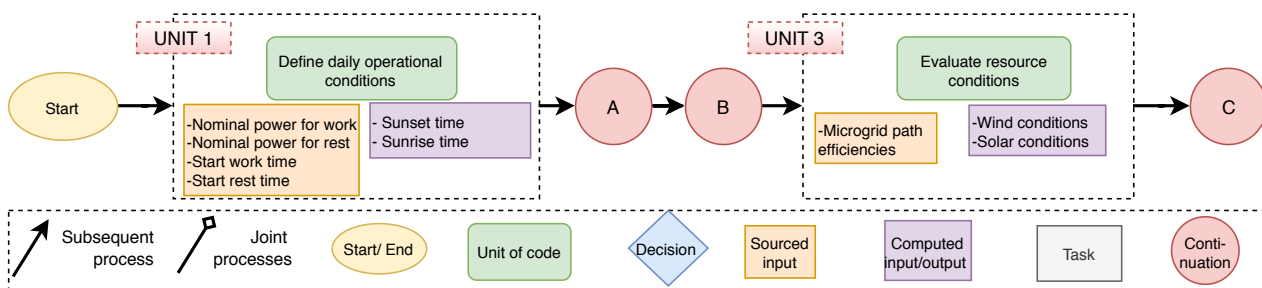


Figure 9.1: Code block diagram of Units 1 and 3 of the performance model with legend included

Unit 2: The second code unit, presented in figure 9.2, computes values of interest for the performance evaluation of the four subsystems, such as the total daily demand. Moreover, it calculates the fractions of the total sol demand that could be directly delivered from the kite and the PV array to the habitat to evaluate what portion has to be delivered through the storage facilities, if any. Nevertheless, for that calculation, the operational periods of the wind and solar subsystems must be known as only during those periods of a Martian sol is direct supply possible. The duration of the periods is explained below and depends on the sunrise and sunsets times. Hence, the total daily demand varies with sunrise, sunset, work, rest times and power values during work and rest periods. Once the direct energy fractions of the two generation systems are computed, the higher is selected as the dominant. As the summer is the only period where solar energy is dominant for the whole season, it is considered to take the solar direct energy fraction for these computations. The implications of this assumptions are later discussed in the sensitivity of the model.

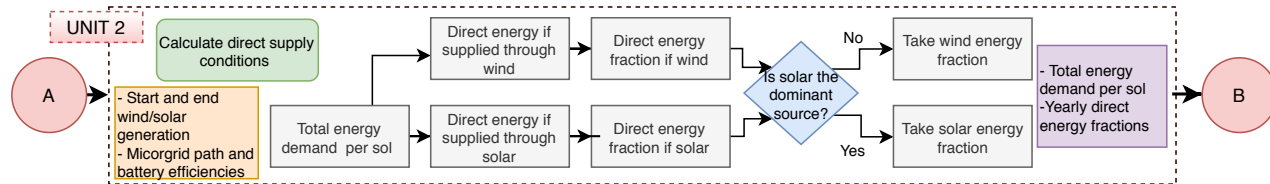


Figure 9.2: Code block diagram of Unit 2 of the system model. Legend is as presented in figure 9.1

Unit 4: Next, the performance of the four subsystems is discussed and can be seen in figure 9.4. The code is executed for every sol of a Martian year. It is important to note that the function is based on a dominant and an auxiliary source and not wind or solar energy as seen in figure 9.3. The final design of the renewable energy system as presented in this report has the wind conditions as be the dominant through the year. This configuration of the function allows for quick iterations with different system configurations.

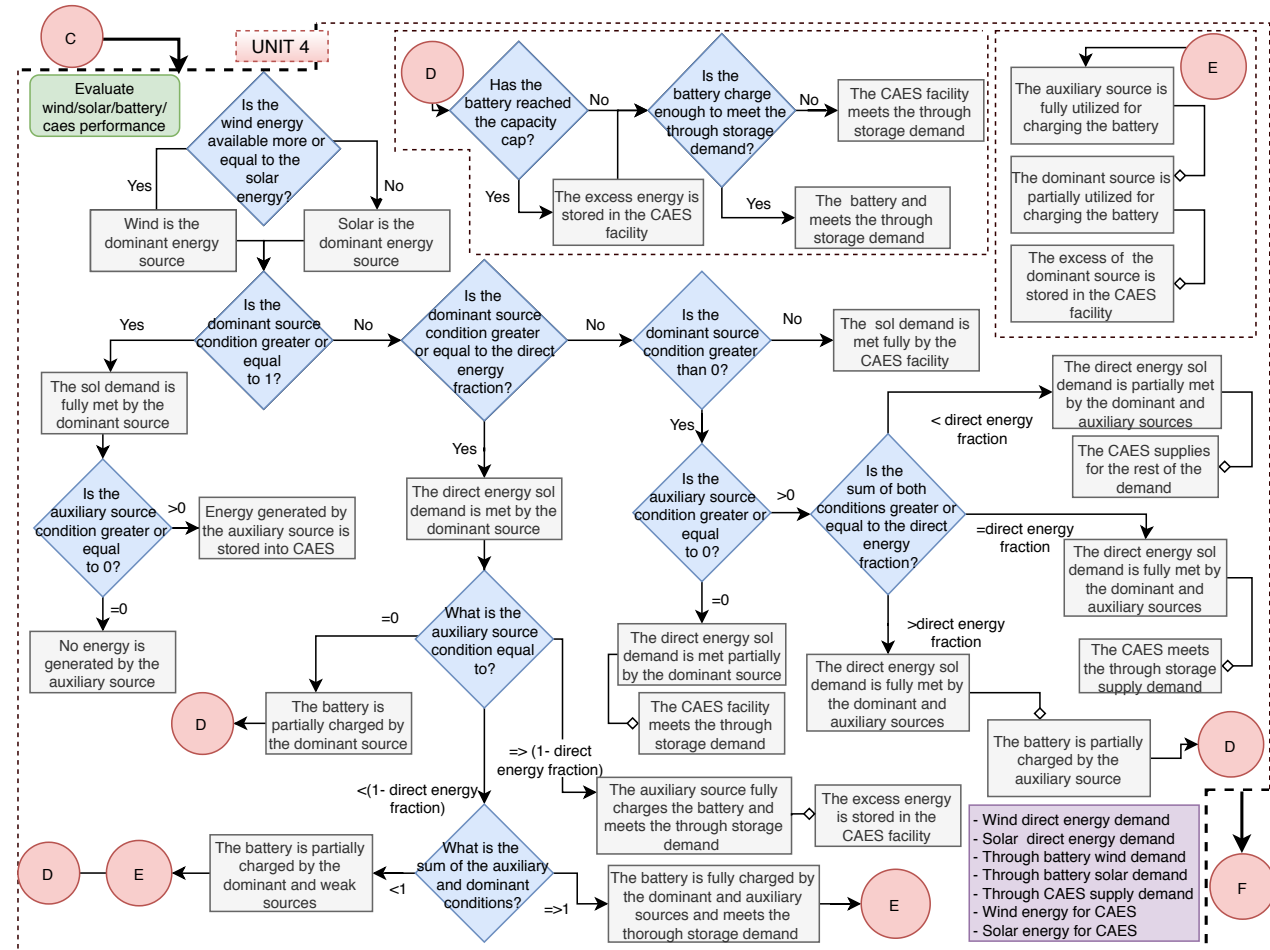


Figure 9.3: Code block diagram of Unit 4 of the system model. Legend is as presented in figure 9.1

It is clear that the function requires inputs such as the wind and solar conditions, the daily operational conditions and the direct energy solar fraction as computed in the previous three code units. This is necessary to evaluate how much of the demand a source can deliver and whether that is sufficient to meet the total, the direct supply demand or the storage demand. Based on the normalised wind resources (the conditions), the supply path could be evaluated and is visualised in the code block diagram of Unit 4. In addition, due to the definitions used in the function (dominant and auxiliary), when computed it is paramount to note that locally the winter operational conditions of the wind system must be specified as different from the rest of the three seasons (± 2 hours from daylight instead ± 1 as explained in next section). Hence a global Boolean variable which indicated whether or not it's winter season is made an input. Similarly, the function also requires an indication of which is the dominant source, in order to evaluate which operational conditions to consider for the dominant and auxiliary sources respectively.

Moreover, the outcome is not only based on the previously discussed parameters which, independently of the

function's outcome vary from sol to sol, but also on parameters which are the results of the conditions from the previous sol. For example, if the conditions of a given sol imply that the battery could only be partially charged during the daytime, whether or not the battery will be utilised for nighttime supply depends on the net battery charge. Even though for the CAES facility same reasoning is valid, the handling methodology is different because it is charged&discharged on a seasonal scale rather than a sol-to-sol basis. Hence, when the fourth code unit is executed for every sol of a Martian year, it is assumed that the CAES facility could meet the demand, allowing the net charge of the facility to be negative. This way, the total storage capacity is given by the most negative value during a year. Thus, the end of the fourth code unit, the direct supply demand from wind and solar is known, along with the battery and CAES supply demand for each sol of a Martian year. Additionally, the required CAES discharge, excluding efficiencies, is computed and stored in array which must be processed in the next unit.

Unit 5: Once the sol demand from each source is computed, it must be evaluated whether or not the CAES facility has been charged sufficiently throughout the year in order to actually fulfil the estimated required supply. This is achieved by, first, evaluating the actual charge input for storage while also considering the compression efficiency and the losses due to the microgrid from the kite and PV array to the CAES' compressor. Next, to evaluate the actual discharge from the CAES facility required in order to output the calculated demand, the value of the demand must be divided by the expansion and storage efficiencies including the losses of transferring the electricity from the CAES to the habitat. Hence, through those calculations, it could be evaluated if the remaining charge in the CAES is positive and if enough energy has been supplied.

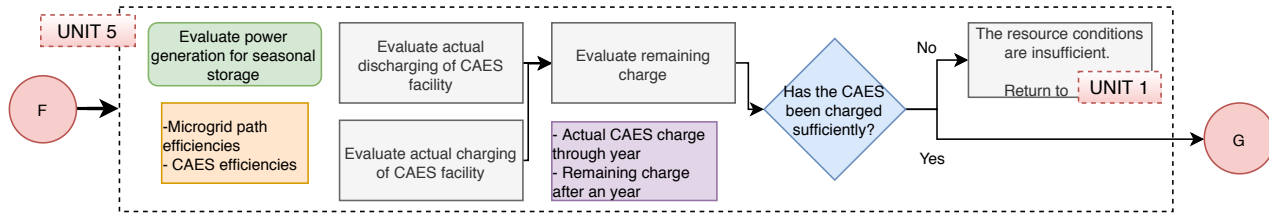


Figure 9.4: Code block diagram of Unit 5 of the system model. Legend is as presented in figure 9.1

Nevertheless, the original and transformed arrays have a different shape heavily dependent on the wind and solar conditions for different system configurations. Therefore, a single mathematical model which automatically verifies the state of the CAES for any configuration has not yet been developed due to the imposed time constraints on the design team. Thus, the decision as visualised by the blue rhombus in figure 9.4 is taken manually by the person handling the model. Even for different configurations a visual inspection is straightforward once it is established that the remaining charge at the end of the year is greater than zero. This is needed as at the beginning of the year, the CAES started from a fully charged state (which is implemented as 0) and it has to be at or above 0, so the following year it can start as fully charged again. The inspection process is further evaluated in section 9.3. Moreover, if it is established that the charge input in the CAES is not enough to provide the discharge output, the model has to be terminated manually and the solar and wind conditions in Unit 1 must be reevaluated. Otherwise, the code will automatically continue.

Unit 6: Following, the energy supply fractions are evaluated in Unit 6.1, while in Unit 6.2 the actual sol demand is calculated through considering the microgrid and the battery efficiencies. Lastly, the nominal operation power output is computed in Unit 6.3 as seen in figure 9.5.

First, the demand energy fractions for different supply methods and paths are calculated. Those are also referred to as the yearly power mix values and would be later presented in section 9.3, which discusses the outcome and sensitivity of the system performance analysis. It is important to note that at this stage it can be evaluated if the wind system delivers more than 50% of the demand and hence complies with the requirements. If the fraction is less than the requirement, the termination of the model must be done manually as otherwise to allow for the examination of system configurations why solar is the overall dominant source. Furthermore, the CAES and battery capacity required can be evaluated in cooperation with the storage facilities.

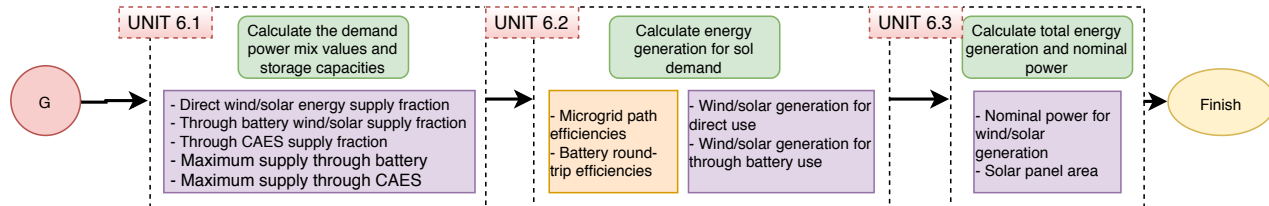


Figure 9.5: Code block diagram of Unit 6 of the system model. Legend is as presented in figure 9.1

Next, Unit 6.2 is not computation intensive. The energy generation for sol demand is computed by dividing the expected supply through the battery by the respective microgrid efficiencies and the round-trip energy efficiencies of the battery. Hence, now that all the required energy generation has been calculated the total energy generation for each sol can be evaluated both for wind and solar sources. Therefore, the actual production of the kite can be compared to the expected production and the approximate solar array size can be evaluated and its performance compared to the expected one. Additionally, in Unit 6.3 the nominal power output of the two subsystems is evaluated as the microgrid design is dependent on those values. Once, all those computations are performed sufficient information has been acquired to conclude the compatibility of all the present sub-systems. Depending on the conclusion the design is reiterated if needed.

9.2. Model Inputs and Task Execution

In this section, a more in-depth elaboration on the specific inputs and task computation is presented to aid the reproducibility of the performance model analysis and to add clarity to the process. The documentation of the processes is presented separately for the six code block units.

Unit 1: Define daily operational conditions

- Nominal power for work and rest: The values are as evaluated in the previous chapter in section 8.5.3 and follow from the previous stakeholder requirement and the considered astronaut power demand. Hence, the nominal power demand for work is 10kW while the nominal power for rest is 5kW.
- Start of work and rest times: The daily work and rest duration are evaluated from the astronaut schedule proposed in section 8.5.3 where a total of 14 Martian hours are dedicated for working purposes while 10 hours are estimated to be the approximate rest duration.
- Sunrise and sunset times: Those are obtained through evaluating the change from the equinox sunrise and sunset times of 6 and 18 o'clock, respectively. The minute variation is obtained through reconstructing a graph computed for 40°Martian latitude by Thomas Gangale¹. From the graphical representation, 25 data points are obtained both the sunrise and sunset curves and the values are linearly interpolated for the rest of the sols. Those values in minutes are then converted to Martian hours though dividing it by 61.625 minutes per Martian hour; as previously explained in section 8.5.3 the time keeping method on Mars will resort to a redefinition of the duration of one second. Then, the deviation in Martian hours is summed with the equinox sunrise and sunset times and the absolute local times are obtained. It is paramount to note that one hour of daylight saving time is included in the computation for sols 80 to 360 as also given by Thomas Gangale.

Unit 2: Calculate direct supply conditions

- Solar generation period: The operational period of a solar farm is easy to evaluate as it depends on the presence of sunlight. Hence, the solar farm is assumed to be generating energy from sunrise to sunset which could also be observed from the calculations by Delgado-Bonal et al. [29] for the obtainable solar energy in the Gale crater as a function of Local Mean Solar Time and season.
- Wind generation period: The wind sub-system daily operational period is not as straightforward to evaluate. As explained with the wind resource evaluation (section 11.3), there is diurnal characteristics of Martian winds. This implies that there is a big difference between the wind available during the day-times and night-times on the red planet. Hence, for a preliminary estimation for the kite operational period, one hour before sunrise and after sunset are taken as a start and end points for spring, summer and autumn. This is considered reasonable, as for the starting time, even if the sun has not yet risen on the site of interest, it is already heating the area east of the site, and hence, creating a thermal gradient and creating wind. Similar logic can be applied for the end of the daily wind generation duration. Moreover, for the winter season, ±2 hours from sunrise and sunset are taken respectively as the wind speeds are higher and there is not as conclusive evidence for the diurnal behaviour of wind during the winter seasons. Nevertheless, even there is a possibility for nighttime energy generation with the kite system for

¹http://ops-alaska.com/time/gangale_mst/daylight.htm [Cited 12 June 2020]

the winter season, from operations, maintenance, and risk points of view, it would be irrational to fully rely on the continuous kite operation for about 150 days. Hence, the kite operational hours during winter are two hours before sunrise and two hours after sunset.

- Microgrid efficiencies: In order to evaluate the direct energy fraction not only the generation and operational conditions must be known but also the microgrid efficiencies for the direct and trough battery supply must be known along with the roundtrip efficiency of the battery. The microgrid values and reasoning are as found table 10.5 while the battery efficiencies are elaborated upon in section 13.5

Hence, with all necessary inputs computed the direct energy fractions could be computed through the following steps:

1. The direct supply for wind E_{wind_direct} , excluding efficiencies is calculated with the following equation, where t_{work} is the clock time at which work begins and t_{wind_start} is the start of wind generation for the sols. P_{rest} and P_{work} are the nominal power required. In the exactly the same manner E_{solar_direct} is evaluated but taking the starting time solar generation.

$$E_{wind_direct} = (t_{work} - t_{wind_start}) \cdot P_{rest} + (t_{wind_end} - t_{work}) \cdot P_{work}$$

2. The total supply for a day excluding efficiencies is computed through the following equation. Where Δt_{work} is the work duration of the astronaut schedule (14 hours) and Δt_{rest} is the rest duration (10 hours). Hence, for the given requirements E_{total} results to be 190kW.

$$E_{total} = \Delta t_{work} \cdot P_{work} + \Delta t_{rest} \cdot P_{rest}$$

3. Now, the actual energy generation could be calculated by subtracting the directly supplied energy through wind/solar from E_{total} and dividing the resultant by the microgrid battery path efficiencies from the respective source and the round-trip battery efficiency. The found values are denoted with $\widehat{E_{wind_battery}}$ and $\widehat{E_{solar_battery}}$.
4. Following, the actual energy generation for meeting the direct supply could be evaluated through dividing E_{wind_direct} by the efficiency of the grid from the kite to the habitat where the result will be denoted with $\widehat{E_{wind_direct}}$. Similarly, $\widehat{E_{solar_direct}}$ is calculated with path efficiency from the PV array to the habitat.
5. Then the total power generation through each source required to meet the demand of 190 kW considering the efficiencies is calculated by summing E_{wind_direct} with $\widehat{E_{wind_battery}}$ and E_{solar_direct} with $\widehat{E_{solar_battery}}$. The results are denoted by $\widehat{E_{wind_total}}$ and $\widehat{E_{solar_total}}$.
6. The direct supply energy fraction are calculated by dividing E_{wind_direct} or E_{solar_direct} by $\widehat{E_{wind_total}}$ or $\widehat{E_{solar_total}}$, respectively.

The resultant fractions indicate how much of the total generation is needed to meet the direct supply demand and how much has to go to the secondary battery. Hence, it is possible to evaluate what portion of the demand the wind and solar resource are will be able to meet. The computation of those two respective conditions is as described below while a visualisation of the results is presented in section 9.3.

Unit 3: Evaluate resource conditions

- Wind conditions: In order to evaluate the wind resource conditions, it must be evaluated how the energy generation per sol varies throughout the year for a given kite and how that compares with respect to the generation required, $\widehat{E_{wind_total}}$, to meet a sol's demand as explained above. Therefore, an input from the kite sizing model is required, namely, the energy generation including the change of operational duration throughout the year. It is paramount to understand that the kite sizing also needs an initial reference array with the required energy generation as an output of the performance analysis. Hence, this is an iterative process and multiple data files were exchanged between the design teams until a converged design was achieved. When a file containing the kite's output is received, it is normalised by dividing it by the previously evaluated $\widehat{E_{wind_total}}$.
- Solar conditions: On the other hand, the solar conditions are estimated through normalising the solar irradiance available as evaluated in section 12.3. This is achieved through setting the maximum solar condition equal to 0.35 for the presented design, corresponding to the sol with maximum solar irradiance. Then, the rest of the solar conditions are computed through taking the current irradiance value and multiplying it by the maximum solar condition and dividing it by the maximum solar irradiance of the year. In addition, in order to also account for different energy generation required values throughout the year due to the direct energy fractions and the efficiencies, the solar conditions are divided by one more term, which is the sum of the direct energy fraction for solar generation divided by the microgrid path efficiency from the PV array to the habitat, and the through storage supply fraction (its equal to $1 - directfraction$) divided by the respective path efficiency and the round trip battery efficiency.

Hence, it can be estimated how much of the daily demand the kite and solar array can meet throughout a Martian year and how that compares to the direct supply required and the total demand which is equivalent to 1 when the resources are normalised as later seen in the graph in section 9.3.

Unit 4: Evaluate wind/solar/battery/CAES performance

For the execution of the all previously computed parameters along with the other relevant inputs as mentioned in the Model Description section must be fed to a function which operates as visualised in the code block diagram in figure 9.3. Additionally, it at the beginning of the year the net charge in the battery and the CAES are considered to be zero. The result for the direct supply per sol from each source and the through storage supply is visualised in following section.

Unit 5: Evaluate power generation for seasonal storage

- Actual discharge: The discharge values are computed through dividing the expected supply by the expansion, storage and microgrid efficiency.
- Actual charge: The charge values are computed through multiplying the energy inputted into the CAES by the compression and microgrid path efficiency.
- Actual charge: The remaining charge is equal to the last value of the array as the initial condition of the charge is numerically equal to zero.

Thus, it could be evaluated if the CAES storage has been charged sufficiently through visual inspection of the graph presented in figure 9.12. The implementations of the data transformation described above could be observed in the same graph where the actual charging stage has a less steep slope than first computed; while, the actual discharging has steeper slope.

Unit 6: Evaluate power mix values, total energy and nominal powers

- Power mix values: These are obtained by summing the energy supplied by each subsystem for a year and later dividing it by the total yearly supply.
- Energy generation for sols: The energy generation for sols is evaluate by dividing the direct supplied energy by the the direct supply path efficiencies and dividing the through battery supply by the respective microgrid efficiencies and the battery efficiency.
- Total energy generation: This is obtained by summing the energy required for sol and seasonal supply both for wind and solar generation.
- Nominal power: These are computed by dividing the total energy generation required by the operational duration of each energy harvesting system throughout the year.
- Solar array area: This is obtained by comparing the power generation required to the actual harvesting capabilities of a farm of a given size. The power of the solar array is computed by the formulas and efficiencies in chapter 12.
- Battery capacity: The battery capacity is estimated considering the maximum required supply though the battery in a year and the efficiency of 0.88% and operational range of 0.8% as later described in section 13.5.
- CAES capacity: The CAES required supply is estimated by considering the supply for the four different seasons and the total supply through them. Then if there are two consecutive season where the CAES is continuously discharged, the supply for the two season is summed and that is considered the maximum supply. Otherwise, the season with the highest supply value is taken as reference for the maximum. Lastly, the supplied energy is divided by the expansion, storage and microgrid efficiencies.

9.3. Results and System Sensitivity Analysis

In the following section the results of the system performance model with the above described inputs are presented. Following, a different system configuration is proposed in order to examine the sensitivity of the system performance.

9.3.1. Results and Contingencies

The results of the model are visualised in the following figures and discussed below.

Unit 1: Define daily operational conditions

The operational conditions of the astronauts is computed for the whole year as seen in the following image 9.6. Moreover, the sunrise and sunset times including one hour of Daylight savings are also presented.

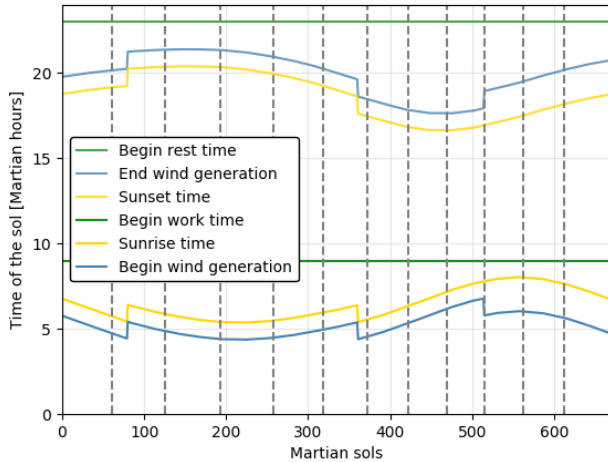


Figure 9.6: Operational times for astronauts, and wind and solar generation

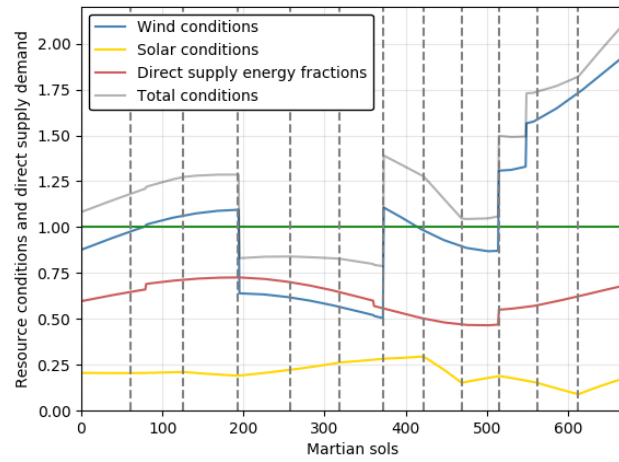


Figure 9.7: Energy conditions and direct energy supply fraction

Units 2 and 3: Evaluate direct supply and resource conditions

The first part of the second unit involves the computation of the operational conditions of the wind and solar energy subsystems. Those are also presented in figure 9.6 as for comparison with the astronaut operations; note that the sunrise and sunset times correspond with the begin and end of solar generation.

While, the resource conditions and the direct supply energy fractions are visualised in figure 9.7 above. It is important, to note that only during summer the total conditions are less than one; this implies that during this season, the CAES facility has to be utilised.

Unit 4: Evaluate wind/solar/battery/CAES performance As a result the fourth unit of code, the yearly expected performance of the complete system is evaluated given inputs and parameters. First, the directly supplied energy is visualised through the graph in figure 9.8. It is important to note that the solar supplied energy is added on top of the wind energy in order to better visualise the complementary the two subsystems. The same is also true for the evaluated excess energy (corresponding to total resource condition greater than one) as presented in figure 9.9. The generation over summer is due to the fact that the battery has been fully charged so the energy must be redirected to the seasonal storage.

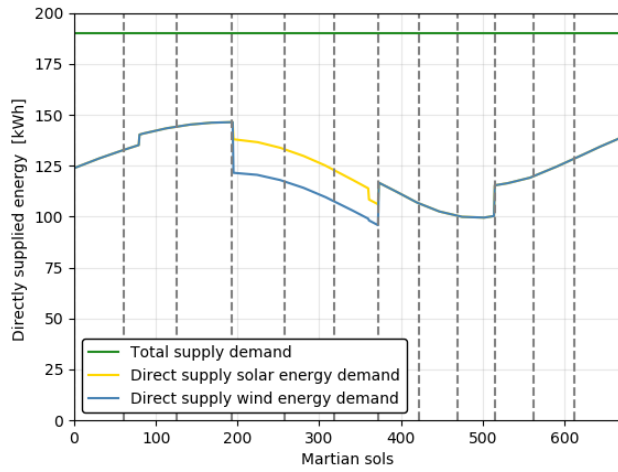


Figure 9.8: Direct supplied energy from the wind and solar sources.

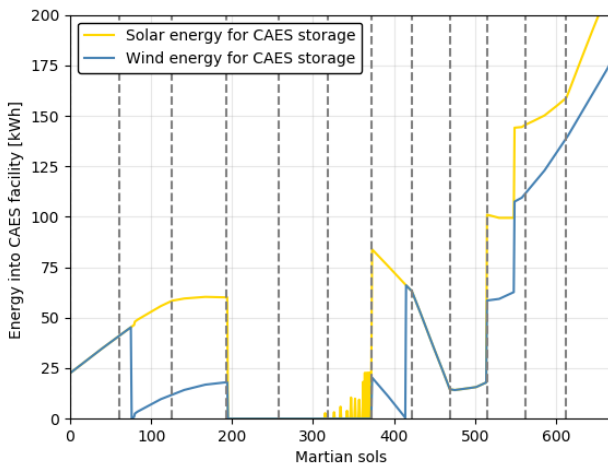


Figure 9.9: Energy supply to the CAES facility from the wind and solar sub-systems.

In addition, the storage supply is also evaluated for the year. Moreover, the arrays are presented in figure 9.10 where the through battery supply with wind and solar are distinguished with different colours. The drop from the beginning of winter corresponds to the increase of wind generation period per sol and hence the energy which could be directly supplied. Furthermore, it is clear that in the beginning of spring and end of autumn, the battery is fully charged by both energy generation sources. While in summer the conditions allow for partial charging of the battery as also seen in the close-up version of the previously discussed graph, presented in

the next image (figure 9.11). It is observed that approximately every other day the battery is fully charged by the solar energy source, while for the days when the charge is not sufficient, the CAES facility provides energy to meet the demand.

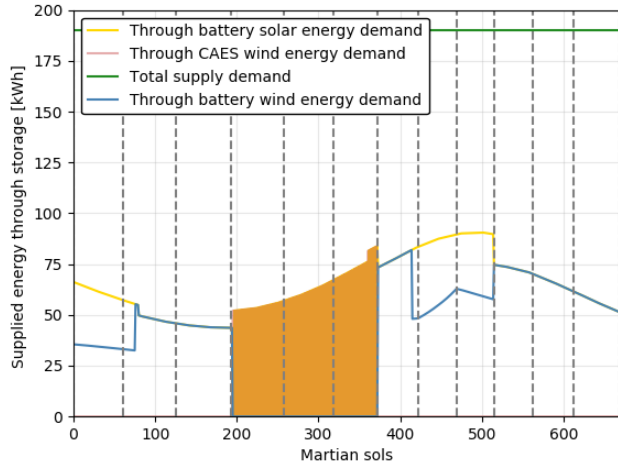


Figure 9.10: Through storage (battery/CAES) supply

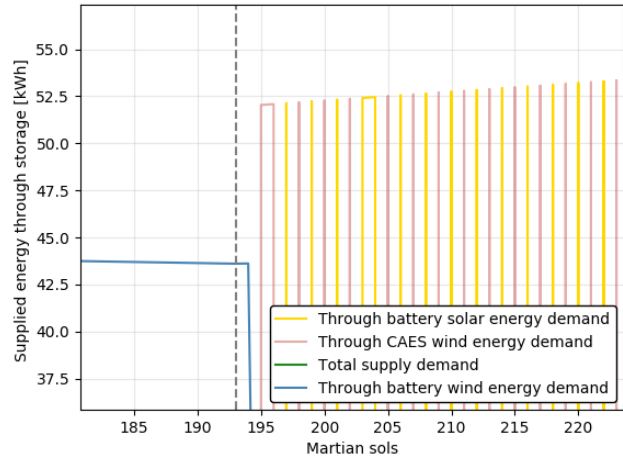


Figure 9.11: Close-up of through storage (battery/CAES) supply

Nevertheless, in order to evaluate the actual energy generation of the subsystems, separate arrays that represent the actual charge provided to and from the battery also must be computed. The sum of the arrays with the direct energy supplied from the wind and the solar sources are represented by the more translucent blue and yellow lines in figure 9.13. However, before the energy generation for sols is generated, it must be verified if the CAES facility has been charged sufficiently for the considered system design.

Unit 5: Evaluate power generation for seasonal storage

The actual CAES charged is computed and could be visually compared to the output of Unit 4 in the following figure 9.12. Furthermore, though visual inspection it could be concluded that CAES has been charged sufficiently. As a matter of fact there are approximately remaining 10MWh of energy stored in the CAES after a year of use. This might make the system seem over-designed, however, there are several factors that must be considered when this is examined.

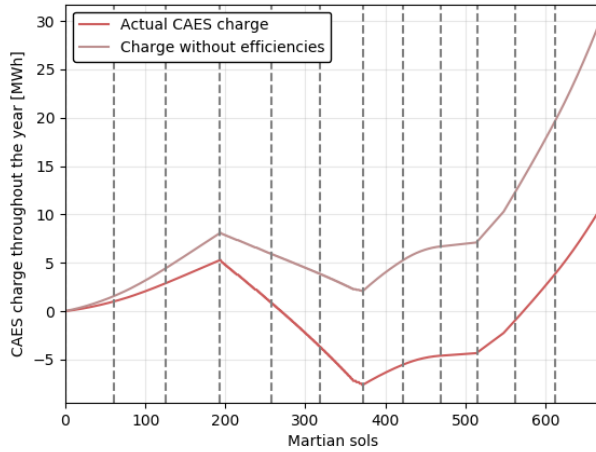


Figure 9.12: The energy charge of the CAES facility as a result of Units 4 and 5

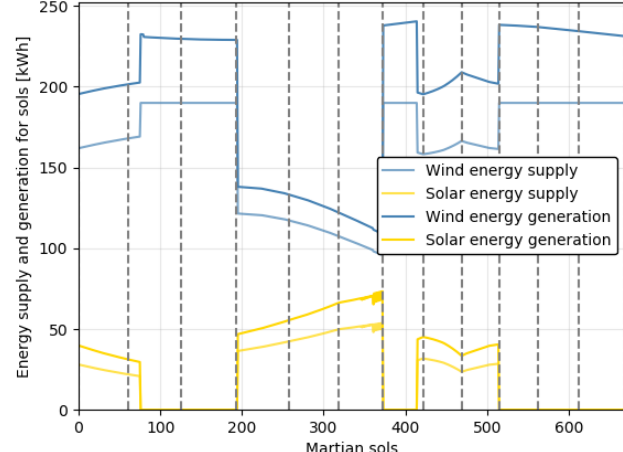


Figure 9.13: Energy generation by the wind and solar sub-systems for sols demand

First, the assumed thermodynamic efficiencies of the CAES facility as later described in chapter 13, are optimistic and might be significantly lower. Furthermore, the CAES facility is over-charged due to the way Unit 4 is modelled. The unit takes any extra amount of energy into the CAES no matter how small it is. In real life, there will be a minimum power required to drive the compressor in order to actually be able to create stored energy. Additionally, the over-charging occurs during winter so if one would like to reduce it the kite

or the solar array must be made smaller (in terms of energy output). However, this on the other hand, would result in a bigger CAES facility required for the summer season. Therefore, after a couple iterations it was considered that increasing the required supply from the CAES to more than approximately 7MWh could make the design unrealistic due to the extremely high pressure ratios required due to the low density of the ambient air. Therefore, a design where the CAES does not exceed that value was converged upon and later presented in the following chapters.

Unit 6: Evaluate power mix values, total energy and nominal powers

Once, it is concluded that a sufficient energy charge has been input into the CAES facility, the power mix fraction are evaluated to verify that the the wind energy sub-system supplies more than 50% of the yearly demand.

Table 9.1: Power mix values for direct and through storage supply on the left and power mix values for sol and seasonal supply on the right

Direct wind	Direct solar	Through battery	Through CAES	Through wind	Through solar	Through CAES
0.64	0.02	0.29	0.05	0.85	0.10	0.05

The calculated supply power mix values are presented in the above table 9.1 and it is evident that the requirement is complied with. Once, that has been established, the total energy generated to meet the sol demand is calculated through considering the microgrid and battery efficiencies. The change in the total wind and solar energy required to meet the sol demand is visualised in the above graph in figure 9.13. On this graphs, the solar conditions are not presented as complimentary but rather the absolute values are shown for clear understanding of the data transformation performed.

Furthermore, with those values for each sol, the total energy generation required by the solar and wind subsystems to meet the sol plus seasonal habitat demand is computed. The sum of the previously discussed energy generation for sol demand and the energy supply to the CAES is presented in figure 9.14. Note that the energy generation for sols is included for the sake of visualising what portion of the total generation is for the sols and what for seasonal storage. Similarly, the sum of the total wind and solar energy generation of the year is included as noted by the grey coloured data. Moreover, the nominal operational power for the Martian sols is computed from the previously discussed values and are presented in figure 9.15.

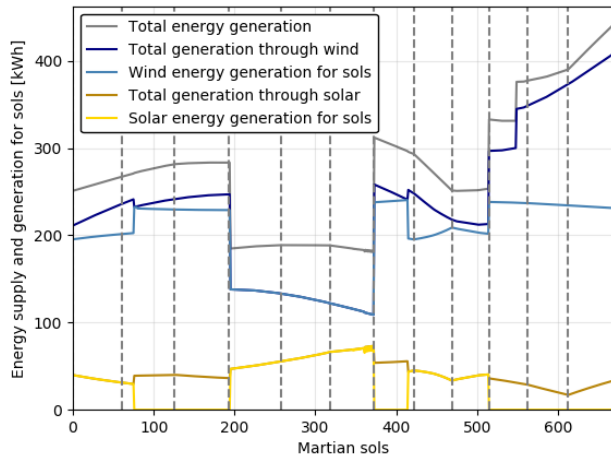


Figure 9.14: Total energy generation by the wind and solar sub-systems

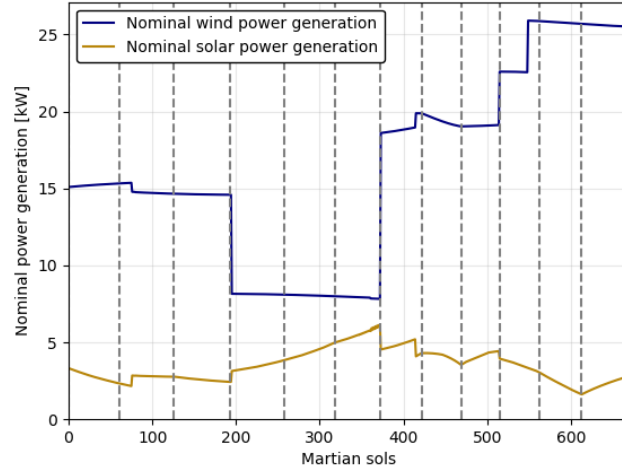


Figure 9.15: Nominal power generation by the wind and solar sub-systems

Therefore, once the whole data transformation has been completed, it still must be evaluated if the system performance analysis model computes the expected wind energy supply accordingly to the actual available energy from the kite subsystem. Lastly, it is further investigated what size solar array is needed to meet the expected yearly solar energy supply. In figure 9.17, the nominal power excepted from the solar array and the actual power generated by a 70m^2 PV array and compared and estimated to be sufficient. Lastly, the maximum supply through the battery is computed to be 86kWh while the total capacity with the considered efficiency result in 116kWh. Furthermore, the total capacity delivered by the CAES is equal to 6.5MWh and the capacity is later estimated in chapter 13. Lastly, it must be noted that the system performance analysis is

not perfect and there are modelling errors which need to be further investigated. The implementation of those modelling errors are that the converged design might result to be slightly bigger or smaller than the estimate. Therefore, design contingencies are considered, where 5% of contingency is taken for the solar array size, the battery and the microgrid, and 10% of contingency for the CAES design as this output is more input sensitive than the remaining of the outputs.

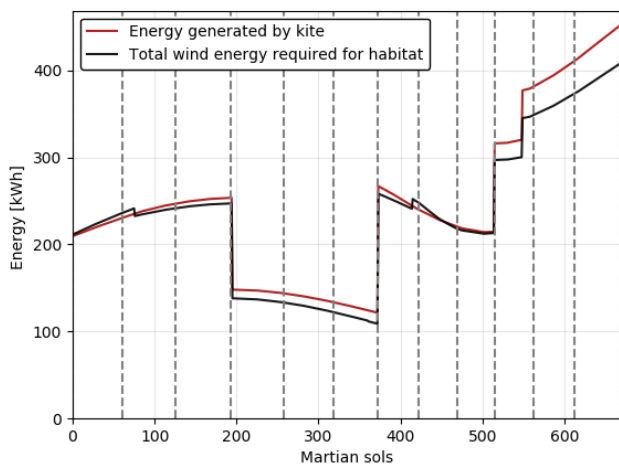


Figure 9.16: Wind energy required by system performance analysis and actual output of the designed kite

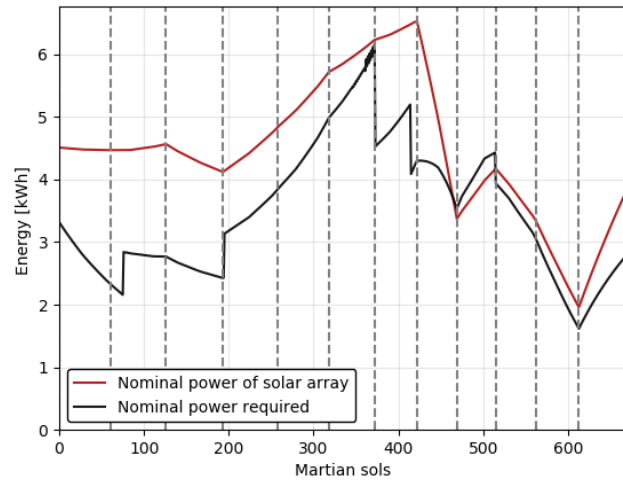


Figure 9.17: Solar power required by system performance analysis and actual output of the designed PV array

9.3.2. Sensitivity Analysis of System Design

In the following subsection a sensitivity analysis of the system design is presented. By doing this, it can be evaluated how does the design scales down if the power requirements are changed and how does this affect the overall mass, cost and volume of the developed renewable energy system.

At the beginning of this analysis, it was of interest to evaluate how the required system size changes as the power requirement is reduced to 5kW of continuous power both for work and rest operations. Nevertheless, it was quickly established that the kite sizing model developed for the purposes of meeting the previous requirement, and does not execute fully correctly when a kite of too small size is considered (most likely due to modelling errors). Thus, the sensitivity of the system performance is evaluated through considering power requirements of 7.5kW for the work operations and 5kW for the resting period.

In order to evaluate the required kite size to meet the new requirements, the previously evaluated kite production as for the original design is scaled by a fraction and run through the system performance model in order to evaluate the required solar array size. Then, the expected energy generation for the sols is provided to the kite design team as a reference for scaling down the kite. Once, that has been completed, the new annual yearly energy production is taken as a reference for computing the wind conditions. With the new input it is evaluated if the complete system is actually capable of delivering the previously estimated supply.

Nevertheless, it is important to note that the scaling of the complete system is not as straightforward as the scaling of single sub-system or a component. This, is due to the fact that for this lowered energy requirements a different ratio of the wind and solar complementary behaviour can be taken. For example, one could choose to go with the same sized kite as the original design while reducing the required solar array area and CAES storage. This could be implemented in the model through taken the old kite production as a reference for the computation of the wind conditions while also lowering the maximum solar condition of 0.35. However, even if the mass and cost are reduced for this case, the reliability of such system also drops.

Hence, in order to exemplify the change in the system considered in this report, the maximum solar conditions remains as 0.35. Then, it is important to note that new energy production required and actually generated by the kite produces approximately 0.8 of the energy output of the original design. How the mass of the new kite changes accordingly is discussed in chapter 11. Additionally, the new required solar array size is equal to 55m² while the battery capacity is 93.5kWh. Moreover, the nominal power which should be handled by the grid lowers to approximately 21kW. Lastly, it is evaluated that the required supply through the CAES facility changes only to 6.25MWh from 6.55MWh. This is due to the fact that the CAES meets the storage supply for about every other rest period during the summer season. Hence, as the nominal power required for the rest periods is still 5kW, there is minimal change in the total required output for this reiterated smaller design. Therefore, the individual sensitivity analysis of the CAES sizing is evaluated in a different manner.

9.4. Verification and Validation

The verification and validation of the system performance analysis is discussed in the following section. It is separated to unit verification and validation, and system model verification and validation procedures.

Verification and validation code units

The six units described above are tested individually to examine the independent outputs of those code blocks and if the data is transformed as expected. For Unit 1, the only piece of code that must be verified is the one which linearly interpolates the 25 reference points and estimates the sunrise and sunset times throughout the year. Furthermore, once the offset of sunrise and sunset times are sourced from Thomas Gangale's work². It is determined that the total error of the linear approximation when compared to the model is less than 2%. Furthermore, for the validation of this simulation aspect, one could independently model the relationship for sunrise and sunset times for a full Martian year though considering through following the steps proposed by Michael Allison by developing an accurate time keeping tool [4]. Additionally, there is an already existing tool developed by NASA, Mars24³, which accurately outputs the solar times of interest for specified point in time and longitude. As the java code of the program is available online, it could also be modified as to show sun time duration but rather than a single time (it works like a clock rather than a timer).

In addition, for Unit 2, the computation of the direct supply energy fractions and the total energy demand, the following unit verification checks are considered. As seen in figure 9.7, the curve representing the direct supply fractions has three steps. The first and second are due to the one hour of daylight savings while the third one corresponds to the increase in wind generation period during winter. Hence, if those are made equal to zero, the red line must appear as a smooth curve. Additionally, the curved nature of this data arises from the considered sunrise and sunset time changes throughout the year as following from Unit 1. Hence, if the sunrise and sunsets time are also kept at 6 and 18 o'clock, respectively, for the whole year, the direct energy supply fraction will appear as a straight line. Additionally, it is considered that if the nominal power demand for work is equal to the nominal power demand for work, the straight line will have a value equal to 0.5 as the direct supply period is equal to a half of the sol.

Furthermore, the outputs of Unit 3 (wind and solar conditions) are not verifiable by comparing it to reference models. The first indication that the wind and solar conditions have been computed numerically correctly is when the model outputs figures 9.16 and 9.17. Furthermore, please note that the numerical normalisation of the wind energy generated and solar resource present has been reevaluated on multiple occasions during the design phase. The computation that results in the most accurate performance evaluation is presented in this report. Additionally, from the two graphs it is clear that the wind energy approximation is more accurate than the one for the kite. This is due to the fact that solar is the auxiliary resource throughout the how year and hence, the wind direct energy fractions are considered. While in reality the there are two different direct energy fractions for a single sol corresponding to fully wind or solar supply. Hence, there is a modelling error due to the adopting of single value for the direct supply which is also a reason for the included contingencies.

Moreover, the verification process of the fourth unit is considered most crucial for the adequate analysis of the system performance. Before, function defining the systems' operations given the solar and wind conditions is tested with the actual resource availability, dummy condition arrays are created to facilitate the unit verification process. The dummy arrays are made such that for each of the twelve months a different path will be taken as shown in figure 9.3 and it could be evaluated if the outputs are as predicted. For example, it is inspected if the solar/wind condition is zero for a given a month, that there should not be supply from that source; also if both conditions are zero, the CAES has to meet the total sol demand. Additionally, a verification test which terminates the model if for a single sol multiple of the operational loops are entered. This unit verification also prints the numbers of the two entered loops. Moreover, another unit verification test for the function is evaluating the sum of the total direct supply from the dominant and auxiliary sources plus the total through battery supply from the dominant and auxiliary sources plus the though CAES supply for a single sol. If that sum divided by total supply per sol minus one exceeds 10^{-5} , the model is terminated. This is basically that the supply through different paths is calculated correctly as once it is summed up it adds up to the required supply demand.

Lastly, as the computations performed in Unit 5 and 6 are not calculation intensive and there is little room for errors, general verification techniques have been applied. It has been double checked that all inputs are correct and the appropriate arrays are used when need instead of arrays with similarly names. Moreover, when estimating the supply power mix values for a Martian year, it is examined if the sum is equal to 1. If that is not the case, an error is presented for the computation of this output.

²http://ops-alaska.com/time/gangale_mst/daylight.htm [Cited 12 June 2020]

³<https://www.giss.nasa.gov/tools/mars24/> [Cited 12 June 2020]

Verification and validation complete model

As a reference model that evaluates the interaction between an airborne kite and PV array though the medium of the microgrid has not been found, the complete model verification and validation is done in the following manner. Note that exactly because of the fact that there is no reference models or theory to consult, the unit verification process as explained above is considered crucial and has been thoroughly implemented.

As for the model verification, first, the outputs of the system performance model have been examined by evaluating the performance for different system configurations. This was done by initially considering non-hybrid operation energy system configuration where CAES is required to meet the spring and autumn demand [24]. Additionally, the changes observed during conducting of the system's sensitivity analysis also support the observation that the model functions accordingly. Furthermore, testing for various astronaut operational conditions (duration between start and end of work time) also results in correct computations as long as the equation for the direct energy supply, presented in the inputs description of Unit 2, and derived from the astronaut schedule in figure 8.7 remains the same. Furthermore, for a couple of sols, all the model computations have been carefully performed by hand to have a clear indication for the lack of programming errors in the model.

Furthermore, it is considered that this model cannot be validated at the current design stage. As it is simulating the power distribution over the year considering the given energy resource availability and the technology at hand, the quantified values of all those must be validated before the system performance model. Additionally, one of the most critical aspect that must be evaluated before the validity of this model could be estimated, is the operations software of the central power control unit. As the model described defines the supply paths through the examination of the dominant, auxiliary and direct supply conditions, it must be validated that the power distribution station will be programmed in a similar manner. Otherwise, the function of Unit 4 should be change accordingly to accurately simulate the decisions taken by the control unit.

9.5. Conclusion and Recommendations

In this chapter, the complementary operations of the wind and solar subsystems and the interaction with the battery, CAES and microgrid is evaluated by the developed and documented system performance model. The model considers the astronaut schedule and the variation of in sunrise and sunset times as a result of the eccentricity of Mars' orbit and planet inclination angle. Moreover, the system design is iterated through exchanging required energy production and actual kite energy production data files with the airborne wind energy design team. From those, the normalised wind conditions representing what fraction of the total supply can be met are computed. Similarly, from the variation in solar irradiance through the year, the solar conditions are evaluated by setting a the maximum condition to be equal to 0.35. Furthermore, the generation periods for the wind system are defined to be equal to -1 hour from sunrise and +1 hour from sunset for spring, summer and autumn; for winter the offset from the sunrise and sunset is equal to 2 hours.

With those inputs the function defining the systems operation as presented in figure 9.3 is executed for each sol and the results are visualised in graphs 9.6 to 9.17. Moreover, the power mix values are presented in table 9.1 and the final evaluated subsystems sizes are the following. First, the kite size and the uncertainties are documented in chapter 11. The solar array must have an area of 70m^2 with 5% contingency. The required battery capacity is 116kWh with 5% contingency. The microgrid should be able to facilitate a power input of 26kW with a contingency of 5%, and lastly the required supply through the CAES is equal to 6.5MWh with a contingency of 10% as this is the most input sensitive subsystem. Furthermore, from the net charge of the CAES it could be evaluated that the mission should be started in autumn/winter in order enough energy to be stored for the summer supply. Additionally, a sensitivity analysis of the system design is performed and the new design sizes are evaluated for a different power requirements. The configuration selected depicts a system which must deliver a power output of 7.5kW for work operations and 5kW for rest and the results are discussed in subsection 9.3.2. Following, the verification and validation procedures for examining the credibility of the following model are documented in 9.4.

The weak parts of the model have been examined and recommendations included on how to improve these. First, it is evident that there is modelling error associated with the assumption of the direct energy fraction of the dominant source for the supply evaluation of the auxiliary one as part of the computations of Unit 4. In order, to rectify that a more in-depth analysis of the system interactions during the hours of a Martian sol must be evaluated. It should be modelled what the daily nominal energy generation of each subsystem is and how those interact with each other to meet the demand. Furthermore, the function that defines the operational path selected by the power distribution control unit is not optimal. The function facilitates the simulation of hybrid, non-hybrid, wind- or solar-dominant system configurations at the expense of modelling errors. Therefore, a new or modified function must be programmed for the specific system design which simultaneously evaluates the supply and generation through considering the actual decision the power control unit will take given the generated energy.

Power Management and Distribution System Design

Every energy system requires a well-engineered power management and distribution system. Its purpose is to ensure the reliable delivery of electrical power to the habitat. The system consists of a microgrid, and it integrates the primary and secondary energy resources, as well as energy storage. After the establishment of its requirements in 10.1, a summary of the trade-off is provided in 10.2. The system's architecture and interfaces follow in 10.3, after which the subsystem sizing in 10.4 is treated. The cost breakdown in 10.5 is presented, followed by an assessment of the risk associated with a microgrid on Mars in 10.7, and sustainability and retirement is also taken into account in 10.8. In the penultimate section 10.9 of this chapter, a compliance matrix is set up and a sensitivity analysis is done. The chapter is concluded with 10.10, containing recommendations for further design activities.

10.1. Requirements

The requirements from section 5.2 that are relevant for the design of the power management and distribution system are displayed again in table 10.1.

Table 10.1: Power Management Requirements List

Requirement ID	Description
REM-Sys-N06-01	The power distribution system shall be able to support a peak power input of 26 kW.
REM-Sys-N06-05	The power distribution system shall have a maximum mass of 400 kg.
REM-Sys-N06-06	The overall efficiency of the power management and distribution system shall be at least 85%.

10.2. Trade-off Summary

Many configurations for a power management and distribution system are possible. In order to choose the best one for this mission, two trade-offs were performed. In the first one, a DC microgrid was traded off against an AC microgrid. The DC microgrid was selected, mainly because this grid type requires less power converters, which is favourable in terms of mass, volume and efficiency. Subsequently, a feasible cable infrastructure for distribution was selected, for which the three options were: underground; on-ground and overhead. After a qualitative trade-off, the underground cable option was chosen. This provides better protection from the Martian environment, and lower material needs as opposed to an overhead infrastructure. The on-ground infrastructure was deemed too hazardous. For the complete documentation on the trade-offs, the reader is referred to the Mid-term report [24]. The selected design options are DC microgrid and underground cable infrastructure.

10.3. System Architecture and Interfaces

The microgrid is the system which interconnects the distributed energy resources (DERs), the energy storage facilities, and the habitat, where consumption of the electrical energy happens. A schematic of the system architecture is shown in figure 10.1. It shows how each subsystem is integrated into the energy distribution system. The most critical system elements of the microgrid are the following:

- **Power Electronic Converters:** In order to connect a power source to the DC bus, it must be ensured that the output voltage is electronically transformed to the correct DC bus voltage, which is held constant at a certain value for distribution. Furthermore, if the power source generates AC power instead of DC, it must be converted through a rectifier. Similarly, the voltage needs to be transformed for a power sink, and if necessary, the direct current must be converted to AC using an inverter. All power electronic converters present in the microgrid are represented by the square boxes in the figure.

- **DC bus:** The grid bus is the common connection to which all power sources and sinks are connected in parallel. Together with the power cables, the function of the bus is transmission of electrical power.
- **PDU:** The Power Distribution Unit (PDU), is a component that monitors the flow of electrical power, and distributes it according to the algorithm described in section 9.1.
- **Central controller:** this component exchanges information with the local controllers, the PDU and the habitat. The communication links are depicted in figure 10.1. The central controller collects measurements of the state of the electrical power at various points, and gives commands to ensure an adequate generation, distribution and consumption of electrical power.

The schematic shows blue arrows, indicating power losses over various components in the grid. The efficiency of these components will be further elaborated upon in section 10.4.

Finally, the system boundary of the microgrid is indicated by the purple dotted area. At this boundary, power is injected into (or withdrawn from) the microgrid by the energy subsystems and the habitat.

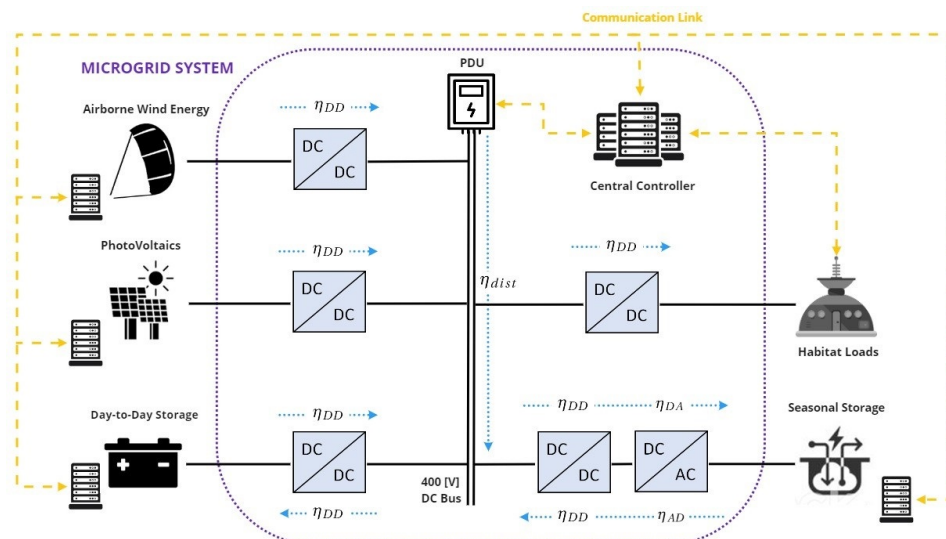


Figure 10.1: Schematic of the microgrid system architecture and its interfaces

10.4. Subsystem Sizing

In order to do a proper analysis of the performance of the complete energy system, it is crucial to get acquainted with the power losses in the microgrid. In effect, a fraction of the electrical power is lost by transmitting it through the conducting cables, as well as by transforming it to higher or lower voltages, or by converting it from AC to DC and vice-versa. But before the efficiencies of the converters and the distribution cables can be defined, a feasible voltage for the grid must be chosen.

As a consequence of a literature study on optimal voltage levels for DC microgrids [5], it was chosen to go for a bus voltage of $U_{grid} = 400$ V. This is a relatively high voltage, and is motivated by the fact that a high voltage reduces the current that flows through the system for the same amount of power. This is beneficial for the transmission efficiency, as will be seen later in this section. Furthermore, this voltage level has already been used in DC datacentres, which means that it is likely that technology is more available for this voltage level.

10.4.1. Power Converter Selection

As explained in section 10.3, many power electronic converters are required for an adequate distribution of power in the grid. They must be properly selected in order to guarantee the highest efficiency, for the lowest mass and volume. This turned out to be a great challenge. Off-the-shelf components for Earth applications were deemed unfeasible, because they are generally too bulky and heavy. On the other hand, space-qualified converters are typically designed for lower power and voltage ratings, and don't fit the purpose of this project either.

Advances in material technologies will allow for compact high-power converters in the near future. A promising technology is Silicon Carbide (SiC), which is a game changer for aerospace power electronic applications because with this material, high power densities can be achieved. For our mission, state-of-the-art SiC power

converters for Aerospace applications were selected. These converters have similar power ratings as the ones from the DC microgrid, which accommodates a voltage of $U_{grid} = 400$ V and a peak power of $P_{peak} = 26$ kW. From datasheets, the most relevant parameters were taken and summarised in table 10.2.

It should be pointed out that these components are designed for use on Earth. The Martian environment has a substantially different impact on the equipment. In order to guarantee the proper functioning of these power converters, protection is needed from the Martian environment that is harmful to the equipment and their operation. That is, it needs to be protected from cosmic ionising radiation, solar radiation, extreme temperatures and their fluctuations along with dust.

Due to extra measures taken to protect the power converters from the hostile Mars' environment, the mass, volume and cost (which will be further elaborated in section 10.5) of these components are assumed to increase by 20%, 10% and 50% respectively. The efficiency is considered a design parameter and is assumed to be kept the same. The adjusted parameters are presented in table 10.3.

Table 10.2: Power electronic converter data

Type	Efficiency	Mass [kg]	Volume [m^3]
DC/DC ¹	$\eta_{DD} = 95\%$	11.0	$2.3 \cdot 10^{-2}$
DC/AC ²	$\eta_{DA} = 98\%$	0.9	$6.2 \cdot 10^{-3}$
AC/DC ³	$\eta_{AD} = 97\%$	6.4	$5.3 \cdot 10^{-4}$

Table 10.3: Data after accounting for protection from Mars' environment

Type	Efficiency	Mass [kg]	Volume [m^3]
DC/DC	$\eta_{DD} = 95\%$	13.2	$2.5 \cdot 10^{-2}$
DC/AC	$\eta_{DA} = 98\%$	1.1	$6.9 \cdot 10^{-3}$
AC/DC	$\eta_{AD} = 97\%$	7.7	$5.8 \cdot 10^{-4}$

10.4.2. Efficiency of the DC Microgrid

Now that the efficiencies of the power electronic converters are established, the next step is to compute the cable losses in the distribution system, η_{dist} . Because these power losses depend on the cable length, first the microgrid layout and the positions of the subsystems on the site location must be decided. A few aspects require specific attention.

From equation 10.3, which will be derived in the upcoming paragraphs, it becomes clear that the power losses in the conducting cables are increased when the cable length is increased. From this point of view, all the subsystems should be located as close as possible to each other and the habitat. However, from a safety point of view, the CAES must be placed away from the habitat and the other subsystems. Therefore it is placed at a minimum distance of 150 m from all other subsystems.

Furthermore, the PV system must be placed such that no shadows are cast on the system. Therefore, it is placed directly south of the pumping kite power system, at a distance of 375 m from the ground station. With a maximum tether length of 400 m and a minimum elevation angle of 25 degrees, the kite can never fly directly above the PV system. Moreover, because the habitat is located on the northern hemisphere of Mars, the Sun is always on the south side of the system. Therefore the kite cannot block any incident sunlight on the PV system. The final energy system layout is schematically visualised in figure 10.2.

With the cable length known, the distribution efficiency η_{dist} can be approximated for each electrical path. That is, the power losses that occur inside the conducting cables due to DC resistance, for each possible path from supply to demand. The power loss is expressed as:

$$P_{loss} = I^2 \cdot R \quad (10.1)$$

Where I is the current flowing through the conductor, and R is the DC resistance of the conductor. The latter is computed as:

$$R = \rho_{DC} \cdot \frac{L}{A_c} \quad (10.2)$$

Where ρ is the electrical resistivity of the conducting material, L the length of the conductor and A_c the area of the conductor. By combining equations 10.1 and 10.2, the distribution efficiency can be computed:

$$\eta_{dist} = \frac{P - P_{loss}}{P} = 1 - \frac{I^2 \cdot R}{P} = 1 - \frac{\left(\frac{P}{U}\right)^2 \cdot \rho_{DC} \cdot \frac{L}{A_c}}{P} = 1 - \left(\rho_{DC} \cdot \frac{P \cdot L}{U^2 \cdot A_c} \right) \quad (10.3)$$

¹<https://www.tame-power.com/en/dc-dc-converters/dcdc-non-isolated-converters> [Accessed 15 June 2020]

²<https://www.ie-net.be/sites/default/files/Siemens%20eAircraft%20-%20Disrupting%20Aircraft%20Propulsion%20-%20OO%20JH%20THO%20-%2020180427.cleaned.pdf> [Accessed 15 June 2020]

³<https://www.craneae.com/Products/Power/datasheets/PSLB4230.pdf> [Accessed 15 June 2020]

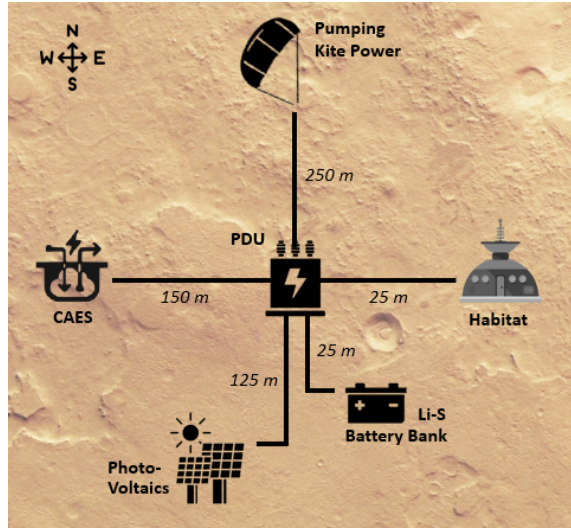


Figure 10.2: Schematic visualisation of the microgrid layout

In this equation, U is the grid voltage, and P is the electrical power (U times the current through the conductor). One can understand that the power in the system is not constant at all times; hence the efficiency also varies throughout the day and throughout the season. For computing the distribution efficiency, a value of 26 kW is taken, which is slightly above the peak power that may occur during a Martian year. The area of the conductor was based on off-the-shelf cables with similar power and voltage ratings. Lastly, a conductor material needs to be selected for the cables. The two most common materials are aluminium and copper. Although copper has a lower resistivity, it does not weigh up to the volumetric mass density of aluminium, which is about three times smaller than the density of copper [89]. Therefore, aluminium is chosen as the conducting material for the cables. The cable parameters are summarised in table 10.4. It is noteworthy that, unlike the power converters, the cables do not increase in size or cost, because it is assumed that the cables are already sufficiently shielded from Mars' hostile atmosphere by installing them underground.

Table 10.4: Cable parameters used for sizing the microgrid

Cable Parameters		
Area A_c	50	[mm ²]
Power P	26	[kW]
Voltage U	400	[V]
Resistivity ρ_{DC}	$29 \cdot 10^{-9}$	[Ω · m]
Volumetric mass density ρ	2700	[kg · m ⁻³]

With the cable parameters from table 10.4 and the lengths from figure 10.2, the distribution efficiency can be computed for each electrical path using equation 10.3. As documented in chapter 9, the power generated can be supplied to the load in three ways. Either directly from supply to load, or through the battery or CAES storage system. These are different electrical paths, and all have their own efficiency, because the total length of cable traversed by the current is different. The cable length can be graphically determined for each electrical path from figure 10.2. The resulting distribution efficiencies are presented in table 10.5.

Finally, the electrical path efficiency can be calculated by taking the product of the distribution efficiency, and the efficiencies of all power electronic converters that are on that particular path. For example, the path efficiency from the PV system to the load via the battery is: $\eta_{dist} \cdot (\eta_{DD})^4 = 80\%$, because 4 DC/DC converters are required to distribute the power on this electrical path. The calculation is done for every possible electrical path, and the results are shown in the last column of table 10.5.

10.4.3. Mass and Volume of the DC Microgrid

With the data from the previous subsection, an estimate on the mass and the volume of the system can be done. As figure 10.1 suggests, the microgrid requires a total number of 5 DC/DC converters, 1 DC/AC converter and 1 AC/DC converter (this is because accommodating the CAES into the system requires a rectifier and an inverter separately). With the power converter parameters from table 10.3, it adds up to a total mass of 74.8 kg, and a total volume of 0.133 m³ for all power electronic converters together.

Table 10.5: Electrical path efficiencies

Electrical path	Cable length [m]	Distribution efficiency [%]	Path efficiency [%]
Kite - Load	275	97.4	87.9
Kite - Battery - Load	325	96.9	79.0
Kite - CAES - Load	575	94.6	72.5
PV - Load	150	98.6	89.0
PV - Battery - Load	200	98.1	79.9
PV - CAES - Load	450	95.8	73.4

Concerning the power cables, they consist of an inner core of aluminium, which is the conducting material, and an outer shell of insulating material. The sum of all cables, as determined from figure 10.2, has a total length of $L = 575$ m. The cross-sectional area of the conductor is $A_c = 50$ mm². Therefore the total volume of the conducting material is $V = L \cdot A_c = 0.029$ m³. As the density of aluminium is known from table 10.4, the mass is easily computed, resulting in a value of $m_{conductor} = 78$ kg.

Now, the estimation for the insulation material is a bit more difficult. This calculation is based on a typical ratio of conductor weight to insulator weight, derived from the aluminium cables from Helukabel⁴. It is derived that for a relatively small conductor cross-section of 50 mm², the weight of the conductor and the insulator together are typically 150% of the weight of the conductor alone. Therefore the total cable mass is estimated to be: $m_{cable} = 1.5 \cdot 78 = 117$ kg.

With these calculations, the subsystem sizing is concluded. The design results are summarised in the next section.

10.5. Cost Breakdown

In order to present a preliminary cost estimation, the cost of the power converters and cables was investigated. As this data is not publicly available, the companies that develop these components were contacted. Concerning the cables, the cost per meter is €4 [A. Veltman, personal communication, 18 June 2020]. For a total cable length of 575 m, this adds up to a total cost of €2300 for the power cables.

The power electronic converters are more expensive. As for the DC/DC converters, they are priced at €6000 per component [P. Plantard, personal communication, 15 June 2020]. The AC/DC converter is slightly cheaper; it comes at a cost of ca. €5000 [S. Lai, personal communication, 19 June 2020]. Unfortunately, it was impossible to gain information on the cost of the DC/AC converter. However, because the inverter is extremely compact for its power rating, it is assumed that this component is more costly. The cost is estimated at €10000.

As explained in section 10.4, the cost of the power electronic converters is assumed to increase by 50% as a result of adjusting the equipment to the Martian environment. Therefore, the cost of the DC/DC converter, rectifier and inverter become €9000, €7500 and €15000 respectively. The total cost of the DC microgrid will be summarised in the next section.

10.6. Subsystem Design Results

In the previous sections, the architecture of the DC microgrid has been established, and the power converters and cables have been sized. The path efficiencies have been calculated and are accounted for in the sizing of the other subsystems. A total of 5 DC/DC converters, 1 DC/AC and 1 AC/DC converter are required for power distribution. The mass, volume and cost of the DC microgrid are summarised in table 10.6.

Table 10.6: Subsystem Design Results

	Mass [kg]	Volume [m³]	Cost [€]
Power converters	74.8	0.133	67500
Power cables	116.4	0.102	2300
Total	191.2	0.235	69800

⁴https://www.helukabel.com/publication/de/brochures/cw/cw_brochure_aluminium_2015_en.pdf [Accessed 17 June 2020]

10.7. Risk Assessment

Now that the sizing of the power management and distribution has been completed, it is time to assess the risks associated with the microgrid. Power management makes or breaks the continuous supply, as even if the energy is generated at one place, it has to be transported to the habitat. There is little to no margin in operation, thus the threats and risks associated with it have to be evaluated. The FMA and the scores of likelihood and impact can be seen in table 10.7 and the risk matrix before mitigation is presented in figure 10.3.

Table 10.7: Failure mode analysis of power management

ID	Failure mode	Likelihood	Impact
DC-01	Mismatch in supply and demand	3	5
DC-02	DC-DC converter failure	3	3
DC-03	Rectifier failure	2	5
DC-04	Inverter failure	2	5
DC-05	Transmission cable failure	1	5

Table 10.8: Revised likelihood and impact scores of power management after mitigation

ID	Likelihood	Impact
DC-01	2	5
DC-02	2	3
DC-03	1	5
DC-05	1	5
DC-05	1	4

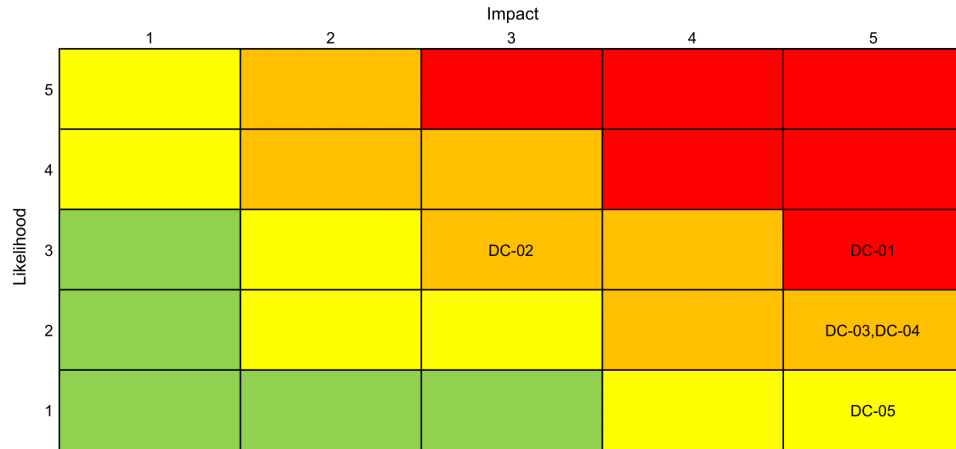


Figure 10.3: Risk matrix before mitigation of power management (red: extreme risk, orange: high risk, yellow: moderate risk, green: low risk)

In order to mitigate the risks, the following measures were established:

- **DC-01:** In the worst case scenario, the grid can experience a total blackout if there is a mismatch in supply and demand. By implementing dedicated control strategy, and by monitoring the power input and output, system balance can be guaranteed. On the other hand, one can make sure that the demand is always met: either by oversizing the supply (by the CAES and secondary battery) or by energy dissipation when the demand is lower.
- **DC-02:** The worst case scenario is a total blackout. Careful measurements of power input & output have to be implemented. In case one fails, the grid can still operate as there is a small voltage margin that it can work with.
- **DC-03/04:** These elements are used for CAES and are not yet mature. The likelihood of the risks can be reduced by additional research and timely inspection& maintenance.
- **DC-05:** Circuit breakers can be implemented in each power line, so if one fails energy can be sourced from other location. When a transmission cable fails, emergency mode has to be initiated after which the power supply can be continuous until the cable is fixed.

Besides these measures and due to the importance of power management, each component has to be inspected and monitored on a regular basis to avoid any of these risks. The revised likelihood and impact scores can be see table 10.8 and the risk matrix after mitigation in figure 10.4.

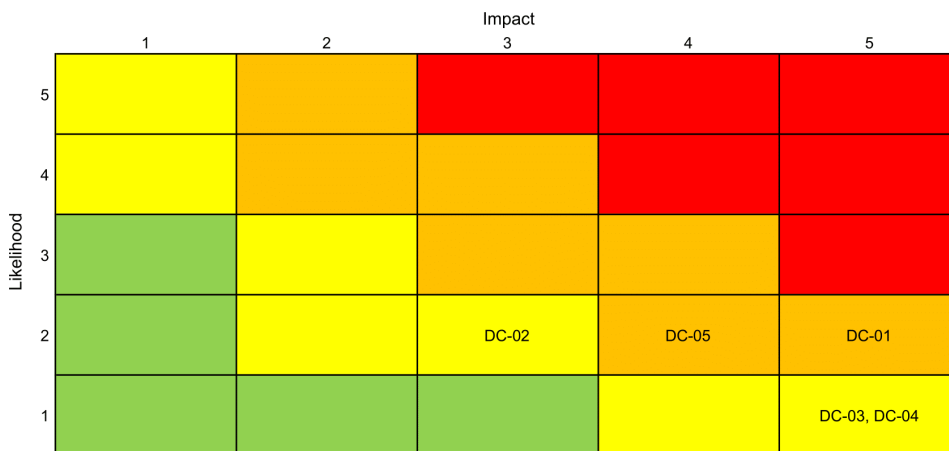


Figure 10.4: Risk matrix after mitigation of power management (red: extreme risk, orange: high risk, yellow: moderate risk, green: low risk)

10.8. Sustainability and Retirement

For the operation of the power management circuit, the biggest impact on the Martian environment will be the installation of the underground cabling. As was concluded in the Midterm Report [24], this is still preferred over on-ground cables, due to lower vulnerability to damage (thus less replacement material) and no additional manufacturing nor transportation for support structures. For the construction of the underground cabling, the rovers from the Rhizome Habitat team will be used, using only in-situ resources. As the cable life-time is in all probability longer than the life-time of the entire system, these can still be used if the mission is extended after five Martian years. Otherwise, the cables can be recycled after-life,⁵ preferably on Mars, if the tools will be available, and otherwise on Earth. The same goes for the PDU. Existing PDUs show a potential recyclability ratio of 55% with current recycling methods⁶, which will hopefully continue to improve in the coming years.

10.9. Requirement Compliance and Sensitivity Analysis

In table 10.9, it is discussed whether or not the design of the power management and distribution subsystem complies its requirements, established in section 5.2.

Table 10.9: Power Management System Compliance Matrix

ID	Compliance	Proof (which section)
REM-Sys-N06-01	Yes	Subsections 10.4.1 and 10.4.2, this was a design criterion and the power conversion equipment and cables have been sized after this requirement
REM-Sys-N06-05	Yes	Section 10.6, the total mass is estimated at ca. 190 kg
REM-Sys-N06-06	Probable	This requirement is difficult to evaluate and arguably irrelevant. Because of the complex power flow, each electrical path has its own efficiency, the lowest being 73.2% and the highest being 89.0%, as presented in table 10.5

Before the design of the subsystem is concluded, it is important to address the effects of slight changes in design parameters through a sensitivity analysis. As the power management and distribution efficiency has a big impact on the size of the other subsystems, it is needless to say that a slight change in e.g. power conversion efficiency will have a considerable effect on the entire energy system. A few scenarios are suggested and worked out. For each scenario, one parameter changes while the others remain constant.

1. The day-time power requirement is decreased to 7.5 kW as described in section 9.3.

As a result from reducing the power consumption, the peak power in the microgrid is decreased from 26kW to 21kW. For the same grid voltage, this reduces the amount of current that is transmitted through the system and hence increases the distribution efficiency as stipulated by equation 10.3. It will probably

⁵https://www.helukabel.com/publication/za/spec_pages/heluwind-wk-powerline-alu-105-c-0-6_1kv.pdf [Accessed 21 June 2020]

⁶https://download.schneider-electric.com/files?p_enDocType=Product+environmental&p_File_Name=GWOG-8WKL2C_R0_EN.pdf&p_Doc_Ref=SPD_GWOG-8WKL2C_EN [Accessed 21 June 2020]

also be possible to select smaller power electronic converters, designed for slightly lower power ratings, saving mass and volume.

2. The distance of each subsystem to the habitat is increased.

In this situation, all length units from figure 10.2 are increased by a factor 2. This means that the power needs to be transmitted over longer distances, which decreases the distribution efficiency as governed by equation 10.3. Straightforwardly, if the cable length is doubled, then also the mass and volume increase by a factor 2.

3. The efficiency of each power electronic converter is lowered by 2%.

As depicted in figure 10.3, the power must be transmitted over quite a few power electronic converters. Each time it is passed through such a component, the distribution efficiency is multiplied by the efficiency of that specific component. As will be seen from table 10.10, it is clear that the total efficiency drops a lot in this scenario: almost by 10% in some cases.

4. The grid voltage is set to 200 V

When the grid voltage is set to a lower value, the distribution efficiency reduces substantially, because the voltage is squared in equation 10.3. This has a significant impact on the total path efficiency. For some cases, it even decreases with more than 10% as can be seen from the last column in table 10.10.

The effect of the changes in design parameters from the different scenario's described above is summarised in table 10.10. It can be observed that many factors influence the efficiency of the microgrid. It should be pointed out that designing a renewable energy system is an iterative process. Due to time constraints, the project only allowed for a few iterations. Perhaps by reiterating a few design choices, the efficiency can be even further increased in the future.

Table 10.10: Sensitivity analysis of the electrical path efficiencies

Electrical path	Efficiency [%]				
	Design	Scenario 1	Scenario 2	Scenario 3	Scenario 4
Kite - Load	87.9	88.4	85.6	84.2	80.9
Kite - Battery - Load	79.0	79.4	76.5	72.5	71.5
Kite - CAES - Load	73.2	74.0	69.0	64.5	60.6
PV - Load	89.0	89.2	87.7	85.3	85.1
PV - Battery - Load	79.9	80.2	78.4	73.4	75.3
PV - CAES - Load	74.1	74.8	70.9	65.3	64.3

10.10. Recommendations

In this chapter the design of the power management and distribution system has only been designed and presented to a certain preliminary level. The design of the subsystem can be further refined if the following recommendations are taken into account.

Firstly, it should be pointed out that no verification and validation has been performed for this subsystem yet. To verify the behaviour of the power management and distribution system, it is recommended to model and simulate the complete renewable energy system in Simulink. A more elaborate description of this is presented in section 18.3.

Next, the PDU and the central controller have been neglected in the subsystem sizing. These are complex system components that govern power flow in the system. Using optimisation algorithms, power flow can be controlled such that the power losses in the microgrid are even further reduced. One of the next steps in power management and distribution design, would be to put effort into researching these components, and to adopt efficient control strategies.

Furthermore, it would be advised to design for the protection and grounding of the subsystem. As stated in the mid-term report [24], this is one of the challenges that is faced in DC microgrids. This will be particularly difficult on the Martian surface.

Also, a great deal of research should be done on power electronic equipment. If SiC power converters are uniquely designed for the ARES mission, efficiencies of 99% can be reached. Using high switching frequencies (in the order of MHz), significant weight reductions can be achieved, while still being able to withstand loads from the launching environment. Research must also provide a solution for how these power converters are to be protected from the Martian environment. Especially cosmic radiation is harmful to SiC semiconductor material, as it interferes with the electric field inside the converter, limiting the voltage blocking capability of the material.

Lastly, it must be stressed that thermal regulation of the equipment should be taken care of in future design steps. Not only for power management equipment, but for example also the generator and supercapacitor from the ground station, and the lithium-sulphur battery bank need dedicated thermal control. The operating temperature range for this equipment is much narrower than the fluctuations in temperature that occur in the Martian atmosphere. In addition, the extremes in temperature (especially the low temperatures) are far outside the operating temperature range of the sensitive components of the renewable energy system. Reliability of the power management and distribution system can only be guaranteed if thermal control of the system is taken care of.

Primary Energy System Design

In this chapter, the process and results of the primary energy system design are described and presented. After listing the requirements in section 11.1, a summary of the trade-offs performed in the baseline and midterm is given in 11.2. The wind resource is assessed in 11.3, followed by a description of the system architecture in 11.4. The system model is elaborated upon in 11.5, after which the sizing process and its results are presented in 11.6. A structural and material analysis is performed in 11.7. The system cost is broken down in 11.8, the model verification and validation procedures are discussed in 11.9, which is followed by a risk assessment in 11.10. System sustainability strategy is given in 11.11, after which the requirements compliance matrix along with the sensitivity analysis results are shown in 11.12. Finally, recommendations on future design steps are given in 11.13.

11.1. Requirements

The following requirements, shown in table 11.1, were either given or generated for the AWE system.

Table 11.1: Primary energy system requirements

Requirement ID	Description
REM-Sys-N02-01	The primary energy system shall have a maximum mass of 200kg.
REM-Sys-N02-02	The primary energy system shall have a cut-in wind speed of 7 m s^{-1} .
REM-Sys-N02-03	The primary energy system shall have a cut-out wind speed of 35 m s^{-1} .
REM-Sys-N02-05	The tether shall withstand a tether force of up to 22500 N.
REM-Sys-N02-06	The tether shall have a creep SSL longer than the mission duration.
REM-Sys-N02-07	The tether shall have a bending fatigue SLL longer than the mission duration.
REM-Sys-N02-08	The ground station total mechanical-to-electric power efficiency at nominal wind velocity shall be above 90 %.
REM-Sys-N02-09	The ground station generator shall be rated at 80 kW.
REM-Sys-N02-11	The ground station shall be able to power the motor with 18.5 kW.
REM-Sys-N02-12	The ground station shall support a reel-out speed of 10 m s^{-1} .
REM-Sys-N02-13	The ground station motor shall support a reel-in speed of 25 m s^{-1} .

11.2. Trade-off Summary

During the midterm report phase of this project, trade-offs were made to decide on the design of the wind energy system. The first big trade-off was between a Vertical-Axis Wind Turbine (VAWT) of the inflatable buoyant type and an Airborne Wind Energy (AWE) system. The AWE concept won in the trade-off, outperforming VAWT significantly with regards to specific power and ease of system installation.

Whilst the gravitational force is not as strong on Mars as on Earth, the average air density is way lower. To produce enough lift to counteract the kite weight, it was found that an almost six times higher flight velocity than on Earth was required. This made using heavy rigid wing structures similar to ones used on Earth unfeasible, and removed the feasibility of using drag-type systems. Aerostatic AWE designs were considered too similar to the discarded VAWT concept. Rotary AWE technology did not reach sufficient technology maturity to allow for its design, and drone-like concepts were found to violate mass and volume constraints heavily. Based on these findings, a pumping kite power system was chosen as the final AWE concept.

A tensairity kite concept (semi-rigid wing) was chosen for its high specific performance. The tether was chosen to be made of braided HMPE DM20 fibres in 12 strands (6 clockwise, 6 anti-clockwise).

11.3. Wind Resource

In order to be able to assess the performance of the wind system, the wind distribution has to be known throughout the mission duration. So far, winds have not been recorded at an altitude of more than 1.5-2 m

[61] and no Mars wind field has been established as of yet [95]. The kite is to be operated at altitudes of hundreds of metres, thus a vertical wind profile is needed in order to correctly estimate the power output of the system. On the other hand, this poses great risks to the project as errors in assumed wind profiles can exceed 100%¹. Nevertheless, to be able to continue, two profiles were established: log wind profile and power law wind profile. The log wind profile has already been used in the past in Martian conditions [85, 93], while the power law wind profile is used to determine a second set of values. These mark the boundaries of the operational regime, which is necessary to check the sensitivity of the calculations.

Lorenz [70] fitted the Viking II data to Weibull distributions for different sol ranges. In order to account for the different location, the General Circulation Model was used from Fenton and Richardson [46] and no changes were made as the two locations show similar velocities. The mean wind velocities were determined for spring, summer, autumn, winter and dust storm season. The values can be seen in table 11.2.

The log wind profile is given by equation 11.1. The first term represents the logarithmic profile, while the second one is the stability term. The contribution of ψ can be neglected, when neutral stability is assumed. The assumption is valid as the stability term is usually not used in the industry and also omitted by Read and Lewis [85].

$$u = \frac{u^*}{\kappa} \left[\ln \left(\frac{z}{z_0} \right) + \psi(z_a, z_0, L) \right] \quad (11.1)$$

The Von Kármán constant (κ) is taken to be 0.4, equal as on Earth [85, p.190][93, p.24556]. Heavens et al. [53] used an analytical model and satellite data to determine the surface roughness (z_0), which is 3.16 cm at the site location. The friction velocity can be calculated with the mean wind velocities and the fact that the measurement unit of Viking II is located at 1.6 m. Once the operational altitude is also known, the mean wind velocity at altitude z_a is given by equation 11.1, which together with k (table 11.2) defines a Weibull probability distribution function (equation 11.2).

$$f(v) = \frac{k}{u} \left(\frac{v}{u} \right)^{k-1} \exp \left[- \left(\frac{v}{u} \right)^k \right] \quad (11.2)$$

The power law wind profile is given by equation 11.3. The early work of Kármán [65] showed that under neutral stability conditions the exponent (α) is 1/7 as is also confirmed by Spera and Richards [91]. As before, reference height ($z_r = 1.6m$) and reference velocity (u_r) are based on Viking II measurements.

$$\frac{u}{u_r} = \left(\frac{z_a}{z_r} \right)^\alpha \quad (11.3)$$

Combining the two results, a wind velocity regime can be established as seen in figure 11.1. The grey shaded areas are bounded by the power law and the log wind profiles as calculated before and define the extreme values for the Weibull distribution.

Moreover, the length of the seasons in order to calculate the power output of the respective season can also be seen in figure 11.2². Spring, summer, autumn and winter are consecutive and make up a full year, 669 sols. Dust storms last for approximately 35-70 sols and are frequent, but do not occur every year [6]. A single dust storm lasting 35 sols per (each) year was assumed for the sizing purposes of this mission. As the team is simulating only one year (instead of five distinct Martian years) and considering that the longest ever recorded global dust storm in 2018 lasted for 100 days, statistically 35 sols over two or three years is quite reasonable [51].

Local and regional dust storms can occur, but as these are usually only a few sols long, they were not considered in the analysis [77].

Table 11.2: Seasonal wind characteristics

Season	Mean wind velocity [$m s^{-1}$]	Friction velocity (u^*) [$m s^{-1}$]	k [-]	Length [sol]
Spring	3.5	0.357	1.3	194
Summer	2.6	0.265	1.58	178
Autumn	4.5	0.459	1.28	142
Winter	7.5	0.764	1.6	154
Dust storm	6.5	0.662	1.3	35

¹https://mepag.jpl.nasa.gov/meeting/2017-09/05_092517-MEPAG35-Aeolus-Colaprete.pdf [Cited 10 June 2020]

²<https://mars.nasa.gov/allaboutmars/extreme/martianyear/> [Cited 11 June 2020]

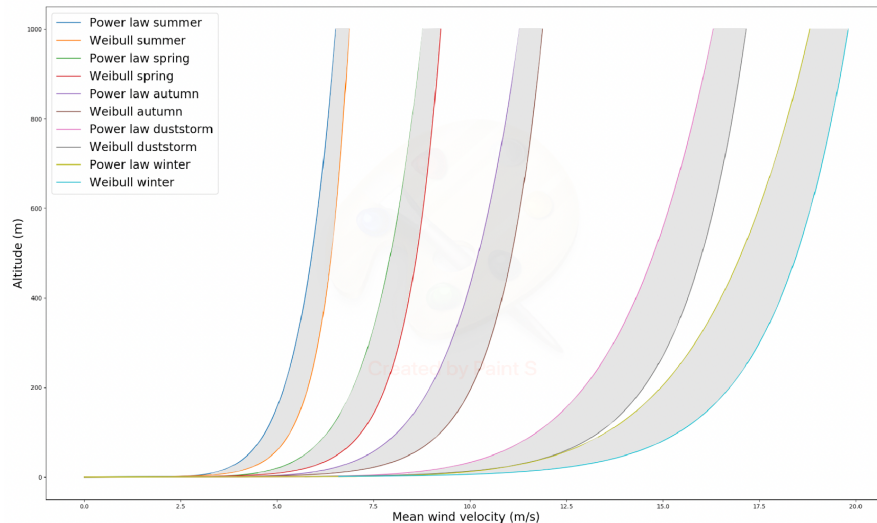


Figure 11.1: Height dependence of mean wind velocity for spring, summer, autumn, winter, dust storm season obtained from log and power law wind profile

Many researchers showed the strong diurnal characteristics of Martian winds, for example by von Holstein-Rathlou [99]. Although, this might be misleading as the diurnality is claimed based on wind direction and not wind velocity. Furthermore, as orbiters are usually in a sun-synchronous orbit, the measurement are taken at 2AM and 2PM in this case, which is then used to determine the wind distribution of the day³. Inspecting the Insight mission weather data, one can observe that wind speed variation from night to day are not significant⁴. The reason may be two-fold: at the time of writing this report (11 June 2020) the Insight rover was in the winter, which has the highest and most persistent wind speeds. On the other hand, the rover is located close to the Equator (3.0°N ; 154.7°E), where in general the wind speeds are the highest on the planet [46].

Due to these reasons, operable wind conditions are assumed to start one hour before sunrise and last one hour after sunset during spring, summer and autumn. For winter months two hours before sunrise and two after sunset are added to the day operation hours. These conditions were used in section 11.6.

11.4. System Architecture and Interfaces

The pumping kite power system combines a tether reel-out phase, in which the kite unwinds its tether from a drum connected to a generator; and a reel-in phase, in which a portion of this generated power is used to retract the kite back. The kite flies in cross-wind manoeuvres, thus increasing its apparent velocity above that of just the wind speed, and therefore producing larger aerodynamic forces. This aerodynamic force produces tension in the tether.

The tether is connected from the kite to the ground station, buried under ground. Out of this ground station, the kite can be released, and reeled back in if the current wind does not allow for operation or if maintenance is required. The ground station contains a drum, onto which the tether is wound. This drum is connected to an axial flux machine (motor/generator), which acts as a generator, producing energy during the reel-out phase, and as a motor, wounding the tether back onto the drum during the reel-in phase. The generated energy is sent mainly to the grid, but some of it is also sent to a supercapacitor in the ground station. The supercapacitor then provides both a smooth baseload to the grid along with the required energy to the motor to reel in the kite. A spindle mechanism is also present, ensuring that the tether is wound onto the drum in an appropriate way, along with brakes.

The ground station control system communicates with the central computer system, setting system operation mode based on the Habitat and wind conditions (measured by an anemometer). A three-region operational mode is ran, with tether force and generator power output as variables monitored by the sensors in the ground station.

The kite control unit (KCU) oversees the real-time operation of the kite, and through a combination of sensing units and actuators connected to a tether bridle system, can affect the aerodynamic properties, and thus manoeuvre the kite. This is done in order to control the tether force and thus the power generated by the system, described in 8.5.2.

³https://mepag.jpl.nasa.gov/meeting/2017-09/05_092517-MEPAG35-Aeolus-Colaprete.pdf [Cited 11 May 2020]

⁴<https://mars.nasa.gov/insight/weather/> [Cited 11 June 2020]

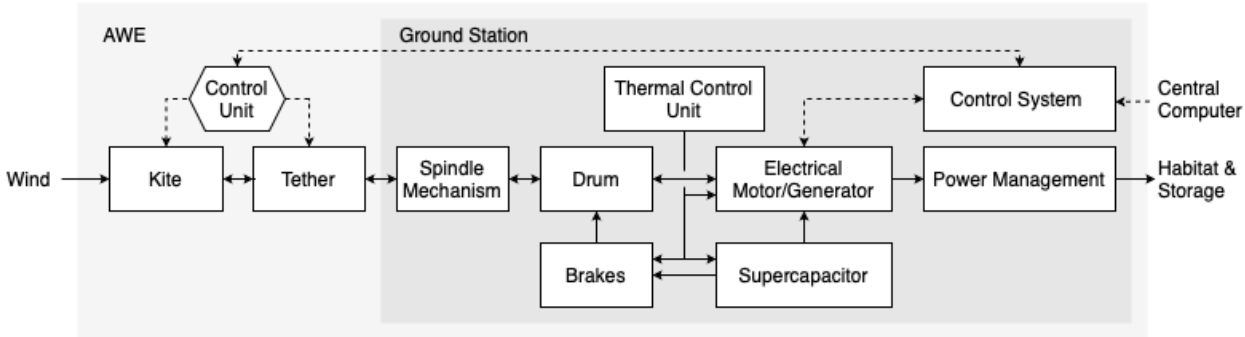


Figure 11.2: AWE system architecture. Solid lines stand for energy flows and dotted lines for communication flows.

11.5. AWE System Model

The various parts of the system model used to size and analyse the performance of the AWE system are presented in this section. After an aerodynamic analysis of the kite in 11.5.1, a description of the model from Luchsinger [71] is given in 11.5.2. In 11.5.3 an overview of the model used for more detailed ground station analysis from Fechner and Schmehl [42] is given, and the section ends with a detailed tether analysis model from Bosman et al. [15] in 11.5.4.

11.5.1. Aerodynamic Analysis

A tensairity kite was found to be the best option for this mission, mainly because of its specific performance and aerodynamic properties.

The drag coefficient of the airborne system can be divided into drag caused by the kite and by the tether. The following equation expresses the relation between the two and how the total drag coefficient is calculated [7]:

$$C_D = C_{D,k} + C_{D,t} = C_{D,k} + \frac{1}{4} \frac{d_t l_{top}}{A} C_{D,c} \quad (11.4)$$

Where $C_{D,k}$ and $C_{D,t}$ are the kite and tether drag coefficients respectively, d_t is the tether diameter, $l_{top} = 300\text{m}$ is the tether operational length which is assumed to be halfway between the ends of reel-out (400 m) and reel-in (200 m) phases, A is the kite projected area and $C_{D,c}$ is the cylindrical drag coefficient of the tether. To find this cylindrical drag coefficient first the Reynolds number is calculated for Mars using:

$$Re = \frac{\nu_w d_t}{\nu} \quad (11.5)$$

Where ν_w is the wind speed, d_t the tether diameter and ν the air viscosity on Mars, which is $5.17 \cdot 10^{-4} \text{ m s}^{-25}$. Assuming the tether to be subjected to a wind velocity ranging between 7 m s^{-1} and 35 m s^{-1} and a tether diameter of 6.5 mm, the Reynolds number is calculated to be between 90 and 440. For these Reynolds numbers, $C_{D,c}$ ranges from 1.2 to 1.8^5 . To account for the majority of the operational wind speeds, a single $C_{D,c} = 1.6$ value is used to calculate the tether drag.

The following table summarises the aerodynamic parameters of the system:

Table 11.3: System aerodynamic properties [17]

Property ...	Value
C_L	0.6	$C_{D,k}$	0.06	Wing span	15 m
C_D	0.077	$C_{D,t}$	0.017	Wing chord (avg)	3.33 m

11.5.2. Performance Analysis

The power produced in the reel-out phase and the power consumed in the reel-in phase depend on the reel-out and reel-in speeds respectively, which can be optimised in order to reach maximum overall cycle power. Two dimensionless factors are defined, $\gamma_{in} = \frac{v_{in}}{\nu_w}$ and $\gamma_{out} = \frac{v_{out}}{\nu_w}$, which represent the ratios between reeling speeds and wind speeds.

⁵<https://www.intechopen.com/online-first/aerodynamics-of-mars-2020-rover-wind-sensors>

⁶<http://brennen.caltech.edu/fluidbook/externalflows/drag/dragonaspHERE.pdf>

Considering a range of wind speeds, at some point along that range the system will have either reached its nominal tether force, or its nominal generator power. Three regions are defined based on these in a model made by Luchsinger [71], each using a different optimisation algorithm to maximise cycle power.

Region 1 $T_{out} < T_{nom}, P_{out} < P_{g_{nom}}$

The first region considers a wind speed where neither the nominal tether force nor the nominal power is reached. The following equation can be used to optimise the normalised cycle power f_c [71]:

$$f_c = \max_{\gamma_{in}, \gamma_{out}} \left\{ \left((1 - \gamma_{out})^2 - \frac{F_{in}}{F_{out}} (1 + \gamma_{in})^2 \right) \left(\frac{\gamma_{out} \gamma_{in}}{\gamma_{out} + \gamma_{in}} \right) \right\} \quad (11.6)$$

Where $F_{out} = \frac{C_L^3}{C_d^2}$, $F_{in} = C_d$ are the force factors during reel-out and reel-in phase. Factors γ_{out} and γ_{in} are independent of the wind speed in this region.

Region 2: $T_{out} \geq T_{nom}, P_{out} < P_{g_{nom}}$

The second region is defined by the range of wind speeds where the nominal tether force has been reached, but the nominal power has not. The reel-out tether force may not be increased beyond this point but the reel-out velocity may, allowing for the increase of the power output whilst accounting for limiting tether force:

$$P_{out} = T_{nom} v_{out} \quad (11.7)$$

The ratio between the wind speed and the nominal wind speed at which the nominal tether force is reached is defined as $\mu = \frac{v_w}{v_{n,T}}$. Considering this region, a new optimisation algorithm needs to be used to find the maximum cycle power. Since the reel out speed is now increased beyond the optimal value, a nominal factor γ_{out}^n is used and the maximisation function only optimises for the γ_{in} :

$$f_{c,\mu} = \max_{\gamma_{in}} \left\{ \left(\frac{1}{\mu^2} (1 - \gamma_{out}^n)^2 - \frac{F_{in}}{F_{out}} (1 + \gamma_{in})^2 \right) \left(\frac{\gamma_{in} (\mu - 1 + \gamma_{out}^n)}{\mu \gamma_{in} + \mu - 1 + \gamma_{out}^n} \right) \right\} \quad (11.8)$$

Region 3: $T_{out} \geq T_{nom}, P_{out} \geq P_{g_{nom}}$

The third region occurs when both the nominal tether force and the nominal power are reached and therefore both are limited from this point. This means that due to the relation between power and force, the reel out speed also has reached a constant nominal value. Therefore, the function can only optimise for the reel-in speed, along with decreasing F_{out} (reducing C_L):

$$f_{c,\mu} = \max_{\gamma_{in}} \left\{ \left(\frac{1}{\mu^2} (1 - \gamma_{out}^n)^2 - \frac{F_{in}}{F_{out}} (1 + \gamma_{in})^2 \right) \left(\frac{\gamma_{out}^n \gamma_{in}}{\gamma_{out}^n + \mu \gamma_{in}} \right) \right\} \quad (11.9)$$

Power Generation

As can be seen from the optimisation equations 11.6, 11.8, and 11.9, the different regions have different values for γ_{in} and γ_{out} .

These parameters can be used to calculate the reel-out and reel-in forces for the different regions and different wind speeds using:

$$T_{out} = \frac{1}{2} \rho v_w^2 A (1 - \gamma_{out})^2 F_{out} \quad T_{in} = \frac{1}{2} \rho v_w^2 A (1 + \gamma_{in})^2 F_{in} \quad (11.10)$$

Which, along with cycle times calculated by the equation below;

$$t_{out} = \frac{l_c}{v_{out}} \quad t_{in} = \frac{l_c}{v_{in}} \quad t_c = t_{out} + t_{in} \quad (11.11)$$

Provides enough values to continue the analysis and sizing of the system, see section 11.5.3.

11.5.3. Ground Station Analysis

In order to conceptualise the design of the ground station for the AWE system, it was first necessary to understand the requirements and constraints imposed on the system to ensure adequate operation and sufficient power generation. The characterisation of the operational envelope and performance of the system heavily relies on the nominal machine parameters of the ground station; however, the selection of the ground station machinery itself depends on the operational envelope as described by the AWE system performance analysis in subsection 11.5.2.

An implicit design obstacle is thus encountered, and for this reason, an iterative design approach was necessary to obtain an initial estimation of the annual wind energy production. The values for the first iteration were based on the parameters used by Fechner and Schmehl [42] for a 20 kW kite system concept, and the ground station of the Delft University of Technology as documented by Fechner et al. [45].

The maximal reel-in and reel-out speed were set to 8 m s^{-1} , the nominal tether force was set to 4 kN, and the nominal electrical generator power to 20 kW. Additionally, the radius of the drum was set to 16.15 cm, with a tether diameter of 4 mm, which translates into a ratio of $D/d_t = 80.75$. Using these parameters with the model-based efficiency analysis of a pumping kite power system as described by Fechner and Schmehl [42], the motor and generator efficiencies could be computed.

Firstly, it is important to realise that the efficiency of the generator is a function of the torque and rotational speed necessary to produce the optimal retraction force and reel-in speed. Likewise, the efficiency of the motor is a function of the optimal traction force and reel-out speed. Assuming that the optimisation algorithm of each of the three regions yields varying γ_{in} and γ_{out} , the reel-in and reel-out velocities can be computed for all wind speeds from the cut-in to the cut-out. With these values, the traction and retraction forces are calculated using equation 11.10, with which the reel-in and reel-out torques and rotational speeds can then be computed:

$$\tau_{in/out} = T_{in/out} \cdot r_{drum} \quad \omega_{in/out} = \frac{v_{in/out}}{r_{drum}} \quad (11.12)$$

Where $\tau_{in/out}$, $T_{in/out}$, and $v_{in/out}$ are the reel-in/out torque, tether force, and speed respectively; and r_{drum} is the radius of the drum around which the tether is wound. Using these values, the motor/generator friction torque can be computed as:

$$\tau_{fin/out} = \tau_{sin/out} + c_{fin/out} \cdot r_{drum} \cdot \omega_{in/out} \quad (11.13)$$

Where $\tau_{sin/out}$ is the (constant) static contribution to the friction torque and $c_{fin/out}$ is the dynamic friction coefficient. Using these values, the gross mechanical generator/motor torque can be obtained by:

$$\tau_g = \tau_{out} - \tau_{fout} \quad \tau_m = \tau_{in} + \tau_{fin} \quad (11.14)$$

And thus the gross mechanical actuator powers follow straightforwardly:

$$P_{m_g}^g = \tau_g \cdot \omega_{out} \quad P_{m_m}^g = \tau_m \cdot \omega_{in} \quad (11.15)$$

Where the sub-subscripts g/m refer to the generator and the motor respectively. These gross mechanical torques and rotational speeds will later be used to define the operational envelope of both actuators over the entire wind speed range. Once the aerodynamic loading experienced by the kite has been converted into a gross mechanical actuator torque, the losses pertaining to the conversion from mechanical to electrical power must then be accounted for. For this, we need to obtain the inverse of the torque constant ($c_{g/m}$) of the generator/motor to relate the gross mechanical torque to the associated electrical current. These are constant values expressed in A N m^{-1} and are usually provided by the manufacturer.

With this, the actuator current can be calculated through $I_{g/m} = \tau_{g/m} \cdot c_{g/m}$. With the terminal resistance (per phase) of the actuators ($R_{g/m}$), and assuming that the actuators use a three-phase winding configuration, the electrical losses ($L_{e_{g/m}}$) can be computed with:

$$L_{e_{g/m}} = \frac{3 \cdot R_{g/m} \cdot I_{g/m}^2}{k_{g/m}} \quad (11.16)$$

Where $k_{g/m}$ is a factor accounting for the higher resistance at operating frequency due the skin effect, stray-load losses, and other not explicitly modelled losses [42]. The gross electrical power of the generator ($P_{e_g}^g$) and the motor ($P_{e_m}^g$) can then be expressed as:

$$P_{e_g}^g = P_{m_g}^g - L_{e_g} \quad P_{e_m}^g = P_{m_m}^g + L_{e_m} \quad (11.17)$$

From which the actuator efficiencies can be computed by:

$$\eta_g = \frac{P_{e_g}^g}{P_{m_g}^g} \quad \eta_m = \frac{P_{e_m}^g}{P_{m_m}^g} \quad (11.18)$$

The pumping efficiency (η_p) could then be computed through:

$$\eta_p = \frac{P_{m_g}^g \cdot t_{out} - P_{m_m}^g \cdot t_{in}}{P_{m_g}^g \cdot t_{out}} \quad (11.19)$$

And the cycle efficiency follows by dividing the pumping efficiency by the loading factor defined in equation 11.26:

$$\eta_c = \frac{\eta_p}{F_L} \quad (11.20)$$

It is important to recall that during the reel-in phase, the motor is actually consuming energy. To avoid unwanted losses resulting from taking energy directly from the grid, a supercapacitor is present in the ground station which is charged during the traction phase, such that it can provide the necessary energy for the recovery phase. To account for this, first the gross electrical energy can be identified as the numerator of equation 11.21, where η_{sc} is the supercapacitor efficiency. With this, the gross electrical efficiency can be computed with:

$$\eta_e = \frac{E_e^g}{E_m^g} = \frac{P_{e_m}^g \cdot t_{out} - \frac{P_{e_m}^g \cdot t_{in}}{\eta_{sc}}}{P_{m_g}^g \cdot t_{out} - P_{m_m}^g \cdot t_{in}} \quad (11.21)$$

The system efficiency (η_s) is then defined by the ratio of net-to-gross electrical energy:

$$\eta_s = \frac{E_e^n}{E_e^g} = \frac{E_e^g - E_{br} - E_{sp} - E_{th}}{E_e^g} \quad (11.22)$$

Where E_e^g is defined by the numerator product of equation 11.21; E_{sp} is the energy required to power the spindle motor that operates the traversal mechanism, which ensures that the tether is wound around the drum optimally, and with as little damage as possible [67]; E_{th} is the required thermal control energy per cycle to ensure adequate temperature control for optimised performance; and E_{br} is the required braking energy per cycle, which for the scope of the report is estimated based on the maximum kinetic energy experienced by the drum:

$$\begin{aligned} E_{br} &= \frac{\int_0^{\omega_{max}} I_{drum} \omega d\omega}{\eta_{br}} \\ &= \frac{I_{drum} \omega_{max}^2}{2 \cdot \eta_{br}} \end{aligned}$$

Where I_{drum} is the mass moment of inertia of the drum, $\omega_{max} = \frac{v_{inmax}}{r_{drum}}$, and η_{br} is the electrical conversion efficiency of the brakes.

All the aforementioned efficiencies can then be combined to find the total system efficiency, η_t , which is defined by:

$$\begin{aligned} \eta_t &= \eta_c \cdot \eta_e \cdot \eta_s = \frac{t_{out}}{t_{cycle}} \cdot \frac{E_m^g}{P_{m_g}^g \cdot t_{out}} \cdot \frac{E_e^g}{E_m^g} \cdot \frac{E_e^n}{E_e^g} \\ &= \frac{E_e^n}{P_{m_g}^g \cdot t_{cycle}} \end{aligned}$$

Which results in an expression from which the cycle power (P_c) can be derived:

$$P_c = \eta_t \cdot P_{m_g}^g = \frac{E_e^n}{t_{cycle}} \quad (11.23)$$

After equation 11.23 was derived, the nominal generator power, maximum reeling speeds, drum radius, and the machine parameters of the actuators are the remaining free variables that can be fine-tuned to obtain the optimum power generation approach.

The nominal generator power is a value that follows directly from the performance analysis, which sets the requirement on the power that the primary energy system should be able to generate. Based on this value, the optimum reeling speeds are found using aforementioned 3-region strategy, keeping in mind that the associated rotational speed (and thus drum radius) should not exceed a value of 1500 RPM, since otherwise the design

would become unrealistic. For this same reason, the optimum drum radius can be found by iteration such that the output power per cycle is maximised. The machine parameters follow directly from the manufacturer, and have a direct effect in the total system efficiency. All input parameters used in the model are shown in table 11.4 below:

Table 11.4: Input parameters for power generation analysis

P_{gnom}	80 kW	v_{cutin}	7 m s ⁻¹
T_{nom}	7.5 kN	v_{cutout}	35 m s ⁻¹
$l_{tethermin}$	200 m	$\tau_{sin/out}$	3.18 Nm
v_{outmax}	10 m s ⁻¹	$c_{fin/out}$	0.799 Ns
v_{inmax}	25 m s ⁻¹	$R_{in/out}$	0.108 Ω
$c_{g/m}$	0.083 A Nm ⁻¹	$k_{g/m}$	0.9 [-]
l_{tether}	420 m	A_k	50 m ²
r_{dinner}	0.26 m	r_{douter}	0.27 m

11.5.4. Tether Analysis

As mentioned in section 11.2, the chosen tether material is HMPE-DM20. Computations need to be performed to both size the tether and make sure it won't fail over its lifetime.

Starting with the sizing, the first thing that needs to be computed is [15]:

$$MBL = T_{nom} F_D \quad (11.24)$$

Where MBL is the minimum breaking load of the tether, T_{nom} is the nominal tether force during reel out and F_D is a design safety factor, for which a common industry value of 3.0 is used [15, p.6]. The MBL can then be used to estimate the mass per 100 meters and diameter of the tether. This is achieved by linearly interpolating in a DM20 properties table provided by the manufacturer Dyneema .

After sizing, two lifetime structural analyses need to be done to make sure that the tether will be able to finish its mission without failing. The first one concerns itself with tether creep failure, and the second one with (bending) fatigue failure. During its lifetime the tether is loaded in tension causing it to stretch or 'creep'. If the creep becomes too large, the tether could snap, causing the system to fail. To calculate the system lifetime considering creep, first the tension acting on the tether needs to be calculated using the following equation:

$$\text{Tension} = \frac{T_{nom} \cdot 100}{(1 - cc) \cdot m_t} \cdot \rho_{lin} \quad (11.25)$$

Where cc is the coating content of the tether with a commonly used value of 0.1, m_t is the tether mass and $\rho_{lin} = 970 \text{ kg m}^{-3}$ is the linear density. Using this tension the Safe Working Life (SWL) can be read from figure 11.3. This lifetime needs to be multiplied by a couple of operational factors. The tether loading during traction phase is much higher than during retraction, therefore the retraction forces can be disregarded. Since the tether reel-out is only a part of the cycle, its lifetime needs to account for that. This loading factor can be calculated using:

$$F_L = \frac{t_{out} + t_{in}}{t_{out}} \quad (11.26)$$

The creep resistance also becomes a lot better at lower temperatures. Since the graph in figure 11.3 is made for a temperature of 20 degrees Celsius and Martian temperatures are generally 100 degrees Celsius lower than that [102], the lifetime increases significantly. The daily and seasonal temperature factor are computed using the following equations [15]:

$$F_{T_{daily}} = \frac{24}{12 \cdot 1 + 12 \frac{1}{3 \frac{\Delta T_{daily}}{10}}} \quad F_{T_{seas}} = \frac{668}{334 \cdot 1 + 334 \frac{1}{3 \frac{\Delta T_{seas}}{10}}} \quad (11.27)$$

Since the temperatures are so low on Mars, both the daily and seasonal temperature factors become approximately 2. Now, the Safe Service Life (SSL) is calculated by multiplying the SWL by these three factors. The SSL needs to be higher than 5 Martian years to make sure the tether does not fail because of creep during its lifetime.

⁶https://www.moremarine.nl/pdf/dyneema_dm20_specs.pdf [Cited 12 June 2020]

The second lifetime check that needs to be done considers the tether bending fatigue. As the tether is repeatedly wound and unwound from the ground station drum, bending stresses are present in the fibres. The higher the drum to tether diameter ratio, the lower the bending stresses and the longer the lifetime. Figure 11.4, shows the number of cycles to failure of Dyneema SK75 fibres. Since Dyneema DM20 has very similar tensile and bending properties⁷, it is assumed that the same graph can be used for bending fatigue lifetime of the DM20 fibre. Therefore, using this figure, the amount of cycles to bending fatigue failure of the DM20 tether can be found. A special type of Dyneema DM20 is available, called DM20 XBO (due to the XBO coating), with very low creep and very good bending performance. According to Dyneema, the cycles to failure of this fibre can be up to 10 times higher using this XBO coating than for regular DM20⁸. This fibre still has approximately the same creep performance and mass. Using figure 11.4 and DM20 with the XBO coating, the total amount of cycles to failure can be computed. Dividing this number by the cycle time, the SSL considering bending fatigue can be computed.

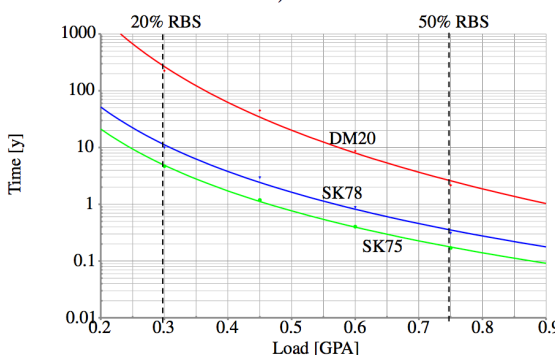


Figure 11.3: Creep lifetime [15, p.21]

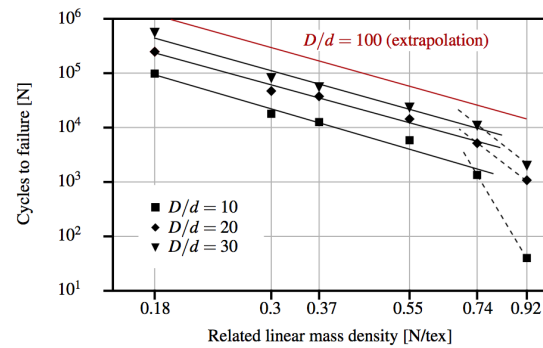


Figure 11.4: Bending fatigue Cycles to Failure [15, p.21]

11.6. AWE System Sizing

Combining the method shown in 11.5.2 with 11.5.3, these models can be extended to calculate not just the power of a single cycle for one wind speed, but the annual energy production of the system. Below in figure 11.5a functional flow block diagram of the code used in the sizing process is shown.

Computing the seasonal average power generation can be done by integrating the product of the cycle power of the particular wind speed with its Weibull probability density (where the $\cos^3(\phi)$ term accounts for the elevation angle $\phi = 25^\circ$ [71]):

$$P_{av} = \int_{v_{cut,in}}^{v_{cut,out}} P_c(v_w) g_W(v_w) \cos^3(\phi) d v_w \quad (11.28)$$

⁷<https://extreemsoftslings.com/wp-content/uploads/2019/02/Dyneema-UHMWPF.pdf>

⁸https://www.dsm.com/dyneema/en_GB/our-products/dyneema-fiber/dyneema-xbo-technology.html

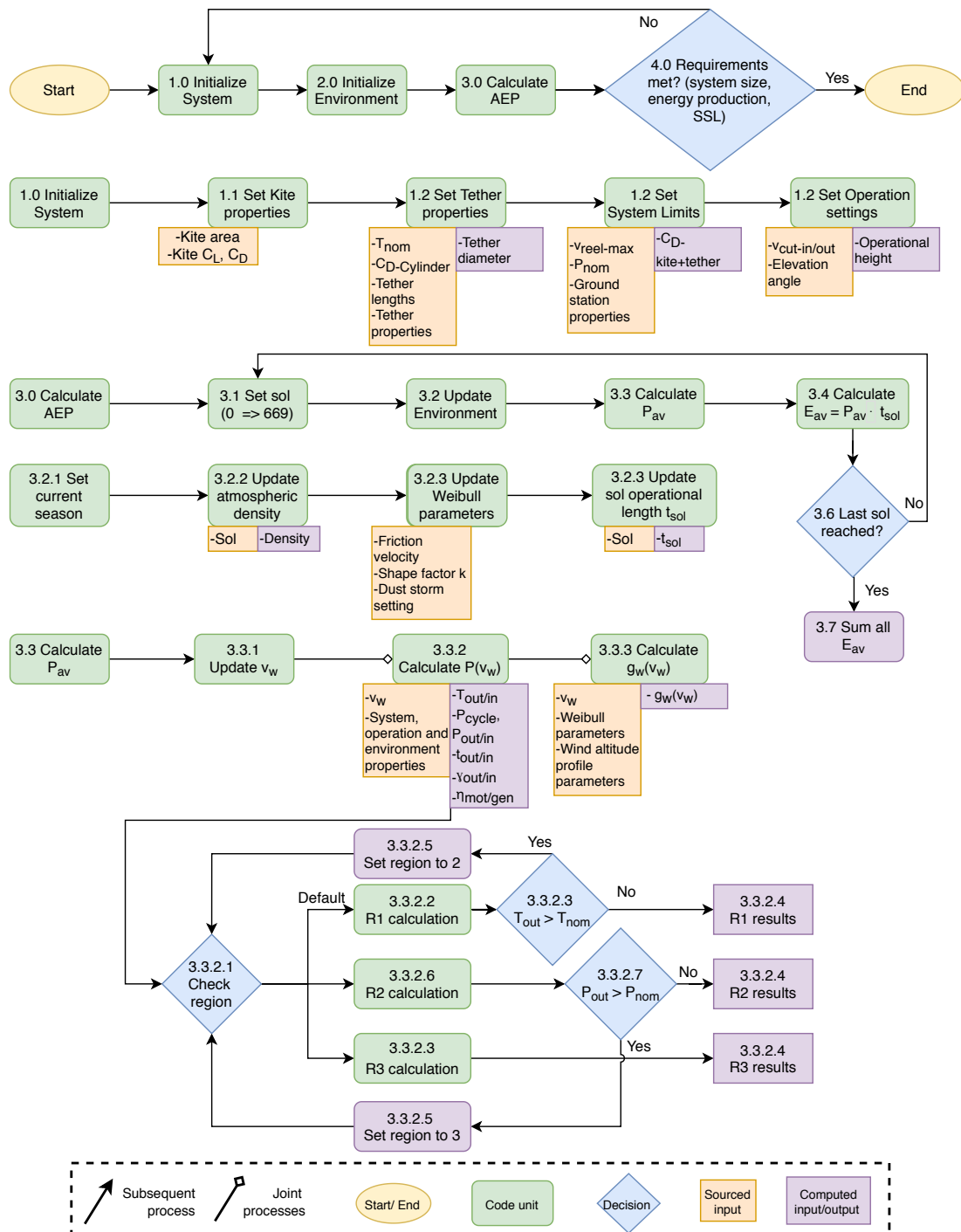


Figure 11.5: AWE annual energy production software flow diagram

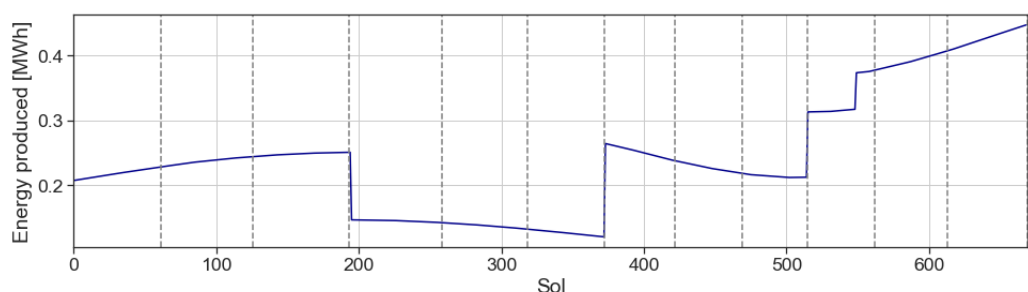


Figure 11.6: Daily wind energy production

Using figure 11.5, the operational envelope and the annual energy production (AEP) can be modelled. The mass of the different elements of the AWE system depend on the input attributes that are used to initialise the model. These input attributes include nominal generator power, nominal tether force and drum radius, among others. In order to find the optimal configuration, single attributes were varied at a time. Based on this, a sensitivity analysis can be performed to evaluate the effect of different attributes on the AEP and the associated operational envelope. This was performed until the system mostly converged to a single configuration with the highest specific power, fulfilling the power requirements at the lowest system mass.

The kite (flattened) area turned out to be 50 m² with an area density of 0.108 kg m⁻² as shown in section 11.7. The tether length equals 420 meters and the tether diameter equals 6.5 mm, the material being DM20 XBO as mentioned in section 11.5.4. The following table shows all the masses and volumes that were found:

Table 11.5: System mass and volume breakdown

Sub-System	Component	Mass [kg]	Volume [m ³]
Kite	Wing	5.4	0.006
	KCU ⁹	5.0	0.025
	Bridle system	2.0	0.003
	Vacuum pump ¹⁰	0.3	0.001
Tether	-	12.7	0.013
Ground station	Motor/generator ¹¹	152.6	0.119
	Drum (11.29)	48.3	0.349
	AC/DC Converter (10.4)	23.2	0.017
	DC/AC Converter (10.4)	1.1	0.001
	Spindle ¹²	25.2	0.120
	Supercapacitor [28, 36]	9.3	0.010
	Brakes ¹³	3.0	0.005
TOTAL		288.1	0.669

Many of the masses were possible to be computed using the component sizes as per the sizing model and the component density properties. For the KCU and the bridle system, it was assumed that units of similar sizes and weights could be designed for the Mars kite as per Schmehl and Fechner [90]. The ground station components, save for motor/generator and the drum, were sized by looking at off-the-shelf components, literature and through company inquiries. The steps for ground station sizing can be found in section 11.6.1. It is important to note that as the volumes account for external dimensions of components, the packing volume of the system can be lower than the estimated 0.669 m³, as for example the spindle, motor/generator and the drum can be assembled, saving space (the volumes account for external dimensions of components, internal space is neglected).

Using a programme called Surfplan ¹⁴, a visual rendering of this design was made. Figures 11.7, 11.8 and 11.9 show the front, top and bottom view of the kite respectively. The puppet is used to indicate the scale of the kite.

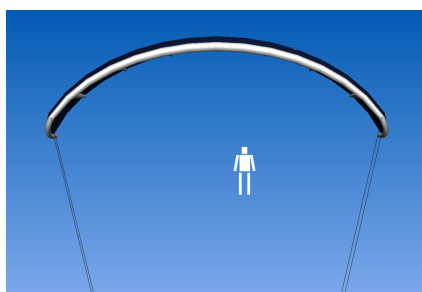


Figure 11.7: Front view of the kite



Figure 11.8: Top view of the kite



Figure 11.9: Bottom view of the kite

⁹<http://www.kitepower.eu/technology/3-system-components/51-kite-control.html> [Cited 18 June 2020]

¹⁰<https://www.gardnerdenver.com/en-nl/thomas/wob-l-piston-pumps-compressors/2110z-series> [Cited 17 June 2020]

¹¹<http://www.alxion.com/products/stk-alternators/>, <http://www.alxion.com/products/stk-motors/> [Cited 18 June 2020]

¹²<https://www.amacoil.com/products/rg-linear-drives/specifications/> [Cited 18 June 2020]

¹³<https://www.altraliterature.com/-/media/Files/Literature/Brand/matrix-international/catalogs/p-7805-mx.ashx> [Cited 18 June 2020]

¹⁴<http://www.surfplan.com.au/sp/> [Cited 18 June 2020]

11.6.1. Ground Station Sizing

Referring back to figure 11.2, where the different elements within the ground station can be distinguished, special focus was brought to the sizing of the motor/generator and drum. Naturally speaking, the remaining elements of the ground station should be sized according to level of detail necessary to finalise a well-rounded concept; however, due to lack of time and for the sake of compactness, it will be a consideration for the next steps of this project.

Generator Sizing

Based on the three-phase strategy for the pumping cycle as described in subsection 11.5.2, the operational envelope of the ground station can be extrapolated with the numerical model depicted in figure 11.5.

Two of the most critical elements that compose the ground station is the motor that will drive the drum during reel-in, and the generator that will convert the mechanical energy into electrical energy. To be able to make an appropriate selection of such machines, first the operational envelope must be defined to obtain a power, torque, and RPM rating that will be used to size the generator. It was found by iteration that a nominal generator power of 80 kW results in an adequate AEP and daily energy production requirement fulfilment as specified by the performance analysis in section 9.3, from which the operational envelope of the ground station can be simulated for all three regions as defined in 11.5.2, shown in figure 11.10 below.

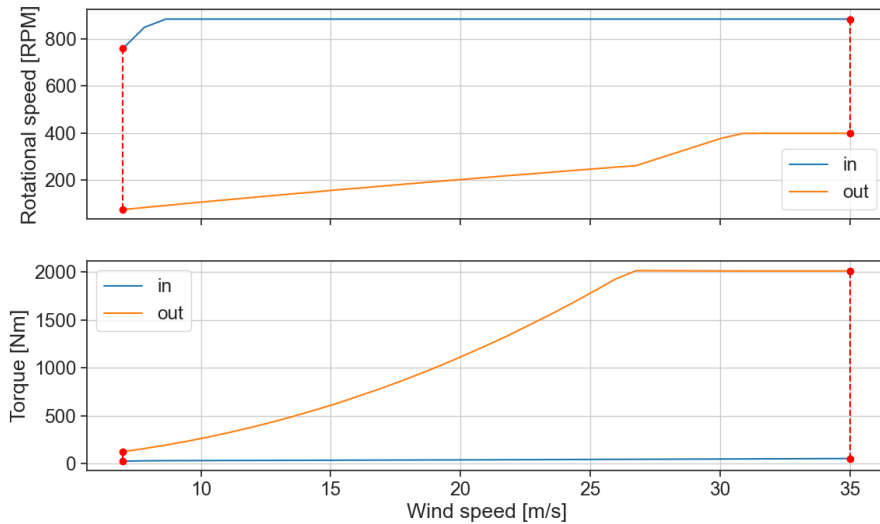


Figure 11.10: Operational envelope of the ground station

The simulated operational limits of the machine can be distinguished by the red dots, which sets a requirement for the axial flux machine to operate at a rated power of 80 kW, peak torque of 2015 Nm, and peak rotational speed of 884 RPM. The efficiencies of the generator and the motor are also computed and are 94.6% and 99.9% respectively. To find an appropriate machine that meets these operational requirements, information from specialised manufacturers was obtained to get a first-order estimate of the sizing of the actuator [27]. For this, the mass of the actuator was assumed to be similar to that of an alternator, with an addition of the mass of a direct drive electrical motor. Although an alternator is capable of working as a motor, the addition of a separate mechanism that can take charge of the reel-in phase was considered to keep the estimation conservative.

An important limitation to be considered, is that the available data used to estimate this sizing, was obtained from manufacturers that do not specialise in the production of space-rated actuators. For this reason, the resulting estimation of the actuator's sizing might not be completely accurate; it is expected that this approach will nonetheless yield a conservative but still sensible estimation. This can be supported by the fact that electrical generators scale linearly with their torque rating [H. Polinder, personal communication, June 17, 2020]: the SP200D electric motor developed by Siemens set the benchmark in this sense as it achieved a torque rating of 1000 Nm with a total mass of around 50 kg. Assuming a similar specific torque of $\frac{1000 \text{ Nm}}{50 \text{ kg}} = 20 \text{ N m kg}^{-1}$, the mass of a 2015 Nm generator would weigh approximately 100 kg. This serves as a good reference point to provide a sanity check of the resulting values for the sizing of the generator.

Drum Sizing

As it is described in subsection 11.5.3, the size of the drum has a direct effect on the overall performance of the AWE system in terms of its total annual production. Due to the complex interdependence of all input

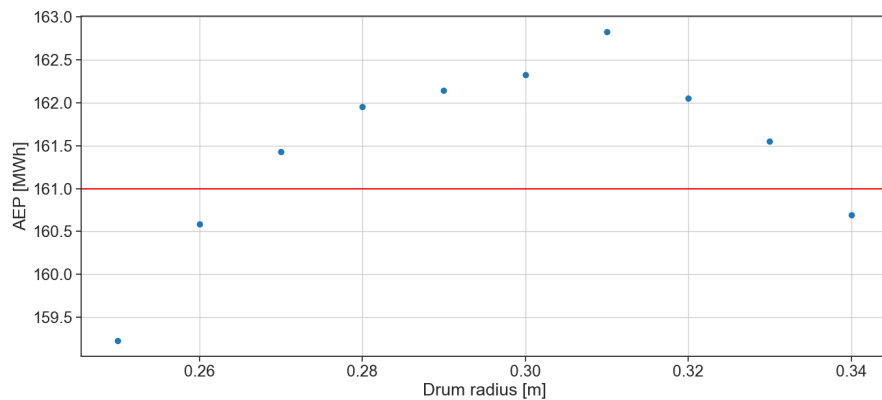


Figure 11.11: Results of optimisation run of AEP vs. drum radius

parameters in the procedure to calculate the total AEP, several rounds of iteration were necessary in order to understand the sensitivity of the model with varying drum radius. Figure 11.11 shows the results of an optimisation to evaluate the change in AEP as a function of drum radius. It can be seen that the drum radius that maximises AEP at a nominal generator power of 80 kW and a nominal tether force of 7.5 kN is equal to 0.31 m. The associated AEP is nonetheless higher than what it needs to be, according to the minimum AEP threshold imposed on the AWE based on requirement **REM-NRG-03**. It must be noted, however, that the selection of the optimum radius was based on a threshold of 161 MWh, which corresponds to the required AEP determined by an earlier iteration of the AWE performance analysis. For the sake of simplicity, it was decided that this value for the drum radius was going to remain unchanged, and was used for the weight estimation of the drum.

Having a final value for the drum (outer) radius of $r_{drum} = 0.27$ m, the next step was to determine the minimum size of the drum length; the estimation of this other drum dimension followed directly from the fact that the tether must be wound onto the drum in a single layer. This is done in order to avoid possible cutting of the tether in the underlying layers, and to further reduce the risk of tether slip [67]. Based on this, a back-of-the-envelope calculation can be done to estimate the minimum required length to ensure that a tether length of 400 + 20 m can be wound onto as follows:

$$l_{drum} = \frac{l_{tether_{max}} + 20 \text{ m}}{2\pi \cdot r_{drum}} \cdot d_{tether} \quad (11.29)$$

Where the extra 20 m is the length of the tether that corresponds to the so-called “dead wraps” which are necessary to ensure that the tether load is conserved at all times. This number of dead wraps is a value that is usually determined by regulatory bodies, and a minimum of three dead wraps are kept on the drum at all times [55]¹⁵. To ensure that the tether stays attached safely to the drum, this value was increased to an approximate equal of twelve dead wraps (i.e. ≈ 20 m).

Based on these now determined dimensions, and assuming a drum inner radius equal to 0.26 m, the volume, mass and inertia of the drum can be modelled as a simple hollow cylinder, with a constant material density of 1810 kg m^{-3} associated with the AZ91D Magnesium alloy [9]:

$$V_d = l_d \cdot \pi \cdot (r_{d_{outer}}^2 - r_{d_{inner}}^2) \quad m_d = \rho \cdot V_d \quad I = \frac{1}{2} m_d (r_{d_{outer}}^2 + r_{d_{inner}}^2) \quad (11.30)$$

Finally, the preliminary architecture of the electrical equipment is illustrated in figure 11.12:

¹⁵<https://www.ingersollrand.com/en-eu/lifting-equipment-material-handling/Support/winch-selection-support/drum-capacity-definitions.html> [Cited June 22, 2020]

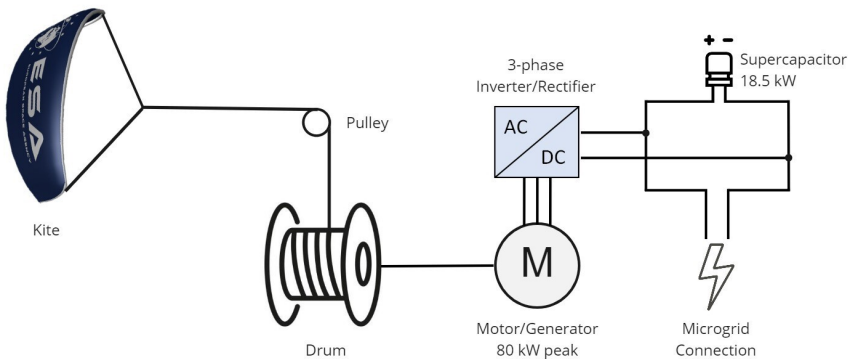


Figure 11.12: Electrical block diagram of the ground station

11.6.2. Conceptual Challenges

For the ground station, an operational temperature of at least -40°C should be maintained for nominal operation of power electronics and the axial flux machine, along with the necessity of having protection against radioactivity for the sensitive electronic equipment. This challenge is to be solved by an under-ground ground station concept, in which the ground station equipment is in an excavated cavity, dug by the same robots and in the same manner as the Rhizome habitat. This can ensure a degree of thermal insulation along with protection against radioactivity that could otherwise only be solved by a heavy insulated casing, at very little weight added. This cavity could share the same heating system as the habitat.

Furthermore, as the temperature varies throughout the day and the kite fabric is permeable, measures should be taken to keep the inflatable stiffening elements of the kite at their optimal pressure with respect to its current environment. This is achieved by including a small vacuum pump on the kite [J. Breuer, personal communication, June 11, 2020], the mass and volume of which is accounted for in the system sizing, yet remains to be designed further in the following design process.

The operational tether length was decided to be between 200 and 400 metres, based on a similar Earth-based system [98]. However, due to the lower gravitational force and density on Mars, the particular flight mechanics for the environment could be investigated further to see if this operational tether length does allow for good system performance.

The launching and stowing away system is yet to be designed in further detail. Whilst taking up some mass and volume, it is possible that a well-designed launching mechanism could increase the system cut-in wind speed by allowing kite take-off even with low wind resource.

11.7. Material and Structural Characteristics

Now that the system components were sized with respect to their functional attributes, their materials are chosen and their structural characteristics are analysed. This allows for mass, volume and cost estimations, along with ensuring that the material composition will be able to complete this mission.

Starting with the tether, as mentioned in section 11.5.4, the best fibre material turned out to be Dyneema DM20 with a XBO coating. To see whether this fibre composition will fail during its lifetime the method described in this section together with figures 11.3 and 11.4 is used. The nominal tether tension was found to be 0.267 GPa, the drum to tether diameter ratio equals $\frac{0.54}{0.0065} = 83.08$, the loading factor $F_L = 3.5$ and the cycle time on average about 30 seconds. The found structural characteristics of this tether design are shown in table 11.6 - the SSL is shown in Martian years.

Table 11.6: Structural characteristics of the DM20 XBO tether

Mass [kg]	Diameter [m]	Length [m]	Creep SSL [y]	Bending fatigue SSL [y]
DM20 XBO	12.7	0.0065	420	3723.40

As can be seen from this structural analysis, the lifetime of the tether corresponding to creep is way higher than the 5 year mission lifetime so there is almost no chance the tether will break because of creep. On the other hand, the lifetime corresponding to bending fatigue is only 1.04 years, which means that to complete the mission at least five tethers need to be brought. To increase bending fatigue SSL once could either first; increase the drum diameter. However, this would increase the system weight more than the extra tethers. Second, the

tether design factor could be increased - however, that would increase the tether thickness and thus tether drag even more, and it was found that this would make the system operation unfeasible.

Thus, third; bringing four more tethers, was discovered to be the best option. The chords that connect the kite to the airborne KCU will probably be made from Spectra fibres, but for this no structural analysis has been made as of yet.

Considering the kite, a range of materials is available. Materials need to be chosen both for the inflatable stiffening tubes, and the skin of the kite. Also a coating will be required to safeguard the kite against things like UV-exposure, radiation and other types of physical wear.

According to a paper written by Breukels et al. [97], the best material to use for the inflatable tubes is called Dacron¹⁶ which is a relatively heavy polyester textile. The material used for the sheets between tubes could be a lighter Rip-stop polyester, for which the Dyneema Composite Fabric was chosen to be the best option¹⁷. Looking at figures of a similar kite made by Kitepower¹⁸, it was estimated empirically that when looking at the flat area of the kite, about 15% was occupied by the inflatable tubes and 85% by the regular fabric. These material ratios are used in the kite sizing process.

Since the tubes technically have fabric both on the top and on the bottom of the kite, it is assumed that the area corresponding to the 15% could be doubled. A 5 micrometer thick polyurethane coating is chosen to be most suitable for this mission [80]. Finally, Dyneema fibres with the same XBO coating have been chosen for the stitches that connect the skin to the inflatable tubes due to their good bending performance, high strength and low mass. It is assumed that approximately 4 metres of this fibre will be present per square meter, which was used to compute the average mass per square meter of kite flat area. Using all of this information the following table was generated, showing both the kite materials and their respective kite contribution:

Table 11.7: Kite materials

	Area [m ²]	Area Density [kg m ⁻²]
Dyneema composite fabric	42.5	50
Dacron	15.0	170
Polyurethane (coating)	100.0	5.5
Dyneema fibres (connections)	50.0	3.52

These values are used to calculate the total kite mass shown in table 11.5, the average kite area density is 0.108 kg m⁻². No structural analysis has been made on the kite itself as of yet. As the kite is a semi-rigid structure with many flexible components, the complexity of an analysis is beyond the scope of this project. In future steps of the design however, this should definitely be included to see whether the kite can withstand the imposed loads.

A more elaborate representation on all the materials present in the AWE system can be found in section 17.2, which also includes all the materials that are present in the ground station and the kite control unit.

11.8. Cost Breakdown

As one of the goals of design is often to make the system cost effective, a production cost requirement of €500.000 per primary energy unit was accounted for the mission.

The parameters that were computed in the sizing part of the design, can be used to estimate the total AWE system cost. As the kite surface was sized to be 50 m², the following cost estimation table can be made for the kite:

Table 11.8: Kite cost estimation

	Area [m ²]	Cost [€]
Kite	50	1510
Dyneema ¹⁹ composite fabric	42.5	1300
Dacron ²⁰	15	210

¹⁶<https://www.extremtextil.de/en/dacron-woven-polyester-sailcloth-170-mt-170g-sqm.html> [Cited 18 June 2020]

¹⁷<https://www.extremtextil.de/en/dyneema-composite-fabric-ct5k18-50g-sqm.html> [Cited 18 June 2020]

¹⁸<https://www.tudelft.nl/en/ae/organisation/departments/aerodynamics-wind-energy-flight-performance-and-propulsion/wind-energy-research/kite-power/> [Cited 18 June 2020]

¹⁹<https://www.extremtextil.de/en/dyneema-composite-fabric-ct5k18-50g-sqm.html> [Cited 17 June 2020]

²⁰<https://www.extremtextil.de/en/dacron-woven-polyester-sailcloth-170-mt-170g-sqm.html> [Cited 17 June 2020]

In order to make a cost breakdown for the rest of the system, a cost estimation model is used that computes the cost of these AWE subsystems [41]. Table 11.10 shows all the subsystems that the model is able to find the costs of, along with respective equations used.

Each of the subsystems uses different parameters and constants to estimate its cost. First, the kite area $A_k = 50 \text{ m}^2$ and kite mass $M_k = 5.40 \text{ kg}$ are used in computing the cost of the KCU and the launch/landing system. To find the price of the controls electronics inside the KCU, the rated continuous power $P_{rat} = 0.2 \text{ kW}$ is used, which was estimated using the KitePower KCU²¹ where two motors are present that require 0.1 kW of power. The price of the drum is computed using the drum diameter $d_{dr} = 0.54 \text{ m}$ and the drum mass $M_{dr} = 74.9 \text{ kg}$. The model uses a HMPE tether and therefore can be assumed to be accurate for tether cost estimation, the estimation is done using tether length $L = 420 \text{ m}$ and the tether diameter $d_t = 6.5 \text{ mm}$. The nominal generator power $P_{nom} = 80 \text{ kW}$ can be used to compute several ground station costs like the power electronics and the cover frame (TBD, as under ground ground station design would change this). Combining P_{nom} and the nominal rotational speed ω_{nom} the motor and generator cost can be estimated. The nominal rotational speed is $\omega_{nom} = 884 \text{ rpm}$ for the motor and 400 rpm for the generator. The constants shown in the estimation equations are found in P. Faggiani [40] and are shown in table 11.9.

Table 11.9: Cost estimation constants

Constants...	[-]	...	[-]	...	[-]	...	[-]
c_{em}	1208	$c_{cf,1}$	10	$c_{kcu,1}$	2000	c_t	0.045
c_{dr1}	1.54	$c_{cf,2}$	300	$c_{kcu,2}$	100	c_{co}	10960
c_{dr2}	5000	c_{ll}	10	c_{thb}	50	c_k	48
c_{pe}	108						

Some ground station components costs could not be estimated using this model and therefore have been found individually. The spindle motor has a cost of €390 (\$440)²². The ground station also has three AC/DC and one DC/AC converter, their costs were retrieved by personal communication with the companies that manufacture them and are €5000 and €20000 per each unit as will be shown in section 10.5. Three AC/DC converters (used in parallel) are required so in total their price becomes €15000. Finally, the supercapacitor capacity required for the system and its requirements is determined to be approximately 0.14 kW h, and using literature specific energy cost values [28, 36], cost can be estimated to be €700. The following table shows all the estimated subsystem cost together with the total primary energy system cost.

Table 11.10: Cost estimation for the kite

Subsystem	Estimation equation	Cost [€]
Electrical machines	$C_{em} = c_{em} \omega_{nom}^{-0.6} P_{nom}$	4300
Drum	$C_{dr} = c_{dr,1} M_{dr} + c_{dr,2} d_{dr}$	2820
Power electronics	$C_{pe} = c_{pe} P_{nom}$	8640
Tether handling and bearings	$C_{thb} = c_{thb} F_{t,max}^{0.5}$	140
Cover frame	$C_{cf} = c_{cf,1} P_{nom}^{0.85} + c_{cf,2}$	710
Launching and landing system	$C_{ll} = c_{ll} M_k A_k^{0.5}$	380
Kite Control Unit	$C_{kcu} = c_{kcu,1} + c_{kcu,2} A_k^{0.5}$	2710
Tether	$C_t = c_t L \pi d_t^2 / 4$	630
Controls	$C_{co} = c_{co} P_{rat}^{0.2}$	7940
Kite	C_k	1510
Supercapacitor	C_{sc}	700
Spindle motor	C_{sm}	390
Converter AC/DC	$C_{AC/DC}$	22500
Converter DC/AC	$C_{DC/AC}$	15000
Total	C_{total}	68370

The total cost estimated for the AWE system is thus €68350, which complies with the €500000 requirement. An important consideration to make is that for further refinement of the design, probably more investigation will be done on special space-grade materials. These materials will decrease the system mass significantly

²¹<http://www.kitepower.eu/technology/3-system-components/51-kite-control.html> [Cited 18 June 2020]

²²http://www.okcoil.com/buy-linear-actuator-online-shop.html?page=shop.browse&category_id=8 [Cited 17 June 2020]

but will also likely add cost. Luckily, there is still a lot of leeway in the budget as approximately €431650 can still be spent on improving the AWE system.

11.9. Model Verification and Validation

The model that is described in section 11.5 calculates many different performance parameters which in turn are used to size the entire AWE system. To make sure that the design fulfils its intended purpose and that all its requirements are met, it is important to verify and validate the created model.

Unit Verification

The equations for computing the variables used in the code were lumped into units of code based on their resulting intermediate outputs, if they could be checked against the literature from which the physical models were provided. This was possible both for the main part of the model from Luchsinger [71] and the motor and generator efficiency models from Fechner and Schmehl [42]. When a unit of code was written, it was tested for its fidelity by using the inputs and comparing them to the outputs presented in said literature. These units were then connected to see their combined effect - if their output corresponded to the outputs in literature. Where this was not possible, the correctness of the code was judged by checking the magnitudes against standard values in the industry.

Module Verification & Validation

Verification and validation of the integrated final model is also done by using a different model by van der Vlugt et al. [96]. This validated model uses a quasi-steady approach to analyse the kite's performance. Using the same input parameters as used in the team's model, the results of separate calculation modules can be compared and thus verified.

The first module that is compared, is the one that calculates the tether force during reel-out and reel-in phase. In order to do so, the forces are computed for both models over a range of wind speeds and plotted, the graphs are shown in figures 11.13 and 11.14. It can be seen for all the verification graphs that the range of wind speeds chosen is slightly different. This is because for the verification model for wind speeds below 9 m s^{-1} the wind speeds are apparently too low for the kite to stay in the air. A physical consideration for this has not been implemented in the system model as of yet, and might be a useful consideration for any next design steps, shifting the cut-in wind speed requirement up.

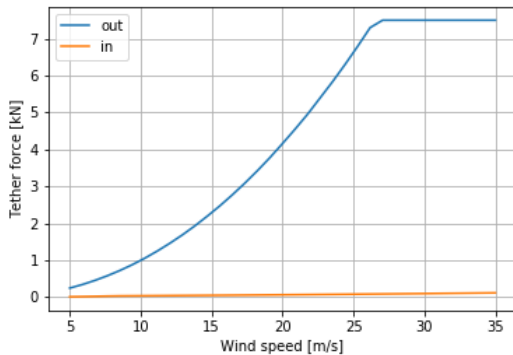


Figure 11.13: Tether force for the system model

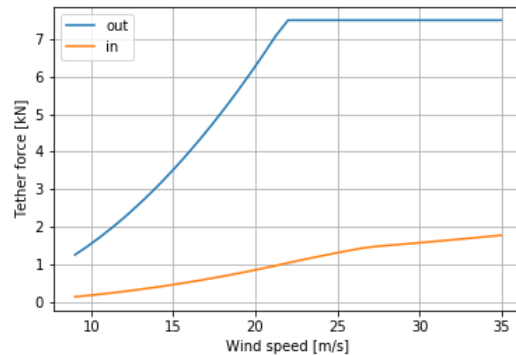


Figure 11.14: Tether force for the verification model

Now both graphs are analysed and compared, starting with the reel out tether force. The tether force limit of 7.5 kN is reached at a slightly different wind velocities for both models. The system model enters region 2 at a wind velocity of 27 m s^{-1} and the verification model at 22 m s^{-1} - this difference is not that significant. The biggest contrast can be seen in the tether force during reel-in. It can be seen that the system model tether force is significantly lower than the tether force of the verification model at each point in the wind speed range. This is caused by the way the models compute the forces on the kite, the system model estimates the force factors where the reel in force factor $F_{in} = C_d$. It was found when iterating aerodynamic parameters that this force factor estimation provides poor results when the drag coefficient is low. The verification model on the other hand uses a different approach to compute the forces on the kite. A real-time aerodynamic analysis of the forces is done at each point during the flight, accounting for the fact that whilst the kite C_L is lowered, it is still accounted for in order to ensure stable flight. Since the drag coefficient found for this tensairity kite is 0.06

(add onto it the tether drag, calculated in an identical way for both models, as per 11.5.1) which is relatively low, the forces during the reel-in phase may be poorly estimated, explaining the big difference in this graph. In future iterations of the system model, a more accurate approach should be taken that is able to find the F_{in} factor that would account for a minimum required C_L as well. But in general it can be said that this module of the AWE model can be verified as even in this first iteration of the design the results are decently close considering the point that were just mentioned.

The next step is verifying the power the system produces during reel-out, reel-in and the total cycle power. Figures 11.15 and 11.16 show these values for both the system and the verification model.

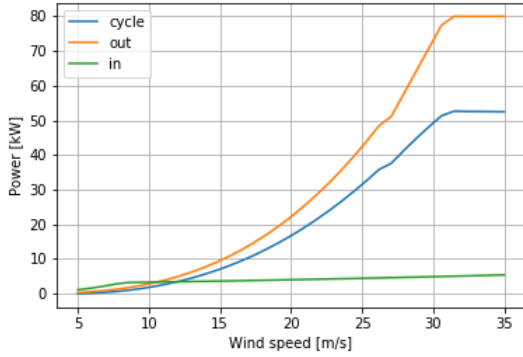


Figure 11.15: Power for the system model

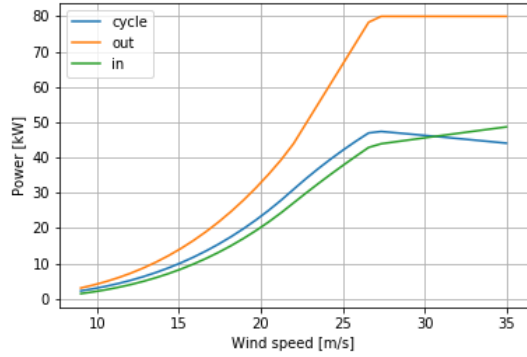


Figure 11.16: Power for the verification model

Comparing both graphs it can be seen that region 3, which is when the nominal generator power of 80 kW is reached, is entered at 31 m s⁻¹ for the system model and at 27.5 m s⁻¹ for the verification model. Both the reel-out power and the cycle power are relatively similar for the two models. Again a significant difference can be seen during the reel-in phase, which can be attributed to the same reason as for the tether force difference. Since the rest of the graphs seems to be almost the same and that the cycle power follows approximately the same path, this module can be said to be verified as well.

The final module to analyse is one for the reel-in and reel-out speeds, shown in figures 11.17 and 11.18.

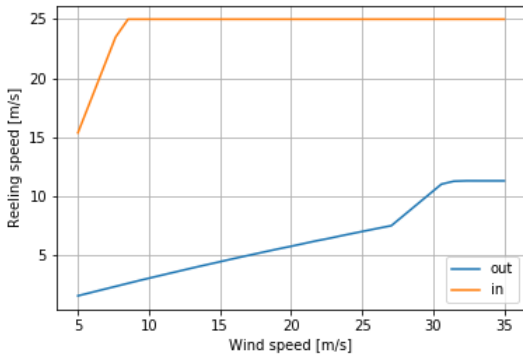


Figure 11.17: Reeling speed for the system model

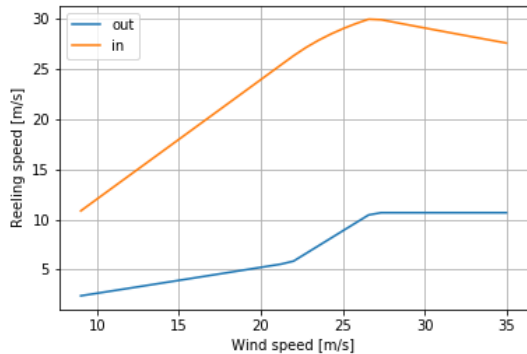


Figure 11.18: Reeling speed for the verification model

First considering the reel-out phase, the shape of the reel-out speed graph is very similar and it ends at approximately the same reeling speed. The only difference is that it is slightly shifted to the right for the system model. The reel-in speed graph first increases for both models but the maximum is reached sooner for the system model than for the verification model. Also after the maximum is reached the system model stays constant and starts decreasing in the verification model. This difference is most likely caused by the fact that the verification model takes the trajectory manoeuvres of the reel-in phase into account. In general, considering the reasons stated, this module is verified. Computing the AEP flows directly from these modules and should be the same for both models. Therefore since the previous modules are verified and because unit testing and sanity checks have been performed for the energy calculations, the entire system model can be considered as verified.

11.10. Risk Assessment

In order to guarantee the success of the AWE system, its reliability, availability and the robustness have to be assessed. Also, the safety of personnel and equipment has to be maintained. The only available comprehensive FMA was conducted by Salma et al. [88] to date. The risk assessment and FMA are solely based on the findings of this article due to the lack of others. It is important to highlight that due to this reason the analysis might be biased. Furthermore, AWE technology is still maturing in 2020; it has not yet been commercialised on Earth, let alone on extraterrestrial applications. The main challenges to be overcome before AWE can be introduced to Earth market are: high complexity, lack of proven reliability and limited knowledge. The present technology readiness level (TRL) is estimated to be between 3 and 5 and the commercialisation period is approximately 10 years [54]. Also, technical problems have to be addressed in order to reach a TRL allowing for Martian deployment, such as durability of materials, erosion testing in Martian conditions or greater design convergence. [100] The high level risks associated with these challenges are:

- *AWE not being technologically mature*: substantial research has to be conducted in the field of fluid-structure interaction analysis of the kite for example. Studies are ongoing, but before proving the financial viability to stakeholders, these will remain in a small scale.
- *AWE not commercialised on Earth*: as mentioned earlier, the projected time for commercialisation is 10 years, which is prone to delays. These setbacks can originate from slow scientific development or unwillingness to invest.
- *AWE not being financially viable for Mars*: even if the system is commercialised on Earth, additional research has to be done in order to account for Martian conditions. Capital expenditures may be estimated less initially, which can also set back the system's financial viability.

The failure modes of the AWE system can be seen in table 11.11. Likelihood and impact scores are defined in chapter 4. The failure modes can be divided into four categories with the ones belonging to these:

- *Crucial HW problems*: These involve failure modes that pose high risk to the safe operation of the system. If any of these should fail, it would mean the loss of control over the system, which cannot be retrieved during flight.
 - WE-01, WE-02, WE-15, WE-16, WE-17, WE-20, WE-25
- *Non-crucial W problems*: In case of failure of any of these components, the system detects the failure, maintains control and safely brings down the kite for maintenance.
 - WE-09, WE-11, WE-13, WE-22, WE-23, WE-26, WE-28
- *Crucial SW problems*: Similar to *Crucial HW problems*, a failure would result in the loss of control over the system. First, the retrieval of control shall be attempted by respecting the respective SW or otherwise a back-up, emergency system shall safely take down the kite.
 - WE-06, WE-08, WE-19, WE-19, WE-21
- *Non-crucial SW problems*: These involve SWs that either have a back-up or are to optimise performance, but not essential for the safety of the system. Any of these fails, the system has to be taken down for maintenance to restore its efficient use, but this can be done by the system itself had there been no failure.
 - WE-03, WE-04, WE-05, WE-07, WE-10, WE-12, WE-14, WE-24, WE-27, WE-29

Table 11.11: Failure mode analysis of AWE system [88]

ID	Failure mode	Likelihood	Impact
WE-01	Tether break	3	5
WE-02	Kite not steerable	3	5
WE-03	Airborne communication software (SW) failure	2	3
WE-04	Ground communication SW failure	2	3
WE-05	Airborne main data-link hardware (HW) failure	3	4
WE-06	Airborne backup data-link HW failure	2	5
WE-07	Ground main data-link HW failure	3	4
WE-08	Ground backup data-link HW failure	2	5
WE-09	Inertial measurement unit (IMU) HW failure	3	4
WE-10	IMU SW failure	2	3
WE-11	Global Positioning System (GPS) HW failure	3	4
WE-12	GPS SW failure	2	3
WE-13	Sensor box HW failure	3	4

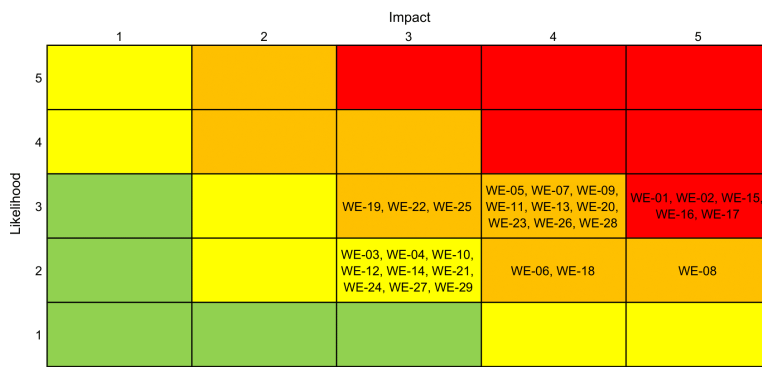
Continued on next page

Table 11.11: Continued from previous page

ID	Failure	Likelihood	Impact
WE-14	Sensor box SW problem	2	3
WE-15	Left motor HW failure	3	5
WE-16	Right motor HW failure	3	5
WE-17	Motor driver microcontroller unit (MCU) failure	3	5
WE-18	Motor driver MCU SW failure	2	4
WE-19	Flight SW problem	3	3
WE-20	Primary CPU HW problem	3	4
WE-21	System state controller SW problem	2	3
WE-22	Maximum power point tracker charger HW failure	3	3
WE-23	Battery pack HW failure	3	4
WE-24	Winch control SW problem	2	3
WE-25	Ground control HW problem	3	3
WE-26	Wind sensor HW failure	3	4
WE-27	Wind sensor SW failure	2	3
WE-28	Force sensor HW failure	3	4
WE-29	Force sensor SW failure	2	3

One can observe that all failure modes have a likelihood of 2 (unlikely) or 3 (possible). The system is considered when it is fully developed and deployed on Mars, thus it is expected not to have high likelihood of failures. On the other hand, impact of the failures are generally high as most of these would result in a downtime and thus not being able to meet the continuous power requirement. Also, some can even result in physical harm to an operator or an object, which would be detrimental to the project.

The risk matrix before mitigation can be seen in figure 11.19. There are five extreme risks of which all are related to the loss of control over the system. Most of the risks are high and some are moderate. Considering the nature of the mission, it is evident that such a project is unsafe and thus the risks have to be mitigated.

**Figure 11.19: Risk matrix before mitigation of AWE system (red: extreme risk, orange: high risk, yellow: moderate risk, green: low risk)**

The revised likelihood and impact scores can be seen in table 11.12. Naturally, some failure modes have similar mitigation measure, thus the related ones are treated together. The mitigation measure for the risks are as follows:

- **WE-01:** In case a tether breaks, the kite is depowered naturally and the kite flies away. A safety zone has to be marked out to guarantee if this happens no object or personal is hit by the tether nor the kite. To be able to continue with mission, it is necessary to have a spare tether and also a spare kite is advised as this can also be damaged in this scenario.
- **WE-02/15/16/17/20/25:** These are part of the crucial HW failure modes. The kite might not be steerable for various reasons. In any of these cases, first regaining control should be attempted. In case of not succeeding, the kite has to be depowered. This can be done by a wire cutter mechanism, which would cut a separate line attached to the tether, but not the tether, so it can be reused. In this case, spare rope, wire cutter, and parts for the failed component are needed to continue with the mission, and a spare kite is advised as this can also be damaged in this scenario.

- **WE-03/04/10/12/14/24/27/29:** These failure modes are part of non-crucial SW failure. Each individual situation has to be assessed by the flight computer or by the operator and the decision has to be made if it is safe or not to operate the kite in such condition. If it is not safe to operate, the kite has to be reeled in immediately. Otherwise, if it is the SW shall be rebooted or maintenance scripts shall be run to overcome the problem, if necessary. The system can be fully repaired after the end of operational period for that day.
- **WE-05/07:** When the airborne or ground data-link HW fails, the back-up has to take its place immediately to continue operation. When the kite is reeled in at the end of the operational period, the main data-link HW can be repaired. It is advised to have spare HW components to be able to repair it.
- **WE-06/08:** The back-up data link is only used if the main had already failed, thus the failure of the back-up means for either airborne or ground station both data-links have failed. Thus, the kite has to be reeled in immediately for maintenance.
- **WE-09/11/13/22/23/26/28:** These are the non-crucial HW failures. Similar to non-crucial SW failure, the safety of operation has to be assessed by the flight computer or the operator. If it is not safe, the kite has to be reeled in immediately. Otherwise, if it is deemed safe, operational conditions have to be reassessed and the kite shall be operated accordingly until the end of the day's operational period. After this, the system can be fully repaired. It is advised to have spare parts of the systems to be able to repair the failed HW.
- **WE-18/19/21:** These are part of the crucial SW failures. Problems associated with these systems can potentially lead to loss of control if not fixed immediately. Thus, the safety of the situation has to be assessed and a decision shall be made accordingly.

Based on these measures the revised likelihood and impact scores can be seen in 11.12 and the risk matrix after mitigation is presented in figure 11.20. One can observe that the majority of the risks is still high, but there are no extreme risks after mitigation. Furthermore, five are moderate and nine are low risks.

Table 11.12: Revised likelihood&impact scores of the AWE system after mitigation

ID	Likelihood	Impact	ID	Likelihood	Impact
WE-01	3	3	WE-16	3	4
WE-02	3	3	WE-17	3	3
WE-03	1	3	WE-18	1	4
WE-04	1	3	WE-19	1	3
WE-05	2	4	WE-20	3	3
WE-06	2	3	WE-21	1	3
WE-07	3	3	WE-22	3	2
WE-08	2	3	WE-23	3	3
WE-09	3	3	WE-24	1	3
WE-10	1	3	WE-25	3	2
WE-11	3	3	WE-26	3	3
WE-12	1	3	WE-27	1	3
WE-13	3	3	WE-28	3	3
WE-14	1	3	WE-29	1	3
WE-15	3	4			

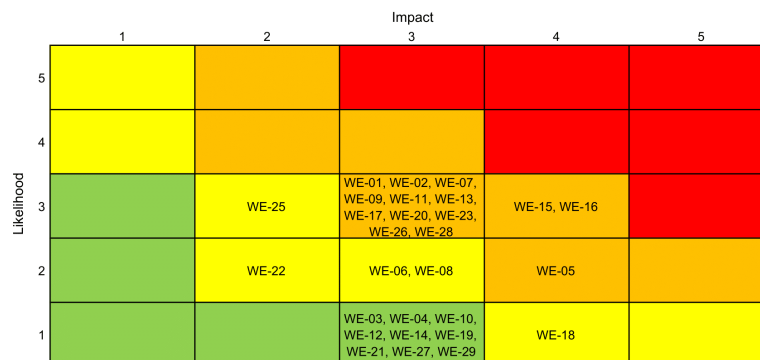


Figure 11.20: Risk matrix after mitigation of AWE system (red: extreme risk, orange: high risk, yellow: moderate risk, green: low risk)

11.11. Sustainability and Retirement

The sustainability of the wind energy system with respect to its production will be discussed in more detail in chapter 17.

Regarding the installation and operation of the primary energy system, one of the big advantages of AWE systems is their minimal impact on the environment. For the installation on Mars, the only adjustment to the environment is the digging of a ground station cavity. This will be done by making use of the same technology as the Rhizome Habitat team, using only local resources to strengthen the structure. During operation, the AWE system does not produce any emissions. The biggest impact of the AWE system will be in the replacement of the tether over life-time, the appliance of lubrication oil and in the worst case, replacement of kite components in case of failure [101], as these will require (human) interventions.

For the retirement, the AWE system consists of several components interesting for reusing and/or recycling on Mars. The kite's fabric, tether and cords could all get a new purpose in the habitat. The fabric could be recycled into storing bags, separation screens, hammocks or any other possible fabric use. The tether and cords can be used as rope, for any installation or binding purposes.

For the KCU, the vacuum pump and most of the ground station components, disassembly would be required, with the possibility to reuse some of the components. Currently on Earth, electrical motors are disassembled into its main parts, which are then shredded, followed by material separation by different properties: metals can be recycled; plastics are recovered; ceramics and recovery/recycling losses have to go to the landfill. This process compensates for up to 62 % of the environmental impact of the manufacturing of the motor [8]. If some of the components outlive the mission span, these can be reused on Mars, otherwise the motor/generator should be brought back to Earth and undergo such a recycling process on Earth.

The created cavity of the ground station, could at end-of-life of the wind system, either be reused for a successor, or be used for another purpose of the habitat, assuming the habitat will continue to grow once settled.

11.12. Requirements Compliance and Sensitivity Analysis

Compliance Matrix

To check whether the AWE design meets its requirements, a compliance matrix is generated. The following table shows the compliance matrix of the primary energy system requirements:

Table 11.13: Primary Energy System Compliance Matrix

ID	Compliance	Proof (Section)
REM-Sys-N02-01	No	Section 11.6, but mass will decrease when considering space-grade materials in the design.
REM-Sys-N02-02	Yes	Kite area density allows for flight for wind velocities above 7 m s^{-1} [24].
REM-Sys-N02-03	Yes	Subsection 11.5.3, the AWE system has been designed using this parameter as an input.
REM-Sys-N02-05	Yes	Subsection 11.5.4 and 11.5.3, the system is designed for a $T_{nom} = 7.5 \text{ kN}$ with a design factor $F_D = 3$.
REM-Sys-N02-06	Yes	Section 11.7
REM-Sys-N02-07	No	Section 11.7, multiple tethers will need to be brought to successfully complete the mission
REM-Sys-N02-08	Yes	Subsection 11.6.1, the generator efficiency is 94.6%.
REM-Sys-N02-09	Yes	Subsection 11.5.3, the AWE system has been designed using this parameter as an input.
REM-Sys-N02-11	Yes	Section 11.6, the motor and its power source (supercapacitor) have been designed to allow for this.
REM-Sys-N02-12	Yes	Subsection 11.5.3, the AWE system has been designed using this parameter as an input
REM-Sys-N02-13	Yes	Section 11.6, the motor and its power source (supercapacitor) have been designed to allow for this.

Sensitivity Analysis

To check how the model reacts to certain changes in inputs, a sensitivity analysis is performed. Several parameters are altered and their impact on the outcome in AEP and system mass are analysed.

The first parameter that was checked is the nominal tether force, which currently has a value of 7.5 kN. Its impact can be seen in figure 11.21. Increasing the nominal tether force results in an increase in mass due to the tether and ground station size increasing, so this behaviour that is shown makes sense. For the AEP, it can be seen that the peak is reached at 8 kN and afterwards it starts decreasing again. It was found that the system only requires the energy output corresponding to 7.5 kN, but if in future iterations higher energy production is required, increasing the nominal tether force could be an option.

The next input parameter to analyse is the nominal generator power, a range of powers around the current 80 kW value are plotted in figure 11.22. The first thing that draws the attention is that changing the nominal generator power does not affect the system mass. This is caused by the current generator/motor size estimation method, as a manufacturers guide of different generators and motors have been used to estimate their size. The issue is that these generators have a very wide range of nominal powers, the one that has been chosen currently ranges from approximately 20 kW to 90 kW. With the generator that is a grade below this one, not being able to comply with the energy production requirements. But in future design steps, a more detailed design model of the ground station will be integrated, possibly using a novel generator design for weight-saving purposes rather than one of a few off-the-shelf ones. Concerning the AEP, similar behaviour is shown as for the nominal tether force. Although the current 7.5 kN does not result in optimal energy production (the drop at 8 kN is due to the set drum radius), it is the most effective mass-wise.

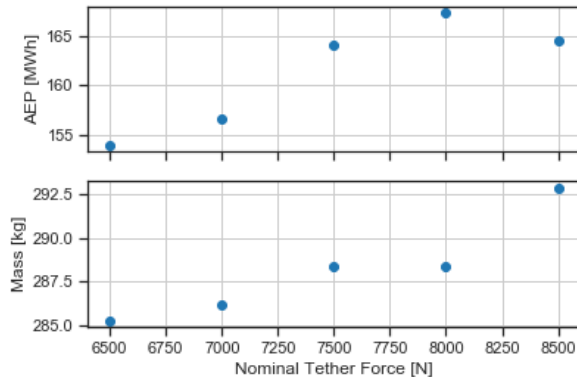


Figure 11.21: Sensitivity analysis: nominal tether force

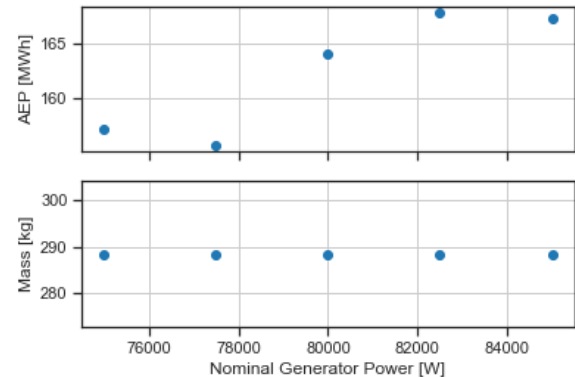


Figure 11.22: Sensitivity analysis: nominal generator power

A parameter found to be relevant in optimising the design, is the drum outer radius, currently set to 0.27 m. It can be seen that this value is a local maximum, caused by an increase in size in other ground station components. It was found that each nominal tether force had its optimal drum radius which maximised the system's energy production, thus requiring a large number of design iterations before the chosen values were converged upon.

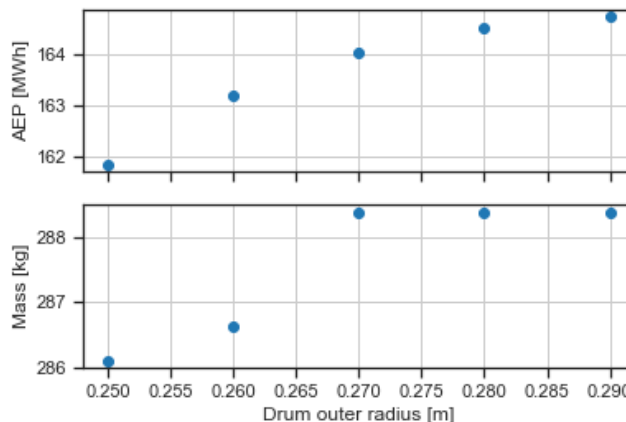


Figure 11.23: Sensitivity analysis: drum radius

The last parameter to be checked are the cut-in wind speeds. As the quasi-steady model by van der Vlugt

et al. [96] has shown, it is a possibility that a higher cut-in wind speed may need to be accounted for by the design; the results show that such a design-change would decrease the AEP quite a lot, hence requiring more extensive system redesign.

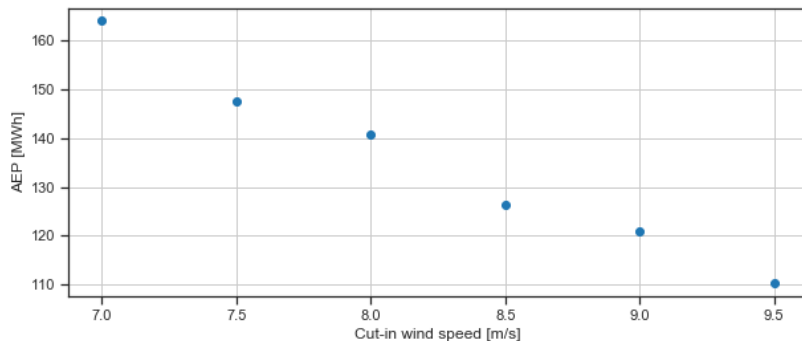


Figure 11.24: Sensitivity analysis: cut-in wind velocity

11.13. Recommendations

The KCU is a large part of the system design-effort wise, and there are many considerations to designing such a system for Mars rather than for Earth. Whilst water-proofing of the casing would not be required, radiation protection for the electronics inside should be taken into account. A preliminary decision has been made to adapt the ground station underground, as evidence shows that the Martian regolith is suited to provide sufficient radiation protection for electronics [6]; however, the feasibility of such a concept must be investigated in more detail in the future stages of the design.

A battery system for the KCU system is assumed, as the tether drag computed in 11.5.1 is already quite high, and including a conducting cable in the main tether would only increase the tether diameter and thus its drag - this would require some type of an automated charging system for the ground station as well. It might even prove that due to the radiation considerations due to the sensitive electronics inside, either its mass, cost or safe service life would reach an unsatisfactory value. This could require a different concept to be used (e.g. multiple tether control from the ground station). Also, a replacement for the GPS system used on Earth for kite control would be needed, as there is no equivalent satellite constellation providing such a service on Mars with such accuracy as on Earth.

The ground station material selection is another big factor - many of the components that are required to be in the ground-station are designed for terrestrial applications in which mass nor volume does not play a large role. Redesigning the axial flux machine (152.6 kg out of the total system mass of 288.1 kg) for the given conditions should be a priority. As an example, considering the use of a magnesium-based alloy in place of an aluminium one, 26.6 kg of mass was saved on the ground station drum mass. A drum thickness of 1 cm was assumed based on similar Earth systems, and were a structural analysis to be performed, weight saving on the drum would surely follow as well.

As section 11.9 has shown, creating a higher-fidelity sizing model which would account for the kite's flight trajectory and mass could give rise to changing the cut-in wind velocity, for the kite to stay airborne in the air. Given time, this should be investigated further, as increasing cut-in wind velocity does reduce the system's AEP generation potential significantly (figure 11.24). Thus, computations could be made as for the validity of having such a cut-in speed as done through the analysis as per [24].

Secondary Energy System Design

In this chapter the preliminary design of the secondary energy system will be further refined. System requirements are given in 12.1, followed by a trade-off summary in 12.2. After an investigation of the solar resource in 12.3, a more careful analysis of the solar cell technology is made in 12.4, regarding the performance on Mars. What follows are the mass and volume estimations stemming from the sizing process in 12.5, along with a system architecture description in 12.6. After that, a cost estimation for the system is made in 12.7, system risks are assessed in 12.8, and its sustainability and retirement is elaborated upon in 12.9. Lastly the design will be checked for compliance with the requirements in 12.10, and future design recommendations are given in 12.11.

12.1. Requirements

To ensure that the design satisfies the mission needs, subsystem requirements were determined for the secondary energy system. These can be found in table 12.1.

Table 12.1: Secondary Energy System Requirements

Requirement ID	Description
REM-Sys-N12-02	The secondary energy system shall have a maximum mass of 550 kg.
REM-Sys-N12-03	The secondary energy system shall have a maximum volume of 1 m ³ .
REM-Sys-N12-04	The secondary energy system shall provide less than 50% of the total power.
REM-Sys-N12-05	The secondary energy system shall have a life-time of more than 5 Martian years.
REM-Sys-N12-06	The dust removal percentage shall be more than 90%.
REM-Sys-N12-07	The axis-system shall maintain an accumulative Sun tracking error of less than 1% per sol.

12.2. Trade-off Summary

In order to determine which design concept was best suited for the secondary energy system, a design trade-off was performed. Following the evaluation of a design option tree in the Baseline report [25], two main candidates were selected as plausible options: geothermal and solar energy generation.

After an extensive trade-off and sensitivity analysis as documented in the Midterm report [24], it was found that the solar energy generation concept was more appropriate for the mission. This was mainly because geothermal power plants generally supply power in the order of 10^8 W, whereas the power requirement for the mission is in the order of 10^4 W. Moreover, its volume and mass performance were deemed unsuitable for the mission due to the constraints imposed on maximum payload mass and volume. Solar energy generation, on the other hand, was found to be able to fulfil these top-level requirements.

The next step was to perform a trade-off for each of the elements comprising the design of a solar energy generation system. A selection for the cell technology, module level design, tilt & orientation mechanism and dust handling mechanism then followed. After another trade-off and sensitivity analysis were performed, it was found that the best performing solar energy generation system consists of a solar panel with a planar module of multi-junction, III-V semiconductor cells, with a bi-axial tilt mechanism, and a hydrophobic dust protection coating.

12.3. Solar Resource

Regardless of the system architecture, in order to assess the power that can be generated from the incoming sunlight, the yearly available solar resources need to be known. Although the irradiance could be calculated analytically at the exact site location, taking into account all sources of solar irradiance was deemed as time inefficient and thus not applicable to this short term project [10]. Rather, the data measured by the Viking II lander was taken as this already incorporates every aspect and gives the actual irradiance values [6].

The data set can be considered representative as the lander is located 48°N, while Deuteronilus Mensae is at 39°N. It gives the solar insolation per sol in kWh m^{-2} over one Martian year. This includes a major dust storm starting in the middle of Autumn, also present in the beginning one third of Winter. It is important to point out that such a storm does not occur every year, but for the purpose of this analysis it was considered appropriate. The data set can be seen in figure 12.1. One can divide the values by the length of the sol, which results in the solar irradiance (figure 12.2). The values are linearly interpolated for the remaining sols through the same function utilised for the sunrise and sunset times, the evaluation of which has been already verified. Moreover, the solar irradiance is computed through dividing the solar insolation by the sunlight duration as evaluated in chapter 9.

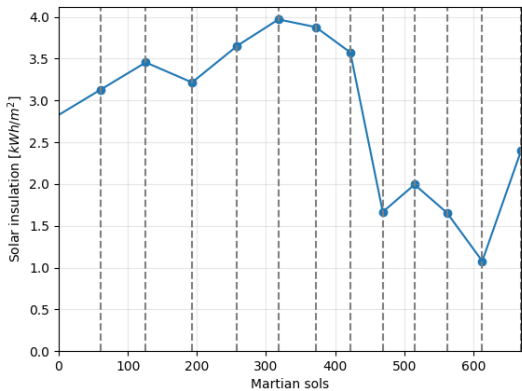


Figure 12.1: Solar insolation resource as obtained from the Viking II lander [6]

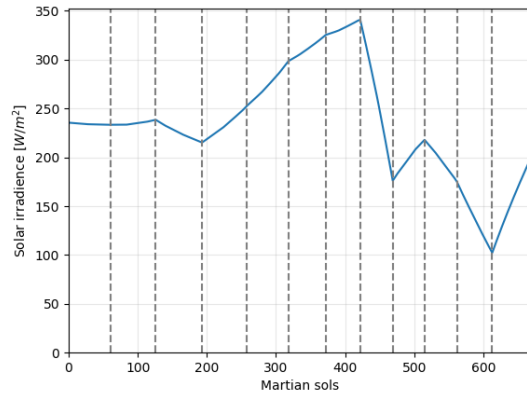


Figure 12.2: Solar irradiance computed for the given insolation value

12.4. Optimising Secondary Energy System for Mars

As mentioned previously, in the trade-off phase the cell technology was determined to utilise III-V semiconductor cells. It was not yet determined which III-V specifically, as this would warrant a more in-depth analysis of the solar spectrum that is present on the Martian surface and its large temperature range. In this section, these aspects are further explored.

12.4.1. Mars Solar Spectrum

To find the cell technology that is most suitable for Mars, and consequently with the highest efficiency, an important factor is how well the cell fits the spectrum. Most solar cells are optimised to function at AM0 or AM1.5 - meaning either for direct light from the Sun, or through the Earth atmosphere respectively. A previous study performed by NASA on the Mars Exploration Rovers [66], analysed the Martian surface spectrum with two photometrically-calibrated cameras. One set of cameras was put on the Opportunity rover which landed at Meridiani Planum, and another set was put on Curiosity, which landed in the Gusev Crater. The measurements from both rovers were then compared to the AM0 spectrum to determine the prominent wavelengths at the Martian surface. These measurements were combined in figure 12.3, where the ratio between the measured values and the AM0 spectrum is portrayed. The optical depth (τ_{opt}) at the time of measurement, is $\tau_{opt} \approx 0.94$. This is an indicator for the dust concentration in the air, where 0 is perfect visibility and 2 is comparable to a Martian dust storm [69].

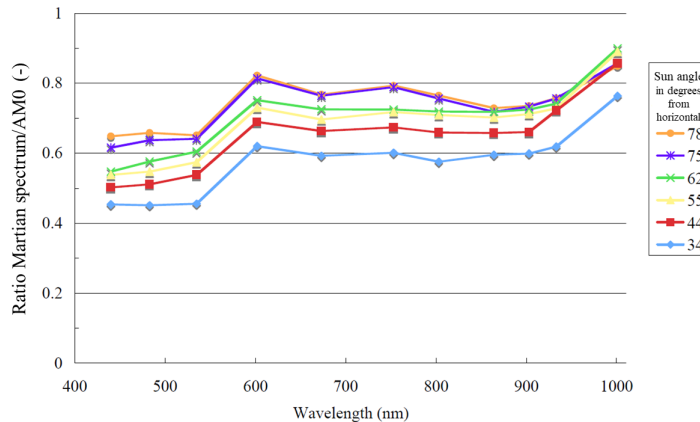


Figure 12.3: “Atmospheric transmission for the global sunlight, 400 nm to 1000 nm, for varied Sun angles (averaged for Spirit and Opportunity data, tau approximately 0.94).” [66]

From this figure it can be seen that due to the high concentration of red dust particles in the air, the blue light gets filtered out partially. With this known, the semiconductor materials for the multi-junction can be selected, to ensure optimal spectrum coverage.

12.4.2. III-V Technology

To gain high conversion efficiencies, one can use multiple semiconductors with different bandgaps to absorb as much energy from the photons as possible. This is the basis for multi-junction cells. When arranging the subcells from the largest bandgap to the smallest (in the order the light travels through the junctions) one can perform so called “spectrum splitting” in the cell. If the energy of a photon is larger than the bandgap of the top semiconductor, it gets absorbed. If the energy is lower, it passes through the next junction to be absorbed, in case of a double junction. More junctions can be added, however the extra gain decreases with each added junction [72]. Thus essentially splitting the spectrum and distributing the different wavelengths to the corresponding subcell. Furthermore, when using multi-junction, it is favourable to have lattice matched subcells. This allows for thinner subcells, as less lattice mismatches will occur during production. Moreover, having less lattice mismatches also guarantees better performance.

When taking these aspects into consideration, there is a III-V triple junction cell technology that seems suitable, namely GaInP/GaAs/Ge. Each of these compounds has very similar lattice constants of around 0.565. Furthermore, the collection of bandwidths fit the spectrum mentioned in the previous subsection. GaInP has a bandgap of 1.85 eV, GaAs of 1.39 eV and Ge of 0.67 eV [72]. This allows GaInP to filter out most of the blue light in the Martian atmosphere, leaving red rich light for the GaAs. The longest wavelengths are captured by the bottom Ge subcell. This increases the performance of the GaAs subcell, as was found in the study performed by Landis et al. [66].

However, as this cell technology was initially designed to perform optimally at AM0, there are some challenges to applying it on Mars. The increase in performance of the GaAs subcell poses a problem to the current matching of the cell. As the light has little blue light and more red light in the spectrum, the GaInP produces a lower current when compared to the GaAs [35]. This limits the current density of the cell, as the total cell current is limited by the subcell generating the lowest current. Edmondson et al. [35] succeeded in matching the currents of the two subcells and optimising a Spectrolab solar cell to the Martian spectrum, gaining 4.6% in power output. As Spectrolab has continued optimising the solar cells for Mars, it was decided to select the Spectrolab GaInP/GaAs/Ge cells for the secondary energy system.

12.4.3. Exergy Considerations

As mentioned in the midterm report [24], a previous study has shown exergy efficiency on Mars to be very low. [29] This is due to the heating up of the panels through the radiation, as the density of the air is not high enough to provide efficient cooling. As the panel temperature exceeds the ambient temperature by a large enough margin, it will generate high thermal losses by losing the heat. The study suggests using panel cooling mechanisms to avoid their heating and thus thermal losses. This should increase the exergy efficiency of the panels if the panel temperature matches the ambient one. An option to be explored in the future would be e.g. either the use of heat sinks as a passive solution, or phase change materials.

To guarantee performance at low temperature however, one can also make use of Low Temperature Low Intensity (LILT) solar panels. This does not negate the exergy efficiency losses; nonetheless it does increase the power output of the panel, as the panel is designed to produce power at low temperatures. The Spectrolab

GalnP/GaAs/Ge cells have a LILT adaptation, with an efficiency of approximately 32% at 1.5AU: the XTE-LILT¹. These cells are not current matched to the Martian spectrum, however as the method for this is known, the performance of the cells will mostly be as expected.

12.4.4. Efficiency Losses due to Anti-dust Coating

The last consideration for the cell performance is the possible decrease in efficiency due to the hydrophobic coating used to prevent dust adhesion. The transparency of the coating was a criterion when designing the coating [105]. The transparency of a normal cover for the cells is 92.0%, whereas the average transmittance of the coating is 92.9%. After temperature shock and radiation tests, the transparency slightly declined to 91.6%. This means there is discrepancy of 0.04% between a coated- and a non-coated panel cover. This decrease in transparency is expected to be negligible and will therefore not be considered further in the sizing of the panel.

12.5. Subsystem Sizing

In general, the secondary energy system can be split into two parts. There are the photovoltaic (PV) panels, which are made up out of the PV modules, and there is the dual axis-system. In this section the sizing, mass and volume estimations of these two will be discussed.

12.5.1. PV Panels

For the PV panels, first the size of the full array must be determined. From there, an estimation of the mass of the full array can be made. This is just considering the panels that make up the array, as the axis-system will be considered in the next subsection.

Size Estimation

The sizing of the PV panels starts with determining the area from the power requirement that is gained from the performance analysis. For this, the same method is used as discussed in the midterm report [24], using the following formula [22, 68] to obtain the area:

$$P_{sa} = S_{in} \cdot A \cdot \eta \cdot I_d \cdot L_d \cdot \cos(\Theta) \quad (12.1)$$

As the specific cell to be used has been chosen, it is now possible to make a more careful area estimation of the array. The required solar power P_{sa} for the habitat is determined throughout the year based on the performance of the kite system as discussed in chapter 9. The solar flux S_{in} is also evaluated throughout the different seasons as described in section 12.3 and the inherent degradation I_d will remain the previously assumed 0.9. The incidence angle Θ will also continue to be assumed as 0°, since the dual axes should keep Θ minimised. From the specifications of the XTE-LILT it can be found that the efficiency η is 0.32 at beginning of life 1.5AU. Lastly, the life-time degradation L_d for the XTE-LILT for a 10 year mission at LEO (with a fluence of 10^{14} electrons/cm² at 1MeV) is 0.93. However at the Martian surface there is a fluence of 10^{11} [3] for the same 1MeV. Thus the L_d was assumed to 0.95 for a life-time of 10 years at the Martian surface.

Using these efficiencies and factors, together with the seasonal change in required power and available irradiance, it can be determined that the largest area is needed in the last month of summer, as there is a peak in the power needed from the solar array due to lower wind resource availability. From this, the second estimate for the area of the PV array is 70 m². A small contingency of 5% is used for any inaccuracies in the performance model due to assumptions, giving an area range of ±3.5 m². This is a considerable decrease from the initial estimation of 934.8 m², which makes the design significantly more sensible.

Mass and Volume Estimation

Once the area of the array is known, its mass estimation can be started. Spectrolab offers fully assembled solar panels for the preceding cell technology of the XTE-LILT, named the XTJ. This cell technology is made with the same triple junction materials, yet provides lower power and efficiency. Aside from this, the mass and volume will be very comparable. Therefore the weight per square meter of the XTJ panel was taken to estimate the weight of the XTE-LILT panel. The XTJ panel weighs 1.76 kg m⁻², with a 9 mm approximate thickness². With the current area estimation, the total mass of the panels would be 123.2 kg. The total volume with a thickness of 9 mm would be 0.63 m³. Of course, this does not fully illustrate if the volume fits with the launch requirement, as it should be ensured that the panels fit into the launch volume by width and height as well.

¹<https://www.spectrolab.com/photovoltaics.html> [Cited 8 June 2020]

²<https://satsearch.co/products/spectrolab-space-solar-panels> [Cited 9 June 2020]

12.5.2. Dual Axis-System

To ensure optimal performance of the PV system, it was decided through a trade-off that a dual axis-system would be used. This can minimise the incidence angle θ and improve the power output of the panel. The specific design for this system is beyond the scope of this project, however some mass estimations can be made.

As the design for the axis-system is pending, off-the-shelf dual axis-systems were used as a baseline. These systems are usually made for crystalline silicone panels, which have a higher mass. Thus, the axis-system is designed to carry more weight, increasing the mass of the whole. Furthermore, the axis-systems designed for commercial use (and by extension for larger scale panels of the scale of the secondary energy system) are not built with mass restrictions in mind. Often steel is used, whereas the system on Mars has strict mass considerations, thus different materials will be considered. Furthermore a higher structural rigidity has been ensured on Earth due to the possibility of high speed wind gusts (up to 50 m s^{-1}) at higher air density. The axis-system that was used as main reference weighs 750 kg for a panel the size of 30 m^2 and can carry a PV panel mass of 375 kg at maximum³. The structure is made of steel, using linear motors and slew drives to follow the Sun through azimuth tracking of a Sun simulation. To support the total area of the secondary energy system, the mass of the dual axis-system would come out to be $1.8 \cdot 10^3 \text{ kg}$. This greatly exceeds what would be a reasonable mass given the requirements. An option is to make use of more lightweight materials, such as aluminium, which seems to have sufficient corrosion resistance on Mars [20], as the XTE-LILT panels are lighter than the axes were designed for. The control unit has an approximate mass of 124 kg for the whole, and deducting this from the total mass, the mass for a similar system using aluminium can be estimated to be 665 kg. This remains more than what would be reasonable as the complete system is very close to the 800 kg launch mass, therefore more research should be done to limit the mass of the dual axis-system by e.g. looking at composite materials on Mars or a magnesium structure, other axis configurations and performing an analysis of the loads present. The volume estimate comes out at around 0.2 m^3 . An advantage is that the foundation of the axis-system can be manufactured on site, using the regolith concrete that will be used for habitat construction as well, saving mass and volume from having to be transported. All sizing estimates were verified by means of hand calculations and sanity checks.

12.6. System Architecture and Interfaces

The system architecture of the secondary energy system is schematically shown in figure 12.4. Here it can be seen that the energy flow in the system starts with irradiance from the Sun reaching the PV panel. The power that is generated is then transported to the power management subsystem, which transfers the power to the habitat and storage as required. The central computer sends the inputs from the Sun simulation to the control system, which in turn commands the control unit of each of the axes, rotating the panels as required. The electromotors that rotate the panels, gather power either directly from the panels, or through the power distribution system.

In case of a dust storm, the central computer can give a signal which puts the panels in a horizontal position to reduce shear forces on the axis, and thus protect the system.

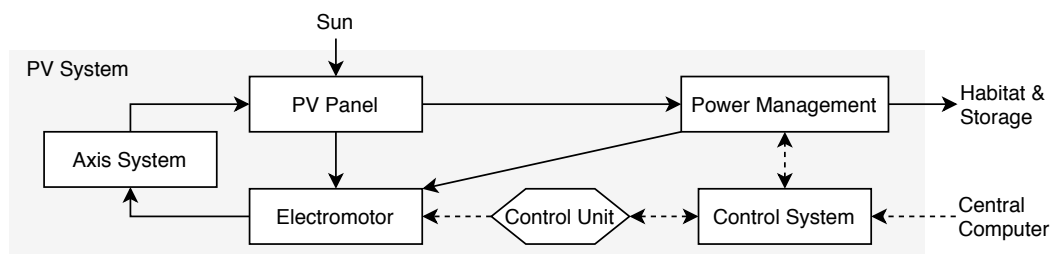


Figure 12.4: Communication (dotted) and energy (solid) flows in system architecture of the secondary energy system

12.7. Cost Breakdown

In this section an estimate of the cost for the PV panels and the axis-system will be made, based on reference material and resource costs.

³<http://www.solar-motors.com/gb/solar-tracker-2-axis-st54m3s30-w-slewing-drive-for-30-m2-0099-st54m3s30-without-concrete-block-i557.shtml> [Cited 9 June 2020]

12.7.1. PV Panels

The first step of estimating the system cost was determining the cost of the cells. Each cell (including cover-glass interconnects and bypass diodes) has an area of 27.22 cm^2 , and costs \$275 [S. Alexander, personal communication, June 11, 2020], or €242. As the area that was previously obtained includes the packing factor, the effective cell area will be taken as 63 m^2 . This area would require 23.3k cells, which means the total cost for the cells comes to €5.65 million.

As the largest cost in the panels will be the cells, it is assumed the panel assembly is around 20% [56] of the cell cost. This makes the total panel cost €6.78 million. This a considerable amount when it is compared to the other sub-system prices. However the higher price required for GaInP/GaAs/Ge when compared to e.g. silicon panels, is negated by the significantly smaller mass and volume. This will save cost later in the project, as less launches will be required to transport the system.

12.7.2. Dual Axis-System

As there is no definitive design for the axis-system, an initial cost estimation is based on the same axis-system as was used for the mass estimation. Since the mass estimation assumed the use of a more light weight material than steel, the price for this reference system needs to be adjusted similarly. For the sake of the the cost estimation, it was assumed aluminium would be used for the structure of the axis-system.

Using the average price of aluminium per tonne (as of 10 June 2020) and the total aluminium mass from subsection 12.5.2 when excluding the hardware, the cost of aluminium in the whole system was estimated to be €773. The cost of the motors and cabling can be taken as €3328^{4,5}, leaving €3576 for added labour cost, production cost and the like. This all leads to a price of €7677 for an equivalent Sun simulation axis-system made out of aluminium. This is considered a reasonable cost within the budget of the mission.

12.8. Risk Assessment

PV panels have been present in the space industry for a long time. The first spacecraft powered by solar panels was launched in 1959⁶. The panels continued to power the spacecraft for more than six years⁷. This proves that already in the beginning of the space era, solar energy was reliable, which has only increased since.

Currently, state-of-the-art solar arrays qualified for Low Earth Orbit and Geostationary Orbit can reach efficiency beyond 35%⁸. Despite the high efficiency and reliability, these are qualification for space and not extraterrestrial use. Although space-grade solar panels are of the highest quality available, the environment for which these are designed for differ from Martian conditions. These factors that are not present in space, but extremely relevant to Martian conditions are: [47]

- *UV radiation* can initiate chemical reactions and degradation of the polymers. As the Martian atmosphere is thin, it cannot filter UV radiation, which is therefore usually high.
- *Wind* can introduce constant static loads on the panels or gusts can apply dynamic loading. This is extremely important during the winter season and dust storms, when the mean wind velocities are the highest.
- *High/low temperatures* introduce thermo-mechanical stress. On Mars, daily temperature change can exceed 100 K, thus this is a major concern [102]. Low temperature tend to slow down chemical processes, which most night are. While high temperature increase stress, but as highest recorded temperatures are in the order of 20-30°C, this is not a major concern.
- *Dust particles* act as an abrasive material and can damage all surfaces, resulting in frosting of the glass and coating damage.

Furthermore, the failure and degradation of PV panels should be clarified. Failure and degradation are used interchangeably, as excessive degradation could also result in certain requirements not being reached.

The failure modes of a solar panel system can be seen in table 12.2 with the likelihood and impact scores defined in chapter 4. Note that not all failure modes are listed here, only the most relevant or applicable to a Mars mission are shown. Furthermore, it is important to note that these risks are for one individual solar panel, thus failure in one panel does not mean the failure of the entire system.

⁴<http://www.solar-motors.com/gb/slewing-drives/slewing-drives-g142.shtml> [Cited 10 June 2020]

⁵<http://www.solar-motors.com/gb/solar-linear-actuator-motor-sm4s600m3nc-0092-sm4s600m3nc-i546.shtml> [Cited 10 June 2020]

⁶<https://web.archive.org/web/20150321054447/http://code8100.nrl.navy.mil/about/heritage/vanguard.htm> [Cited 16 June 2020]

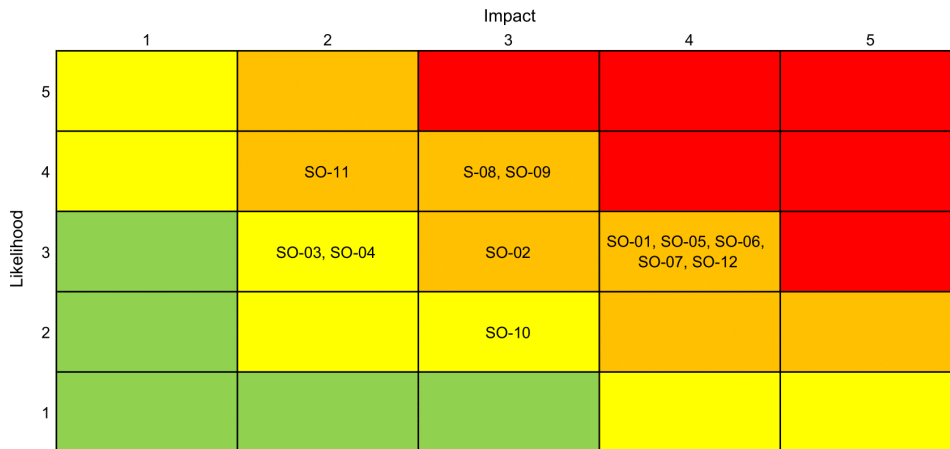
⁷<https://nssdc.gsfc.nasa.gov/nmc/spacecraft/display.action?id=1958-002B> [Cited 16 June 2020]

⁸<https://www.cesi.it/space-solar-cells/> [Cited 16 June 2020]

Table 12.2: Failure mode analysis of a solar panel system [47, 58, 64]

ID	Failure mode	Likelihood	Impact
SO-01	Mechanical solar panel orienting HW failure	3	4
SO-02	Orientation SW failure	3	3
SO-03	Short-circuited cell	3	2
SO-04	Open-circuited cell	3	2
SO-05	Short-circuited module	3	4
SO-06	Open-circuited module	3	4
SO-07	Glass breakage	3	4
SO-08	Delamination of encapsulant and solar cell	4	3
SO-09	Hot-spot failure	4	3
SO-10	By-pass diode failure	3	2
SO-11	Encapsulant degradation	4	2
SO-12	Structural failure	3	4

The risk matrix before mitigation can be seen in figure 12.5. Due to the TRL of solar panels at the moment, no risk is classified as extreme risk. The reason for this is the nature of the mission. PV panels have never been operated in extraterrestrial environment, thus this poses uncertainties and risks.

**Figure 12.5: Risk matrix after mitigation of a PV panel (red: extreme risk, orange: high risk, yellow: moderate risk, green: low risk)**

Risk mitigation measures have to be taken in order to reduce the risk associated with the solar energy system. Similarly to the AWE system, some risks have similar mitigation measures allowing for their grouping:⁹

- SO-01/12: In case of a mechanical failure, an assessment has to be made if it is safe to operate the adjacent solar panels. If it is and the performance reduction is not sufficient, the corrective maintenance can be done during the night. Otherwise, if the safety of other panels is at risk, repair needs to be done immediately.
- SO-02: If the SW fails, first it shall rebooted or if this is unsuccessful fixed immediately. This does not endanger the operation of other panels, thus time of repair is independent of time of the day.
- SO-03/04/05/06: If open- or short-circuit failure happens in a cell or module, the system should remain operational. Thus, the busbars of cells and wiring of modules shall account for this.
- SO-07: Glass breakage usually happens due to dynamic loading caused by wind gusts. These are usually unforeseen, thus a wind velocity threshold shall be established and in case of wind speeds exceeding this, the panel shall be oriented to reduce loading as much as possible.
- SO-08: Module delamination is often the result of thermal stress. To reduce the likelihood, materials have to be researched that have high resistance against temperature fluctuations or thermal control of the panel has to be assessed.
- SO-09: Hot-spots can have numerous underlying causes. Thus to reduce the likelihood, research has to be done for Martian solar panels.

⁹https://www.pveducation.org/pvcdrom/modules-and-arrays/degradation-and-failure-modes#footnote1_oi59yfb [Cited 16 June 2020]

- SO-10: By-pass diodes in Earth environment fail due to undersizing, or high temperatures. As cold temperatures are prevalent on Mars, if sizing is done correctly, this likelihood should be sufficiently lowered.
- SO-11: UV radiation can cause degradation of the encapsulant. Thus, if possible, it shall be avoided by doing additional research and applying the findings, otherwise it has to be monitored and repaired when needed.

After taking these mitigation measures, the revised likelihood and impact scores can be seen in table 12.3 and the risk matrix after mitigation in figure 12.6.

Table 12.3: Revised likelihood&impact scores of a solar panel system after mitigation

ID	Likelihood	Impact	ID	Likelihood	Impact
SO-01	3	3	SO-07	3	3
SO-02	1	3	SO-08	4	2
SO-03	3	1	SO-09	4	2
SO-04	3	1	SO-10	3	1
SO-05	3	3	SO-11	3	2
SO-06	3	3	SO-12	3	3

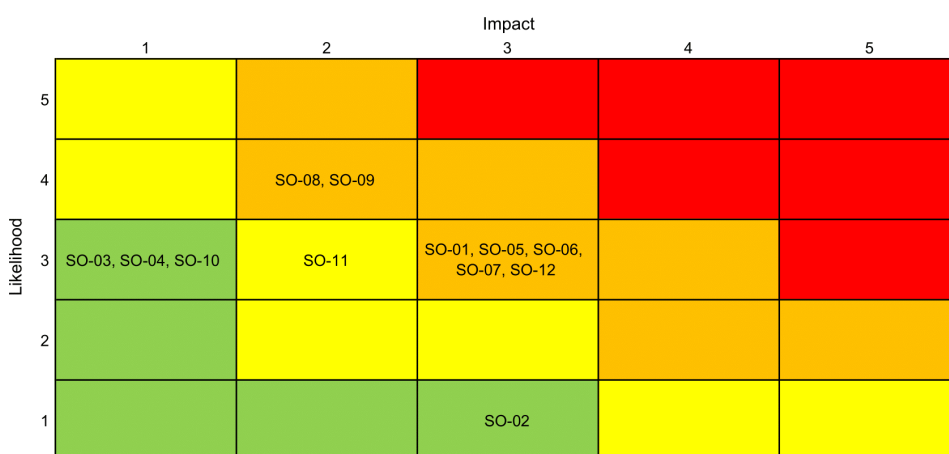


Figure 12.6: Risk matrix after mitigation of a solar panel system (red: extreme risk, orange: high risk, yellow: moderate risk, green: low risk)

12.9. Sustainability and Retirement

As PV panels produce no emissions during their life time, they are a very sustainable option for energy generation. A bottleneck for these PV panels however, are the materials needed for manufacturing. The main materials like aluminium are readily available, due to its wide use in many industries. However, the processing of these metals does have an adverse effect to the environment, and waste is a big issue. The rare metals used in the semiconducting cell however, are more impactful as they are not easily mined and may have adverse health effects. Indium, germanium and gallium are very rare or non-existent in nature in their pure form and have to be refined, which also leaves a lot of waste material. Arsenic and phosphorus also have adverse effects to the environment, where arsenic can potentially damage living organisms and the overproduction of phosphorus has damaged its natural cycle¹⁰. Thus the production of the required resources can have adverse effects on the environment. However when looking at the lifetime of a solar panel, the pollution that is negated by the zero emissions of the energy system make it a much more sustainable option of energy generation compared to methods fossil fuel methods, for example.

As for the retirement of the Martian PV system, several other challenges present themselves. To recycle the PV panels, facilities are required to disassemble them and purify the metals used in the cells [48]. These facilities will not be present on Mars and the panels cannot really be re-purposed. Therefore, the only solution

¹⁰<https://www.lenntech.com/periodic/periodic-chart.htm> [Cited 17 June 2020]

to avoid leaving an impact on Mars at mission end, is to bring the panels back to Earth so that they may be recycled. The axis system however can be disassembled, where the circuits could be reused together with the electromotors present in the axis. The aluminium frame could be used in new structures on Mars if required.

12.10. Requirement Compliance and Sensitivity

To ensure the design meets the requirements, the requirements compliance is checked as seen in table 12.4. Please note, that **REM-Sys-N12-06** and **REM-Sys-N12-07** are still dependent on further research, as they are part of a more detailed design phase.

Table 12.4: Secondary Energy System Requirements

ID	Compliance	Proof (Section)
REM-Sys-N12-02	No	Subsection 12.5.1 and subsection 12.5.2, further research is needed to decrease axis mass
REM-Sys-N12-03	Yes	Subsection 12.5.1 and subsection 12.5.2 show the volume of the system to meet the requirement
REM-Sys-N12-04	Yes	Chapter 9 maintains the secondary energy contribution below 50%
REM-Sys-N12-05	Yes	Subsection 12.5.1 accounts for the 5 Martian years life-time
REM-Sys-N12-06	Probable	Dust removal coating is very new and shall mature in the coming years. More research is required to incorporate the dust removal percentage in the analysis
REM-Sys-N12-07	Probable	More research is needed to develop the Sun simulation, however the system is likely to achieve a high accuracy

Next, to confirm the design is reliable a sensitivity analysis is performed. This is done using the method shown in section 9.3, where the system is downsized to investigate its sensitivity. The solar area will be decreased to 55 m^2 for this analysis. The estimated dimensions of the secondary energy system decrease as expected when the area decreases. Since the calculations used have a direct relation between the array area and the sizing estimates of the system, an equal decrease was expected in the system dimensions. Decreasing the area as mentioned, means a decrease of 21.4%. When the dimensions are resized, the systems decreased with 21.4% as expected. Therefore the system parameters adapt satisfactorily with the sensitivity analysis, and the method is therefore assumed to be sound for usage in this preliminary design phase of the system.

12.11. Recommendations

There are several steps that can be taken in the next phase of the design to further develop the secondary energy system. Firstly, the axis-system needs to be re-evaluated to find a more light weight solution, as the initial mass estimate is higher than favourable considering the mission limits. Secondly, a cooling concept for the solar panels needs to be designed that would be effective in the low density Martian atmosphere, without adding too much mass to the system. Furthermore, the Sun-simulation used by the azimuth Sun tracking system needs to be developed to ensure high performance of the system. Lastly, the specific configuration of the modules and panels needs to be finalised in cooperation with Spectrolab, as they will be manufacturing the panels.

Storage System Design

Storage refers to systems where energy is stored and utilised for the Habitat in times of unfavourable wind and/or solar conditions. The storage system will have two essential components, one being a day-to-day storage solutions, the other being a seasonal storage solution. Both these are designed in more detail in the following sections. Starting with requirements in 13.1, the trade-off summary in 13.2 and the system's architecture in 13.3 which are relevant for both systems, the detail in design in 13.4 and 13.5 of the two systems is described separately for the two. Towards the end of this chapter, the design results are summarised in 13.6 and cost, risk and sustainability are analysed in 13.7, 13.8 and 13.9 respectively. Finally, requirement compliance is checked in 13.10, ending the chapter with further recommendations in 13.11 for the future of the project.

13.1. Requirements

The storage system will consist of a seasonal storage system and a day-to-day storage system. These have their specific requirements which are listed in table 13.1. The requirements will be checked for compliance at the end of this chapter.

Table 13.1: Energy Storage Requirements List

Requirement ID	Description
REM-Sys-N05-02	The seasonal energy storage system shall have an energy capacity of 13 MWh.
REM-Sys-N05-03	The combined energy storage system shall have a rated power of 10 kW.
REM-Sys-N05-04	The components of the total energy storage shall have a maximum mass of 1500 kg.
REM-Sys-N05-05	The energy storage subsystem should make use of ISRU storage options by at least 70%.
REM-Sys-N05-06	The seasonal storage system shall have a compression efficiency of at least 70%.
REM-Sys-N05-07	The seasonal storage system shall have a storage efficiency of at least 96%.
REM-Sys-N05-08	The seasonal storage system shall have an expansion efficiency of at least 60%.
REM-Sys-N05-09	The day-to-day energy storage system shall have an energy capacity of at least 117 kWh.

13.2. Trade-off Summary

The design trade-offs were initiated with a preliminary sizing based on energy storage capacity required, gathered from system performance. It was clear that hardware for gravitational, battery and fuel cell storage would be too massive to meet given mass and volume requirements. For day-to-day storage, the Compressed Air Energy Storage (CAES) system incurs low round-trip efficiency for short cycle and daily usage, while the regenerative fuel cell technology is too complex and incurs overall high operational risk. Battery systems are the most logical solution for a modular, plug and play, short period, daily operational electrical storage system. For a more extensive summary of the storage design trade-off process, refer to the Midterm report [24].

The initial designs and final designs of the trade-off procedures are summarised below. In the following sections the exact battery technology will be selected, which will allow for a more detailed sizing procedure.

Trade-off Design Options

- Compressed Air Energy Storage (CAES)
- Gravitational Storage
- Secondary Batteries
- Regenerative Fuel Cells

Final Designs for Storage Systems

- *Seasonal:* Compressed Air Energy Storage
- *Day-to-day:* Secondary Batteries

13.3. System Architecture and Interfaces

This section includes a diagram of how the energy storage system functions and is integrated. Both CAES and batteries are vital to the workings of the energy system, and they play an interchangeable role as the storage

infrastructure. Figure 13.1 shows the seasonal storage as well as the day-to-day storage components with respect to the energy generation systems and the Mars habitat.

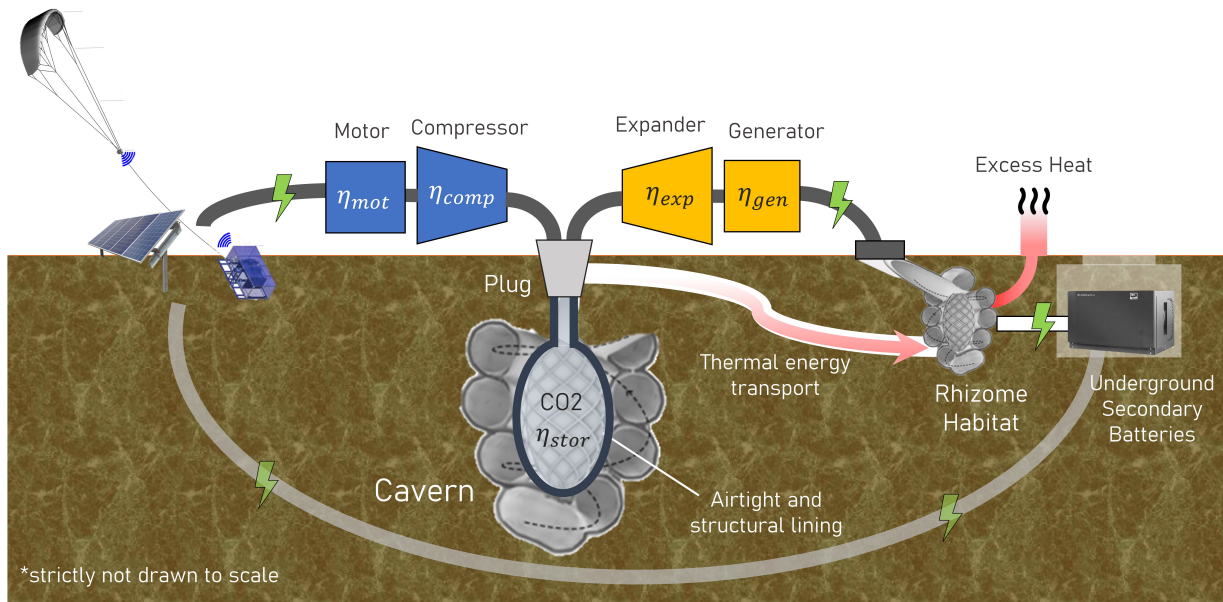


Figure 13.1: Architecture of the energy storage system

Since the CAES and the secondary battery system combine to one system that needs to perform in harmony, this next section will describe how this happens.

Energy is produced by the wind and solar energy systems, which then can go to three different places. A part of the energy is supplied to the habitat for direct use. The excess energy then goes into one of the two storage options. As the batteries need to be used during the night to provide energy to the habitat, these need to be charged first. This means that until the batteries are fully charged the excess energy flows in here. Any additional excess energy after charging the batteries flows into the compressed air storage for long term storage. In the case where the energy production units are not able to provide enough energy to the habitat or to charge the batteries for the night time, the energy needs to be supplied by the seasonal compressed air storage.

A final item to note is that the compressed air storage also produces a lot of heat which results in a loss of efficiency for energy storage. In order to not lose all the thermal energy, it is planned to be reused to heat the habitat. Further detail on the two systems and how these work will be elaborated on in the following sections.

13.4. CAES Design Approach and Sizing

An adiabatic CAES system (A-CAES) is a type of energy storage system that can be adapted to the Martian environment. This is due to the minimisation of required components to meet mission cost and mass budgets. A key modification is that a typical thermal energy storage system of an A-CAES is now a thermal energy transport system, where the heat generated at compression stages is transported to the Habitat.

The grid-scale CAES systems that are currently operational on Earth, but not feasible for Mars, are either diabatic systems (D-CAES) and isothermal systems. In D-CAES, fuel is injected at the expansion stage to increase the effective power retrieved. This means that this option is not fully renewable as energy is stored in the form of fuel, namely natural gas. The third type of CAES is an isothermal system, in which the operational temperatures at compression and expansion stages are to be maintained by constant heat exchange to the environment. Only, this system is only practical for low power levels and more complex.

13.4.1. Design Approach

The sizing of the CAES system, including defining the characteristics and configuration of components can be put through an iterative procedure. Note that there are multiple design criterion of an underground CAES system that needs to be delineated to have a holistic analysis, including volume sizes of caverns or excavations.

tions. This is why the sizing should be done in conjunction with a Mars mission team such as the Rhizome habitat project. This is reflected in Section 13.11.

The first step is to perform a preliminary exergy storage capacity analysis, and the first condition to set is a range of possible storage cavern volumes on Mars. For this DSE, a theoretical ceiling is set (blue line in figure 13.3). The second assumption is that the structural characteristics of the internal lining of the surrounding rock-mass withstands the pressures below this ceiling.

It is considered that the CAES will utilise CO₂ namely, hence its analysis and characteristics take precedence in design. Next, the thermodynamic process overview of the system needs to be understood. These two informing steps aid in selecting the components of segments in a specific configuration. In this report, only the compressor and turbine are sized and selected. Other components (the motor, generator, plug) are delegated to further design stages.

Finally, the total efficiency of the system is verified, which covers **REM-Sys-N05-06** to **REM-Sys-N05-08**. The last test verifies requirement **REM-Sys-N05-05**, where the mass of CO₂ required is determined to be 301812 kg, which is roughly 86% of the total storage system weight (disregarding the regolith material mined and built as inner structural lining material). The first CAES design procedure is complete and the storage capacity and components can be further designed, as recommended in section 13.11.

13.4.2. Subsystem Sizing and Design Parameters

This section details the sizing iterations and consolidates the design parameters, intended for further research and manufacturing of the key components.

Exergy Storage Capacity Analysis

A CAES system functions on converting the work done by expanding compressed air, thus the storage performance can be modelled using thermodynamic relationships. As inferred from the system design process (figure 13.4), the compression/expansion phase can be modelled close to isothermal and may obey the ideal gas law, which is the first key assumption made.

From an initial state *A* to final state *B*, with constant absolute temperature, the (negative) work required for compression or by expansion (positive) can be written as equation 13.1. The ambient pressure p_a on Mars is equal to the starting pressure p_A and the positive work by compressed air lowers the exploitable exergy, which adds a term to equation 13.1 to form 13.2, where B is the exergy capacity required of the storage system and $p_B = p_s$, the pressure of the underground cavern.

$$W_{1 \rightarrow 2} = \int_{V_A}^{V_B} p \cdot dV = \int_{V_A}^{V_B} \frac{nRT}{V} \cdot dV = nRT \ln\left(\frac{V_B}{V_A}\right) = p_A V_A \ln\left(\frac{p_A}{p_B}\right) = p_B V_B \ln\left(\frac{p_A}{p_B}\right) \quad (13.1)$$

$$B = W_{1 \rightarrow 2} = p_s V_s \ln\left(\frac{p_a}{p_s}\right) + (p_s - p_a) V_s \quad (13.2)$$

The cavern storage volume, V_c , required can thus be defined at each exergy storage capacity level as a function of pressure ratios, r , see equation 13.3.

$$V_c = \frac{B}{p_a \cdot \left(r \ln\left(\frac{1}{r}\right) + (r - 1)\right)}, \text{ where } r = \frac{p_s}{p_a} \quad (13.3)$$

The results of the preliminary exergy storage analysis is represented in a graph that contains an 'envelope' where possible design trade-offs between available volumes on Mars, whether existing Martian caverns are utilised or excavated by the Rhizome habitat team. This is also defined by structural rigidity and resistance to pressurised deformations. In order to minimise overall volume needed, Point *B* is selected at the exergy

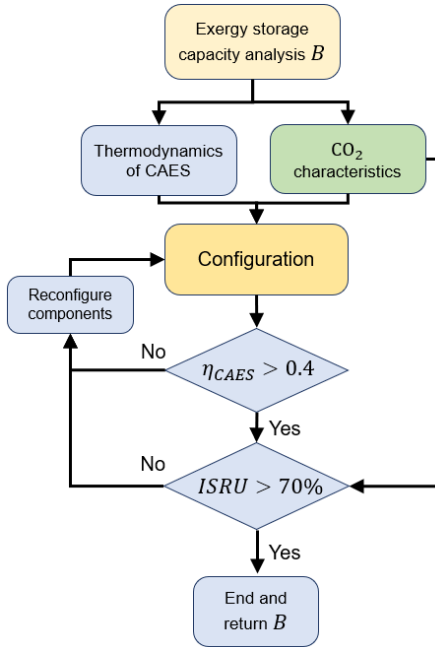


Figure 13.2: Flow chart of CAES design

capacity design point, with a pressure ratio of 175. Although this value seems high, this ratio means the pressure stored in the cavern is 105175 Pa, which is roughly 4% more compared to Earth's surface pressure. Hence, there is existing compression technology for space applications that already pressurised spacecrafts and will be used for Martian habitat adaptations to accommodate the human physiology¹. However, a problem arises when sizing the turbine, as expanding compressed air with high ratios might decrease efficiency of turbine performance. This is highlighted in section 13.4.2. In addition, the volume of storage cavern needed is high, which almost poses a design challenge and risk.

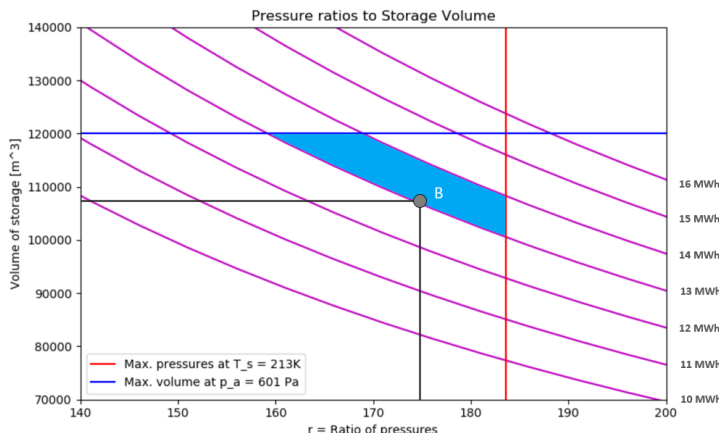


Figure 13.3: Exergy storage capacity envelope

CO₂ Analysis

Because of the abundance of CO₂ on Mars (roughly 95.8%) this is an in-situ resource that should be utilised, meeting a functional requirement in the process. Thus, a key assumption made in the sizing of the CAES system is that the compressed air utilises mainly CO₂ properties. Because of novelty of its application and the large deviation in atmospheric temperatures and pressures compared to Earth, a key step in validating the CAES sizing model is to ensure that the compressed air remains a manageable (gaseous) state to avoid operational complexities during all segments. CO₂ is a highly corrosive medium² and the moisture (condensation) must be kept to a minimum. This is a key consideration for the turbine design, as air can be cooled significantly in rapid expansion stages. At low temperatures on Mars, the maximum pressures of CO₂ as the storage air is generally lower. This can also be inferred from a CO₂ phase diagram³. To represent this pressure limit, the red line in graph 13.3 indicates the maximum pressures allowable for the lowest extreme temperatures on Mars considered for CAES operations, which is 213K (-60°C), the highest being 253K (-20°C).

The following assumptions influence the configuration selection, particularly equations 13.6 and 13.5, the compressibility factor of CO₂, z , is assumed to be 1 because even at high pressure ratios up to 160 (where p_s is 0.1MPa), z remains close to 0.98. k is the ratio of specific heats, which is taken as 1.28. R is the gas constant and T_a is the ambient temperature on Mars, which is taken as 233K, a mid-point between the functional temperature range selected for the CAES system.

Thermodynamics of CAES

The CAES system functions on the effectiveness of the compression and expansion stages of the desired gas, thus its sizing relies on thermodynamic flows and properties. Pressure ratios, stage efficiencies and energy losses provides a good indication of the system's configuration performance as a whole. Four key assumptions are also set here.

Figure 13.4 presents the three segments of the CAES system: compression, storage and expansion. The first includes the motor and stages of compression, which produces heat as a byproduct. In the Mars design concept, this heat is led to the environment or directed to the habitat, which approaches an isothermal process, this is key assumption 1. The second segment consolidates the storage with the charging and discharging of system, represented by the exergy streams \dot{Ex}_{cas_in} and \dot{Ex}_{cas_out} respectively. During the storage process, no heat is lost and is in equilibrium with the ambient temperature, this is key assumption 2.

¹<https://journals.physiology.org/doi/full/10.1152/jappl.1999.86.3.1062> [Cited 17 June 2020]

²<https://www.haug.ch/de/produkte-service/gas-kompressoren/haugsirius-75-30-kw.html> [Cited 12 June 2020]

³<https://socratic.org/questions/what-are-the-phase-diagrams-of-water-and-carbon-dioxide> [Cited 17 June 2020]

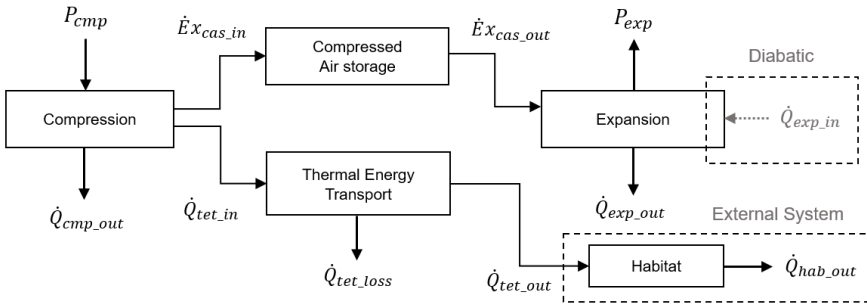


Figure 13.4: Mars CAES System Design Concept

$$\eta_{CAES} = \eta_{comp} \eta_{stor} \eta_{exp} \eta_{others} = \frac{\dot{E}x_{cas_in}}{P_{cmp}} \cdot \frac{\dot{E}x_{cas_out}}{\dot{E}x_{cas_in}} \cdot \frac{P_{exp}}{\dot{E}x_{cas_out}} = \frac{P_{exp}}{P_{cmp}} \quad (13.4)$$

The final expansion stages translates the expanding air into controlled mechanical work to activate the generator. \dot{Q}_{exp_in} is heat input that a diabatic system namely adopts, but it can also represent any additional heat input concept that can increase the efficiency of the expansion stage. For the purpose of this project, additional diabatic components are disregarded. In addition, the cold air formed in the expansion stage is also set to be negligible in the sizing, this is key assumption 3.

The three segments for efficiency analysis play a role in meeting the system's functional requirements. As reflected in equation 13.4, the overall CAES efficiency, η_{CAES} , is the ratio of power extracted from the expansion to the power required to compress the air. This is used for verification of CAES design requirement compliance. The efficiencies of other components are incorporated in η_{others} , which includes losses in generator energy conversion. These losses are neglected in this sizing, this is key assumption 4.

Configuration Selection - Compressor and Turbine

The two subsystems of a CAES system to design for a Martian adaptation at this stage are the compressor(s) and turbines(s). Motors and generators can be adapted later on, which is also demonstrated in the development of the primary energy system's ground station.

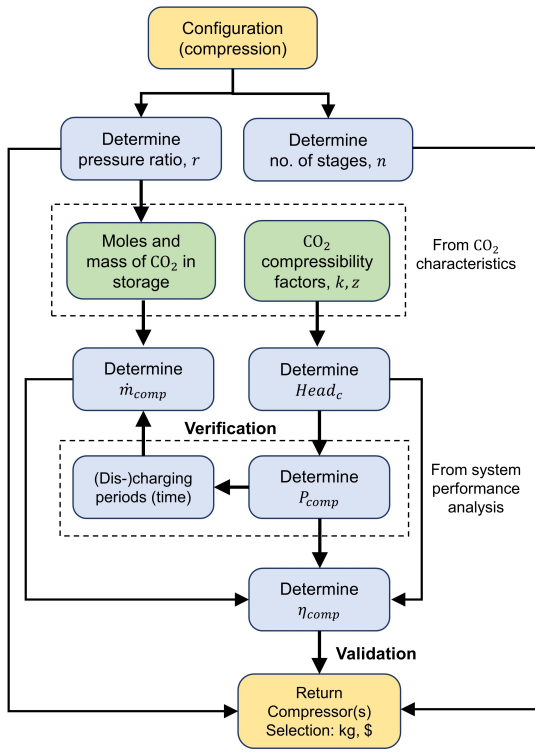


Figure 13.5 illustrates the procedure for selecting the compressor. The turbine selection follows a similar approach with power, efficiency and mass flow variants, and some practical alterations regarding compression and turbo-expansion technology. Following key assumption 1, both the compression and expansion stages are isothermal processes in order to simplify the preliminary analysis, which implies T_a in equation 13.5 remains the same in the event of multiple stages. The logic behind this follows that the compression segment is spread over To take into account temperature differences between different stages, a sensitivity analysis is carried out in section 13.11.

From CO₂ analysis, assumptions are carried forward about the quality of . The mass of the this compressed CO₂ is determined by molar mass and number of moles at set pressure, temperature and volume. $Head_c$ is the measure of amount of energy required to elevate the pressure of a fixed amount of air to a higher level in a *centrifugal compressor*, given by equation 13.5.

$$Head_c = \frac{k}{k-1} z RT_a \left[r_c^{\frac{k-1}{k}} - 1 \right] \quad (13.5)$$

Figure 13.5: Flow chart of (compressor) configuration selection

From systems performance analysis (section 9), using initial inefficiencies, during the charging (compression) periods, the power required of the compression segment, P_{comp} , is 17.2 kW. With the total charging time, over an average of 2 hours per day for 40 days, the mass flow \dot{m}_{comp} , is calculated as 1.106 kg/s and is assumed to constant through the segment. The power extracted from each stage of the compressor is reflected by the variable $P_{comp,i}$, where i represents the compressor stage, which is equally segregated from total power required P_{comp} . η_{comp} is the efficiency of the compression segment as a whole.

$$\eta_{comp} = \frac{\dot{E}_{cas_in}}{P_{comp}} \approx \prod_{i=1}^n \frac{\dot{m}_{comp} \cdot Head_c}{P_{comp,i}} \quad (13.6)$$

To select a compressor technology, these parameters are critical; r_c , \dot{m}_{comp} , P_{comp} and η_{comp} . Hence, the requirement for the seasonal storage compression efficiency can be validated. The mass and costs of the selected compressor is considered and if respective budget requirements are met, the compressor selection is complete. The compressor selected within this iteration is the HAUG Sauer Sirius centrifugal compressor⁴. The total segment efficiency η_{comp} is determined to be 76.3%. Table 13.2 consolidates the compressor model selection and design parameters for its operation.

Table 13.2: Compressor Selection

Pressure Ratio r_c [-]	Stages n [-]	Mass flow \dot{m}_{comp} [kg/s]	Power Required P_{comp} [kW]	Efficiency η_{comp} [%]	Weight [kg]	Cost [€]
13.5	2	1.106	17.2	76.3	400	400 000

A parallel analysis is done for the turbine selection, with a few discrepancies. Because turbines can handle lower pressure ratios and still retain optimal functionality, the initial number of stages is set to 3, with a pressure ratio of 5.7. The peak power supplied to the habitat (via power management) by the expansion segment is 11.8 kW, and P_{turb} is the nominal power required by the turbine based on an initial efficiency, η_{exp} , estimate of 65%, taken to be 18.1 kWh. As opposed to $Head_c$, $Head_t$ represents the measure of energy released during the expansion phase, in which the difference in pressures power the generator. The mass flow is calculated as 54.5 g/s, over an average of 12 hours per sol for 120 sols. Finally, η_{exp} is determined to be 65%. Table 13.3 consolidates the turbine model selection and design parameters.

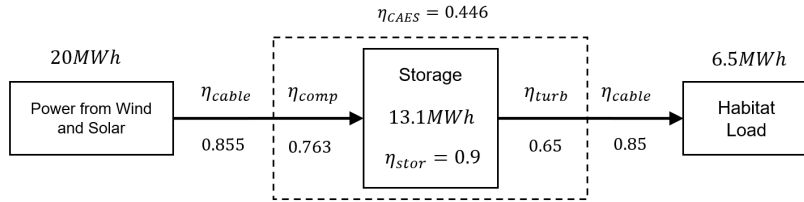
$$\eta_{exp} = \frac{P_{exp}}{\dot{E}_{cas_out}} \approx \prod_{i=1}^n \frac{\dot{m}_{turb} \cdot Head_t}{P_{turb,i}} \quad (13.7)$$

Table 13.3: Turbine Selection

Pressure Ratio r_t [-]	Stages n [-]	Mass flow \dot{m}_{turb} [kg/s]	Power Required P_{turb} [kW]	Efficiency η_{exp} [-]	Weight [kg]	Cost [€]
5.7	3	0.0542	18.1	65.0	660	850,000

The implications of the efficiencies of the selected components and stage configuration can should still allow the storage system to function with the sufficient energy inputs and outputs. One key check is that the power received by the CAES from wind and solar direct is sufficient through the year. This check is to conform the configuration values with the ones achieved from the systems performance analysis (chapter 9), in particular, the plots 9.9 and 9.12, which showcases the energy stored and the charging of the CAES system and the energy stored as a function of time through a Martian year respectively. Figure 13.6 presents an overview of inefficiencies and power requirements at each stage of the current design for one Martian year.

⁴<https://www.haug.ch/de/produkte-service/gas-kompressoren/haugsirius-75-30-kw.html> [Cited 12 June 2020]

**Figure 13.6: Efficiency and power compliance for one Martian year**

Remaining Components

These are the design parameters for the remaining components of the CAES system. Both the sizing of the motor and the generator can begin from the relationship described by equation 13.8⁵, where Tq is the torque of the component, P is the power input/output and RPM is the revolutions per minute, which is an estimated number based on the compression and expansion segment conditions and mass flow requirements, as well as reference values for typical compressor motor and turbine generators. Two final key assumptions are reemphasised here; the electrical-to-mechanical energy losses (and vice versa) between the motor/compressor and turbine/generator (respectively) is negligible. Secondly, the multiple stages of the segments coincide at this point of intersection, which means the RPM is the combination of multiple stages. This is done by multistage-integrated gearbox design⁶. The final motor and generator selection are shown respectively in table 13.4 and 13.5.

$$Tq = 9.5488 \cdot \frac{P}{RPM} \quad (13.8)$$

Table 13.4: Motor Selection

Power required P [kW]	Torque Tq [Nm]	Rotational Speed RPM	Mass [kg]	Cost [€]
17.2	326.57	500	100	250,000

Table 13.5: Generator Selection

Power output P [kW]	Torque Tq [Nm]	Rotational Speed [RPM]	Mass [kg]	Cost [€]
18.1	115.22	1500	240	500 000

The last component of the CAES system to size for is the plug⁷. This component controls flow at the ground surface. For the scope of this DSE, the design of the plug is not included as this is also highly dependent on the site characteristics where the storage cavern is located. The plug is thus incorporated into both compression and expansion segments, treating the compressor and turbine caps as the control of mass flow. However, the plug can also be identified to be a substantial cost in terms of material volume needed on Earth. This could be another pitfall of the CAES design selection. A recommendation is to first investigate whether the plug design can be produced with in-situ additive manufacturing, and this is done in conjunction with the research planned for cavern volume design, elaborated upon in section 13.11.

13.4.3. Materials and Structural Characteristics

For the CAES system, the main components, also shown in figure 13.1, are the compressor, motor, turbine, generator, plug, and structural linings of the cavern. The detailed list of materials likely used in a compressed air energy storage system is consolidated in table 13.10 below. Note, that the materials listed below account for the bulk (>70%) of the total component weight. Lastly, the materials listed here is meant as a reference, there are multiple design adaptations required for Martian-bound applications of existing 'off-the-shelf' components. An instance is the material for the structural lining of the cavern, this resource is highly dependent on further

⁵http://wentec.com/unipower/calculators/power_torque.asp [Cited 19 June 2020]

⁶<https://www.neugart.com/en/planetary-gearbox/multi-stage-gearbox/> [Cited 19 June 2020]

⁷<https://www.sciencedirect.com/science/article/pii/S1674775515001171> [Cited 20 June 2020]

investigation into Martian rock mass rigidity, possibly by the Rhizome habitat team. This is also mentioned in further recommendations of CAES design.

Table 13.6: Material considerations for CAES system

Part	Material	Part	Material
Compressor	Nickel Graphite	Turbine	Anti-corrosive Steel
	Carbon-Manganese		Aluminium
	Titanium		Nickel-based Alloy
	Aluminium		Thermoplastics
Motor	Silicon steels	Plug	ISRU: Rock mass
	Cobalt		Alternative: Low specific-weight steels
	Copper	Cavern lining	ISRU: Rock mass
	Aluminium		Alternative: Low specific-weight steels
Generator	Electrical Steel		
	Magnesium		
	Copper		

Lastly, in order to size the materials needed for inner structural lining, the maximum membrane stress of the (idealised) spherical cavern, σ_{cavern} needs to be determined. This is the normal stress the inner lining needs to withstand, in addition to being airtight and thermally insulated ideally. These are considered in further recommendations. By equation 13.9, where r_{cavern} is the radius of the cavern and t is the thickness of the structural lining, which is assumed to be 0.5 m, σ_{cavern} is determined to be 3.1 MPa. Note, this relation can only be used based on thin-wall theory, where $r_s/t > 10$.

$$\sigma_{cavern} = \frac{p_s r_{cavern}}{2t} \quad (13.9)$$

This is significantly lower than the yield stress of most steels. It can be extended that the additive manufacturing product (a regolith-alloyed spray) of the Habitat-building rovers will have the capability to meet this stress criteria. Hence, mass of the lining, as a material that is transported from earth, and the regolith in-situ resource is utilised. A mass budget of the regolith⁸, using a density of 1.52 g/cm^3 , and a volume of 5468 m^3 (from a spherical surface area idealisation and thickness), indicates 8 310 tonnes of material needs to be mobilised.

Remote sensing techniques will certainly be initially used to identify rock structures to determine feasible sites for underground construction before committing a Martian colony to a site. This can be done in conjunction with the CAES construction.

13.5. Battery Design Approach and Sizing

Now that the Seasonal Storage system has been designed, the secondary batteries need to be as well. In the next subsections the design method will be described.

13.5.1. Design Approach

To come up with a suitable design and size for the day to day batteries, it is important to select the right battery type. The two most viable options for space that have been researched are lithium-ion and lithium-sulphur. One must however keep in mind that lithium-sulphur is still in development whereas lithium-ion is already widely used. The characteristics of each battery type [94] are given in table 13.7.

The battery types are consequently sized as to trade-off which type is more applicable to the mission at hand.

13.5.2. Subsystem Sizing and Budget Breakdown

To size the batteries⁹, the following approach was used. First, the required capacity (C_{req}) is given from the system performance analysis. Based on this, the capacity at end of life and beginning of life are calculated with equations 13.10 and 13.11, respectively [68].

$$C_{EOL} = \frac{C_{req}}{\eta_{bat} * DOD} [\text{Wh}] \quad (13.10)$$

⁸<https://www.lpi.usra.edu/meetings/LPSC98/pdf/1690.pdf> [Cited 19 June 2020]

⁹<https://www.valispace.com/how-to-size-a-satellite-battery/> [Cited 10 June 2020]

Table 13.7: Battery properties

Properties	Lithium-Ion	Lithium-sulphur
Energy density [Wh l ⁻¹]	200	350
Specific energy [Wh kg ⁻¹]	100	300
Lifetime [years]	5	5
DOD [-]	0.8	0.8
Usable energy [-]	0.8	0.8
Efficiency [-]	0.88	0.88
Fading factor [-]	0.92	0.92

$$C_{BOL} = \frac{C_{EOL}}{F_{fading} * N_{years}} \quad (13.11)$$

The mass and volume of the batteries result from equations 13.12 and 13.13, respectively.

$$M_{bat} = \frac{C_{BOL}}{m_{sp}} \quad (13.12)$$

$$V_{bat} = \frac{C_{BOL}}{e_{density}} \quad (13.13)$$

The summary of the results are shown in table 13.8.

Table 13.8: Battery sizing results

Property	Lithium-Ion	Lithium-sulphur
C_{req}	117.0	117.0
C_{EOL}	166.2	166.2
C_{BOL}	36.1	36.1
M_{bat}	361.3	120.4
V_{bat}	180.6	103.2

Now that both options have been sized according to the necessary capacity requirement, a battery needs to be chosen. The trade-off for these is performed as was done in the Midterm Report [24].

Table 13.9: Trade-off between lithium-ion and lithium-sulphur batteries

Category	Aspect	Weight	Score	
			Lithium-ion	Lithium-sulphur
Development cost	Research cost	4	7	3
Development risk	Achievable manufacturability	4	5	3
Mass performance	System mass	5	5	8.9
	Specific capacity	3	5	7
Volume performance	System volume	4	3	7
Sustainability	Production	3	5	7
	Retirement	3	5	7
Regained energy		4	5	7
Sum category weights			Weighted Score	
		24	5	6.1

Table 13.9 shows the trade-off for the battery technology. It can be seen that the lithium-sulphur batteries win the trade-off with a grade of 6.1. This is mainly because they perform so well in mass and volume compared to the lithium-ion batteries. However, the important thing to note about the new technology is that it is still under research and is not yet commercialised like lithium-ion batteries are. Thus, their properties are not yet guaranteed and it is still unsure whether these really are a good option for space travel compared to lithium-ion batteries which are already widely used for space applications. The research cost here is thus much higher, scoring a lower grade for lithium-sulphur than the lithium-ion batteries. The same argument can be made for the achievable manufacturability. Furthermore, sustainability aspects were taken into account for retirement and production of the batteries. What makes lithium-sulphur so interesting is that these are more recyclable than lithium-ion batteries currently are. Finally, the lithium-sulphur batteries have a higher general performance than the lithium-ion batteries and thus are chosen despite still needing to be researched further.

Two more additional considerations are made for the batteries. One being that it needs to be stored in a protective cover for protection from radiation and Martian environment. This cover would most likely be some sort of a box which will insulate the batteries as well as protect it from radiation.

The other consideration is that the battery is heavy, which means that it would be best if the battery was modular to make installation on Mars easier. This would also mean that when one of the modules fails it can be easily replaced by a new module. These single modules could for example be around 25 kg each of the total mass of 120.4 kg.

The final size of the lithium-sulphur batteries which contribute to the budget of the energy storage system will be a mass of 120.4 kg and a volume of 103.2 l.

13.5.3. Materials and Structural Characteristics

For the design of the batteries there are not any structural characteristics to take into account for now. The most structural part of the design would be the protective casing, however this will not be designed in this part of the project. The other materials are those considered in the production of the batteries. These would naturally include the chemicals lithium and sulphur and any other materials used to encase the batteries. The full list of materials likely used in the lithium-sulphur batteries can be seen in table 13.10.

Table 13.10: Materials in a lithium-sulphur battery for different component

Part	Material	Part	Material
Positive Electrode	Graphene oxide	Cell container	Aluminium, ingot
	Sodium thiosulfate		PP
	PVP		PE
	HCl		Aluminium, ingot
	Carbon Black		Copper, billet
	PVDF		PP
	Aluminium, ingot		PE
Negative Electrode	NMP	Separator	Aluminium, ingot
	Lithium, billet, primary		ABS
	TEOS		Copper, wire
Electrolyte	Copper, billet		Integrated, circuit
	LitTFSI		Polymer
	DOL		Aluminium, ingot
	DME		Ethylene glycol
BMS	LiNO ₃	Cooling system	Aluminium, ingot
	BMS		Steel, billet
			Copper wire
Pack packaging			

13.6. Subsystem Design Results

At this juncture, the 2 storage subsystems have been designed and need to integrated as one. In the following, the two systems will be briefly summarised.

CAES

The CAES system consists of a compression segment, which includes the motor and compressor. Its total weight estimation is 500 kg with an efficiency of 76.3%. The storage segment consists of a plug (which is currently integrated in the other two segments) and the storage cavern with a volume of 107 500 m³, holding a pressure of 105175 Pa with an efficiency of 90%. The final segment is the expansion which consists of the

turbine and generator and its total weight is 900 kg with an efficiency of 65%. Overall, the efficiency of the CAES system is 44.6% and is required to store 13.1 MWh in a Martian year.

Battery

In summary for the short-term storage, the day-to-day storage system will be made of lithium-sulphur batteries with a mass of 120.4 kg and a volume of 103.2 l. They will be stored in a protective box and modularity of the batteries will be an important aspect of their design.

13.7. Cost Breakdown

The cost of the system is a challenge to estimate as these technologies are not readily used. However, a preliminary estimate was compared to values in existing CAES systems today, namely the Hundorf and McIntosh plant, as well as the design parameters for the ADELE A-CAES concept¹⁰.

The total cost estimation for the parts to be transported from Earth, which adds up to 1400 kg is €2 000 000. This is excluding the material considerations of cavern structural lining, harnessing and use of CO₂ and plug design. The total costs of the implementation the CAES system is to be incorporated with these activities, which is part of the habitat team in site construction, in terms of materials, available equipment (excavation rovers etc.) and man hours (astronauts).

For the batteries, the lithium-sulphur type is still under development and there are no companies already selling the batteries off-the-shelf. Thus, the team needs to depend on estimations.

A first estimation that was found and stated by a company called Oxis Energy¹¹, states that by the time these batteries can be mass produced, it can be priced as low as 200 €/kWh. Many other sources state that one of the aspects that make these batteries such a viable option is the fact that they are forecasted to be a lot cheaper and more affordable than lithium-ion batteries. As such, this estimate is taken to be accurate enough for a first cost estimation.

From the Beginning of Life Capacity calculated in table 13.8 follows that the cost of the batteries will be around \$7225. Converted to euros and rounded up this ends up at around €6450 for the lithium-sulphur batteries.

13.8. Risk Assessment

CAES has not yet been commercialised nor used in a decentralised microgrid applications. Four projects exist of which only two are commercial grid-scale plants. [81] The FMA conducted here is not site specific, but rather applicable for the CAES itself. The site specific risks are detailed in chapter 4.

Furthermore, the FMA of the secondary battery is not specific to lithium-sulphur but is based on the findings of Lyu et al. [73] for lithium-based batteries. The risks associated with the development and the TRL of the system are evaluated in chapter 4.

The failure modes of the CAES and the lithium-sulphur secondary battery are given in table 13.11

Table 13.11: Failure mode analysis of CAES and secondary battery

ID	Failure mode	Likelihood	Impact
Compressed Air Energy Storage [81]			
CA-01	Uplift failure	3	5
CA-02	Rock mass deformation	3	4
CA-03	Buckling failure of steel lining	3	5
CA-04	Fatigue failure of steel lining	3	5
CA-05	Concrete plug instability	3	4
Secondary battery [73]			
SB-01	Fracture in cathode	3	4
SB-02	Mechanical failure of anode	3	4
SB-03	Degradation of anode	4	3
SB-04	Dendrite formation	3	3

¹⁰<http://www.rwe.com/web/cms/mediablob/en/391748/data/235554/1/rwe-power-ag/press/company/Brochure-ADELE.pdf> [Cited 10 June 2020]

¹¹<https://oxisenergy.com/technology/> [Cited 10 June 2020]

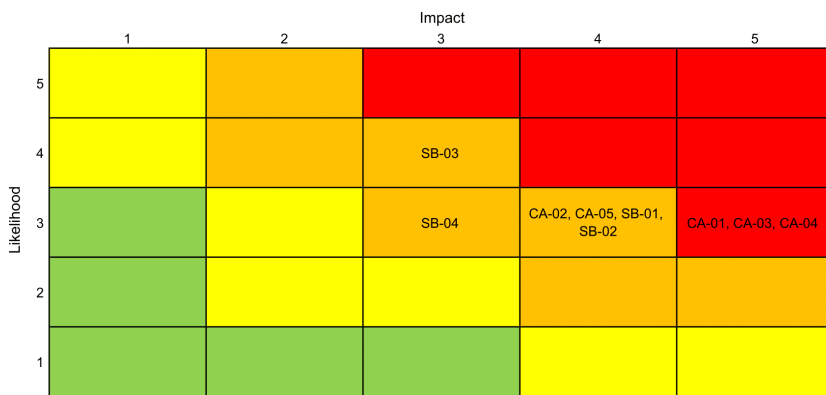


Figure 13.7: Risk matrix before mitigation of CAES and CAES and lithium-sulphur secondary battery
 (red: extreme risk, orange: high risk, yellow: moderate risk, green: low risk)

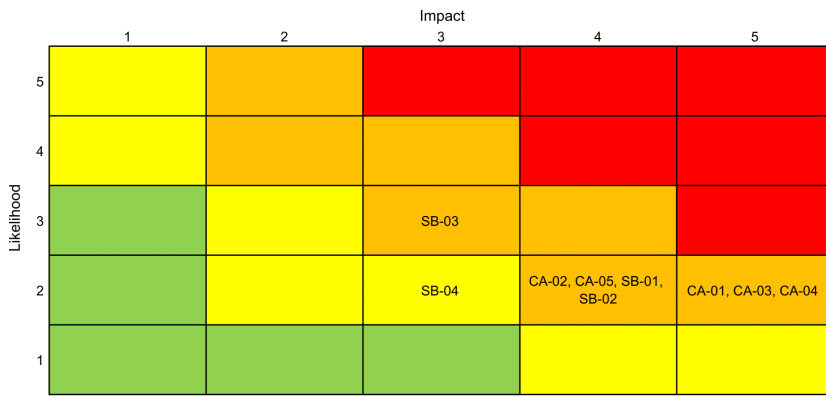


Figure 13.8: Risk matrix after mitigation of CAES and CAES and lithium-sulphur secondary battery
 (red: extreme risk, orange: high risk, yellow: moderate risk, green: low risk)

It is important to emphasise that the failure modes of the CAES are based on an Earth system. Thus, it is likely that the definition of these failure modes will change. The main failure modes identified lead to the destruction of the storage cavern, which has severe impacts all around. Currently, they are driven by the functional requirements. For example, to maximise ISRU, a different lining material might be used than steel (CA-03, CA-04), and using 3D printed regolith-rock mass mix as the lining might be a potential solution. The same applies to CA-05: instead of conventional concrete, the regolith mix will be used. Thus, as the CAES system is still under early stage development, exact mitigation strategies are difficult to be established, but will have to be updated when new information arise.

Lithium-based batteries are widely used in all sectors, but similarly to CAES lithium-sulphur batteries are in the development phase. Again, low TRL means that the detailed design is not known yet, thus no exact mitigation plan can be established, but will have to be revised.

Thus, for both systems thorough research has to be conducted to reduce the likelihood of the failure modes. The risk matrix before mitigation can be seen in figure 13.7.

Although, the exact mitigation measures are not known, all of these is to reduce the likelihood of failure. The revised likelihood and impact scores can be seen in table 13.12 and the resulting matrix in figure 13.8. One can observe that except one, all of the risks are high. This originates from the fact that these storage technologies are in the R&D phase, thus there is high risk associated with these.

Table 13.12: Revised likelihood&impact scores of CAES and lithium-sulphur secondary battery after mitigation

ID	Likelihood	Impact	ID	Likelihood	Impact
CA-01	2	5	SB-01	2	4
CA-02	2	4	SB-02	2	4
CA-03	2	5	SB-03	3	3
CA-04	2	5	SB-04	2	3
CA-05	2	4			

13.9. Sustainability and Retirement

With the goal to source as much material as possible on Mars, decreasing the mass that needs to be transported and thus emissions, the CAES system helps achieve this. For the storage, either a cavity built by rovers from the habitat or an already existing cave that meets the size requirements can be used. From a sustainability point of view, the latter is preferred as the creation of the cavern normally has a significant impact on the environment [16] and no extra adjustments to the environment would be preferred. Still, these options have to be explored in further design steps, along with gaining more knowledge of the habitat site by further exploration. After end of life, this cavern, whether natural or constructed, could be reused for the habitat, assuming the habitat will continue to expand once the first humans landed on Mars. Regarding the other components of the CAES, the compressor could be reused to pressurise the habitat as this will be needed to create living conditions. The motor, turbine and generator could be dismantled and parts reused in projects that are set up in the habitat. As there is no knowledge yet on these activities, it is difficult to say anything about a predestined purpose already.

Regarding the sustainability of the battery, the choice for a lithium-sulphur battery instead of a lithium-ion battery, already makes a big difference. Though the lithium-sulphur battery is still under development, the battery already shows to be more environmentally friendly than its competitors [30]. One of the main contributors to this is the fact that sulphur is abundantly available on Mars [74] and less harmful to the environment than the heavy materials in conventional lithium-ion batteries. For the Mars mission, further investigation on the abundance of sulphur shall be made as it is not known to what extent sulphur is available at site location [62]. Only the provision of tools needed for acquisition and processing of the sulphur on Mars could be a bottleneck for this. Still, when it is assumed that the Martian habitat will keep on growing once settled, providing these tools would be an interesting consideration to make.

After life, the battery needs to be recycled. In this aspect also the lithium-sulphur battery shows promising advantages over its competition. Although, as the battery is yet under development, at the moment the recycling process only includes material recovery, because the recycled materials do not meet the high-quality standards of materials for battery manufacturing yet [30]. Assuming these techniques will be developed before the mission takes off bringing tools for material recycling on Mars would be of high interest.

13.10. Requirement Compliance and Sensitivity Analysis

The systematic approach taken with the CAES sizing implies that at each iteration, key parameters are being updated. The sensitivity of these changes are described below.

Increase in exergy capacity required: To form a preliminary sizing of the volume and pressures, the efficiencies and demand of the habitat load is taken into account. If the efficiency of the turbine, η_{turb} , decreases from 65% to 60%, the exergy capacity increases to 14.2 MWh and the envelope in figure 13.3 moves up one step. A combination could be a pressure ratio of 180 with a volume of 113 000 m³.

Compressibility factor of CO₂: At 1 atm, which is roughly the pressure in the cavern, as well as the lowest temperature considered for Martian fluctuations (213 K), carbon dioxide incurs a compressibility factor of 0.985 in equation 13.5 and in determining mass of air in cavern. This decreases the efficiency of the compressor by 2%, and the efficiency of the turbine by 3%, which also has a direct influence on the exergy capacity required, increasing by 4.61%, and the iteration above begins again. This is why CO₂ analysis was an early step in the CAES sizing.

Increase in radius of cavern: The pressures that the structural lining can withstand is highly dependent on the cavern radius, r_s . If the radius is increased by 1 m (which corresponds to a 10.5% increase in spherical volume), the cavern membrane stress, σ_{cavern} , increases by 3.4% to 3.21 MPa. To maintain the stress as it was, the thickness of the membrane could be increased by 2 cm, increasing the required regolith mass to 9 260 tonnes.

A note about the last point is that with the changing radius, the distance from the habitat increases. This is to ensure to minimise impact of a catastrophic event by the CAES system. This margin is preferably set at over ten times of the radius itself, including a safety margin of 1.5.

The batteries size changes relatively strongly to the general system performance. The required capacity directly influences how big and heavy the batteries need to be. Applying the sensitivity analysis explained in section 9.3 to the batteries gives the following results:

Indeed table 13.13 shows that decreasing the power needed gives a lower required capacity resulting in smaller lighter batteries. These effects are naturally positive and do not influence the trade-off as these arguments are still valid when it comes to choosing lithium-sulphur over lithium-ion batteries.

Finally, this section gives an overview of compliance with the requirements in table 13.14.

Table 13.13: Battery sizing results from sensitivity analysis

Property	Lithium-sulphur
C_{req}	93.4
C_{EOL}	132.8
C_{BOL}	28.9
M_{bat}	96.2
V_{bat}	82.5

Table 13.14: Energy Storage Compliance Matrix

ID	Compliance	Proof (Section)
REM-Sys-N05-02	Yes	Section 9 and 13.4.2 with stage inefficiency and power validation
REM-Sys-N05-03	Yes	Section 9
REM-Sys-N05-04	No	Section 13.6
REM-Sys-N05-05	Yes	Section 13.4.2, based on the use of CO ₂ as storage air and use of in-situ printed regolith as structural lining of storage cavern
REM-Sys-N05-06	Yes	Section 13.4.2, the compression segment efficiency is sized
REM-Sys-N05-07	Probable	Storage efficiency not looked into too much detail in this report, further investigation needed
REM-Sys-N05-08	Yes	Section 13.4.2, the expansion segment efficiency is sized
REM-Sys-N05-09	Yes	Section 13.5.2

13.11. Recommendations

In this section, the recommendations for the CAES and battery are given.

CAES

Because the design of the CAES relies heavily on different technical perspectives of stakeholders, namely the Rhizome Habitat team, the procedure to continue with future CAES sizing can be integrated as an iterative tool that can be accessed and utilised by the Habitat team. Figure 13.9 presents a flow chart of this tool integrated with the DSE's Exergy Analysis B .

The cavern volume is first initialised, which is dependent on the two factors that will become more clear in the future, one is the capabilities of the Rhizome habitat team in excavating a sizeable cavern or the availability of hard rock caverns that can be found underneath the Martian surface.

This volume is used to determine the maximum pressures allowed in the storage component, based on the maximum stresses the rock-mass formation and the rock lining can handle. This would inform a limit to the pressure ratios, which can be examined in the exergy storage capacity analysis, similar to the one done in this DSE.

The exergy storage B is juxtaposed with the B_{design} that is required by the habitat, if values are within a set error margin, the optimal cavern volume can be determined and the next steps for detailed operation plans can be carried out.

Both the cavern pressure and exergy storage analysis can undergo verification. The former can model stress paths and states along the storage boundaries and the latter may use well-researched CAES systems to validate model accuracy.

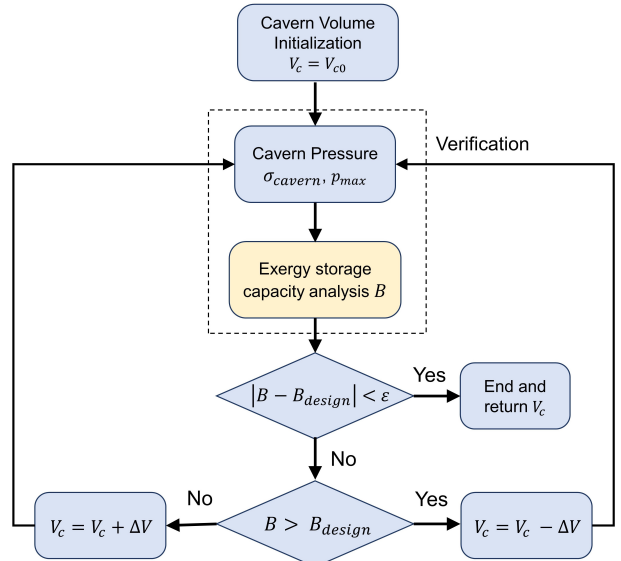


Figure 13.9: Flow chart of CAES design as integrated with the Rhizome habitat team

To increase the fidelity and feasibility of the design to the true application, the following characteristics regarding the sizing and design of the CAES can be considered:

- Investigate inter-cooling and heat transfer between compression and expansion stages to validate or increase overall efficiencies. On Mars, the density of air is less than 2% that of Earth [102]. Intuitively, this implies that mass transfer, and thus the carried heat, is reduced compared to Earth. This has consequences on the assumptions presented in the CAES sizing, where processes are modelled as isothermal, but this might be far from reality. Modelling simulations of the airflow through the stages is recommended as a further step.
- Investigate the structural properties of the Martian terrain below its surface. This could be a critical make-or-break factor for a CAES system feasibility on Mars. One aspect of this is to look at existing caverns on Mars¹². Another aspect is further research into Martian rock mass formation. This is due to the fact that understanding deformations and stresses under the cyclical (de)pressurisation stages is key to design for reliability and longevity of the CAES system. Exploration into different compressed air storage technologies is also recommended, as lightweight tanks that can be built in-situ with additive manufacturing equipment, or rigid balloon-like structures¹³.

One key design consideration that can be looked into as the next step is by increasing the number of storage caverns available, which reduces the efforts in locating a singular large enough facility. On Earth, there are two grid scale CAES systems, the McIntosh (USA)¹⁴ with a single salt cavern of 540 000 m³ and the Huntorf CAES plant (Germany)¹⁵ with two underground caverns with total of 310 000 m³. For a spherical idealisation, the cavern capacity can be analysed with an equation, where r is the radius of the corresponding i^{th} cavern. Accordingly, the mass and cost of the structural lining can be estimated.

$$\text{Total volume} = \frac{4}{3} \sum_n^i r_i^3 \quad (13.14)$$

Following the exergy storage envelope (figure 13.3, for every ten-step increase in ratio of pressures, volume can be reduced by 10%. The final recommendation is to integrate mass, cost and sustainability models to the procedure described in this report.

Battery

The level of design of the batteries for this report is high level and has not gone into full detail yet. This section will elaborate on the items that need to be improved on to finalise the design. More research should be done to check the viability of the chosen battery technology in space. As it is still in development, it may need extra research and development. Since this mission would only start 5-10 years into the future, there should be time to be able to do this. Moreover, the thermal insulation and protection from the Martian radiation is also needed. The specific materials used for this would need to be further investigated. Finally, the battery parameters and modularity of the design need to be further researched in order to come up with a more robust design.

¹²<https://www.foxnews.com/science/nasa-underground-cavern-mars-good-candidate-to-contain-life> [Cited 18 June 2020]

¹³<http://euanmearns.com/a-review-of-underwater-compressed-air-storage/> [Cited 18 June 2020]

¹⁴<https://www.smithsonianmag.com/innovation/salt-power-plant-most-valuable-180964307/> [Cited 18 June 2020]

¹⁵<https://oxisenergy.com/technology/> [Cited 18 June 2020]

Data and Communication Handling

In this chapter the data flow through the system and the communication will be explained. A block diagram is used to depict these flows.

To show the flow of data going in and out of all the subsystems and other mission components, a data handling block diagram is made and presented in figure 14.1. Both the flow of the data and of the commands is displayed. It is shown how the subsystems are connected to the main computer, which has a central processor, a memory and a watchdog timer which is used to detect and recover from computer failures. A communication system is also implemented to send and receive data from the earth station.

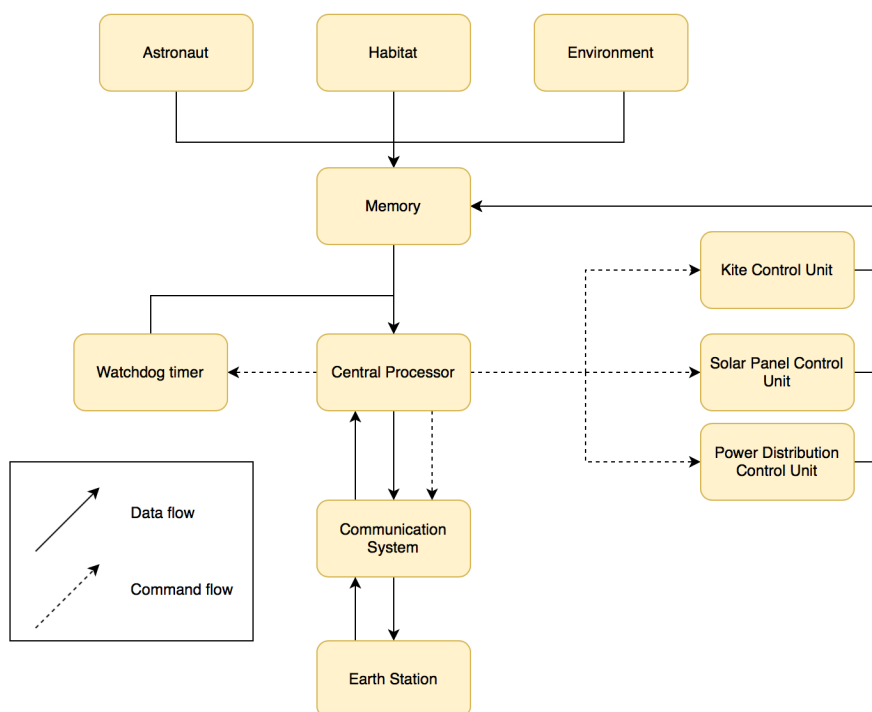


Figure 14.1: Data Handling Block Diagram

It can be seen that a central processor is present to send commands and data to all parts of the system. You can not just use any kind of processor on Mars due to the rough environmental conditions. To see what kind of computer is required for this kind of mission, similar missions are inspected. The chosen reference was the Mars rover Perseverance as this is one of the newest Mars missions, expected to launch in 2020¹.

This rover has a radiation-hardened central processor with PowerPC 750 Architecture and a BAE RAD 750 which operates at 200 MHz. It has 2 GB of flash memory, 256 MB of dynamic random access memory (RAM) and 256 kB of electrically erasable programmable read-only memory (EEPROM). Now this is of course the data handling system of one rover and not of an entire energy system but since no actual energy system has been installed on Mars as of yet, not a lot of information can be found on its computers. Therefore this seemed to be the most viable option to withstand the Martian environment while also performing properly.

¹<https://mars.nasa.gov/mars2020/spacecraft/rover/> [Cited 17 June 2020]]

Reliability, Availability, Maintainability and Safety

In this chapter the RAMS characteristics of the mission are discussed. First the reliability and availability characteristics are discussed in section 15.1, then in section 15.2 the maintenance procedures are analysed and finally in section 15.3 the required safety actions are shown.

15.1. Reliability and Availability

Assessing the reliability and availability of the system design is very important for the successful completion of the mission. Therefore these aspects are analysed for each subsystem design, starting with the primary energy system.

Primary energy system: As detailed in section 11.10, AWE is in the beginning of the development phase on Earth. The extraterrestrial use will require additional research before it reaches a sufficient TRL. The only comprehensive work to date on reliability and availability of an AWE system has been conducted by Salma et al. [88], but this is not sufficient for this project. The kite system in this article has a lower TRL than is acceptable for a Mars mission. Thus, it is important to note that the values presented here have to be reevaluated as the technology matures.

The unavailability of the kite power system after seven days of operation is 2.70% with a Fussell-Vesely importance of 86.31% [88], which "measures the overall percent contribution of cut sets containing a basic event of interest to the total risk"¹. This is unacceptable for a space mission as high unavailability could result in loss of mission or crew.

For these reasons, the group suggests to conduct thorough testing of the kite system simulating the hostile Martian environment for example in the Aarhus Mars Simulation Wind Tunnel².

Secondary energy system: Photovoltaic modules have long been used in space missions. The first spacecraft ever to be powered by solar energy was the Vanguard-1 with a mission duration of six years³. The International Space Station has been in service for more than twenty years solely relying on solar energy⁴.

Jordan et al. [58] recorded the failure rate of terrestrial PV modules from 2000 to 2015 to conclude that that every 5 of 10000 failed. This translates to a reliability of 99.95% over fifteen years. The value is expected to increase when space-grade materials are used.

On the other hand, as before the group suggest to conduct thorough simulation and testing of operation in Martian conditions.

Energy storage - CAES: Huntorf CAES was the first to be built. After twenty years of operation, Crotogino et al. [26] concluded that during its lifetime the system had no major malfunction. The only maintenance required was associated with the well heads and the valves. Furthermore, the production string fractured due to material failure, which was investigated and refitted afterwards. The rock bed did not deform or deteriorate significantly either.

The caverns at this plant is comparable size to the one designed in this report, thus one may conclude that CAES is reliable. It is important to note that limited work and knowledge is available on reliability of CAES as it is not a well-spread technology. Hence, if it is to be used in a Martian setting, the group highly encourages to run a pilot project on Earth.

Energy storage - secondary battery: Lithium-sulfur batteries are still in the development phase, thus reliability cannot be analysed yet. An other lithium-based battery is lithium-ion (Li-Ion), which is widely commercialised and been in use for more than twenty years.

¹<https://www.nrc.gov/docs/ML1216/ML12160A479.pdf> [Cited 18 June 2020]

²https://www.esa.int/ESA_Multimedia/Images/2019/05/Aarhus_Mars_Simulation_Wind_Tunnel [Cited 18 June 2020]

³<https://web.archive.org/web/20150321054447/http://code8100.nrl.navy.mil/about/heritage/vanguard.htm> [Cited 19 June 2020]

⁴https://www.nasa.gov/mission_pages/station/structure/elements/solar_arrays-about.html [Cited 19 June 2020]

The yearly cycle number based on the performance analysis (chapter 9) is around 500. Conventional Li-Ion batteries have a cycle duration of 400-1200⁵ [103]. One can assume that space-grade batteries will at the higher end of the threshold or exceed it. On the other hand, lithium-sulfur batteries are expected to outperform Li-Ion in terms of reliability. Depending on the increase in cycle duration, one or two battery will be needed for the duration of five Martian years.

Power management system Power management play an essential role in the life of the habitat. Even short outages can have a detrimental effect. Although, power system are complex, the reliability on Earth is high due to its high societal importance⁶.

As the power transmission cables are underground, the Martian weather can have no impact. As for others parts of the design, space-grade materials are going to be, thus the reliability of power management can only increase compared to Earth.

Thus, one may conclude that due to the high TRL, this aspects of the infrastructure is going to be reliable.

15.2. Maintainability

Throughout the systems lifetime maintenance will need to be performed to reduce the number of failures. This maintenance will be done by the astronauts present at the site. There are two types of maintenance: scheduled and non-scheduled maintenance activities. Non-scheduled maintenance activities consist of what to do when a failure mode is reached and these are explained in the risk assessment of the subsystem chapters.

Considering scheduled maintenance activities, the main goal is that no failure mode is reached by applying regular maintenance. This is done for both hardware and software.

Schedule Hardware Maintenance

Primary energy system

- To make sure the tether does not break during its lifetime, regular maintenance is performed. Every day the tether will be checked for tears or cuts by an astronaut and if any are present it will be repaired. Proper material, maintenance guidelines and equipment will be brought that can be used to patch up the tether and reensure its structural integrity.
- Since the kite is partly inflatable, any tears could also turn into terrible consequences. Fortunately, the kite is flexible and therefore less likely to break when colliding with an other object. After the tether is checked, the kite will also be checked daily for any structural issues. In the case a tear is present then again the astronauts are provided with the material, the guidelines and the equipment required to repair the kite.
- The points where the tether is connected to the kite also need to be checked regularly. These points are structurally reinforced with Dyneema fibres but again any tears here could lead to system failure. The same maintenance and repair approach is taken here as for the rest of the kite.
- Scheduled maintenance also needs to be performed for the ground station. It will be checked whether the entire station is still properly connected to the ground and that all its sub-components are still structurally sound. Any type of connection like bolts, adhesives, welding etc. will also be checked to see if no tears or breaks are present here. If any issues do appear, the right tools will be present to reinforce the connections or fix other problems.
- At this stage of design the AWE system the sizing of the kite, the tether and the ground station has been done. But components like, force sensors, communications systems etc. have not yet been considered. Therefore the same general maintenance approach will be taken for all of these. The astronauts will be given the guidelines and the tools necessary on how to inspect and fix these components if necessary.

Secondary energy system

- First of all, the glass on the solar panel needs to be checked every week. Minor damage to the panel could eventually lead to glass breakage, which is something you want to prevent. If minor damage is present, maintenance needs to be performed by the astronauts to repair the glass, proper equipment and a reparation coating will be brought to reinforce the panel.

⁵<https://web.archive.org/web/20150520021436/http://www.thermoanalytics.com/support/publications/batterytypesdoc.html> [Cited 19 June 2020]

⁶<https://energiforskmedia.blob.core.windows.net/media/23663/reliability-evaluation-of-distribution-systems-energiforskrapport-2017-462.pdf> [Cited 20 June 2020]

- The solar panels stand on structures for stability and orientation. Similarly to AWE ground station, both the structural components and the connections need to investigated regularly. If any structural weak spots are found, the astronauts are given the guidelines, materials and tools to repair the structural components or the connections.
- Considering the rest of the secondary energy system, the cells, the modules and the orienting system will all be checked often just like the rest of the system. But no actual specifications on maintenance can be made as of yet, since the design of this system is not detailed enough to provide proper guidelines.

Energy storage system

- For the compressed air energy storage (CAES) several aspects need to be inspected regularly. Things like the rock mass around the storage systems and the steel linings could deform and if they do this must be noticed quickly. A disadvantage is that it is often hard to find any deformations in the CAES visually since a lot happens on the inside and it is hard to disassemble it. Several options are available enable investigations of these system components, the best one would probably be to bring some kind of non-destructive test that is able to scan the storage system from above ground, for example using ultrasound testing. If any deformations are found then either certain parts need to be replaced or they need to be reinforced, the proper tools and materials will be brought to make this possible.
- For the battery several other components are important to maintain. The anode and cathode need to be checked often to make sure they are still in good shape. A physical or visual inspection might be hard since it is a confined system. The best way to maintain the repair is to apply regular checks on the battery, seeing whether its input and output are still what you expect them to be. If not then guidelines will be available to check what part of the battery might be causing an issue and then this part could either be repaired or replaced.

Power management system

- In the power management system a list of things could happen and it might be hard to find out what part of the system is causing certain issues. Therefore it is important to regularly apply testing to this system. Interfaces will be available for the astronauts to show whether all the components of the power management system are getting the correct input and are providing the right output. If not, tests will be available to see which component is the problem. The equipment, parts and guidelines will be present for the astronauts in case a system component requires repair.

Scheduled Software Maintenance

- The software used to drive the energy system, is built in such a way that it is robust and self-healing⁷. This has been done to make sure that if any problems occur the software will react correctly, it will realise that a problem is present and shut down the respective systems. So the software performs maintenance on itself.
- Daily checks will also be done by the astronauts outside operational window to make sure that no bugs are present and that the software is functioning properly. Guidelines will be given to the astronauts to do these maintenance checks and if a problem has presented itself guidelines will also be present on how to update the software and fix the issue at hand.
- Finally a watchdog timer is also implemented in the software system. This is an application widely used in space travel, which makes is used to detect and recover from computer related issues. The timer is normally reset regularly by the computer, but if due to hardware or software issues it does not reset the watchdog timer, it will run out and send out a timeout signal. This signal will be used to initiate any actions required to fix the system.

15.3. Safety

Safety is a big consideration for the mission. Everything from production of the systems, integration on Mars to operation needs to be safe. If safety is not enforced the astronauts and the habitat can be subjected to severe consequences. Safe integration and operation could mean for the astronauts the difference between life and death. Therefore a safety plan is made for each of the three stages, where guidelines by the American Institute of Aeronautics and Astronautics⁸ have been considered a good starting point. First the production safety procedures are discussed.

System production

The workers that manufacture all the system components need to be safe when doing so.

⁷<https://ubiquity.acm.org/article.cfm?id=1241853> [Cited 16 June 2020]

⁸<https://www.aiaa.org/> [Cited June 21 2020]

- The first step in achieving workplace safety is providing proper manufacture and safety guidelines, so no foreseeable mistakes are made.
- Next, the workers will also be given safety equipment to make sure that if something happens no harm occurs. Safety equipment will range from protective glasses, protective gloves, a proper work suit and a mask when working with dangerous gasses or other poisonous materials.
- If an accident on the workplace does happen, tools will be available to help workers with any possible minor injuries. Bandages, disinfectant etc. will be present at several locations in the workplace.

Integration on Mars

Integration on Mars might be one of the most dangerous parts of the mission and therefore extensive safety measures need to be present.

- The first step in mission integration happens when the systems are unloaded from the spacecraft. Since at this moment no habitat is present yet and the energy systems that require integration are going to provide the power to make the habitat, the astronauts will have to live in their spacecraft. This makes safety a big consideration, during departure and entry of the spacecraft special measures will be taken to make sure no breaches occur that could endanger the entire team.
- During integration of the systems by the astronauts, the astronauts will be given special safety equipment to perform the required mechanical actions. Their oxygen supply will be way bigger than what they will actually need, in case of an emergency. Finally, another astronaut will always be on stand-by in case of any astronaut emergencies. This astronaut will be given the right training and equipment to be able to save his fellow astronauts.

Operation on Mars

Finally, operation of the energy systems on Mars can also be a risk. Luckily, most of the systems have been designed in such a way that very few manual operation is required, significantly reducing the possibility of something going wrong. Still some safety considerations need to be made.

- The two considerations that were mentioned in the previous bullet points, can also be applied to the operation of the energy systems.
- When hazardous machines are in use, caution will be taken during operation. The astronauts will receive the proper education on what to be cautious of.
- Maintenance of the energy systems will usually be done manually, therefore certain things are brought to ensure safety. The equipment used for maintenance and repair is safe to use, making it hard for an astronaut to injure him/herself. The materials used for repair will not contain any hazardous substances. Finally, very strict safety guidelines are taught to the astronauts for maintaining the energy systems.
- During end-of-life procedures, the same rules can be applied as for maintenance. This will probably be a dangerous part of the missions. The astronauts will need to deconstruct an entire energy system and afterwards need to either recycle it or bring it back to earth on a spacecraft. Therefore extra caution will be taken at this final stage of the mission.

16

Budget Analysis and Resource Allocation

In this chapter the changes in the budget for the mass, volume, power and cost for the project will be elaborated upon and an updated budget will be presented. Furthermore, the resource management will be discussed and updated.

16.1. Budget Analysis

An initial budget analysis was performed in the Baseline Report [25] and contingencies were established for the budget. After performing mass, volume and cost estimations on the preliminary designs it becomes apparent that the initial assessment of the budget underestimated the cost and mass of the CAES and the secondary energy system. When including the contingencies of 30% for the cost and 35% for the mass for both systems, they still largely exceed the budget by 92% and 67% for the CAES respectively and 5118% and 95% for the secondary energy unit respectively. For the CAES system, the volume was also underestimated by 114% with a contingency of 40%. The power management only exceeds its mass budget by 42% with a contingency of 32%.

This underestimation can be explained by the fact that not all the technologies for energy storage, power management and the secondary energy units had been determined in the Baseline Report. Thus the estimations of the previous budget were based on the other subsystem parameters and the desire to limit the launches required to two.

As the budget in the Baseline Report accounted for a primary energy system with two kites, the mass was estimated to 400 kg. However as the final design only includes one kite, the mass budget decreases to 200 kg, putting the primary energy system 31% over budget.

Aside from these underestimations and the higher mass for the primary energy system, all the system parameters are within budget. This means the system will require four launches to Mars for transport, of which the CAES needs two launches for its shipment. An updated budget was made to incorporate the new mass and volume requirements for each of the subsystems, maintaining the previously established contingencies. The new budget can be found in table 16.1.

Table 16.1: Updated Technical Budget

	Mass [kg]	Volume [m ³]	Power	Cost [€]
Primary energy unit	300	1	30 kW	70 000
Secondary energy unit	800	1	5 kW	7 000 000
Day-to-day storage solution	150	0.25	116 kWh	8 000
Seasonal storage solution	1500	6	14 MWh	2 000 000
Power distribution unit	220	0.5	-	80 000
Total	2970	8.75	-	9 158 000

It is evident that these increases in the budget should be avoided and are not preferable. However, the added mass volume and cost were a direct consequence of maintaining system integrity, where maintaining the previous budget would have been unfeasible for a sensible design.

16.2. Resource Allocation

The resource allocation was performed in the baseline report and is still largely valid. Therefore the definition of the human resources, technological resources and the sustainability resources will remain the same and are re-stated below. The resource allocation will be updated slightly as to encompass a ten year development track, which will be elaborated on further later in the report in chapter 21, and the increased budget for the project.

16.2.1. Human Resources

The human resources relevant to this project are listed here to ensure smooth operation and that all necessary functions are attended to.

- **HM - Managers:** Managers spearhead the respective tasks. There are many types of managers, including human resource manager (team manager), business and financial managers, and technical managers (highly-qualified and experienced engineers) to name a few.
- **HE - Engineers:** (Certified) engineers are involved in all stages of design, development, testing and certification. They are further specialised into different engineering fields: aerospace, chemical, energy, electrical, software, structures etc.
- **HT - Technicians:** Technicians are individuals that received technical training in product development, manufacturing. These individuals often work under the instructions of engineers, that have specific skill sets and work stations in production line.
- **HA - Astronauts:** Individuals that transport, set up (integration to habitat) and operate the energy system on Mars. Astronauts are also engineers, scientists, pilots or highly-qualified technicians.
- **HO - Others:** Ground Station Professionals, Sustainability Officers, Marketing Officers etc.

16.2.2. Technological Resources

Technological resources are the non-physical resources such as software and information, and the physical resources such as hardware needed in production.

- **TM - Machinery:** This includes prototyping, testing, manufacturing and production equipment.
- **TS - Software:** Software consists of simulation tools, computational analysis tools, modelling, application programming interfaces. It also includes components of cyber-security measures like user authentication, encryption tools and firewalls.
- **TH - Hardware:** This includes any functional hardware that supports the project, such as computer systems and storage capacities. It also includes other organisational tools such as air-conditioning, servers, laptops, office work stations.
- **TI - Information:** The relevant information and data sets, at times data acquired from external parties (NASA's Mars Insight Mission). Also includes processes such as transmitting of data to relevant parties such as the launch site or ground control.
- **TIP - Intellectual Property:** The utility and adoption of novel innovation technologies and proprietary tools. As well as new developments of inventions spun from the project's design process.

16.2.3. Sustainability Resources

The sustainability resources are used to ensure a sustainable development track. Carbon equivalents and the waste are used to examine the sustainability of the project.

- **SW - Waste:** Evaluates the ergonomics and efficiency in reducing the waste of materials and resources through the project. Naturally, the bulk of the waste would be testing and manufacturing processes. It is difficult to have a general category for waste due to the diverse materials applied to the project, however this metric will be rated from 1 to 10, one being little waste budget allocated and 10 being the maximum waste expected to be produced.
- **SEE - Energy and Emissions:** Energy is required at all stages of the project. This can be quantified by carbon equivalents, taking into account energy use on Earth. The total carbon equivalents dedicated to the project's entirety is 2000 kWh and a cap of 500 tons of CO₂.

The resource allocation can be found in table 16.2, and is updated to include the new budget and schedule. The ten year development track can be found later in the report as mentioned, in chapter 21 together with a budget for the total project. The total length of the mission is approximately ten years as well, making everything from conceptual design to end-of-life last over twenty years. For the development phase, which is taken as conceptual design to production, working days of eight hours were assumed (working hours of a single person, not accounting for multiple people), and from there on the hours were counted as full 24h days, as the system should operational all times of the day. The conceptual, preliminary and detailed design do not correspond with the phases of the DSE, but with the phases of the total development, of which the DSE spans half-way into the preliminary design.

Table 16.2: Resource Allocation

	Cost (% of total)	Schedule (hours)	Human resources	Technological resources	Sustainability (Waste, CO₂ %)
Conceptual design	0.1	240	HM, HE, HO	TS, TH	(1, 3)
Preliminary design	0.1	1200	HM, HE, HO	TS, TH, TI	(1, 3)
Detailed design	0.2	5760	HM, HE, HO	TM, TS, TH, TI	(3, 9)
Testing	20.1	3360	HE, HT	TM, TS, TH	(6, 20)
Production (on Earth)	46.6	11720	HM, HE, HO	TM, TS, TH, TIP	(8, 65)
Installation (on Mars)	2.4	6048	HA	TS, TH, TI	(4, -)
Operations	23.1	82440	HA, HO	TS, TH, TI	(1, -)
End-of-life process	2.4	12096	HM, HT, HO	TH, TS	(3, -)

LCA of the Primary Energy System

In this chapter, a preliminary Life Cycle Assessment (LCA) of the kite system is performed. Following the ISO standards 14040 [1] and 14044 [2], an LCA contains four steps: determining the scope and goal of the analysis, performing an inventory analysis, evaluating the impact of the inventory and interpreting the results. These steps done in the following sections: in section 17.1, the goal and scope of the LCA are discussed, in section 17.2, the inventory analysis and impact assessment are performed and in section 17.3, an interpretation of the results is given and the room for improvement is discussed.

17.1. Goal and Scope

The goal of the LCA is to get an overview of all resources needed for the production of the kite and their impact on Earth. With this knowledge, the contributors could be looked at that have a big environmental impact, and the improvements that could be made to decrease these in further design steps of the kite. The unit used to measure the impact on Earth, is the CO₂ equivalent, widely used to compare the Global Warming Potential (GWP) of different materials.

As a quantitative analysis of the whole life cycle of the kite (including launch and installation, operation and end-of-life) was not achievable within the scope of this project, a cradle-to-gate approach is followed for the LCA of the kite. Its boundaries are illustrated in figure 17.1. The aspects of the sustainability of the system during life-time and retirement, are discussed in section 11.11.

For the LCA, raw material acquisition and manufacturing are merged in the inventory analysis, as better data could be found for these two phases combined. The raw material acquisition includes extraction from the natural environment and processing of the material to make it usable. Manufacturing includes the production of all the components and the intermediate stages needed for this. The energy needed to transport these components and assemble them, is included under the assembly of subsystems. Finally, the production of the materials needed during the mission for maintenance and repair is also added.

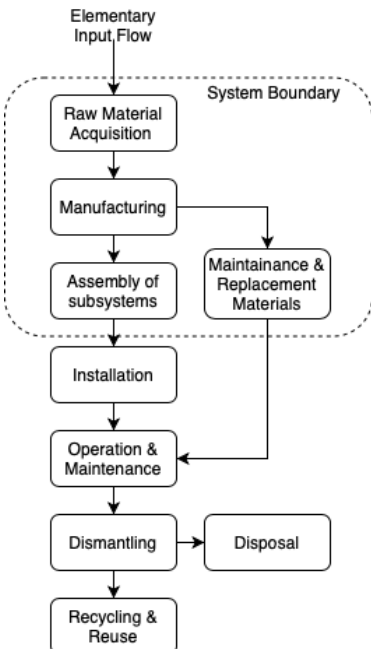


Figure 17.1: LCA Boundary

17.2. Inventory Analysis and Impact Assessment

For the inventory analysis of the LCA, some assumptions had to be made based on simplified calculations to estimate the quantity of each material that is used for the primary energy system. Regarding the materials of the kite, it is now assumed that a combination of Dyneema Carbon Fabric and Dacron will be used. However in future design steps a trade-off between several materials will still have to be performed. The material ratio of 85/15 between the Dyneema Carbon Fabric and the Dacron is based on the TU Delft B3 Kite¹, after which the Dacron area is doubled as these parts will be inflated and thus double-sided. The coating to protect the kite against radiation is assumed to have a thickness of 5 μm [80]. For the stitching of the material, it is approximated that for every square meter, the circumference needs to be stitched. Furthermore, the control lines are assumed to have a total length of 100 m² with a thickness of 5 mm. For the tether, a mass of 12.7 kg is adopted from the AWE sizing, as shown in chapter 11. The mass of the kite control unit is taken to be 5 kg, equivalent to the KCU of Kite Power², and the percentage of the materials are roughly estimated. As vacuum pump for the design, the magnesium dual piston air compressor from Thomas Power³ is used, for which the material distribution is also estimated. For the ground station, the mass of its subcomponents

¹<https://www.tudelft.nl/en/ae/organisation/departments/aerodynamics-wind-energy-flight-performance-and-propulsion/wind-energy/research/kite-power/> [Cited 16 June 2020]

²<http://www.kitepower.eu/technology/3-system-components/51-kite-control.html> [Cited 21 June 2020]

³<https://www.gardnerdenver.com/en-nl/thomas/wob-l-piston-pumps-compressors/2110z-series> [Cited 18 June 2020]

are given in chapter 11. The drum is assumed to be made from titanium and the brakes from aluminium (for the purposes of the LCA, drum design was changed into magnesium later). For the other components, the material percentages are taken from S. Wilhelm [101].

For operation and maintenance, it is assumed that the system needs 500 kg of lubrication oil over its lifetime [101]. Furthermore, the tether will need to be replaced four times during operation, as is estimated in section 11.5.4. It must be mentioned that it is expected some other materials must be brought to Mars for repair, but these are not included in this LCA.

After gathering all materials, a study has been done into their respective CO₂ equivalence per kilogram for acquisition and manufacturing. It is assumed, that after manufacturing these materials have the form needed for assembly, and energy for production of molds and others is not included. For manufacturing, a factor 0.6 of the total material CO₂ equivalent is assumed for emittance [84]. For waste production, it is assumed that half of the total material needed for the system, will be spilled during manufacturing.

Finally, for transportation, in this LCA it is assumed that the total of raw materials needed, have to be transported 500 km by truck to arrive at the location of the factory. As the specialised manufacturers for this international mission are probably scattered all around Earth, it is estimated that the average distance the components need to move is 5500 km (which is the distance to cross the Atlantic Ocean from Amsterdam to New York) by tanker, as this is more sustainable than airfreight [34]. Lastly, it is assumed that all scrap materials need to be transported 200 km by truck to their respective landfill or recycling factory.

The final overview of this inventory analysis and impact assessment is summarised in table 17.1.

17.3. Interpretation & Next Steps

In figure 17.2 and 17.3, an overview is given of the outcome of the LCA. The biggest impact on Earth is the raw material acquisition and processing of the ground station (43%). The kite system (including vacuum pump and KCU) and the tether respectively contribute 0.6% and 0.3% of the total CO₂ equivalent in the course of the production process. The replacement tether and lubrication needed for operations and maintenance (O. & M.), cause 7.2 % of the calculated CO₂ emission. Manufacturing, emissions and waste also have a big impact on the environmental impact of the design (26.3% and 21.9%). Though, it must be said that the values used to calculate them are estimations based on industry. Since most likely, one energy system will be created, these values will have a chance to be reduced as no bulk production will be used and more specified techniques can be used for the wind system. In that case, these values can be seen as an indicator to stress the importance of lean manufacturing for the sustainability of the design.

To conclude, this LCA must be read as a preliminary LCA and thus an indicator of possible impact areas. No exact materials, production processes or manufacturers were known yet. This will automatically improve when more knowledge is gathered during further design steps. Furthermore, for a subsequent LCA it would be preferable to make use of one of the LCA programs on the market, as these were not available for this assessment due to money restricted accessibility. Also, it would be recommended to perform a sensitivity analysis on the final outcomes, since many values are based on assumptions taken.

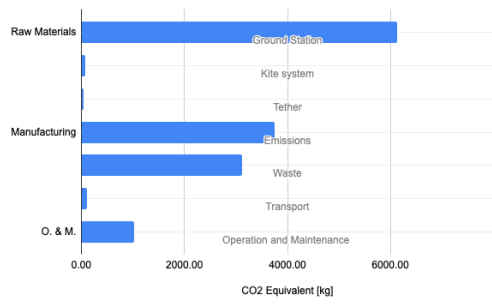


Figure 17.2: CO₂ Equivalence per subsystem or action

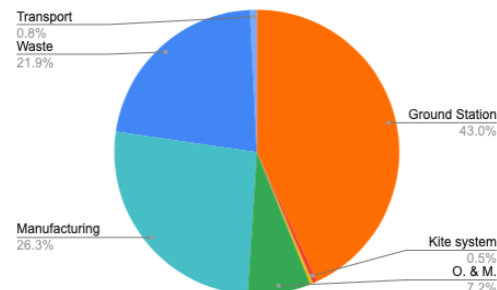


Figure 17.3: Percentage of CO₂ Equivalence

Table 17.1: Environmental impact of the kite production, measured in CO₂ equivalent

Materials Input				
Part	Material	Quantity [kg]	CO₂ Eq./kg	CO₂ Eq. [kg]
Kite	Dyneema Composite Fabric ⁴	2.13	10.60	22.53
	Dacron ⁵	2.55	5.44	13.87
	Polyurethane (coating) ⁵	0.55	3.61	1.99
	Dyneema fibres (stitches)	0.18	2.40	0.42
	Spectra (Bridle system) ⁵	2.00	2.40	4.80
Tether	DM20 XBO ⁶	12.7	3.33	42.29
Kite Control Unit	Electrical Steel ⁷	0.50	49.00	24.50
	Copper [50]	1.00	1.25	1.25
	Other Steels [50]	3.5	1.97	6.90
Vacuum Pump	Magnesium [57]	0.29	3.67	1.07
	Copper	0.03	1.25	0.04
Ground Station	Electrical Steel	83.93	49.00	4112.57
	Low-alloyed steel ⁸	15.56	2.00	31.12
	Other steels	55.70	1.97	109.73
	Cast Iron ⁵	15.50	1.51	23.40
	Aluminium ⁹	8.03	1.60	12.86
	Titanium ¹⁰	48.3	36.00	1738.8
	18CrNiMo7 ¹¹	10.74	1.70	18.25
	Copper	13.77	1.25	17.22
	Alkyd Paint [63]	2.02	19.10	38.59
	Glass fibre	3.72	2.6	9.67
	Chemicals ⁵	2.79	3.00	8.37
	Insulation material ⁵	1.98	1.86	3.69
	Polyethylene	0.46	3.33	1.54
TOTAL	Fiberboard ⁵	0.29	2.2	0.64
		288.1		6246.1
Operation & Maintenance				
Lubrication Oil Replacement	Castrol Braycote 601 EF [21]	500.0	1.70	850.00
	Tether (DM20 XBO)	50.8	3.33	169.16
Manufacturing [84]				
Emissions				3746.7
Waste Production				
Scrap Materials		144.1		3123.1
Transport [34]				
Part	Volume (Tonnes)	Distance [km]	gCO₂/tonne-km	CO₂ Eq. [kg]
Raw Mat. (Road)	1.81	500	62	56.0
Compon. (Tanker)	1.20	5500	5.00	33.1
Scrap Mat. (Road)	0.60	200	62	18.7

⁴https://www.dsm.com/content/dam/dsm/dyneema/en_GB/Downloads/Case%20Studies/DSM_Dyneema_LP_Customer%20information%20sheet_180113.pdf [Cited 16 June 2020]

⁵https://www.winnipeg.ca/finance/findata/matmgt/documents/2012/682-2012/682-2012_Appendix_H-WSTP_South_End_Plant_Process_Selection_Report/Appendix%207.pdf [Cited 15 June 2020]

⁶<https://dielectricmfg.com/knowledge-base/uwmw/> [Cited 16 June 2020]

⁷<https://www.makeitfrom.com/material-properties/ASTM-B631-Class-B-Silver-Tungsten-Electrical-Contact-Alloy> [Cited 15 June 2020]

⁸<https://www.makeitfrom.com/material-properties/SAE-AISI-L6-T61206-Low-Alloy-Tool-Steel> [Cited 16 June 2020]

⁹https://ghgprotocol.org/sites/default/files/aluminium_1.pdf [Cited 15 June 2020]

¹⁰https://arpa-e.energy.gov/sites/default/files/documents/files/METALS_ProgramSummary.pdf [Cited 21 June 2020]

¹¹<https://www.makeitfrom.com/material-properties/EN-1.6587-18CrNiMo7-6-Case-Hardening-Bearing-Steel> [Cited 16 June 2020]

System Verification and Validation

Verification and validation (V&V) procedures are crucial in order to ensure that the design meets all requirements and the product fulfils its intended purpose. In the final design stage of the DSE, a detailed model was developed to simulate the kite power system, and another comprehensive model was created to analyse the performance of the renewable energy system. The V&V activities performed for these models have already been thoroughly discussed in chapters 9 and 11. In this chapter, first a short summary of the performed tests will be presented. Subsequently, a number of tests are suggested to perform as future V&V activities. Then, methods for testing the product are described. Finally, system-wide verification and validation tests are considered.

18.1. Model Verification and Validation

This section discusses V&V procedures of the software tools that were developed in order to size the renewable energy system.

18.1.1. Summary of System Performance Verification and Validation

Many tests have been performed on the system performance model and are shown in 9.4. Its verification and validation methods are summarised below.

Six units have been defined in the system performance analysis and each is tested accordingly. V&V procedures have been performed on the interpolation for the sunrise and sunset distributions and on the calculation of the energy fractions and the total energy demand. Furthermore, the solar and wind resources have been checked and the entire model is tested using dummy conditions. Throughout the making of the model, sanity and syntax checks have also been performed on blocks of code, to check for any obvious errors.

Verification of the entire model was harder because no reference model has been found that shows the interaction between an AWE and a solar energy system. Sensitivity analysis is performed to check how the entire model reacts to input changes, which helps looking for model errors. In general, at this design stage it can be said that this model can be verified and validated. But in future design activities, things like the operation of the central power control unit need to be tested in order to fully accept the validity of the model.

18.1.2. Summary of Primary Energy System Verification and Validation

The verification and validation methods applied on the primary energy system model shown in section 11.9 are summarised here.

Several actions were performed for model verification. Firstly, units of code were checked against the literature that the model theory was from. The outputs that were received were compared with graphs that are shown in the literature to check whether using the same inputs as the literature gives the correct output. If this was not available, then sanity checks were performed to see whether the outputs of certain units made sense. This was done by comparing the output values against standard values in the industry.

Next, a combination of verification and validation was applied to several modules in the model. Computations were performed on the tether forces, powers and reeling speeds against a range of wind speeds. A different model that uses a quasi-steady approach made by van der Vlugt et al. [96] was used to compare with the AWE Luchsinger model made by the team. This verification model has already been validated using experimental data and therefore this model can be used both for verification and validation of the AWE model.

All these actions resulted in the conclusion that the model can be verified and validated at this stage of design. But in future steps more elaborate verification and validation techniques need to be applied on the actual produced system to make sure that the model can be completely accepted.

18.1.3. Future Verification and Validation of the Models

The previous sections showed that the model can to some extent be verified, but in the future more elaborate verification and validation need to be applied to be completely sure that the model works properly. Since this mission is a very new approach to a Martian energy system for the space industry, no actual data is available to compare the system with. There has been no mission yet that has integrated a hybrid energy generation system like this one on Mars.

Therefor, in order to validate the system, a different and more creative approach needs to be taken. An investigation will be done to find data for a kite with similar properties. This data of course will be retrieved from a project done on earth, thus the experiments will have been performed in a different environment than on Mars. The model properties like air density and gravity will be adjusted for Earth. Also the wind resource that was present during these experiments will be put into the Mars mission model. Now that this has all been implemented, a lot of units can be checked with the experimental data to see whether the model does what it is supposed to do.

If it is found that these units can be validated, then it can be assumed that when modelled for Martian conditions the system is validated as well.

18.2. Product Verification and Validation

Next to V&V of the models, the final products also need to be verified and validated. Several approaches exist for checking compliance of the product with its requirements. These have already been introduced in the mid-term report [24]. Here, four different methods are distinguished: test, analysis, inspection and demonstration.

- **Test:** For this method, a realised component or end product is tested to obtain data to verify or validate its performance. Tests are performed in dedicated test facilities.
- **Analysis:** This method makes use of well-validated mathematical and physical models to predict the performance of a design. Based on the calculated data, the design is checked for compliance with its requirements.
- **Inspection:** By visual examination of a realised component or end product, physical design features can be verified. These can be length or volume of a product, but also the mass (weighing the product is considered inspection here).
- **Demonstration:** If none of the above methods are suitable, then a demonstration of the product is an option. It aims to establish compliance of the product with its requirements by operating it.

The requirements for which the final product needs to be tested are listed in table 18.1. For each requirement, it is indicated which method is used to verify or validate compliance of the design. It must be noted that one of the requirements (REM-NRG-09) requires two methods. This is because testing allows to evaluate whether the system is able to withstand the impact by flying particles of dust storms for a short period, but not for four months. It would require further analysis using a computer model to evaluate the durability of the system.

Table 18.1: Methods planned for verifying whether or not the product meets its requirement

Test	Analysis	Inspection	Demonstration
REM-NRG-08	REM-NRG-03	REM-Sys-N05-08	REM-Sys-N02-01
REM-NRG-09	REM-NRG-04	REM-Sys-N06-01	REM-Sys-N05-04
REM-Sys-N02-05	REM-NRG-09	REM-Sys-N06-05	REM-Sys-N06-05
REM-Sys-N02-08	REM-NRG-12	REM-Sys-N06-06	REM-LD-01
REM-Sys-N02-09	REM-NRG-13	REM-Sys-E01-01	REM-LD-02
REM-Sys-N02-12	REM-Sys-N02-02	REM-LD-03	REM-Sys-M02-01
REM-Sys-N02-13	REM-Sys-N02-03	REM-LD-04	REM-Sys-M02-02
REM-Sys-N02-11	REM-Sys-N02-04	REM-COST-01	REM-Sys-N12-02
REM-Sys-N05-09	REM-Sys-N02-06	REM-COST-02	REM-Sys-N12-03
REM-Sys-N12-06	REM-Sys-N02-07	REM-Sys-C02-01	
REM-Sys-N12-07	REM-Sys-N05-01	REM-Sys-C02-02	
	REM-Sys-N05-02	REM-Sys-C02-03	
	REM-Sys-N05-03	REM-Sys-C02-04	
	REM-Sys-N05-05	REM-IAS-02	
	REM-Sys-N05-06	REM-Sys-I01-01	
	REM-Sys-N05-07	REM-Sys-N12-05	

18.3. System Verification and Validation

Systemwise, the Renewable Energy System for a Mars Habitat needs to be verified and validated as well. Three relevant procedures are worked out.

Firstly, a common way to verify the behaviour of an energy system, is to model and simulate it in Simulink. This is a Matlab-based block diagram environment, that allows to model and simulate a design before moving to hardware. The big advantage of modelling in Simulink is that the actual system does not have to be produced yet. The individual subsystems can be modelled as electrical blocks. The inputs to the system are data files containing wind and solar data with a predefined resolution. The power consumption by the habitat can also be modelled. If the load profile is also an input to the system, the model can be run for a simulation time equal to the mission lifetime. During the simulation, the power flow is monitored, and the balance of the system is checked. In this manner, it can be verified if the individual subsystems are sized correctly, and if their integration is successful.

Then, to validate the complete energy system, a different set of tests are needed to be done. It is challenging to analyse the entire system in one place. Different testing facilities are required for different subsystems. For example, the Aarhus Mars Simulation Wind Tunnel¹ is required to accurately simulate Martian atmospheric conditions to test the AWE system [39]. On the other hand, Spectrolab's testing facility for testing the equipment and particularly the solar arrays under Martian solar conditions will be required for validation [35]. These facilities are not in the same place and therefore these tests will have to be done separately.

An efficient way to check how the subsystems interact with each other is to simulate the outputs from the other subsystems using a battery and power management system. When the kite is tested in a wind tunnel, then the simulation system will be present to represent the solar energy system, both types of storage and the microgrid. A model is made to make sure that the simulation system reacts just like the actual subsystems would, a set inputs should result in the correct outputs. How these subsystems react to certain system fluctuations will be found in the other facilities by applying the same methods. If an accurate simulation for each of the subsystems is available than the entire system can be validated without having to build a large test facility that is able to test all the subsystems at the same time.

Lastly, it is of utmost importance to validate the underlying assumptions on the available wind resources in the Martian atmosphere. As discussed in section 11.3, there is no accurate data available on the vertical wind profile because it has never really been measured yet. In order to size the kite power system, a log and power law wind profile has been assumed. This would need to be validated by sending a LiDAR to Mars (Light Detection And Ranging). With the LiDAR, the wind profile can be mapped. With the measurement data, the validity of the assumptions on the wind resources can be checked. If it turns out that the available wind has been overestimated, it will have serious consequences for the design of the renewable energy system.

On a final note, it is needless to say that the V&V activities suggested in this chapter are merely the tip of the iceberg. The exceptional amount of risk that is involved with the project demands for extensive V&V on every imaginable level. In view of time constraints, the planning of these is left for future engineering activities.

¹https://www.esa.int/ESA_Multimedia/Images/2019/05/Aarhus_Mars_Simulation_Wind_Tunnel [Cited 21 June 2020]

Production Plan

In this chapter, the first thoughts have been put into the finalisation of the system during production. In section 19.1, the production strategy is explained. In section 19.2, a preliminary manufacturing and assembling plan is presented.

19.1. Production Strategy

In the following section, general methods and policies for the production of the renewable energy system for a Mars habitat are presented. For the purposes of the mission at hand, during all production processes, lean manufacturing methodology will be applied. The lean manufacturing approach aims to minimise waste in terms of material, energy, time and human resource, while also striving to maximise the efficiency, productivity and quality of the process¹.

Therefore, in order to apply the lean manufacturing policy to this project, it is key to understand the ways resources could be wasted during production periods and how those could be prevented or mitigated to achieve a more efficient and sustainable process. Out of the eight ways waste could be produced² only *excess processing, waiting, inventory, and transportation* are dependent on the system development team. While the remaining four (*defects, overproduction, motion, non-utilised talent*) are not as relevant for having a lean production of the components at hand. First of all, this is a one time mission and no component will be produced in bulk. Secondly, third party contractors are most likely to be responsible for executing the manufacturing processes effectively and on schedule. Nevertheless, the development team is expected to hire appropriate, credible contractors which can guarantee and deliver the expected quality in the desired time periods.

Moreover, in order to address the first four lean manufacturing aspects, the development team must execute the following tasks. First, a detailed production plan must be developed and documented, so that minimal to no *excess processing* is observed during the component manufacturing. This would include a flow chart describing the flow of the processes, a Gantt chart for an overview of the time management and clear descriptions including images clarifying production steps of every component. Furthermore, it is not only the production and assembling that require extensive amount of planning. As for the purpose of manufacturing all the necessary components to a space-grade quality and the required durability, it could be expected that the best manufactures around the globe would be hired for the job. As this would be an international project involving multiple contractors and organisations, the transportation and logistics plan must be extremely well thought off and risk-proof in ordered to minimise the resource waste of the *waiting, inventory, and transportation* aspect of the lean manufacturing methodology. Moreover, please note that this planning is not exclusively for the manufacturing and assembling process; it also involves acquiring and delivering of all the necessary raw materials at the needed times and places. With this planning, the total transportation and production delays and waste must be minimised for the sake of the sustainable execution of this mission in the expected time period.

Nevertheless, before all the raw materials are purchased and the actual parts manufacturing is started, the compatibility of components must be verified and the integrity of the design is as expected. For these purposes, it is recommended to make engineering models or mock up assemblies beforehand, as visualised in figure 19.1. This can be done for example by 3D printing complicated joints and examine if the parts fit together. Moreover, when considering the spindle mechanism of the ground station, an equivalent physical model could be created from cheaper materials for the purpose of examining its functionality and limits. In case experiments do not go as expected or do not demonstrate sufficient quality, the process should be iterated. Once the engineering model has verified the functionality of the design and the mock-up assembly has demonstrated the compatibility of complicated components, the production of the final product can be started.

¹<https://searcherp.techtarget.com/definition/lean-production#:~:text=Lean%20manufacturing%20is%20a%20methodology,not%20willing%20to%20pay%20for> [Cited 19 June 2020]

²<https://www.machinemetrics.com/blog/8-wastes-of-lean-manufacturing> [Cited 19 June 2020]

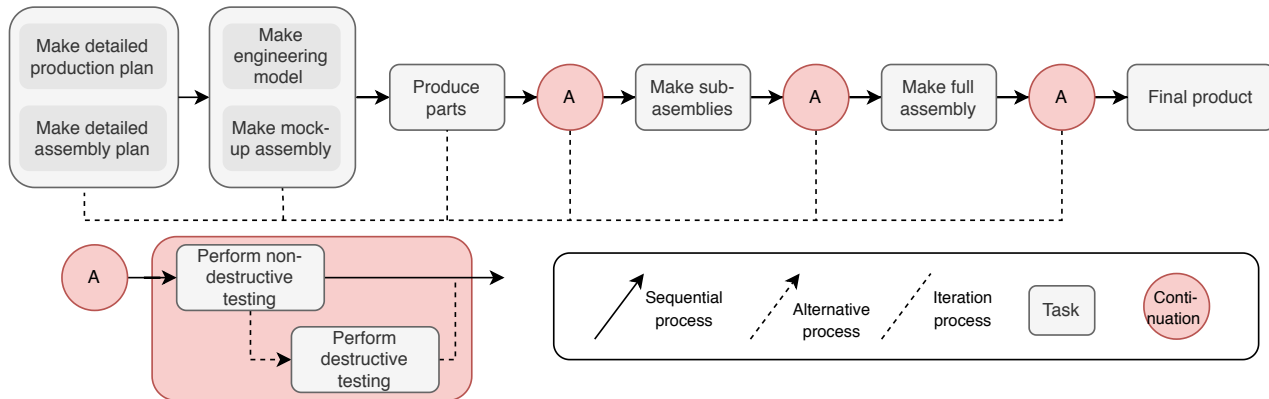


Figure 19.1: Production methodology with included iteration loops for system components

19.2. Manufacturing and Assembling Plan

As mentioned in the previous section, in order to minimise *excess processing*, *waiting*, *inventory*, and *transportation*, a detailed production plan must be created in advance of the production phase. To discover the steps that need to be included in this plan, a preliminary overview is made and shown in figure 19.2. It must be mentioned that as this is just a first overview, more knowledge should be acquired for the production of several components. Also, some components might still be missing. Later, as the design mature, it might be reassessed.

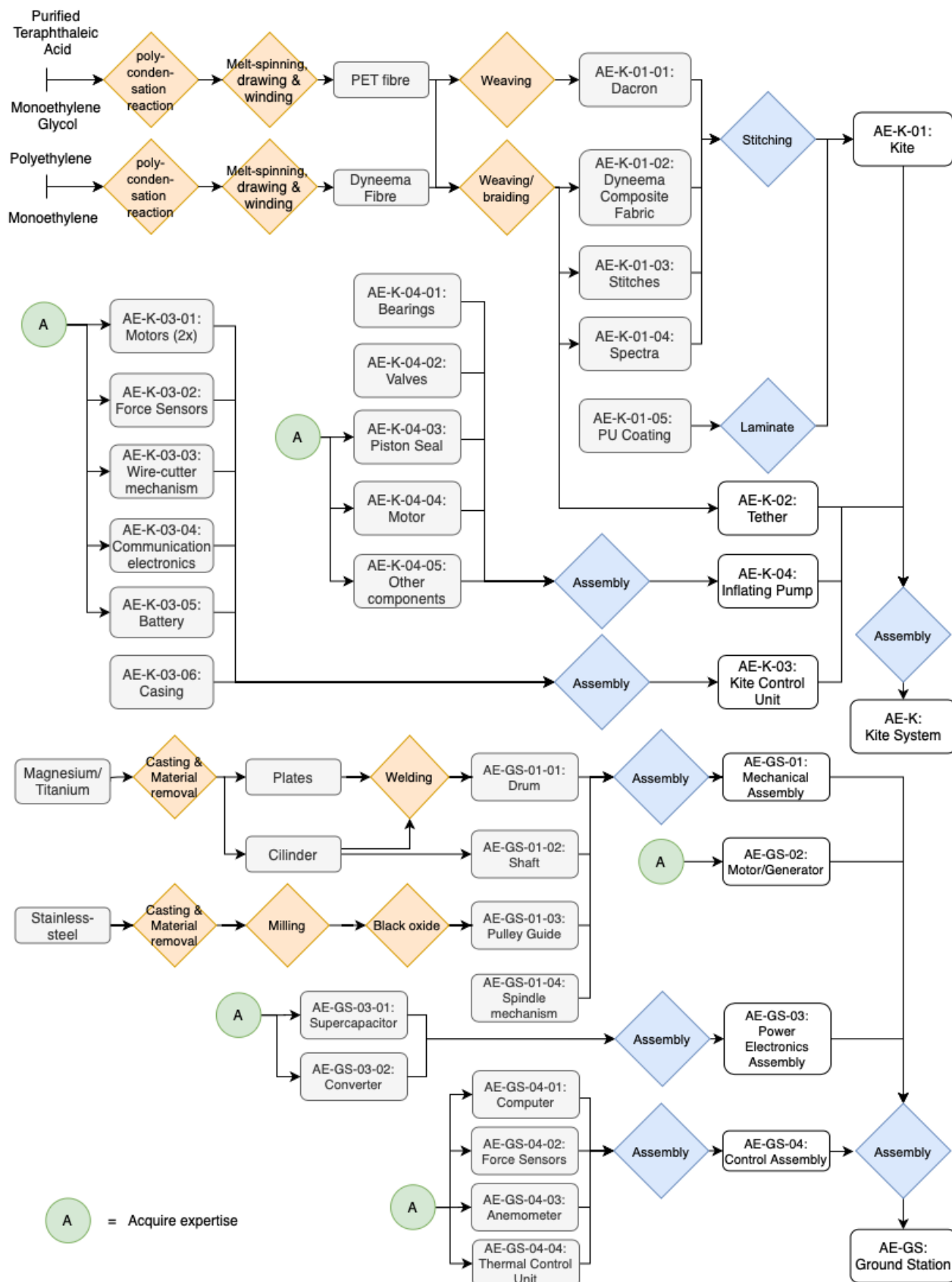


Figure 19.2: Preliminary production plan for the Airborne Wind Energy system

Compliance Matrix

In the compliance matrices, it is summarised whether or not each requirement has been met by the design. This section is subdivided into different subsystems and other aspects, e.g. safety and legal requirements. The requirements of the various subsystems have already been checked for compliance in chapters 10 to 13. For the sake of completeness, they are summarised again in this section. It should be pointed out, that compliance of the design with its requirements rests on analytical and computational models described in this report. To actually check whether the product meets the requirements, dedicated V&V procedures should be performed as presented in chapter 18. Nevertheless, the compliance matrices in this section provide good judgement of feasibility of the design, and show areas to improve on for further design activities. Also sensitivity analysis has been performed on the subsystem requirements and can be found in their respective chapter. Considering the compliance matrices, yes means that the requirement is complied with, no means that it is not yet complied with, probable means that more detailed modelling is required but will probably be complied with and “[TBD]” means that the requirement itself can not be analysed yet but will be in later iterations of the design.

Subsystem Requirements

Power Management System

ID	Compliance	Proof (which section)
REM-Sys-N06-01	Yes	Subsections 10.4.1 and 10.4.2, this was a design criterion and the power conversion equipment and cables have been sized after this requirement
REM-Sys-N06-05	Yes	Section 10.6, the total mass is estimated at ca. 190 kg
REM-Sys-N06-06	Probable	This requirement is difficult to evaluate and arguably irrelevant. Because of the complex power flow, each electrical path has its own efficiency, the lowest being 73.2% and the highest being 89.0%, as presented in table 10.5

Energy Storage System

ID	Compliance	Proof (Section)
Storage requirements		
REM-Sys-N05-02	Yes	Chapter 9 and section 13.4.2 with stage inefficiency and power validation
REM-Sys-N05-03	Yes	
REM-Sys-N05-04	No	
REM-Sys-N05-05	Yes	Section 13.4.2, based on the use of CO_2 as storage air and use of in-situ printed regolith as structural lining of storage cavern
REM-Sys-N05-06	Yes	Section 13.4.2, the compression segment efficiency is sized
REM-Sys-N05-07	Probable	Storage efficiency not looked into too much detail in this report, further investigation needed
REM-Sys-N05-08	Yes	Section 13.4.2, the expansion segment efficiency is sized
REM-Sys-N05-09	Yes	Section 13.5.2

Primary Energy System

ID	Compliance	Proof (Section)
REM-Sys-N02-01	No	Section 11.6, but mass will decrease when including space-grade materials in the design
REM-Sys-N02-02	Yes	Section 11.6, Kite area density allows for flight at velocities above 6.3 m s^{-1}
REM-Sys-N02-03	Yes	Subsection 11.5.3, the AWE system has been designed using this parameter as an input
REM-Sys-N02-05	Yes	Subsection 11.5.4 and 11.5.3, the system is designed for a T_{nom} of 7.5 kW with a design factor F_D of 3
REM-Sys-N02-06	Yes	Section 11.7
REM-Sys-N02-07	No	Section 11.7, multiple tethers will need to be brought to successfully complete the mission
REM-Sys-N02-08	Yes	Subsection 11.6.1, the generator efficiency equals 94.6%
REM-Sys-N02-09	Yes	Subsection 11.5.3, the AWE system has been designed using this parameter as an input
REM-Sys-N02-11	Yes	Section 11.6, the motor is sized for this value
REM-Sys-N02-12	Yes	Subsection 11.5.3, the AWE system has been designed using this parameter as an input
REM-Sys-N02-13	Yes	Subsection 11.5.3, the AWE system has been designed using this parameter as an input

Secondary Energy System

ID	Compliance	Proof (Section)
REM-Sys-N12-02	No	Subsection 12.5.1 and subsection 12.5.2, further research is needed to decrease axis mass
REM-Sys-N12-03	Yes	Subsection 12.5.1 and subsection 12.5.2 show the volume of the system to meet the requirement
REM-Sys-N12-04	Yes	Chapter 9 maintains the secondary energy contribution below 50%
REM-Sys-N12-05	Yes	Subsection 12.5.1 accounts for the 5 Martian life-time
REM-Sys-N12-06	Probable	Dust removal coating is very new and shall mature in the coming years. More research is required to incorporate the dust removal percentage in the analysis
REM-Sys-N12-07	Probable	More research is needed to develop the sun simulation, however the system is likely to achieve a high accuracy

Energy Requirements

ID	Compliance	Proof (which section)
REM-NRG-12	Yes	Section 8.5.3 and Chapter 9
REM-NRG-13	Yes	Section 8.5.3 and Chapter 9
REM-NRG-02	Yes	Section 9.3
REM-NRG-03	Yes	Section 9.3
REM-NRG-04	Yes	Chapters 11 and 12
REM-NRG-05	Yes	Chapter 13
REM-NRG-06	Yes	Chapter 10
REM-NRG-07	No	Subsection 8.1.1, the external team had no research yet on what they needed for a site, in the future a mutual trade-off can be made
REM-NRG-08	[TBD]	The dust storms and its effects on the system have not been analysed yet, but will be in future design iterations
REM-NRG-09	Probable	Still has to be investigated but the metallic structures should be able to withstand these wind speeds

Environmental Requirements

ID	Compliance	Proof (which section)
REM-MENV-01	Yes	Section 9.3, this is a fully renewable system
REM-MENV-02	Yes	Chapter 3 and section 8.5.1, as much recycling integrated in mission retirement as possible
REM-Sys-M02-01	[TBD]	More research is required to give a concrete number to this requirement
REM-Sys-M02-02	[TBD]	More research is required to give a concrete number to this requirement
REM-EENV-01	Yes	Section 17.2, CO2 emission analysed and minimised
REM-Sys-E01-01	[TBD]	More research is required to give a concrete number to this requirement

Launch and Deployment Requirements

ID	Compliance	Proof (which section)
REM-LD-01	No	Chapter 7, but in future design iterations this number will be reduced significantly
REM-LD-02	No	Chapter 7, but in future design iterations this number will be reduced significantly
REM-LD-03	[TBD]	More research is required to give a concrete number to this requirement
REM-LD-04	[TBD]	More research is required to give a concrete number to this requirement

Cost Requirements

ID	Compliance	Proof (which section)
REM-COST-01	Yes	Section 11.8
REM-COST-02	Yes	Chapter 7
REM-Sys-C02-01	Yes	More research is required to give a concrete number to this requirement
REM-Sys-C02-03	Yes	Section 12.7
REM-Sys-C02-04	Yes	Section 10.5

Legal Requirements

ID	Compliance	Proof (which section)
Legal requirements		
REM-LEG-01	Probable	Legal considerations have not been made yet, but will be in future design steps
REM-LEG-02	Probable	Legal considerations have not been made yet, but will be in future design steps
REM-LEG-03	Probable	Legal considerations have not been made yet, but will be in future design steps

Other Requirements

ID	Compliance	Proof (which section)
Other requirements		
REM-IAS-01	Yes	Section 15.3, one of the biggest priorities is keeping the astronauts safe throughout the mission
REM-IAS-02	Yes	Section 15.2, the astronauts will be given the required equipment/material for proper maintenance
REM-Sys-I01-01	Yes	Chapter 8, again astronaut safety is very important and this is therefore integrated in mission operations

21

Next Steps

This chapter elaborates on how the project could continue after the DSE phase has finished. The chapter includes the Project Gantt Chart spanning a period of 10 years up until launch of the system. Furthermore, the Design and Logic diagrams elaborate on the tasks that will be done in the future to make the project a success. Finally, a future cost breakdown structure is established.

21.1. Project Gantt Chart

A project Gantt chart was constructed to establish a timeline for the ten years following the DSE, and can be seen in figure 21.1. The schedule is divided into three phases, the first of which being Engineering Model Development. In this stage of the development, the design will be completed in its theoretical stage. As the DSE will have completed the conceptual design and performed part of the preliminary design of the full system, a more detailed design can be finalised, and simulations will be developed to evaluate the feasibility of the system. Furthermore, simultaneously with this stage, research studies will be performed to further develop the storage technologies. Additionally, the resource availability on Mars will be more carefully examined by possibly sending a rover with testing equipment to the chosen site. This will increase the confidence in the model and the system.

The second phase of the schedule is the Qualifying Model Development. In this stage the transition from theoretical model to hardware will be made. Starting with material tests and from there expanding to sub-system tests under Martian conditions. This will follow a similar structure when compared to the first phase. First a “conceptual design” will be made, meaning determining the structural characteristics of the materials for example, and examining their performance under Martian conditions. Next in the “preliminary design” the materials that were evaluated are used to assemble components of the sub-system and, again the performance can be tested. Finally in the “detailed design” the sub-systems can be assembled and be tested for certification. This allows all parts of the system to be fully verified and validated and allowing for iterations in case of a deviation in expected performance.

The last phase of the schedule focuses on the testing and finalising of the whole system and making it launch ready. The “final design” is the completion of the design using the space grade materials and final testing, which is performed concurrently with the system integration of all the sub-systems. This is followed by full system tests and assembly of the final mission ready system, leading all the way up to the launch.

21.2. Design and Logic Diagram

The schedule in the Gantt chart can be given a visual representation as to the flow of the development of the design. This can be seen in the project design and development logic diagram in figure 21.2. Here it is clearly displayed which tasks are expected to be performed concurrently, and how the iteration is executed. The research studies and the engineering model development are displayed in parallel, as these will be worked on at the same time. The information found in the research studies can be utilised in the design of the theoretical model. From there all parts happen consecutively. Once the engineering model is completed the qualifying model can be started, which is in turn followed by the flight model.

The phases are indicated by the green diamonds and their respective sub-tasks are coloured blue. The iteration loops are coloured yellow for extra emphasis as this is a very important step in the design process, and the transition from one phase to the next is indicated with a red circle. Finally the launch campaign is also indicated with red, as this is the closing step of the design phase that is visualised with this schedule.

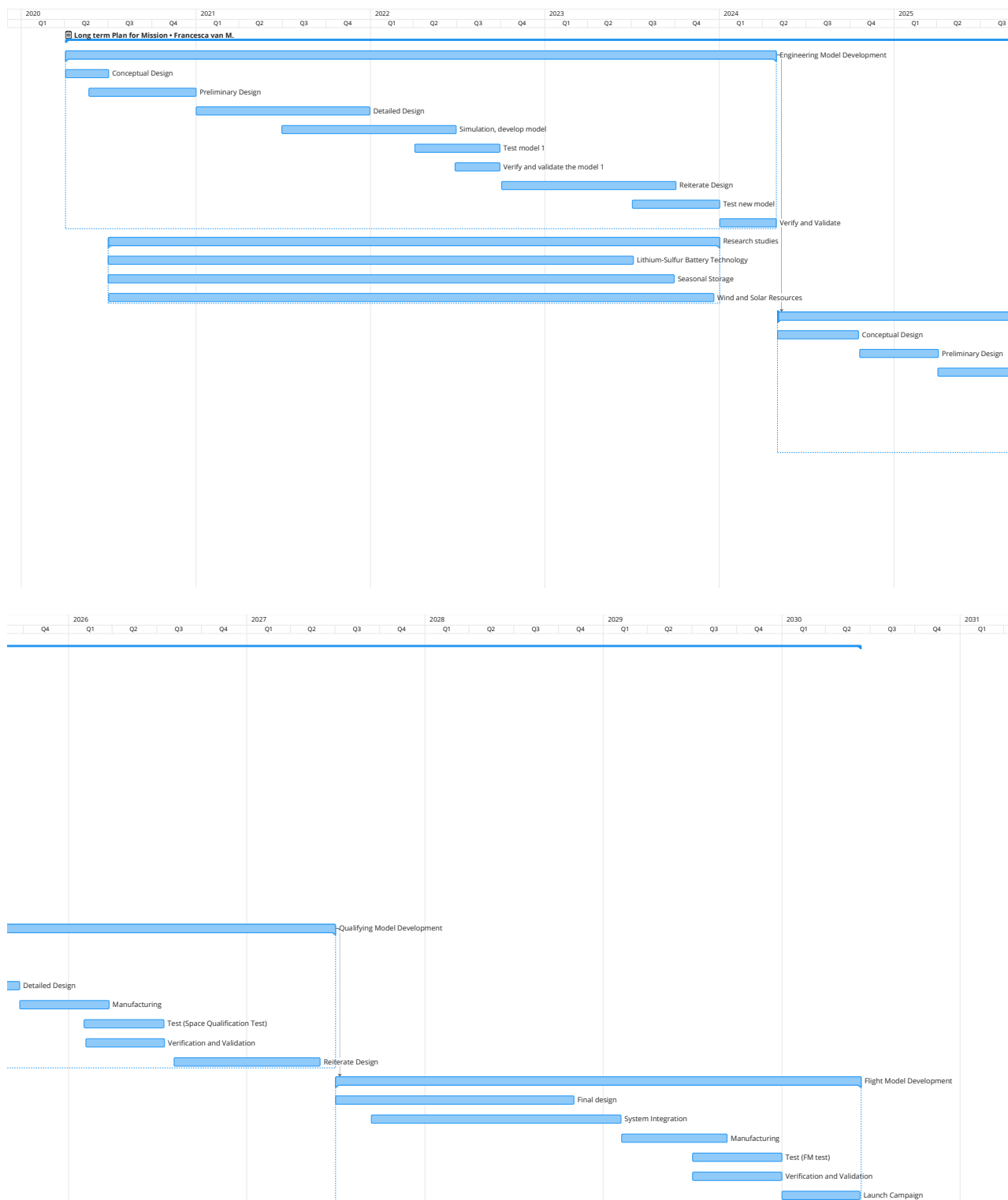


Figure 21.1: Project Gantt chart

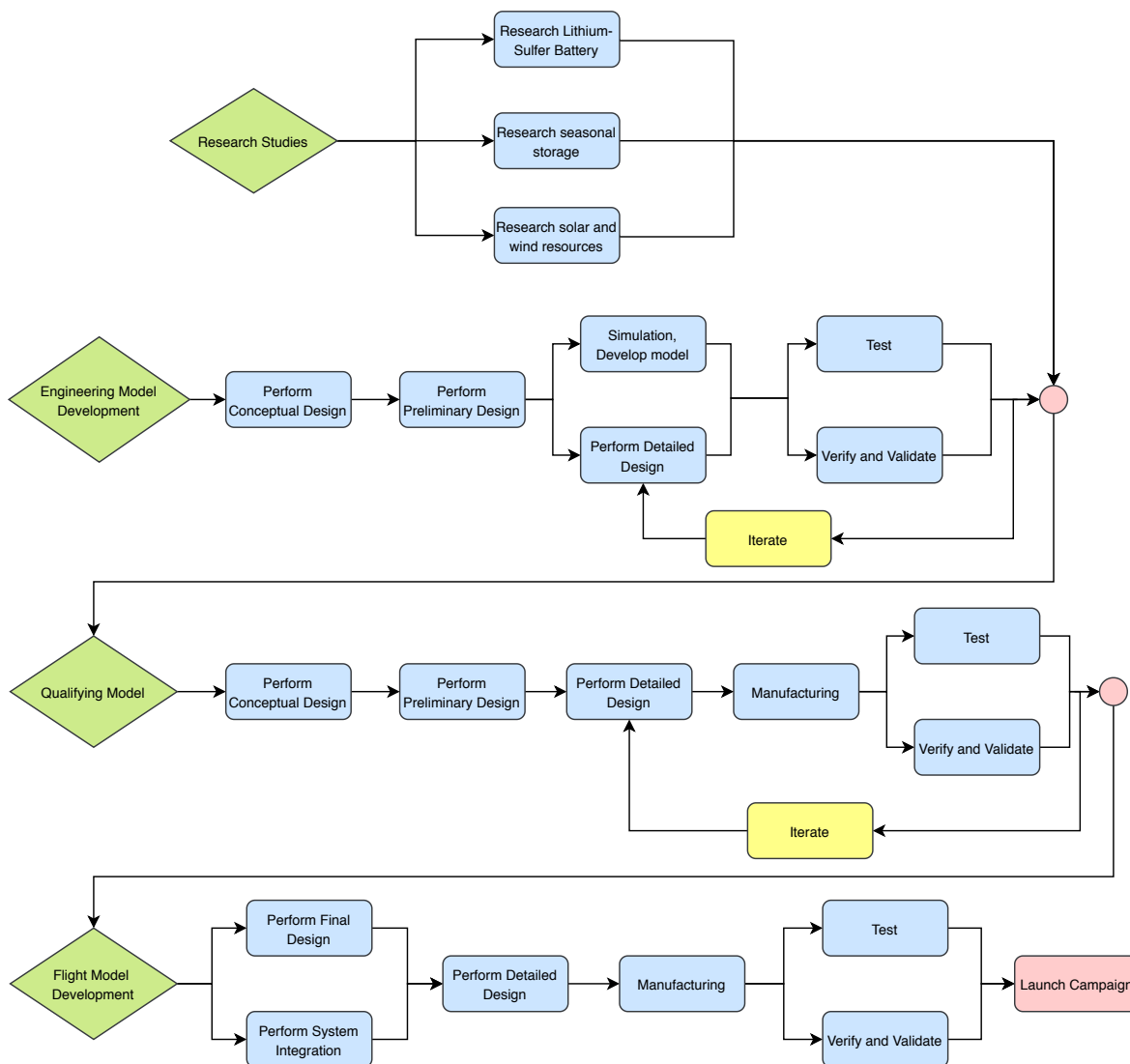


Figure 21.2: Project design and development logic diagram

21.3. Cost Breakdown Structure

The cost breakdown structure for the entire 10 year plan made in the Gantt chart, has been estimated in table 21.1 with values used from table 21.2. Quite some research was done into future planned Mars habitat missions as well as completed rover missions and space agency budgets. They have given a little bit of insight into how high budgets for interplanetary projects can be.

After doing this research and collecting data in an excel sheet, the most important value to have was an estimate for the total cost of the mission. To estimate this, the Mars One mission¹ was looked at. Here they budget 2.3 billion \$ for the preparations that need to be made on Mars before astronauts arrive. This would include the construction of a habitat and likely also an energy system to support it and its vital components. Since this project is only focusing on the energy system, the group decided to halve the total budget to 1.15 billion US \$. After this, the hardware and manufacturing costs are found based on the cost estimation of the designed system, where it was decided to take 3.5 times the cost of the whole system as to account for destructive testing and prototyping. The amount of launchers then gives the cost estimate for launching all payload to Mars. Here a contingency was taken into account for unplanned maintenance missions. The labour cost could also be estimated by assuming a certain number of employees and research their average pay grade per year, to estimate the total labour cost for the 10 year project^{2,3}. It was decided to assume 10 senior engineers would be working on the project, each with their own expertise such as electrical engineering or structural design. Each of the 10 engineers would have a team of 5 skilled labourers to assist in the development. Moreover, 10 astronauts are assumed to be going on the mission to Mars. Their salary is

¹<https://www.mars-one.com/faq/finance-and-feasibility/what-is-mars-ones-mission-budget> [Cited 15 June 2020]

²https://www.payscale.com/research/NL/Job=Aerospace_Engineer/Salary/053c0b86/Mid-Career [Cited 15 June 2020]

³<https://www.nationaleberoepengids.nl/service-engineer> [Cited 15 June 2020]

assumed to be similar to a senior engineer's salary⁴. Furthermore, testing, maintenance, safety and unexpected costs are left. The unexpected costs were simply estimated at 5% of the full budget. The testing costs were estimated at 20% as testing consists of quite a large and costly part of development. This fraction was based on a the budget of a similar study performed by NASA in which an energy system for a Mars habitat was developed [87]. Finally the maintenance cost and safety cost were split equally over the left over amount. The maintenance cost also include the maintenance to be performed during the mission in case extra support for this is needed.

Table 21.1: Cost Breakdown Structure for the long term mission plan

Cost	M€	% of total Cost
Hardware cost	35	0.030
Manufacturing cost	287.5	0.250
Launcher cost	39.21	0.034
Labour cost	31.5	0.027
Testing cost	230	0.20
Maintenance cost	234.6	0.20
Safety cost	234.6	0.20
Unexpected cost	57.5	0.050
Total cost	1150	1.000

Table 21.2: Values used for cost breakdown structure

Item	Value	Unit
Number of launchers	0.3	-
Cost per launch	130.7	M\$
Number of senior engineers	10	-
Number of skilled labourers	50	-
Number of astronauts	10	-
Cost per senior engineer per year	0.07	M€
Cost per skilled labourer per year	0.035	M€
Cost per astronaut per year	0.07	M€

The costs as described above, can be distributed over three categories and the unexpected cost. In the project budget there will be so called investment costs. These are the costs that are one time expenditures, which includes the launch cost and the safety cost. As certification expenses only happen as a design stage is finished, these costs will be payed once only. Next is the fixed cost, which in the case of this project incorporates only the labour cost. The fixed costs are consistent every month, as the engineering teams are assumed to be constant throughout the project, the labour costs should be as well (not considering bonuses and the like of course). Then in the variable costs the costs which are always present but not constant are included. In this case the maintenance, testing and hardware and manufacturing costs are incorporated in this category. As all of these will be performed throughout the project, however the costs might vary based on required materials and methods. The division of the costs between the three mentioned categories and the unexpected costs can be seen below in figure 21.3.

⁴https://www.glassdoor.nl/Salarissen/belgium-senior-engineer-salarissen-SRCH_IL.0,7_IN25_KO8,23.htm?countryRedirect=true
[Cited 22 June 2020]

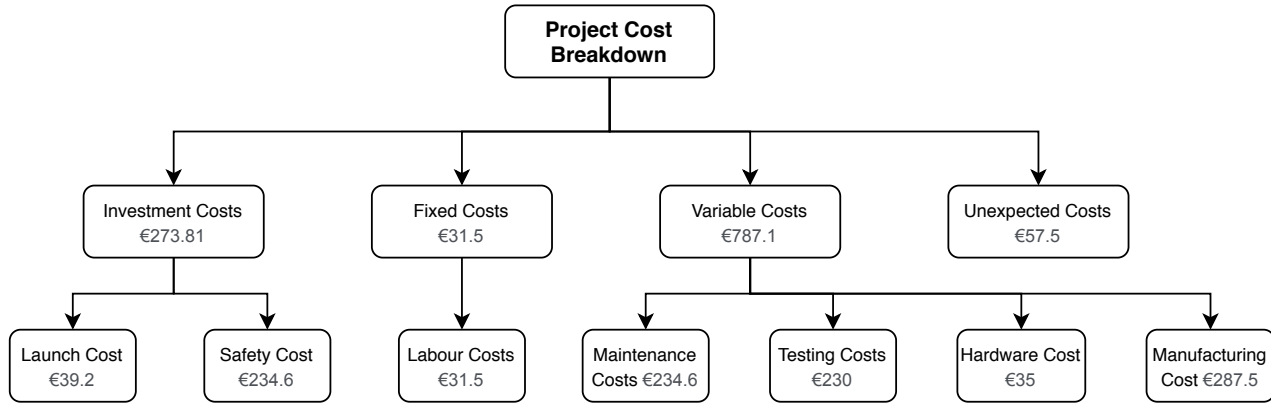


Figure 21.3: Cost Breakdown Structure tree in millions

To conclude this chapter, it is important to remember that the Gantt chart as well as the Cost Breakdown Structure are subject to change and can most definitely be refined once the project continues and more detail is known. The design that has been achieved until now has slightly more detail than a preliminary design would be. For the end of this report, there will be further recommendations on how to continue with the design at hand to follow the schedule made above, presented in the conclusion in chapter 22.

Conclusions and Recommendations

DSE team 23 consisting of 10 students was tasked with designing a renewable energy system for Mars habitats within 10 weeks. As this report comes to an end, it is also time to conclude on the design produced during the DSE. The renewable energy system has been designed to power the habitat without any nuclear or other unsustainable energy sources. This has been done by taking into account sustainability and risk of the project from all aspects as well as thoroughly analysing the market beforehand. The mission need and project objective statements that are guiding the project are as follows:

Mission Need Statement

To provide a renewable energy supply of 10 kW to a Mars habitat.

Project Objective Statement

Design a renewable energy supply system, primarily focusing on wind energy, which continuously provides 10 kW to a Mars habitat, by 10 students in 10 weeks.

Naturally coming up with a design solution, didn't come without any challenges. To bring light to the challenges and the team's creative solutions, the following sections will elaborate on the design solution, the solved and unsolved challenges and finally the recommendations for further development of the project.

Design Summary

Before getting deep into challenges and solutions, the final design will be shortly summarised. The design consists of a power management system, energy storage system, and two energy harvesting systems, namely the primary wind energy system and the secondary solar energy system.

Power management and distribution is the system that connects all the subsystems systems. It is essential for efficient distribution of power from energy harvesters to storage and to the habitat. The DC microgrid has been designed to have an underground cable infrastructure. Its total mass adds up to 191 kg and the system will cost a total of €69,800.

The primary energy system is harvesting energy from the wind and will be a pumping kite system attached to a ground station. The kite area amounts to 50 m² and the total system including the ground station has a mass of 288.1 kg and comes at an estimated cost of €63,500.

The secondary energy system consists of solar panels which will be harvesting energy from the sun. They occupy a total area of 70 m² and use a dual axis system to point in the right direction based on input from the sun simulation. The total system has a mass of 788 kg and costs €6,800,000.

The energy storage system consist of a seasonal compressed air storage system and a day-to-day lithium-sulphur battery solution. They work together to provide storage for the excess energy being produced by the energy harvesting devices. The two systems will have a joint mass of 1,520 kg and joint cost of approximately €2,006,500.

Requirements Compliance

Most of the requirements that were deduced in the baseline report have been complied with. There are still some TBD's left over, however as mentioned in the requirements section, these are mainly items that have not yet been researched into enough detail and will become more relevant as the design progresses further.

The main requirements that have not been complied with are displayed in table 22.1:

Table 22.1: Requirements that aren't complied with

Requirement ID	Description
Energy Requirements	
REM-NRG-07	The location of the habitat and its energy system shall be jointly decided by the external Mars habitat project team and the DSE team.

Continued on next page

Table 22.1: Continued from previous page

Requirement ID	Description
Primary Energy System Requirements	
REM-Sys-N02-01	The primary energy system shall have a maximum mass of 200kg.
REM-Sys-N02-07	The tether shall have a bending fatigue SLL longer than the mission duration.
Secondary Energy System Requirements	
REM-Sys-N12-02	The secondary energy system shall have a maximum mass of 550 kg.
Energy Storage System Requirements	
REM-Sys-N05-04	The components of the total energy storage shall have a maximum mass of 1500 kg.
Launch and Deployment Requirements	
REM-LD-01	The maximum volume for transportation shall be 3 m ³ .
REM-LD-02	The maximum payload shall be 800 kg per flight.

Noticeably, most of the requirements that the design does not comply with, are mass requirements. The design can still be dramatically improved by reducing the mass in many areas. Space-grade and lightweight materials should be investigated to achieve this. In later design iterations, the requirements that currently are not complied with should still be able to be reached.

Furthermore, as there is an ongoing trend in the development of launch vehicle concepts, with the purpose of enabling the transportation of larger payloads to the Martian surface while minimising the required transfer energy and associated costs. This will not only allow for the re-evaluation of the limiting size constraint, but it might also introduce a new framework of scalability for the design of ARES.

Challenges and Solutions

During the DSE period, the team has faced many challenges which include both technical design challenges as well as group organisational challenges. First the group related ones will be addressed.

This year, due to the DSE being online, the group had many organisational challenges. For starters, the project was completely done from home. So the work was done from home through online communication tools. The physical presence of group members was missed by many and this required some getting used to. Additionally, not everyone has the same working conditions from home which can severely influence their productivity. Our team has managed surprisingly well by using Zoom to communicate face to face and Slack for instant messaging. Even the review presentations were performed successfully with only few technical difficulties through Zoom. This proves that remotely working teams can be effective if the members are ready to put in the effort and necessary daily routine adjustments.

One large design challenge the group faced was ensuring that the required power could be provided continuously by purely renewable energy. The goal was initially to provide 10 kW of continuous power to the habitat, however it became clear that this would probably not be possible with the weight restrictions imposed. Many solar panels and very large kites would have been needed for this. To try to resolve this without having to provide some energy with a nuclear energy unit, the group came up with a solution where the energy system would have to provide less during the night. This would be realistic as the astronauts would be resting during this time. This results in 10 kW continuously being provided for 14 martian hours per sol and 5 kW being provided for 10 martian hours per sol solving the challenge and allowing the group to continue its design without a nuclear energy unit.

Unsolved Challenges

Some challenges remain unsolved and would need to be tackled in further development of the project. These include further research for the CAES as this system still consists of many unknowns, especially for a Mars application. The lithium-sulphur batteries are also still under development and if they were not flight ready within the mission timeline, then a different battery type would need to be chosen for the mission.

To actually ensure the mission is possible, it would also be essential to have more data on wind and solar resources at the habitat location on Mars. This would involve sending more rovers to Mars to gather more data.

The kite in its current state is not yet durable enough to last the mission lifetime. This challenge would need to be solved with more in depth research and testing of materials.

Finally, all the subsystem designs need to be adjusted for application on Mars as the planet does not have a friendly environment. This has not yet been investigated enough in detail and needs to be properly included in the flight version.

Recommendations for the Future of the Project

To end the conclusion and the final report of the DSE, some recommendations are proposed for the design to improve in the future development of the project.

For power management, the PDU and the central controller should be included in the design. In addition to this, the use of optimisation algorithms for power flow should be investigated to further increase the efficiency of the DC microgrid, as well as the control. Moreover, a challenge for DC microgrids consists of designing proper protection and grounding for its infrastructure. Finally, further research needs to be performed on the power converters for Mars applications not only to achieve the highest power densities, but also to shield them from the Martian environment and maximise reliability.

For the primary energy system a couple of recommendations and considerations can be made to ensure for design improvement in future iterations. Firstly, a couple of recommendations are made for the KCU as this part of the AWE system has not been designed to the same extent as the rest of the components. The casing of the KCU will need to be radiation proof and the control unit will need to be powered by batteries, which in turn need to be able to be recharged when the kite is on the ground. A kite position tracking system will also need to be created. Another big consideration that can be improved on is the system mass. Right now the primary energy system is slightly too big, but using less standard and more expensive materials that have higher specific mass, could improve the system design. Finally, in future design iterations the cut-in wind speed should be investigated further to optimise the systems annual energy production.

For the secondary energy system a more lightweight solution to the axis-system needs to be found. Furthermore a panel cooling system appropriate to the mission needs to be developed, which will be effective in the less dense atmosphere. Lastly, the sun-simulation of the sun path at the habitat location needs to be developed for the azimuth sun tracking system.

For the CAES, the key factor that determines the overall feasibility of the system is the availability of caverns on Mars and the structural properties of the Martian rock mass formation. The deformations and stresses under the cyclical pressurisation stages is key to design for reliability and longevity of the CAES system. Investigation into different compressed air storage technologies, such as lightweight tanks that can be built in-situ with additive manufacturing is also recommended.

For the batteries, close attention needs to be paid to thermal insulation and protection from Martian radiation. As the batteries still need to be developed, materials for these should also be researched more thoroughly. A more robust design should also be found in order to improve its parameters and the modularity of the design.

As a general recommendation for the entire system, the team says that all components need to be adjusted to work in a Martian environment. Most importantly, what most recommendations have in common is that they need some sort of thermal control as the temperature variations on Mars are extreme.

Finally, the team a few recommendations for the DSE in general. the team feels that an extension on the page limit for the midterm report would be of great benefit to the teams. This would avoid relevant information needing to be cut due to lack of pages. The online DSE has also taught the team a lot and should be reiterated here as recommendations for future groups working as a remote team. There are many ways to communicate through he internet nowadays, but the challenge is using these methods efficiently and for the correct type of communication. An important piece of advice for future teams is to do as many meetings and work sessions with video meetings as possible. This makes it more personal and you feel like you are working with a team even if not physically present. Of course official external communication should still go via e-mail to keep it documented. For quick questions an instant messaging app is best. Avoid whatsapp as this is more for personal messaging, instead one should use something like slack, Microsoft Teams or discord. Finally, keep in mind that members are working from home, which is an environment different for everybody. This means if sometimes members need to attend to something in their home or have other important appointments, the rest of the team should try to stay flexible.

Bibliography

- [1] Environmental management - Life cycle assessment - Principles and framework. ISO 14040:2006, 2006.
- [2] Environmental management - Life cycle assessment - Requirements and guidelines. ISO 14044:2006, 2006.
- [3] M. Alexander. Mars transportation environment definition document. Technical Report NASA/TM-2001-210935, NASA Marshall Space Flight Center, Alabama, March 2001. URL <http://hdl.handle.net/2060/20010046858>.
- [4] M. Allison. Accurate analytic representations of solar time and seasons on Mars with applications to the Pathfinder/Surveyor missions. *Geophysical Research Letters*, 24(16):1967–1970, August 1997. doi: 10.1029/97GL01950.
- [5] S. Anand and B.G. Fernandes. Optimal voltage level for DC microgrids. In *36th Annual Conference on IEEE Industrial Electronics Society (IECON 2010)*, pages 3034–3039, Glendale, AZ, USA, 2010. doi: 10.1109/IECON.2010.5674947.
- [6] J. Appelbaum and D.J. Flood. Solar radiation on Mars. Technical Report NASA-TM-102299, NASA Lewis Research Center, 1989. URL <http://hdl.handle.net/2060/19890018252>.
- [7] I. Argatov, P. Rautakorpi, and R. Silvennoinen. Estimation of the mechanical energy output of the kite wind generator. *Renewable Energy*, 34(6):1525–1532, 2009. doi: 10.1016/j.renene.2008.11.001.
- [8] J. Auer and A. Meincke. Comparative life cycle assessment of electric motors with different efficiency classes: a deep dive into the trade-offs between the life cycle stages in ecodesign context. *The International Journal of Life Cycle Assessment*, 23:1590–1608, August 2017. doi: 10.1007/s11367-017-1378-8.
- [9] AZO Materials. Magnesium AZ91D cast alloy, 2013. URL <https://www.azom.com/article.aspx?ArticleID=9219>. Accessed 1 July 2020.
- [10] V. Badescu. *Mars Prospective Energy and Material Resources*. Springer-Verlag, Berlin Heidelberg, 2009. doi: 10.1007/978-3-642-03629-3.
- [11] L. Barger et al. Learning to live on a Mars day: Fatigue countermeasures during the Phoenix Mars lander mission. *Sleep*, 35:1423–1435, 10 2012. doi: 10.5665/sleep.2128.
- [12] A. Barnard, S.T. Engler, and K. Binsted. Mars habitat power consumption constraints, prioritization, and optimization. *Journal of Space Safety Engineering*, 6(4):256–264, 2019. doi: 10.1016/j.jsse.2019.10.006.
- [13] H. Bier et al. Rhizome: Development of an Autarkic Design-to-Robotic-Production and -Operation System for Building Off-Earth Rhizomatic Habitats. 2nd stage of ESA competition, 2019. URL <http://cs.roboticbuilding.eu/index.php/Shared:2019Final>.
- [14] M.K. Biswal and R.N. Annavarapu. A novel entry, descent and landing architecture for Mars landers. 2018. URL <https://arxiv.org/abs/1809.00062>.
- [15] R. Bosman, V. Reid, M. Vlasblom, and P. Smeets. Airborne wind energy tethers with high-modulus polyethylene fibers. In U. Ahrens, M. Diehl, and R. Schmehl, editors, *Airborne Wind Energy, Green Energy and Technology*, chapter 33, pages 563–585. Springer, Berlin Heidelberg, 2013. doi: 10.1007/978-3-642-39965-7_33.
- [16] E.A. Bouman, M.M. Øberg, and E.G. Hertwich. Life cycle assessment of compressed air energy storage (caes). In *6th International Conference on Life Cycle Management (LCM2013)*, Gothenburg, Sweden, 2013.
- [17] J.C.M. Breuer and R.H. Luchsinger. Inflatable kites using the concept of tensairity. *Aerospace Science and Technology*, 14:557–563, 2010. doi: 10.1016/j.ast.2010.04.009.

- [18] L.M. Burke, R.D. Falck, and M.L. McGuire. Interplanetary mission design handbook: Earth-to-Mars mission opportunities 2026 to 2045. Technical Report NASA/TM-2010-216764, NASA Glenn Research Center, 2010. URL <http://hdl.handle.net/2060/20100037210>.
- [19] Z.A. Caddick, K. Gregory, and E.E. Flynn-Evans. Sleep environment recommendations for future space-flight vehicles. In Stanton N., Landry S., Di Buccianico G., and Vallicelli A., editors, *Advances in Human Aspects of Transportation. Advances in Intelligent Systems and Computing*, volume 484, pages 923–933. Springer, Cham, 2017. doi: 10.1007/978-3-319-41682-3_76.
- [20] L.M. Calle. Corrision on Mars: Effect of the Mars environment on spacecraft materials. Technical Publication NASA/TP-2019-220238, NASA Kennedy Space Center, June 2019. URL <http://hdl.handle.net/2060/20190027256>.
- [21] K. Campbell. Lubricating space exploration. *LUBE MAGAZINE*, 118, 2013.
- [22] A. Cervone and B.T.C. Zandbergen. AE2230-II: Propulsion & power, electrical power systems for aerospace vehicles. Lecture notes, Delft University of Technology, February 2017.
- [23] E.L. Christiansen, J.L. Hyde, M.D. Bjorkman, K.D. Hoffman, D.M. Lear, and T.G. Prior. Micrometeoroid and orbital debris threat assessment: Mars sample return earth entry vehicle. Technical Report NASA-JSC-66287, NASA Johnson Space Center, 10 2011. URL <http://hdl.handle.net/2060/20140001399>.
- [24] F. Corte Vargas, M. Géczi, M. Heidweiller, M. Kempers, B. J. Klootwijk, F. van Marion, D. Mordasov, L.H. Ouromova, E. N. Terwindt, and D Witte. Renewable energy for Mars habitat. Design synthesis exercise - midterm report, Faculty of Aerospace Engineering, Delft University of Technology, 2020.
- [25] F. Corte Vargas, M. Géczi, M. Heidweiller, M. Kempers, B.J. Klootwijk, F. van Marion, D. Mordasov, L.H. Ouromova, E.N. Terwindt, and D Witte. Renewable energy for Mars habitat. Design synthesis exercise - baseline report, Faculty of Aerospace Engineering, Delft University of Technology, 2020.
- [26] F. Crotogino, K. Mohmeyer, and R. Scharf. Huntorf caes: More than 20 years of successful operation. In *Solution Mining Research Institute (SMRI) Spring Meeting*, Orlando, FL, USA, 2001.
- [27] Alxion Documentation: STK Motors Range Complementary data. *PM Brushless Alternators for Direct Drive*. Alxion Automatique & Productique, 2017. URL <http://www.alxion.com/products/stk-motors/>.
- [28] R. de la Garza Cuevas. Kite power in a microgrid. Master's thesis, Delft University of Technology, 2018. URL <http://resolver.tudelft.nl/uuid:7653081f-710b-4511-be05-f1df9e6abc31>.
- [29] A. Delgado-Bonal, F.J. Martín-Torres, S. Vázquez-Martín, and M.-P. Zorzano. Solar and wind exergy potentials for Mars. *Energy*, 102:550–558, 2016. doi: 10.1016/j.energy.2016.02.110.
- [30] Y. Deng, J. Li, T. Li, X. Gao, and C. Yuan. Life cycle assessment of lithium sulfur battery for electric vehicles. *Journal of Power Sources*, 343(12):284–295, 2017. doi: 10.1016/j.jpowsour.2017.01.036.
- [31] SpaceX Documentation. Falcon user's guide. Technical report, Space Exploration Technologies Corp., 2020.
- [32] SpaceX Documentation. Starship user's guide. Technical report, Space Exploration Technologies Corp., 2020.
- [33] M.A. Dornheim. Planetary flight surge faces budget realities. *Aviation Week and Space Technology*, 145:44–46, 1996.
- [34] ECTA Documentation. *Guidelines for Measuring and Managing CO₂ Emission from Freight Transport Operations*, March 2011.
- [35] K.M. Edmondson, D.E. Joslin, C.M. Fetzer, R.R. King, N.H. Karam, N. Mardesich, P.M. Stella, D. Rapp, and R. Mueller. Simulation of the Mars surface solar spectra for optimized performance of triplejunction solar cells. In *19th Space Photovoltaic Research and Technology Conference*, number NASA/CP-2007-214494, pages 67–78, Brook Park, OH, USA, 2007. URL <http://hdl.handle.net/2014/37746>.
- [36] L.R. Elizondo and P. Bauer. DC and AC microgrids. Lecture notes, Delft University of Technology, 2018.
- [37] S. Engler. Forecasting of energy requirements for planetary exploration habitats using a modulated neural activation method. Master's thesis, University of Calgary, 2017. URL <http://doi.org/10.11575/PRISM/26208>.

- [38] S.T. Engler, K. Binsted, and H. Leung. HI-SEAS habitat energy requirements and forecasting. *Acta Astronautica*, 162:50–55, 2019. doi: 10.1016/j.actaastro.2019.05.049.
- [39] ESA. Aarhus Mars simulation wind tunnel, 2019. URL https://www.esa.int/ESA_Multimedia/Images/2019/05/Aarhus_Mars_Simulation_Wind_Tunnel.
- [40] P. Faggiani. Pumping kites wind farm. Master's thesis, Delft University of Technology, 2015. URL <http://resolver.tudelft.nl/uuid:66cddbd2-5f50-4fc7-be0b-468853128f37>.
- [41] P. Faggiani and R. Schmehl. Design and economics of a pumping kite wind park. In R. Schmehl, editor, *Airborne Wind Energy – Advances in Technology Development and Research*, Green Energy and Technology, chapter 16, pages 391–411. Springer, Singapore, 2018. doi: 10.1007/978-981-10-1947-0_16.
- [42] U. Fechner and R. Schmehl. Model-based efficiency analysis of wind power conversion by a pumping kite power system. In U. Ahrens, M. Diehl, and R. Schmehl, editors, *Airborne Wind Energy*, Green Energy and Technology, chapter 10, pages 249–269. Springer, Berlin Heidelberg, 2013. doi: 10.1007/978-3-642-39965-7_10.
- [43] U. Fechner and R. Schmehl. Flight path control of kite power systems in a turbulent wind environment. In *2016 American Control Conference (ACC)*, pages 4083–4088, Boston, MA, USA, 2016. doi: 10.1109/ACC.2016.7525563.
- [44] U. Fechner and R. Schmehl. Flight path planning in a turbulent wind environment. In R. Schmehl, editor, *Airborne Wind Energy – Advances in Technology Development and Research*, Green Energy and Technology, chapter 15, pages 361–390. Springer, Singapore, 2018. doi: 10.1007/978-981-10-1947-0_15.
- [45] U. Fechner, R. van der Vlugt, E. Schreuder, and R. Schmehl. Dynamic model of a pumping kite power system. *Renewable Energy*, 83:705–716, 2015. doi: 10.1016/j.renene.2015.04.028.
- [46] L.K. Fenton and M.I. Richardson. Martian surface wind: Insensitivity to orbital changes and implications for aeolian processes. *Journal of Geophysical Research: Planets*, 106(E12):32885–32902, 2001. doi: 10.1029/2000JE001407.
- [47] C. Ferrara and D. Philipp. Why do PV modules fail? *Energy Procedia*, 15:379–387, 2012. doi: 10.1016/j.egypro.2012.02.046. International Conference on Materials for Advanced Technologies 2011, Symposium O.
- [48] V.M. Fthenakis. End-of-life management and recycling of pv modules. *Energy Policy*, 28:1051–1058, November 2000. doi: 10.1016/S0301-4215(00)00091-4.
- [49] C. Galpin and A. Moncaster. Inclusion of on-site renewables in design-stage building life cycle assessments. *Energy Procedia*, 134:452–461, 2017. doi: 10.1016/j.egypro.2017.09.603. Sustainability in Energy and Buildings 2017: Proceedings of the Ninth KES International Conference, Chania, Greece, 5–7 July 2017.
- [50] S. Grimes, J. Donaldson, and G.C. Gomez. Report on the environmental benefits of recycling. Technical report, Bureau of International Recycling (BIR), October 2008.
- [51] S.D. Guzewich et al. Mars science laboratory observations of the 2018/Mars year 34 global dust storm. *Geophysical Research Letters*, 46(1):71–79, 2019. doi: 10.1029/2018GL080839.
- [52] J. Head, G. Neukum, R. Jaumann, et al. Tropical to mid-latitude snow and ice accumulation, flow and glaciation on Mars. *Nature*, 434:346–351, 3 2005. doi: 10.1038/nature03359.
- [53] N.G. Heavens, M.I. Richardson, and A.D. Toigo. Two aerodynamic roughness maps derived from Mars Orbiter Laser Altimeter (mola) data and their effects on boundary layer properties in a Mars general circulation model (GCM). *Journal of Geophysical Research: Planets*, 113(E2), 2008. doi: 10.1029/2007JE002991.
- [54] K. Hussen et al. Study on challenges in the commercialisation of airborne wind energy systems. Technical Report PP-05081-2016, prepared by Ecorys BV for the European Commission's DG Research and Innovation, Brussels, September 2018. URL <http://doi.org/10.2777/87591>.
- [55] Ingersoll Rand. Drum capacity definitions. Online, 2020.

- [56] International Renewable Energy Agency (IRENA). Renewable energy technologies: Cost analysis series - volume 1: Power sector, solar photovoltaics. Technical report, June 2012.
- [57] M.C. Johnson and J.L. Sullivan. Lightweight materials for automotive application: An assessment of material production data for magnesium and carbon fiber. Technical Report ANL/ESD-14/7, Argonne National Laboratory, September 2014. URL <http://doi.org/10.2172/1172026>.
- [58] D.C. Jordan, T.J. Silverman, J.H. Wohlgemuth, S.R. Kurtz, and K.T. VanSant. Photovoltaic failure and degradation modes. *Progress in Photovoltaics: Research and Applications*, 25(4):318–326, 2017. doi: 10.1002/pip.2866.
- [59] Imran K., Michael W.J., and J. Stephenson. Identifying residential daily electricity-use profiles through time-segmented regression analysis. *Energy and Buildings*, 194:232–246, 2019. doi: 10.1016/j.enbuild.2019.04.026.
- [60] J.-H. Kang and S.-C. Chen. Effects of an irregular bedtime schedule on sleep quality, daytime sleepiness, and fatigue among university students in taiwan. *BMC Public Health*, 9:1–6, 2009. doi: 10.1186/1471-2458-9-248.
- [61] Keck Institute for Space Studies. Unlocking the climate record stored within Mars' polar layered deposits. Technical report, Keck Institute for Space Studies, 2018.
- [62] P.L. King and S.M. McLennan. Sulfur on Mars. *Elements*, 6:107–112, 2010. doi: 10.2113/gselements.6.2.107.
- [63] J.S. Kougoulis, R. Kaps, B. Walsh, K. Bojczuk, and T. Crichton. Revision of eu european ecolabel and development of eu green public procurement criteria for indoor and outdoor paints and varnishes. Technical report, JRC European Commission and Oakdene Hollins Research & Consulting, June 2012.
- [64] J.M. Kuitche. *A Statistical Approach to Solar Photovoltaic Module Lifetime Prediction*. PhD thesis, Arizona State University, 2014. URL <http://hdl.handle.net/2286/R.A.143310>.
- [65] Th. V. Kármán. Über laminare und turbulente Reibung. *ZAMM - Journal of Applied Mathematics and Mechanics / Zeitschrift für Angewandte Mathematik und Mechanik*, 1(4):233–252, 1921. doi: 10.1002/zamm.19210010401.
- [66] G.A. Landis, D. Hyatt, and the MER Athena Science Team. The solar spectrum on the Martian surface and its effevy on photovoltaic performance. *IEEE 4th World Conference on Photovoltaic Energy Conversion*, May 2006. doi: 10.1109/WCPEC.2006.279888.
- [67] B. Lansdorp and W.J. Ockels. Design and construction of a 4 kW groundstation for the laddermill. *IASTED European Power and Energy Systems (EuroPES 2007)*, 2007.
- [68] W.J. Larson and J.R. Wertz. *Space Mission Analysis and Design*, volume 8 of *Space Technology Library*. Springer Netherlands, 3 edition, 1999.
- [69] J.S. Levine, D.R. Kraemer, and W.R. Kuhn. Solar radiation incident on Mars and the outer planets: Latitudinal, seasonal, and atmospheric effects. *Icarus*, 31(1):136–145, 1977. doi: 10.1016/0019-1035(77)90076-8.
- [70] R.D. Lorenz. Martian surface wind speeds described by the weibull distribution. 33(5):754–756, 1996. doi: 10.2514/3.26833.
- [71] R.H. Luchsinger. Pumping cycle kite power. In U. Ahrens, M. Diehl, and R. Schmehl, editors, *Airborne Wind Energy, Green Energy and Technology*, chapter 3, pages 47–64. Springer, Berlin Heidelberg, 2013. doi: 10.1007/978-3-642-39965-7_3.
- [72] A. Luque and S. Hegedus. *Handbook of photovoltaic science and engineering*. Wiley, Chichester, West Sussex, U.K., 2 edition, 2011. doi: 10.1002/9780470974704.
- [73] D. Lyu, B. Ren, and S. Li. Failure modes and mechanisms for rechargeable lithium-based batteries: a state-of-the-art review. *Acta Mechanica*, 230:701–727, 11 2019. doi: 10.1007/s00707-018-2327-8.
- [74] A. Manthiram, S.-H. Chung, and C. Zu. Lithium-sulfur batteries: progress and prospects. *Advanced Materials*, 27(12):1980–2006, 2015. doi: 10.1002/adma.201405115.

- [75] L. Mason and M. Rucker. Common power and energy storage solutions to support lunar and Mars surface exploration missions. In *70th International Astronautical Congress (IAC)*, Washington, DC, USA, 2019. URL <http://hdl.handle.net/2060/20190032521>.
- [76] G.M. Merritt and P.G Smith. *Field Guide to Project Management*. John Wiley & Sons Inc., 2 edition, 2004.
- [77] L. Montabone and F. Forget. On forecasting dust storms on Mars. In *48th International Conference on Environmental Systems*, Albuquerque, NM, USA, 2018.
- [78] R.W. Moses and D.M. Bushnell. Frontier in-situ resource utilization for enabling sustained human presence on Mars. Technical Report NASA/TM-2016-219182, NASA Langley Research Center, 2016. URL <http://hdl.handle.net/2060/20160005963>.
- [79] M. Nolberto. *Risk Management for Engineering Projects - Procedures, Methods and Tools*. Springer International Publishing, 2014. doi: 10.1007/978-3-319-05251-9.
- [80] S.S. Pathak and A.S. Khanna. Sol-□□gel nanocoatings for corrosion protection. In V.S. Saji and R. Cook, editors, *Corrosion Protection and Control Using Nanomaterials*, Woodhead Publishing Series in Metals and Surface Engineering, chapter 12, pages 304–329. Woodhead Publishing, 2012. doi: 10.1533/9780857095800.2.304.
- [81] P. Perazzelli and G. Anagnostou. Design issues for compressed air energy storage in sealed underground cavities. *Journal of Rock Mechanics and Geotechnical Engineering*, 8(3), 10 2015. doi: 10.1016/j.jrmge.2015.09.006.
- [82] J.J. Plaut, A. Safaeinili, J.W. Holt, R.J. Phillips, J.W. Head, R. Seu, N.E. Putzig, and A. Frigeri. Radar evidence for ice in lobate debris aprons in the mid-northern latitudes of Mars. *Geophysical Research Letters*, 36(2), 2009. doi: 10.1029/2008GL036379.
- [83] T. Prater and M.T. Moraguez. In-Space Manufacturing: The Gateway to the High Frontier and an Enabling Technology for Human Space Exploration. In *2019 Tennessee Valley Interstellar Workshop*, Wichita, KS, USA, 2019. URL <http://hdl.handle.net/2060/20200000035>.
- [84] Q. Qiao, F. Zhao, Z. Liu, S. Jiang, and H. Hao. Comparative study on life cycle CO_2 emissions from the production of electric and conventional vehicles in China. *Energy Procedia*, 105:3584–3595, May 2017. doi: 10.1016/j.egypro.2017.03.827.
- [85] P.L. Read and S.R. Lewis. *The Martian Climate Revisited*. Springer-Verlag, Berlin Heidelberg, 2004.
- [86] M.A. Rucker. Mars ascent vehicle design considerations. In *AIAA Space 2015 Conference*, Pasadena, CA, USA, 2015. URL <http://hdl.handle.net/2060/20150016019>.
- [87] M.A. Rucker et al. Solar versus fission surface power for Mars. Technical report, National Aeronautics and Space Administration, 2016.
- [88] V. Salma, F. Friedl, and R. Schmehl. Improving reliability and safety of airborne wind energy systems. *Wind Energy*, 23(2):340–356, 2020. doi: 10.1002/we.2433.
- [89] P. Schavemaker and L. van der Sluis. *Electrical Power System Essentials*. Wiley, 2 edition, 2017.
- [90] R. Schmehl and U. Fechner. Kitepower data 2010–2015. Technical report, Delft University of Technology, 2020.
- [91] D.A. Spera and T.R. Richards. Modified power law equations for vertical wind profiles. In *Wind Characteristics and Wind Energy Siting Conference*, Portland, OR, USA, 1979. URL <http://hdl.handle.net/2060/19800005367>.
- [92] S. W. Squyres. Martian fretted terrain: Flow of erosional debris. *Icarus*, 34(3):600–613, 1978. doi: 10.1016/0019-1035(78)90048-9.
- [93] R. Sullivan et al. Results of the imager for Mars Pathfinder windsock experiment. *Journal of Geophysical Research: Planets*, 105(E10):24547–24562, 2000. doi: 10.1029/1999JE001234.
- [94] R. Surampudi et al. Energy storage technologies for future planetary science missions. Technical Report JPL D-101146, Jet Propulsion Laboratory, 2017.

- [95] R. Tao, T.L. Neil, R.L. Stephen, M. Luca, and Peter L.R. Investigating the semiannual oscillation on Mars using data assimilation. *Icarus*, 333:404–414, 2019. doi: 10.1016/j.icarus.2019.06.012.
- [96] R. van der Vlugt, A. Bley, R. Schmehl, and M. Noom. Quasi-steady model of a pumping kite power system. *Renewable Energy*, 131:83–99, 2 2019. doi: 10.1016/j.renene.2018.07.023.
- [97] R. Verheul, J. Breukels, and W.J. Ockels. Material selection and joining methods for the purpose of a high-altitude inflatable kite. In *50th AIAA/ASME/ASCE/AHS/ASC Structures, Structural Dynamics, and Materials Conference*, Palm Springs, CA, USA, 2009. doi: 10.2514/6.2009-2338.
- [98] R. van der Vlugt, J. Peschel, and R. Schmehl. Design and experimental characterization of a pumping kite power system. In U. Ahrens, M. Diehl, and R. Schmehl, editors, *Airborne Wind Energy, Green Energy and Technology*, chapter 23, pages 403–425. Springer, Berlin Heidelberg, 2013. doi: 10.1007/978-3-642-39965-7_23.
- [99] C. von Holstein-Rathlou. *Wind related evolution of the Martian surface*. PhD thesis, Aarhus University, 2011.
- [100] S. Watson, A. Moro, et al. Future emerging technologies in the wind power sector: A european perspective. *Renewable and Sustainable Energy Reviews*, 113:109270, 2019. doi: 10.1016/j.rser.2019.109270.
- [101] S. Wilhelm. Life cycle assessment of electricity production from airborne wind energy. Master's thesis, Hamburg University of Technology, 2015.
- [102] D.R. Williams. Mars fact sheet, 2020. URL <https://nssdc.gsfc.nasa.gov/planetary/factsheet/marsfact.html>. Accessed 4 May 2020.
- [103] N. Williard, W. He, M. Osterman, and M. Pecht. Reliability and failure analysis of lithium ion batteries for electronic systems. In *Electronic Packaging Technology and High Density Packaging*, pages 1051–1055, 08 2012. doi: 10.1109/ICEPT-HDP.2012.6474788.
- [104] D. Yaghoubi. Emerging technologies for Mars exploration: Mars ascent vehicle. In *IEEE Aerospace Conference*, Big Sky, MT, USA, 2020. NASA Marshall Space Flight Center. URL <http://hdl.handle.net/2060/20200001747>.
- [105] J. Zhang, W. Wang, S. Zhou, H. Yang, and C. Chen. Transparent dust removal coatings for solar cell on Mars and its anti-dust mechanism. *Progress in Organic Coatings*, 134:312–322, 2019. doi: 10.1016/j.porgcoat.2019.05.028.